PhD degree in Molecular Medicine (curriculum in Molecular Oncology)

European School of Molecular Medicine (SEMM),

University of Milan and University of Naples “Federico II”

Settore disciplinare: Bio/11

ESSENTIAL POSTREPLICATIVE FUNCTIONS OF THE SMC5/6 COMPLEX

Demis Menolfi

IFOM, Milan

Matricola n. R09393

Supervisor: Dr. Dana Branzei

IFOM, Milan

Anno accademico 2013-2014

Table of contents

Figures index

Tables index

List of abbreviations

ARS	Autonomously Replicating Sequence
BrdU	5-bromo-2'-deoxyuridine
ChIP-on-chip	Chromatin Immunoprecipitation on chip
DAPI	4',6-diamidino-2-phenylindole
DDT	DNA Damage Tolerance
DSB	Double Strand Break
EdU	5-ethynyl-2'-deoxyuridine
HJ	Holliday Junction
HR	Homologous Recombination
HU	Hydroxiurea
MMS	Methyl metansulfonate
NM	Nitrogen Mustard
NSE	Non Smc Element
PFGE	Pulse Field Gel Electrophoresis
PRR	Post Replication Repair
RFB	Replication Fork Barrier
SCIs	Sister Chromatid Intertwinings
SCJs	Sister Chromatid Junctions
SGA	Synthetic Genetic Array
SMC	Structural Maintenance of Chromosome
STR	Sgs1-Top3-Rmi1
SUMO	Small Ubiquitin-like Modifier
TLS	Translesion synthesis
TS	Template Switching
wt	wild-type

Abstract

The structural maintenance of chromosomes (SMC) complex Smc5/6 is based on a heterodimer of two SMC subunits, Smc5 and Smc6, and six non-Smc element subunits, Nse1-6, all of which are essential for cell viability in most organisms. Smc5/6 safeguards genome integrity via different mechanisms, including stabilization of stalled replication forks, resolution of recombination intermediates, and maintenance of nucleolar integrity. However, the essential functions of Smc5/6 remain elusive. The aim of the present work was to understand when in the cell cycle the crucial functions of Smc5/6 are manifested and to identify them. Through the use of cell cycle regulated alleles, which enabled the restriction of various Smc5/6 subunits expression to either S or G2/M phases of the cell cycle, we uncovered that the essential roles are executed postreplicatively in G2/M. By further genetic screens, molecular approaches and genome-wide studies, we identified three chromosome topology and recombination-related processes that are crucially sensitive to low amounts of Smc5/6 specifically in G2/M. First, Smc5/6 plays a topological role affecting the formation and/or the resolution of Rad5-Mms2-Ubc13 chromatin structures that are later engaged by Sgs1-Top3-Rmi1. Second, Smc5/6 facilitates an epigenetic pathway that ensures silencing of specific loci, such as repetitive DNA regions, thereby preventing unrestrained recombination. Third, Smc5/6 has an anti-fragility function, facilitating replication through natural pausing elements and site-specific replication fork barriers and preventing their breakage in mitosis during chromosome segregation.

1 Introduction

1.1 Architecture of SMC complexes

Structural maintenance of chromosome (SMC) complexes regulate chromosome architecture and organization throughout the cell cycle in both prokaryotes and eukaryotes (reviewed in (Hirano, 2006; Losada and Hirano, 2005)).

SMC proteins are huge polypeptides of about 1,000-1,300 amino acids with a unique domain organization. They contain at the N-terminal and C-terminal domains two nucleotide-binding motifs, respectively Walker A and Walker B. Between these two motifs there are two long coiled-coil that are connected by a non-helical sequence in a way that an SMC monomer folds back on itself, creating an ATP-binding globular 'head' domain at one hand, in which the N- and the C-terminal come in close contact, and a 'hinge' domain at the other. In this way, the ATPase head and the hinge domain are separated by an intramolecular antiparallel coiled-coil.

SMC dimers are formed when two SMC monomers associate with each other through their hinge domain and they can assume highly dynamic structures, including open-V, closed-V and ring-like molecules, as it has been detected by electron microscopy.

The C-terminal domain of Smc proteins contains a so-called C motif, which is characterized by a LSGG(E/Q)(K/R) sequence. ATP binds to a pocket formed by the Walker A and Walker B motifs from one SMC subunit and interacts with the C motif of the second subunit; binding of the ATP to the head domains induces their engagement with the subsequent hydrolysis of ATP which in turn triggers their disengagement. While the head-head engagement requires ATP and it is dynamically regulated by its hydrolysis, the hinge-hinge interaction which mediates the dimerization does not require ATP and it is achieved primarly by β-sheet interactions between the monomers.

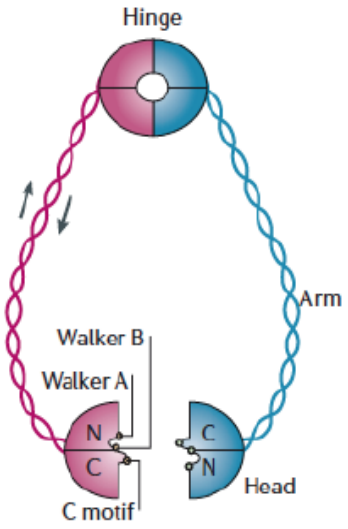

Figure 1.1 General structure of the core of SMC complexes. Adapted from (Hirano, 2006).

1.2 Varieties and functions of SMC complexes

While in prokaryotes SMC proteins form homodimers, in eukaryotes they form heterodimers, and each of these heterodimers further associate with non-Smc subunits in order to become functional complexes.

1.2.1 Prokaryotic SMC complexes

The best characterized bacteria SMC proteins are the *Bacillus subtilis* SMC (BsSMC) and its homologue in *Escherichia coli*, MukB, which form homodimers that are entirely symmetrical. They both associate with two non-Smc subunits called segregation and condensation protein A and B (ScpA, ScpB) in *B. subtilis*, and MukE and MukF in *E. coli* (reviewed in (Graumann and Knust, 2009)). ScpA and MukF are members of the kleisin protein family, which physically connect the two SMC subunits. Different studies suggest that the SMC/MukB complex regulates chromosome compaction and segregation, partly through an effect on DNA supercoiling by suppressing the formation of negative supercoils (Petrushenko et al., 2006). It was shown that SMC interacts with many regions

on *B. subtilis* chromosome (Lindow et al., 2002) and binds DNA in a non-specific manner (Volkov et al., 2003). Furthermore, it is required for the formation of defined assemblies on the nucleoids and it is believed that SMC condenses newly synthetized regions on the chromosome that are moved away from the replication machinery, located in the center, towards opposite cell poles (Volkov et al., 2003). Other bacterial SMC-like proteins, SbcC and RecN, were identified and linked to DNA repair. SbcC plays a role in the repair of inter-strand crosslinks and in the restart of stalled replication forks, likely by promoting Homologous recombination (HR). RecN accumulates at DNA double-strand breaks (DSBs) at early time points *in vivo* and is thought to act as a sensor of DSBs (Mascarenhas et al., 2006).

1.2.2 Eukaryotic SMC complexes

In eukaryotes there are at least six SMC family members, Smc1-6, which form three main heterodimers, known as cohesin (Smc1-Smc3), condensin (Smc2-Smc4) and Smc5/6 (Smc5-Smc6), which are individually discussed below (reviewed in (Wu and Xu, 2012; Jeppsson et al., 2014b).

1.2.2.1 Cohesin

The cohesin complex is composed of four evolutionary conserved subunits, Smc1, Smc3 and two non-Smc proteins, Scc1 and Scc3. Vertebrate cells contain two Scc3 proteins, SA1 and SA2. Scc1 is the kleisin subunit that links the head of Smc3 and Smc1 through its N- and C-terminal regions, respectively, in order to form a tripartite ring; Scc3 is a HEAT repeat-containing protein that interacts with Scc1.

The main function of cohesin is to regulate sister-chromatid cohesion, possibly by topologically embracing the two chromatids inside its ring from their formation during replication until their separation in anaphase. The complex is loaded by Scc2-Scc4 in telophase and G1 before DNA replication (Ciosk et al., 2000), but it becomes cohesive during DNA synthesis through the acetylation of Smc3 by the acetyltransferase Eco1 on

lysines K112 and K113 in budding yeast (Rolef Ben-Shahar et al., 2008; Unal et al., 2008). Timely dissolution of cohesion is required for allowing proper chromosome segregation in mitosis. In budding yeast, Scc1 is cleaved by the protease Separase at the metaphase-anaphase transition and this event triggers sister chromatid separation (Uhlmann et al., 1999; Uhlmann et al., 2000). In vertebrate and mammalian cells, most cohesin is removed from chromatid arms in prophase by Pds5 and Wapl (Gandhi et al., 2006), negative regulators of cohesion, and this process is facilitated by Plk1-dependent phosphorylation of SA2 (Hauf et al., 2005). A small amount of the complex remains associated with pericentromeric regions and it is protected from removal by the shugosin-PP2A complex (Kitajima et al., 2006; Riedel et al., 2006); finally, this pericentromeric/centromeric pool of cohesin is cleaved by Separase at the onset of anaphase (Uhlmann et al., 2000).

Cohesin has been recently involved in a number of new functions, such as the organization of replication factories to promote efficient origin firing and the regulation of transcription, by mediating long-range chromosomal interactions in *cis*, thereby acting as an intramolecular bridge (Jeppsson et al., 2014b).

The chromosomal binding pattern of cohesin was examined at high resolution by Chromatin immunoprecipitation (ChIP) followed by hybridization on DNA tiling arrays (ChIP-on-chip). In metazoan cells, cohesin's interaction sites are consistent with the transcriptional function of the complex. In *D. melanogaster* cohesin colocalizes with RNA polymerase II at transcribed genes (Misulovin et al., 2008) and in humans with the mediator complex (Kagey et al., 2010). Differently, in budding yeast, cohesin preferentially binds intergenic regions between genes that are transcribed in a convergent manner (Lengronne et al., 2004).

Besides its physiological functions in sister-chromatid cohesion and transcription, cohesin plays a crucial role in DSB repair through Homologous recombination (HR)

during S/G2 phases of the cell cycle. During DSB repair sister chromatids are the preferred template for HR. Thus, cohesion at or near DSBs facilitates the proximity of the donor, the undamaged sister chromatid, to facilitate and promote strand invasion and HR. In mammalian cells, cohesin recruitment to laser-induced lesions was shown by immunofluorescence (IF) to be dependent on Mre11 and Rad50 (Kim et al., 2002). In budding yeast, enrichment of cohesin by ChIP studies (Strom et al., 2007; Unal et al., 2007) was detected around an induced DSB in G2/M, but not in G1, and required Scc2/4. Cohesin recruited to DSB is able to establish sister-chromatid cohesion in G2, not only at the DSB but also throughout the genome, independently from DNA replication. This damage-induced cohesion is controlled by the DNA damage response (DDR) factors (Mec1, Tel1, Mre11 and γH2A) and other regulators (Scc2, Eco1 and Smc6). Phosphorylation of the Scc1 subunit at S83 by Chk1 makes Scc1 a better substrate for Eco1, which acetylates K84 and K210 of Scc1 to establish damage-induced cohesion (Heidinger-Pauli et al., 2009). Eco1 has therefore distinct substrates in S phase (Smc3) and damage-induced (Scc1) cohesion.

1.2.2.2 Condensin

Condensin is composed of two core subunits, Smc2 and Smc4, and three non-Smc elements, which in budding yeast are the kleisin, Brn1, and two HEAT domain-containing proteins, Yse4 and Ycg1. In vertebrate cells, there are two types of condensin complexes: condensin I and condensin II. They share Smc2/CAP-E and Smc4/CAP-C, but they differ for the other three subunits. Condensin I contains the kleisin CAP-H, CAP-D2 and CAP-G, while Condensin II contains CAP-H2, CAP-D3 and CAP-G2.

Condensin complexes regulate chromosome organization and condensation during mitosis and meiosis and they are responsible for folding chromatin fibers into highly compact chromosomes to ensure their faithful segregation. In addition to the structural organization of chromosomes, condensin promotes the function of type II topoisomerase

(Top2 in budding yeast) controlling its recruitment and localization. Top2 is required for the disentanglement of sister chromatids allowing their separation in mitosis (Baxter et al., 2011). Inhibition of condensin or Top2 leads to similar phenotypes, including chromosome missegregation and unresolved DNA bridges that connect the chromatids (Bhalla et al., 2002; Coelho et al., 2003).

In metazoans, condensin II is present in the nucleus throughout the cell cycle, but it becomes more stably associated in prophase, while condensin I has a more dynamic association with mitotic chromosomes and binds to them during nuclear envelope breakdown (Ono et al., 2003). In budding yeast, ChIP-on-chip analysis showed that condensin is bound to genes encoding small nuclear RNA and ribosomal proteins and genes under the control of RNA polymerase III, including tRNAs, throughout the cell cycle, while it is enriched at centromeric regions in G2/M. Scc2-Scc4 contributes to condensin association with chromosomes (D'Ambrosio et al., 2008; Haeusler et al., 2008).

One main function of condensin in budding yeast is to control rDNA stability and to regulate rDNA condensation (Tsang et al., 2007). This in turn inhibits intrachromosomal HR at this locus by excluding Rad52 from the nucleolus, reducing the production of extrachromosomal rDNA circles (ERCs) and protecting the integrity of the rDNA array.

1.3 Structure of the Smc5/6 complex

Budding yeast Smc5/6 complex consists of the two Smc proteins, Smc5 and Smc6, and six additional non-Smc elements (Nse), Nse1, Nse2/Mms21, Nse3, Nse4/Qri2, Nse5 and Nse6/Kre29 (reviewed in (Potts, 2009)). In the fission yeast *Schizosaccharomyces pombe* Smc6 was first identified as Rad18 and Smc5 as Spr18 (Fousteri and Lehmann, 2000; Lehmann et al., 1995), and they were shown to physically interact with Rad60 (Boddy et al., 2003), whose budding yeast homologue, Esc2, is genetically and functionally

connected to Smc5/6, but no physical interaction has been reported in this organism (Sollier et al., 2009). Six of the human orthologs genes (SMC5, SMC6, NSE1, NSE2/MMS21, NSE3/MAGE1 and NSE4) were identified. All subunits of Smc5/6 are required for cell viability in *S. cerevisiae* (Zhao and Blobel, 2005), and all but Nse5 and Nse6 are essential in *S. pombe* (Pebernard et al., 2006). Smc5 and Nse2-deficient chicken DT40 cells are viable (Kliszczak et al., 2012; Stephan et al., 2011) and RNAi depletion of Smc5/6 proteins in human tissue culture cells only shows a moderate cell cycle delay (Behlke-Steinert et al., 2009), but knock-out of SMC6 in mouse has been reported to be early embryonic lethal (Ju et al., 2013), suggesting that the complex have essential functions also in vertebrate cells.

Table 1.1 reports all the orthologs of Smc5/6 complex so far identified in model organisms.

S. cerevisiae	***S. pombe***	***C. elegans***	***D. melanogaster***	***X. laevis***	***H. sapiens***
Smc5	Smc5/Spr18	SMC-5	SMC5	SMC5	SMC5
Smc6/Rhc18	Smc6/ Rad18	SMC-6	SMC6/ CG5524	SMC6	SMC6
Nse1	Nse1	-	CG11329	NSE1	NSE1
Nse2/Mms21	Nse2	-	CG13732, CG15645	NSE2	NSE2
Nse3	Nse3	-	Mage	-	MAGEG1
Nse4/Qri2	Nse4/Rad62	-	CG13142	-	NSE4A, NSE4B (EID3)
Nse5	Nse5	-	-	-	-
Nse6/Kre29	Nse6	-	-	-	-

Table 1.1 Smc5/6 orthologs in different model organisms.

Smc5 and Smc6 have the typical structural features of SMC proteins described above. Biochemical studies (Roy and D'Amours, 2011; Roy et al., 2011) showed that both are able to bind dsDNA, but have a clear preference of binding to ssDNA substrates at physiological concentration of salts. These *in vitro* data suggest that Smc5/6 might

directly associate *in vivo* with single stranded DNA intermediates that are originated during DNA replication, repair and recombination. The minimal size of ssDNA required for binding is 40 to 50 nt, much smaller than the size of ssDNA regions detected at replication forks and at sites of DNA damage, suggesting that the formation of ssDNA during these processes can accommodate the binding of several Smc5/6 complexes at each site.

Nse1 contains a RING domain that is usually found in E3 ubiquitin ligases, but however it does not display a ubiquitin ligase activity *in vitro* (Pebernard et al., 2008a). It was proposed that the RING domain could act as a structural element to form a trimeric subcomplex between Nse1-Nse3-Nse4, which associates with the globular heads of Smc5 and Smc6 in fission yeast (Palecek et al., 2006), but only with the one of Smc5 in budding yeast (Duan et al., 2009b).

Mms21 interacts with the coiled-coil of Smc5 via its N-terminal domain, which forms a helical bundle with the arm of Smc5 (Duan et al., 2009a). Mms21 contains in its C-terminal region a modified RING domain called SP-RING (SIZ/PIAS-RING) which is associated with E3 SUMO (small-ubiquitin like modifier) ligase activity both *in vitro* and *in vivo* (Andrews et al., 2005; Potts and Yu, 2005; Zhao and Blobel, 2005). Like Ubiquitin, SUMO (in yeast Smt3, in mammals SUMO-1,-2,-3) is covalently attached to lysine residues on target proteins by a multi-step ATP-dependent enzymatic cascade involving E1 activating, E2 conjugating and E3 ligase enzymes. Although sumoylation affects several substrates, its pathway involves a single E1 (yeast Uba2/Aos1, human SAE1/SAE2) a single E2 (Ubc9) and few ligases. In budding yeast four ligases are known, that are Siz1, Siz2, Mms21 and Zip3, while in human more than ten have been uncovered. SUMO can be conjugated as a monomer or can form poly-SUMO chains. SUMO conjugation is reversible, since hydrolases called SUMO proteases SENPs or ULPs, can remove the modifications from the substrates. Sumoylation has several

functions in the cell and various nuclear pathways, including DNA repair, damage tolerance mechanisms and checkpoint responses are likely to be modulated by these modifications (reviewd in (Bergink and Jentsch, 2009)). Mms21 was shown to catalyze the sumoylation of different targets in various organisms. The list of Mms21 SUMO substrates includes budding yeast Smc5, Ku70 (Zhao and Blobel, 2005), Scc1, Smc1, Smc3 (Almedawar et al., 2012; McAleenan et al., 2012) and the kinetocore proteins Ndc10 and Bir1 (Yong-Gonzales et al., 2012), fission yeast Smc6, Nse3 and Nse4 (Andrews et al., 2005; Pebernard et al., 2008a), and human Smc6, Rap1, SA2, Scc1, Tin2, Trax, Trf1 and Trf2 (Potts et al., 2006; Potts and Yu, 2005, 2007). In addition, *in vitro* and *in vivo* assays show that yeast and human Mms21 can sumoylate itself (Andrews et al., 2005; Potts and Yu, 2005; Zhao and Blobel, 2005). Despite the fact that Mms21 is essential for cell viability, its SUMO ligase activity is not, since in *S. cerevisiae mms21-11,* which encodes a truncated protein that lacks the SUMO ligase domain at the C-terminus, and *mms21-CH,* which encodes an inactive SUMO ligase domain caused by alanine substitutions at the conserved Cys200 and His202 of the SP-RING domain, are compatible with life (Branzei et al., 2006; Zhao and Blobel, 2005). The SUMO ligase activity of Mms21 is however important for efficient DNA damage tolerance and repair (Branzei et al., 2006), as it will be discussed later. Mms21 function in sumoylation is redundant with the other SUMO ligases and double mutants *mms21-11 siz1Δ* and *mms21-11 siz2Δ* are very sick, suggesting an important role of sumoylation for normal growth.

Nse3 is a melanoma-associated antigen gene (MAGE)-like protein (Sergeant et al., 2005). The functions of MAGE family members are not well understood, but they seem to be involved in gene expression, cell-cycle regulation and apoptosis, and they are also specifically expressed in particular cancers (reviewed in (Feng et al., 2011)). Furthermore

they have the ability to bind and enhance the ubiquitin ligase activity of E3 enzymes (Doyle et al., 2010).

Nse4 is the kleisin subunit with helix-turn-helix and winged-helix folds similar to other members of SMC family, such as Scc1, CAP-H and CAP-H2 (Palecek et al., 2006). In human cells the homolog is Nse4a, but it is present also a germ-cell specific isoform, expressed only in testis, called Nse4b/EID3, which is 50% identical to Nse4a (Bavner et al., 2005; Taylor et al., 2008).

Nse5 and Nse6 associate as a dimer near the globular heads of the fission yeast complex (Pebernard et al., 2006), but interact with the hinge domain in budding yeast (Duan et al., 2009b). They have been so far identified only in yeasts and they do not show sequence homology, but they are considered functional homologs just on the observation that they are stable subunits of the complex, their mutations lead to similar phenotypes in both yeasts and the two Nse6 proteins contain similar folding motifs.

A schematic representation of Smc5/6 complexes in budding and fission yeasts is reported in Figure 1.2.

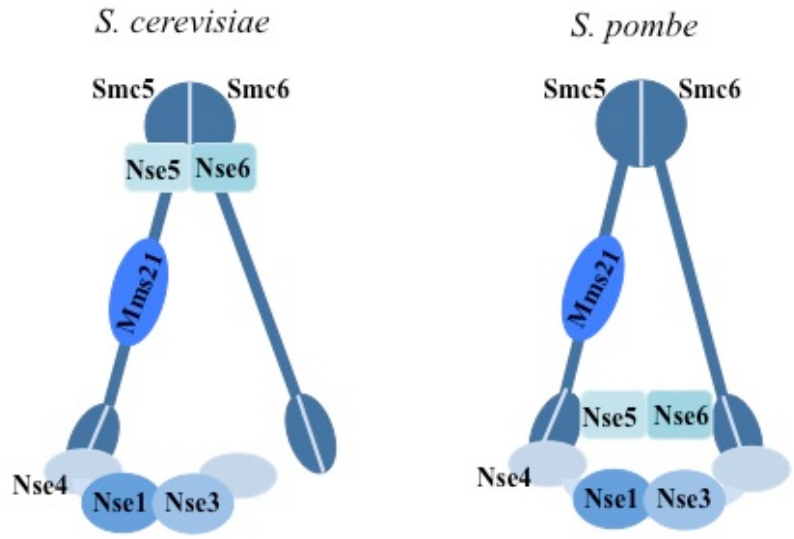

Figure 1.2 Schematic representation of Smc5/6 complex in budding and fission yeasts.

The Smc5/6 complex, differently from cohesin and condensin, does not still have an official name, since its essential functions in chromosome metabolism have yet to be uncovered. However, several lines of work describe its clusters on chromosomes in various phases of the cell cycle and different mutant backgrounds, its role in homologous recombination and DNA damage tolerance, its functions at repetitive DNA elements (CENs, ribosomal DNA array, telomeres). All these findings will be discussed separately in the following sections, making, when possible, a comparison between Smc5/6 in yeasts and higher eukaryotes.

1.4 Chromosomal clusters of Smc5/6

The Smc5/6 complex associates with chromatin in budding and fission yeast and the detailed analysis of the genome-wide localization of the complex was achieved using ChIP-on-chip.

The group of Camilla Sjogren carefully analyzed the ChIP-on-chip profile of Smc6 in each stage of the cell cycle (Jeppsson et al., 2014a; Lindroos et al., 2006). There is almost no association of Smc6 to chromosomes in telophase and in G1. In S phase arrested cells, after HU treatment, Smc6 binds to early origins of replication, suggesting that the complex localizes to chromosome during replication or it is recruited to stalled replication forks. This association to early ARS regions in HU was further confirmed by other studies (Bustard et al., 2012). The most prominent binding of Smc6 is manifested in the G2/M phase of the cell cycle after Nocodazole arrest or following Cdc20 depletion. In G2/M Smc6 binds prominently to centromeric regions of all chromosomes and between convergently transcribed genes, resembling the chromosomal localization of cohesin. However, differently from cohesin, the number of Smc6 clusters increases with the length of the chromosomes, being higher in frequency in longer chromosomes. Smc5/6 chromosome association depends partially on the cohesin loader complex Scc2/4, since in

the temperature sensitive mutant *scc2-4* the overall fold enrichment of Smc6 was reduced by 40.2% compared to wt, with the centromeric localization almost abolished. However, the strong binding in the region downstream the rDNA array on chromosome XII was unaffected, suggesting that it is independent of Scc2/4. By using high-resolution ChIP-sequencing and quantitative ChIP-qPCR it was shown that the levels of Smc6 found on chromosomes were markedly reduced in a mutant of the cohesin kleisin subunit, *scc1-73*, after an S phase at restrictive temperature. Some binding was retained at core centromeres, but all other specific binding sites were abolished. Smc6 recruitment to chromatin not only requires a functional cohesin complex, but is dependent on sister chromatid cohesion. Indeed the binding was prevented in several mutants defective in cohesion, like *pds5-101* and *eco1-1*. The deletion of *WPL1* (*RAD61*) in *eco1-1* restores cohesion and the binding of Smc6. If cohesin and cohesion controls Smc5/6 recruitment, the reverse is not true.

In fission yeast, the chromosomal localization of the complex was addressed by ChIP-on-chip of Nse4 (Pebernard et al., 2008b). Smc5/6 transiently localizes at centromeres when they are replicated in early S phase following HU treatment through a mechanism that is dependent on heterochromatin establishment. Indeed the binding of Nse4 to the outer repeats (*otr*) of the centromere is abolished in the absence of the H3K4 methyltransferase Clr4. As in budding yeast, Smc5/6 is enriched at rDNA loci, suggesting that it has similar functions at these repetitive regions. Furthermore, Smc5/6 loads at tRNA genes across the genome in a TFIIIC and transcription dependent manner and this binding appears to be cell cycle and DNA damage independent. This enrichment at tRNA genes has not been so far reported for budding yeast.

1.5 Smc5/6 and chromosome topology

Several evidences suggest a relation between SMC complexes and DNA topology. Recently, a higher frequency of Smc5/6 binding clusters were detected by ChIP-on-chip on longer chromosomes compared to shorter ones (Jeppsson et al., 2014a; Kegel et al., 2011), implying a possible function of the complex related to chromosome length that could be the sensing of replication-induced topological stress that accumulates during replication. This stress is originated during unperturbed replication by the separation of the two parental strands and the passage of the fork, which causes the DNA ahead of replication fork to become overwound or positively supercoiled. These supercoils have to be removed in order to allow replication fork progression. One way to do so is enzymatically achieved by topoisomerases. Type I topoisomerases (Top1 and Top3 in *S. cerevisiae*) creates a single-strand nick in the DNA to relieve superhelical tension, while type II enzymes (Top2 in *S. cerevisiae*) generate a transient DSB to transfer one DNA double helix through another. Another way to prevent the accumulation of positive supercoil is to allow the replication fork to advance in a rotating manner, following the turn of the DNA helix and leading to the formation of sister chromatid intertwinings (SCIs) or precatenanes behind.

To examine if Smc5/6 binding is a reflection of higher topological tension on longer chromosomes, the authors of the above-mentioned studies performed the following experiments (Jeppsson et al., 2014a; Kegel et al., 2011). They analyzed Smc6 association after Top1 and Top2 depletion. Camptothecin (CPT) inhibits Top1 and did not significantly altered Smc6 binding pattern, while a marked increased by 92% of overall Smc6 binding sites was detected in *top2-4* mutant. Recently it was shown that Smc6 binding around centromeres in *top2-4* was not significantly changed as compared to wt cells, but a strong enrichment was observed along chromosome arms. This increase in chromosome bound Smc6 in *top2-4* cells still requires cohesion, since it is markedly

reduced in the double mutant *top2-4 scc1-73*. Since in *top2-4* replication is unperturbed but the number of SCIs is increased, Smc5/6 association to chromatin could be trigged by SCIs. To verify this, the authors artificially shortened Chr IV, dividing it in two pieces, and the frequency of Smc6 binding sites decreased to the level seen on natural chromosomes of the same size. They also created a circular version of Chr III in which the number of SCIs is expected to increase and Smc6 bound much more on this artificial chromosome compared to the linear wt one as addressed by ChIP-sequencing. The above-mentioned changes in Smc6 distribution in *top2-4* cells and after chromosome shortening or circularization suggest that Smc6 loading is triggered by SCIs. To further verify this, it was demonstrated that the accumulation of Smc6 in *top2-4* requires that the mutant passes through S phase under restrictive conditions, in which SCIs are formed and not resolved, while after inactivation of Top2 in G1 or in G2/M the levels of Smc6 remain unchanged. Moreover, Smc6 dissociates from chromosomes when Top2 function is restored after replication, a condition in which Top2 resolves SCIs. In addition, this feature appears to be specific for Smc5/6, since nor Smc1 and Smc2, subunits of cohesin and condensin respectively, neither the Scc2 loader showed this chromosome length-dependent pattern.

Moreover, the number of catenations between replicated plasmids was lower in a *top2-4 smc6-56* double mutant compared to *top2-4* single, suggesting that defective Smc6 is not able to transfer supercoils to SCIs in a plasmid assay. Finally the authors also proved that *smc5-6* mutants display a late replication delay that specifically affects longer chromosomes, and this phenotype was shared by mutants lacking type I topoisomerases, Top1 and Top3. Deletion of *TOP1* and *TOP3* significantly delays replication of chromosomes that are equal or longer than Chr XIII (~924 kb), while *smc6-56* mutation inhibits replication of chromosomes equal or longer than Chr X (~746 kb).

Type I topoisomerases are required for timely completion of replication of long, but not short, chromosomes, indicating that superhelical tension increases with length. The current model proposes that Smc5/6 complex accumulates on chromosomes that have high levels of SCIs in order to sequester them behind the replication fork, allowing fork rotation and the removal of superhelical tension. In *smc5-6* mutants rotation is inhibited and this leads to an accumulation of supercoils ahead of the replication machinery, responsible for the delay in completing replication of long chromosomes, which are expected to have more SCIs.

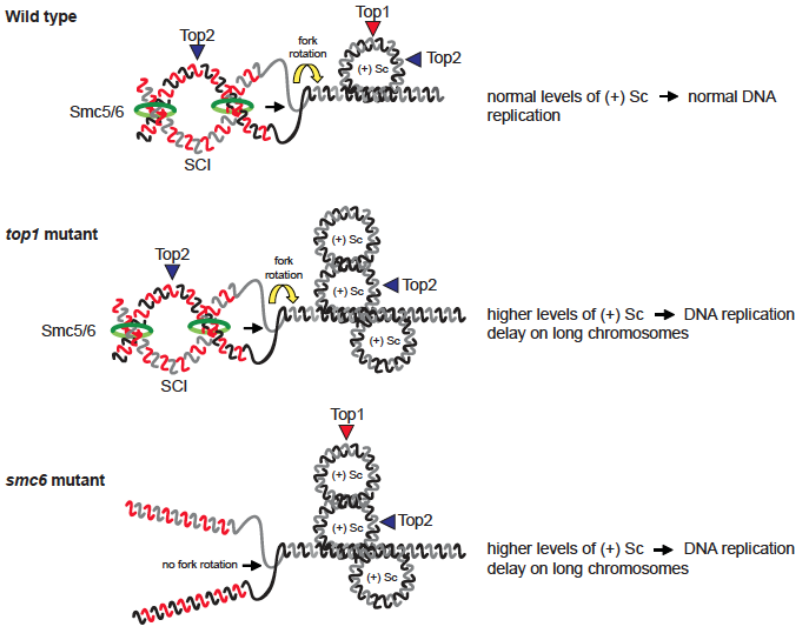

Figure 1.3 Model describing the function of Smc5/6 in releasing topological stress at the replication fork. Adapted from (Kegel et al., 2011).

1.6 Roles of Smc5/6 in DNA damage response and repair

In budding yeast all the eight subunits of the Smc5/6 complex are essential for proliferation and needed for DNA repair. Conditional mutants in Smc5/6 genes have been used to analyze the repair functions of the complex and they all share hyper-sensitivity to a wide range of DNA damaging agents, such as UV, ionizing radiation (IR), methyl metansulfonate (MMS), hydroxyurea (HU), mitomycin C (MMC) and camptothecin

(CPT) (Onoda et al., 2004). These phenotypes are conserved in all organisms so far analyzed. Indeed replication stress and DNA damage sensitivities were found in DT40 *Smc5*$^{-}$ and *Nse2*$^{-/-/-}$ cells (Kliszczak et al., 2012; Stephan et al., 2011), in MMS21 RNAi depleted HeLa cells (Potts and Yu, 2005), in *Smc5*, *Smc6* and *MAGE* mutants in *Drosophila melanogaster* (Li et al., 2013) and in *smc-5* and *smc-6* mutants of *C. elegans* (Wolters et al., 2014). These data suggest conserved functions of Smc5/6 complex and its Mms21 SUMO ligase activity in several DNA damage tolerance and repair processes throughout the eukaryotic kingdom.

It is clear in budding and fission yeast that the sensitivity of *smc5-6* mutants to DNA damage is not due to an inability to activate the checkpoints, since they show wt kinetics and intensity of the checkpoint response after UV, MMS, HU and DSBs (Torres-Rosell et al., 2007a; Harvey et al., 2004). This could suggest that Smc5/6 is a real repair factor with little effect on the damage checkpoint.

1.6.1 Smc5/6, DSBs repair and HR

Epistasis analyses placed the Smc5/6 complex in the homologous recombinational pathway of repair. In fission yeast, *nse2* mutants in which *rhp51* is mutated are sensitive to IR as the single mutant *rhp51* (Andrews et al., 2005); in budding yeast *smc6-56 rad52* show a sensitivity to MMS similar to the *rad52* single mutant(Onoda et al., 2004); in DT40 *Smc5*$^{-}$ cells are sensitive to IR as the double *Smc5*$^{-}$ *Rad54*$^{-/-}$ (Stephan et al., 2011). All these similar epistasis observations suggest an evolutionary conserved function of Smc5/6 in HR. Since while complete absence of HR in yeast is not lethal, but loss of Smc5/6 is, and the concomitant loss of both does not rescue the lethality associated with Smc5/6 gene deletion, the complex must have additional HR independent and essential functions.

DSBs are one of the most threatening alterations of a cell's genetic material and there are two main mechanisms involved in their repair: non-homologous end-joining (NHEJ) and

homologous recombination (HR) (reviewed in (Branzei and Foiani, 2008)). The first one entails the direct rejoining of the broken ends of DNA, is mainly active in G1 but can operate throughout the cell cycle, while the second one involves the search of similar sequences that can be used as a template for repair and is mainly operating in S and G2, when the sister chromatids are present. Following DSB induction, the broken ends of DNA remain associated and checkpoint, repair and structural proteins are required for the DNA damage response. Briefly, DSB is sensed by the heterotrimer Mre11-Rad50-Xrs2 (MRX) in yeast (MRN in human cells), which binds to the broken ends. The nucleases Mre11 and Sae2 initiate the nucleolytic process known as 5'-3' resection and the formation of single-stranded DNA is continued by Exo1, Sgs1 and Dna2. The resected DNA is then coated by the single-stranded DNA binding protein RPA and the recombinase Rad51 is loaded in a step mediated by Rad52. Rad51 forms a presynaptic nucleoprotein filament on the ssDNA that searches for homology and can subsequently pair with the undamaged homologous duplex. DNA strand exchange between the target DNA and the Rad51 filament leads to the formation of the displacement loop (D-loop), which contains the novel heteroduplex DNA and the displaced strand of the donor DNA. This structure facilitates repair using the intact homologous sequence as the template strand and invading ssDNA as a primer for DNA repair synthesis. In mitotic cells, HR proceeds through two recombination pathways which result in non-crossover (NCO) formation, one is the synthesis-dependent strand-annealing (SDSA), the other one, less frequent, leads to the generation of four-stranded DNA intermediates known as double Holliday Junctions (HJs). The STR complex, composed of the RecQ helicase Sgs1, which unwinds DNA in the 3' to 5' direction, the type I topoisomerase Top3 and Rmi1, promotes branch migration of the double HJs to form a hemicatenane which is then dissociated by Top3 action. This process yields NCO products and is known as HJ dissolution.

Cohesin is also recruited to DSBs where it holds sister chromatids together allowing efficient repair (Strom et al., 2007; Unal et al., 2007). ChIP studies in budding yeast (De Piccoli et al., 2006; Lindroos et al., 2006) and in human cells (Potts and Yu, 2005) revealed that Smc5/6 complex is also recruited to HO- and I-SceI-induced DSBs respectively, binding to a region that spans at least 25 kb on each side. In budding yeast, Smc5/6 loading to DSBs depends on Mre11, but does not depend on Mec1 and Rad53, differently form cohesin (Lindroos et al., 2006). In addition, also the BRCT domain-containing protein Rtt107/Esc4, which physically interacts with Nse6, is required for the recruitment of the complex to DSBs (Leung et al., 2011). The function of Smc5/6, like that of cohesin, is to promote sister chromatid recombination at DSBs.

In *S. cerevisiae* the chromosomal association of Scc1 is unaltered after the destruction of *smc6-56* function in G2/M arrested cells, but this mutant is defective in damage-induced genome-wide cohesion, by mean of the higher percentage of cells with separated sisters compared to wt (Strom et al., 2007). Two recent studies in budding yeast revealed Mms21-dependent sumoylation of Scc1. In one study (McAleenan et al., 2012), Scc1 was shown to be sumoylated following DNA damage. Scc1 SUMO defective alleles are able to go to DSBs but are defective in tethering sister chromatids and consequently in establishing damage-induced cohesion both at DSBs and undamaged chromosomes. In addition, the second study (Almedawar et al., 2012) showed that Scc1 sumoylation occurs when cohesion is established and the lack of sumoylation, by fusing a SUMO peptidase domain to Scc1, is lethal due to cohesion defects.

In human cells it was shown that the depletion of SMC5 and NSE2 abolishes the recruitment of cohesin to DNA breaks (Potts et al., 2006), but a more recent study shows that Smc5/6 was dispensable for cohesin loading at DNA damage sites (Wu et al., 2012). In addition, Nse2 sumoylates multiple lysines of the cohesin subunit Scc1 promoting sister chromatid recombination (SCR); cells expressing nonsumoylatable Scc1 mutant

(15KR) maintain sister chromatid cohesion during mitosis, but are defective in SCR and sensitive to IR. Deletion of Wapl rescues the defects in SCR of Mms21-deficient or Scc1K15R-expressing cells, suggesting that Scc1 sumoylation promotes recombination by counteracting Wapl-mediated regulation of cohesion (Wu et al., 2012).

1.6.2 Functional connections between Smc5/6, cohesion and chromosome segregation

Besides the above connection between Smc5/6 and cohesin in DSB repair and damage-induced cohesion, other studies underlined functional interplay between cohesin and Smc5/6 complexes, both in yeast and human cells.

In fission yeast, hypomorphic alleles of Smc5/6 cause lethality in mitosis, where sister chromatids separation fails leading to the cut phenotype, in which the division septum lethally bisects the unsegregated or incompletely resolved chromosomes (Fousteri and Lehmann, 2000; Harvey et al., 2004). The same phenotype was observed when these mutants were exposed to DNA damage or replication stress. The *smc6-74* allele is synthetically lethal with a loss-of-function allele of the topoisomerase II gene *top2*, *top2-191*, and again these cells die at the semi-permissive temperature of 30°C in mitosis. These aberrant mitoses were associated with a failure to strip cohesin from chromosome arms. In these mutants it was observed by ChIP a postanaphase retention of cohesin, which can lead to lethal attempts at chromosome segregation. Overexpression of the protease separase, Cut1 in *S. pombe*, which cleaves the kleisin subunit of cohesin, removes the complex from chromosome arms and suppresses the mitotic defects (Outwin et al., 2009). Moreover, loss of the histone variant H2A.Z, by deleting the *pht1* gene, lowers cohesion levels by up to 50% and this also suppresses mitotic defects in *smc6* mutants (Tapia-Alveal et al., 2014). Furthermore, both the overexpression of Cut1 and the deletion of *pht1* suppress the DNA damage and replication stress sensitivity of *smc6* mutants, indicating that there could be a link between sensitivity, cohesion retention and

mitotic defects. Thus, Smc5/6 might affect chromosome structure, allowing proper removal of cohesin from chromosome arms before segregation and cell division.

In line with what was reported in yeast, a recent study (Gallego-Paez et al., 2014) in human cells depleted for SMC5 or SMC6 show aberrant mitotic chromosome structures. SMC5- and SMC6- depleted cells present abnormal "curly" chromosome conformation, in a 25% of cases associated with a cohesion defect. These cells also display anaphase bridges and lagging chromosomes, suggesting chromosome loss and/or breakage during cell division. Moreover, these aberrant mitoses are accompanied by abnormal distribution of condensin and topoisomerase IIα. Another study in HeLa cells (Behlke-Steinert et al., 2009) showed that RNAi ablation of SMC5 or MMS21 causes a severe delay in mitotic progression, with a high percentage of cells that accumulate in G2/M. SMC5 or MMS21 depleted cells display premature sister chromatid separation and clustering of chromatids around spindle poles before the onset of anaphase. The consequent loss of tension at the prematurely separated centromeres likely triggers the mitotic arrest.

1.6.3 DNA damage tolerance pathways

Besides being the major player of DSB repair, HR is also needed in promoting restart of a blocked replication fork (RF). Bulky DNA lesions or replication fork barriers (RFBs) can impede the progression of RFs leading to transient stalling. If prolonged, dissociation of the replisome can lead to fork collapse and formation of DSBs. HR was also involved in gap-filling and fork restart associated with replication of UV- and MMS-damaged templates (Branzei and Foiani, 2010).

DNA Damage Tolerance (DDT) also requires the *RAD6-RAD18* epistasis group, called Post Replication Repair (PRR), in both yeast and mammalian cells. PRR controls two distinct branches of damage bypass. One pathway involves DNA synthesis across the damaged template by translesion synthesis (TLS) polymerases, which are often mutagenic, and therefore this mode is considered error-prone. The second pathway

involves a recombination-like invasion mechanism, called template switching, in which the blocked nascent strand uses the undamaged sister chromatid as a temporary replication template leading to the transient formation of X-shaped intermediates involving sister chromatid junctions (SCJs) (Branzei, 2011; Branzei and Foiani, 2010).

A central player in PRR is the homotrimeric ring sliding clamp PCNA and its post-translational modifications by ubiquitin and SUMO. Following DNA damage, PCNA is mono- or polyubiquitylated at the highly conserved lysine K164 (Hoege et al., 2002). Monoubiquitylation depends on the Rad6 E2 ubiquitin-conjugating enzyme and the Rad18 E3 RING-finger ubiquitin-ligase (Hoege et al., 2002) and it promotes translesion synthesis, possibly through direct recruitment of TLS polymerases that possess ubiquitin-binding motifs (Stelter and Ulrich, 2003; Kannouche et al., 2004). K63-linked polyubiquitylation of monoubiquitylated PCNA by the E2 conjugating dimer Mms2-Ubc13 and the E3 RING-finger ligase Rad5 (Hoege et al., 2002) promotes instead the error-free branch of template switching with SCJ formation (Branzei et al., 2008).

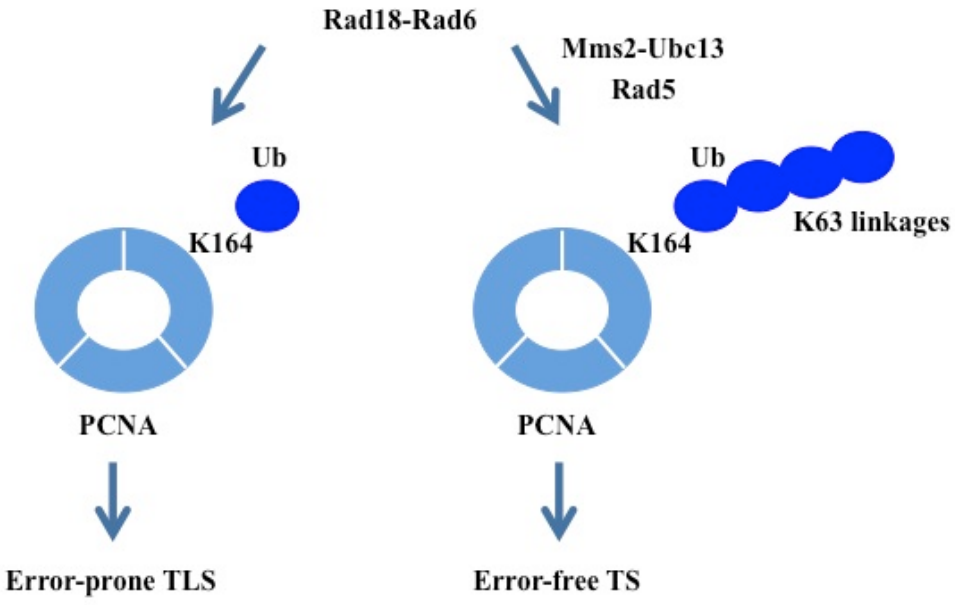

Figure 1.4 DNA damage tolerance pathways.

Besides being ubiquitylated, PCNA can also be sumoylated at two lysines residue, K164 and K127 (Hoege et al., 2002). Sumoylation plays a key role in regulating the metabolism of the SCJs accumulating under MMS conditions. Mutants in the E2 SUMO conjugating enzyme Ubc9, or mutations affecting PCNA sumoylation cause accumulation of cruciform structures in a process that is Rad51-dependent, but Rad5- and PCNA polyubiquitylation-independent (Branzei et al., 2006; Branzei et al., 2008). Thus, in the absence of PCNA sumoylation the error-free PRR pathway is impaired in promoting the formation of Rad5- and PCNA polyubiquitylation-dependent damage-induced SCJs, indicating that SUMO-PCNA, via a yet undefined mechanism, enables the utilization of factors belonging to the previous mentioned error-free PRR (Branzei et al., 2008). Both HR and PRR were shown to be required for gap-filling and SCJ formation following genotoxic stress.

Damage-induced template switch intermediates are potentially recombinogenic and need to be resolved to restore a normal chromosomal structure and ensure chromosome segregation. Sgs1 and Top3 are the major activities involved in template switching intermediate resolution (Liberi et al., 2005; Branzei et al., 2008). Furthermore, *mms21* mutants defective in the SUMO ligase activity, such as *mms21-SP* and *mms21-CH*, are sensitive to damaging agents and are characterized by the accumulation of recombination dependent X molecules during MMS treatment, in a manner reminiscent of *sgs1* mutants (Branzei et al., 2006). In contrast, the other two SUMO ligases of *S. cerevisiae*, Siz1 and Siz2 are not required to counteract the accumulation of SCJs (Branzei et al., 2006). These data altogether suggest an important role of Ubc9- and Mms21-dependent sumoylation in counteracting the accumulation of recombinogenic structures and they might act in concert with Sgs1-Top3 complex. Moreover, Sgs1 is sumoylated in a Ubc9 dependent manner, meaning that or it is directly sumoylated by Ubc9, with which physically interacts, or by another ligase (Branzei et al., 2006). The other SUMO substrates involved

in template switch intermediate resolution are still not known, but they possibly include, among the others, the Smc5/6 complex itself, which is sumoylated by Mms21 and genetically interacts with Sgs1-Top3.

DDT was believed to act directly at the replication fork in S phase, but growing evidences in budding yeast suggest that it rather works in the rear of the forks. A recent study (Karras and Jentsch, 2010) used the Clb2 derived G2-tag, which restricts the expression of a given protein to G2/M and demonstrated that DDT can operate uncoupled from replication forks and is functional if restricted after S phase. TLS polymerases Rad30 and Rev3 were also able to support survival and mutagenesis in the presence of DNA damage if restricted to G2/M, suggesting that they could all act on lesions behind replication fork. The key factors of the error-free branch of PRR, like Sgs1, Rad5, Rad18 and Ubc13 were also restricted to G2/M and found to promote efficiently DNA damage tolerance, strongly indicating that the template switching pathway operates primarily behind moving of replication forks rather that directly at the fork. Finally, recent structural studies (Giannattasio et al., 2014) on the DNA structures mediating recombination-bypass provided evidence that template switching is primarily a gap-filling associated process, with DNA gaps initiating invasion in the homologous duplex and exposure of the newly synthesized strand rather than a replication-coupled process through fork reversal.

In another study (Daigaku et al., 2010), using conditional alleles of *RAD18*, the authors observed that ubiquitin-dependent DNA damage bypass can be effectively delayed until after the bulk of replication is completed, without deleterious effects on cell viability. They also found that, following UV treatment, PCNA remains associated or is reloaded to chromatin after DNA synthesis and this pool of PCNA is target for ubiquitylation in G2/M. These data suggest that, even though the ubiquitin-dependent PRR is normally

active during S phase, its function may be most needed in G2/M, providing a fully functional damage tolerance uncoupled from genome replication.

1.6.4 Smc5/6 functions in the error-free branch of DDT

Different labs provided evidences that besides SUMO defective alleles of Mms21, other mutants in the Smc5/6 complex accumulate SCJs during MMS-induced damage and that Smc5/6 plays a role in their resolution. These physical linkages can be dissolved upon reactivation of Smc6, suggesting that the complex has an active role in their removal (Bermudez-Lopez et al., 2010).

Similarly, *esc2Δ* cells are defective in the resolution of damage-induced X-molecules, phenotypically resembling *sgs1/top3*, *mms21/smc5-6* and *ubc9* mutants, suggesting that all these pathways work in parallel or jointly in their resolution (Sollier et al., 2009; Mankouri et al., 2009). Esc2 is a protein containing two SUMO-like domains, SUMO-binding motifs and different SUMO consensus sites. By two-hybrid analysis, it was shown that Esc2 physically interacts with Ubc9 and SUMO in *S. cerevisiae*, but no evidence yet could be gathered about its interaction with Smc5/6 and Sgs1. In budding and fission yeasts, *esc2* mutants (*rad60* in *S. pombe*) share several phenotypes and functional interactions with *smc6* mutants and genetic evidences suggest that they are both synthetic sick/lethal in combination with each other or with *sgs1* in MMS. The double mutants *smc6 esc2*, *smc6 sgs1* and *esc2 sgs1* are more sensitive to genotoxic stress than the single ones, suggesting that Smc5/6, Esc2 and Sgs1, have also, at least partly, independent functions both in undamaged conditions and in response to MMS.

Initially by 2-hybrid studies, the DNA helicase Mph1 was found to interact with Smc5/6, but it does not appear to be sumoylated (Chen et al., 2009). Mph1, a 3'-5' helicase with DNA dependent helicase activity, is the ortholog of the Fanconi Anemia M (FANCM) protein in mammals and it was shown to dissociate DNA D-loop structures made by Rad51 to limit crossovers during mitotic recombination (Prakash et al., 2009). Deletion of

MPH1 suppresses several defects of *smc5-6* mutants, whereas overexpression exacerbates these effects (Chen et al., 2009). In the absence of Mph1, *smc6Δ* and *mms21Δ* cells are viable, even if very slow growing, indicating that an important function of Smc5/6 is to regulate an Mph1 activity that is toxic during normal growth. Furthermore, the sensitivity to different DNA damaging agents (MMS, HU, UV) of *smc6* mutants is suppressed when Mph1 is deleted, as well as the accumulation of SCJs during MMS treatment. The SCJs are also suppressed by an allele of *MPH1* defective in the helicase activity. These data suggest that Mph1, through its helicase activity, is largely responsible for the accumulation of X-shaped recombination intermediates in *smc6* and *mms21* mutants (Chen et al., 2009; Chavez et al., 2011). Differently, the sensitivity to MMS of *sgs1* mutants and the accumulation of SCJs are not rescued by deleting *MPH1*, suggesting that different types of molecules are induced by replication in the presence of DNA damage and that they are differentially targeted by Sgs1 and Smc5/6 (Chen et al., 2009).

These genetic and 2D gel analyses suggested a role for Smc5/6 in Mph1 regulation and a very recent study (Xue et al., 2014) revealed a mechanism through which this can happen. By affinity pull-down it was confirmed that Mph1 interacts directly with Smc5/6, precisely with the coiled-coil arm of Smc5. *In vitro* experiments show that Smc5/6 inhibits replication fork regression and holliday junction migration activities of Mph1, without affecting its D-loop dissociation and helicase activities. This regulation of Mph1 is independent of DNA binding by Smc5 but stems directly from its physical interaction. Through the use of AFM (Atomic Force Microscope) and EM (Electron Microscopy) the authors were able to demonstrate that Mph1 specifically recognizes the junction point in a mobile replication fork and associates to it as multimeric complexes. The addition of Smc5 reduces the frequency of Mph1-replication forks complexes, indicating that Smc5 prevents Mph1-substrate engagement. Replication fork regression needs to be tightly

controlled and this study proposes a function for Smc5/6 in directly restraining Mph1 fork regression activity.

Besides *mph1* mutations, others were found to assuage *smc5-6* mutants phenotypes when deleted in yeast cells (Choi et al., 2010). Among these there are genes belonging to the Shu complex (*SHU1*, *SHU2*, *PSY3*, *CSM2*), comprising Rad51 paralogs and likely affecting an early recombination step, and mutations in the PRR pathway, such as mutations in the ubiquitin conjugating enzymes Mms2 and Ubc13 required for PCNA polyubiquitylation. Similarly to *mph1Δ*, *shu1Δ* and *mms2Δ* suppress the MMS sensitivity of *smc6* mutants and each individual mutation reduces the levels of X molecules accumulating in these cells, with double deletions conferring greater reduction, suggesting non-overlapping functions between these pathways. Thus, the Smc5/6 complex is required to prevent the accumulation of SCJs generated independently by Shu1- and Mms2-dependent processes, in addition to those generated by Mph1 activity. But differently from *mph1Δ*, nor *shu1Δ* neither *mms2Δ* can rescue the lethality of *smc6Δ* and *mms21Δ* cells.

1.6.5 Smc5/6 functions at stalled and collapsed replication forks

Besides its functions in template switching, an additional role of Smc5/6 during replication of damaged templates was proposed to be in the processing of collapsed replication fork following dissociation of the replisome. Replication stress agents such as HU cause fork stalling, which is a transient event that does not cause replisome dissociation, but occasionally, replicative polymerases and helicases might dissociate from the fork, thus causing it to collapse. Fork collapsing was observed in checkpoint mutants following HU treatment by 2D gel electrophoresis and electron microscopy, and in that context it was associated with formation of regressed forks and single-strand gaps (Lopes et al., 2001; Sogo et al., 2002) .

In budding yeast, Smc5/6 binds to early origins of replication during HU treatment (Bustard et al., 2012; Jeppsson et al., 2014a), suggesting the possibility that it is recruited to stalled replication forks, likely to stabilize and protect them. In a recent paper (Bustard et al., 2012), *mms21-11* and *nse5-ts1* mutants were shown to display replisome instability, since the recruitment of Pol1 and Pol2 to early ARS during HU treatment was dramatically reduced as addressed by ChIP-qPCR. These mutants accumulated Rad51-dependent X-shaped structures during prolonged fork stalling induced by HU, indicating that the forks either collapse or are restarted via HR. These data were interpreted as to suggest that following replication stress, the Smc5/6 complex prevents fork collapse and subsequent recombination mediated fork restart, and promotes the resolution of X shaped intermediates. Furthermore, this study uncouples Smc5 sumoylation from the complex' function at stalled forks. The study describes an *nse5-ts2* mutant defective in Smc5 sumoylation, but not sensitive to HU and not defective in replisome association to stalled forks. At present, the biological significance of Smc5 modification by SUMO remains elusive, it could be a bystander effect, just due to its interaction with Mms21 E3 ligase. However, since *mms21* SUMO mutants display severe defects following genotoxic stress, there are likely Mms21-dependent SUMO targets important for HU and MMS tolerance. Besides sumoylation, it can also be a general structural function of the complex to protect replication forks and prevent them from stalling and/or collapsing.

In fission yeast, a study showed that Smc5/6 association to chromatin is increased upon HU treatment (Irmisch et al., 2009). In *cds1* (*rad53*) cells treated with HU X-shaped replication intermediates remain stable and accumulate in the absence of a functional Smc5/6 complex, while they rapidly decay in $smc6^{+}$ cells. Since Rad52 focus formation is normal in *smc6* mutants, Smc5/6 may function to regulate aspects of HR-dependent DNA processing at a later step in HR, in response to fork collapse. In *smc6* single mutants such X-shaped intermediates were not detected by 2D gel following HU

treatment, but a significant proportion of cells exhibit *cut* phenotypes, due to morphologically aberrant mitosis, suggesting that intertwined DNA structures persist during mitosis and impede proper chromosome segregation.

The viability and the DNA damage hypersensitivity of *smc6-74* mutants can be rescued in fission yeast by overexpression of the BRCT domain-containing Brc1 protein, suggesting that in the absence of Smc5/6, accumulated HR intermediates can be processed and repaired through alternative mechanisms involving Brc1 (Sheedy et al., 2005). Brc1 suppression of *smc6-74* requires the Slx1/4 and Mus81/Eme1 nucleases, which can cleave different substrates, including nicked HJ, D-loops, 5' and 3' flaps. These genetic data suggest that in the absence of a functional Smc5/6 complex, DNA repair intermediates can be processed by alternative DNA damage tolerance pathways, which become essential for cell survival.

The Smc5/6 complex might process collapse replication forks directly or indirectly, since it could act structurally or it could regulate, through its enzymatic activities, factors that are required for the remodeling of collapsed forks and/or the restart of stalled ones. In accordance to this model, *smc5-6* mutants are lethal in *S. pombe* when combined with deletions of several DNA exonucleases, like *RAD2*, *SWI1*, *APN2* (Lee et al., 2007). Thus, replication intermediates that accumulate in the absence of Smc5/6 might depend on exonuclease activity for their resolution.

The above-described functions of Smc5/6 in replication fork restart, stabilization and damage-bypass by template switching are summirized in Figure 1.5.

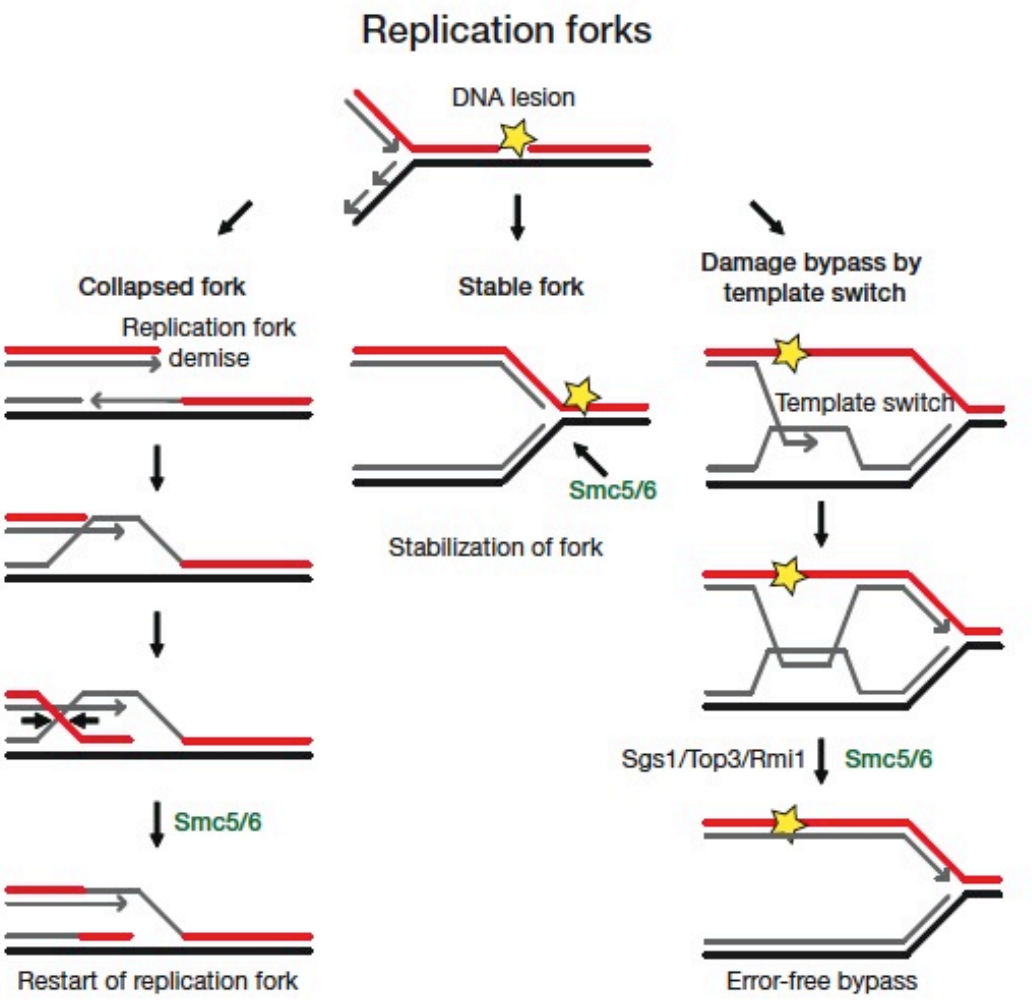

Figure 1.5 Schematic representaiton of Smc5/6 functions in replication fork restart, fork stabilization and error-free template switching. Adapted from (Kegel and Sjogren, 2010).

1.6.6 Smc5/6 suppresses gross chromosomal rearrangements

One of the most common genomic features of cancer cells is known as gross chromosomal rearrangements (GCR). Using genetic assays, *Saccharomyces cerevisiae* provides an easy way to quantitatively measure the rate at which GCRs accumulate in different genetic background. Rearrangements detected include broken chromosomes healed by de novo telomere addition and several forms of translocations, like monocentric, interstitial deletions and dicentric inter- and intrachromosomal fusions.

Several mutants of Smc5/6 complex, including *smc6-9* and *mms21-11*, were found to increase GCR rates compared to wt cells about 80 times (Hwang et al., 2008). *smc5-6* mutants enhance mainly translocations type GCR that are completely dependent on HR.

Specifically, these GCR are produced by Rad52-Rad51 dependent break-induced replication (BIR), indeed deletion of *RAD52* and *RAD51* lower by five folds the increased GCR rates in *smc6-9*. When a DSB occurs in the middle of a chromosome, it can be repaired by gene conversion, using homologous sequences on a sister chromatid or at an ectopic locus. But if only one end of a DSB shares homology with other sequences in the genome, cells utilizes BIR to restore genome integrity. BIR is a Rad52 dependent process in which a DSB is repaired by undergoing recombination-dependent DNA replication with the re-establishment of a unidirectional replication fork, which proceeds to the end of a template chromatid or until it meets a converging replication fork. Pol32, a non-essential subunit of polymerase ∂ dispensable for replication and gene conversion, is uniquely required for BIR.

Translocations that occur in Smc5/6 mutants are generated close to repetitive sequences including Ty elements, ARS and tRNA genes, indicating that these loci are highly instable in the absence of a functional complex and are more prone to break and to become substrates for GCR formation.

The loss of Sgs1 or Top3 increases sister chromatid exchanges rate and HR. The deletion of *SGS1* or *TOP3* synergistically increases the GCR rates in *smc6-9* background. Since both *smc5-6* and *sgs1-top3* mutants accumulate hemicatenane-like molecules after exposure to DNA damage, one possibility is that an increased level of such structures causes the observed increment in GCR rates seen in the double mutants.

1.6.7 Mms21-dependent sumoylation suppresses duplication-mediated genome rearrangements

The human genome contains several “at-risk” sequences that are prone to mutations including repeated sequences, segmental duplications and regions of copy number variations. These elements represent the major source of polymorphism between individuals, but also have been associated with development of cancer and genetically

complex phenotypes. Using genetic approaches, different pathways were found to prevent duplication-mediated genome rearrangements in *S. cerevisiae* (Putnam et al., 2009). One group of genes includes Sgs1-Top3-Rmi1 complex that suppresses HR between divergent sequences. Many genes that are synthetic sick with *sgs1Δ,* such as *RRM3, SRS2, MUS81, SLX4, SLX5, SLX8* also suppress duplication-mediated GCRs. Another group includes Mrc1 and Tof1, suggesting a critical function of the checkpoint in suppressing these deleterious events. Finally, post-replication repair pathway genes, *RAD6, RAD18, RAD5, MMS2, UBC13* act in concert with the replication stress checkpoint to suppress duplication-mediated GCRs formed by HR.

Recently (Albuquerque et al., 2013), it has been shown that the SUMO ligase activity of Mms21 suppresses GCRs mediated by single-copy sequences and has an even more important function in suppressing those mediated by segmental duplication. The deletion of *ESC2* causes a strong defect in suppressing GCRs too, and particularly the duplication-mediated ones, even if less than that caused by *mms21-11*. Few SUMO substrates of Mms21 have been identified so far, among them there are the RNA polymerase I subunit RPA135, the ribosomal protein Fob1 and the SMC proteins Smc1, Smc2, Smc3, Smc4 and Smc5. Notably, the deletion of *ESC2* has a similar effect on sumoylation with the *mms21-11* mutation. Esc2 was shown to interact with Ubc9 and Smt3 and its deletion specifically reduces the sumoylation of Mms21 targets, suggesting that Esc2 positively regulate Mms21 activity *in vivo*, possibly promoting the formation of an active complex between Ubc9 and Smc5/6-Mms21. Since the single deletion of the SUMO ligases *SIZ1* or *SIZ2* does not have appreciable defect in suppressing GCRs, an Mms21- and Esc2-specific sumoylation event plays critical role in preventing duplication-mediated GCR formation.

1.7 Smc5/6 roles at specific genomic locations

1.7.1 Smc5/6 and Centromeres

As mentioned in previous sections, Smc5/6 binds to centromeric regions in both budding and fission yeast, respectively in G2 and in S phase, by ChIP approaches, but the biological meaning of this enrichment remains unclear.

A recent study provides insights into the function of the complex at CEN regions in budding yeast (Yong-Gonzales et al., 2012). In *smc6-56* mutants there is an increased level of recombination intermediates at centromeric regions, detected by 2D gel analysis, and a 3.2 fold increase in the level of CEN-Rad52 foci, showed by live cell imaging, compared to wt cells. These two data indicate that Smc5/6 regulates recombination at centromeric DNA and surrounding regions, besides executing these functions at other loci in the genome. Mutants that are defective in centromere and kinetochore functions also show sensitivity to nocodazole, which is a microtubule and spindle destabilization drug. Moreover, *smc6-56* cells are very sensitive to nocodazole and *rad51Δ* suppresses this sensitivity. A SUMO deficient allele of *RAD52*, *rad52-snm* (*sumo-no-more*), reduces the levels of recombination foci at centromeres and the nocodazole sensitivity of *smc6-56* cells, even if it does not rescue the accumulation of X shaped molecules at centromeric regions, suggesting that *rad52-snm* affects recombination in a different manner than *rad51Δ* in *smc6* mutants.

Centromere sequences are unique in the genome since they are characterized by the binding of more than 60 kinetochore proteins, which assembly and dynamics are highly regulated by different post-translational modifications. The sumoylation of two kinetochore proteins, Ndc10 and Bir1, is strongly decreased in *mms21-11*, suggesting that Mms21 is the main SUMO ligase responsible for their modification. In addition, *mms21-11* negatively affects the spindle localization of Ndc10, in accordance with the fact that sumoylation is required for the proper localization of the protein.

1.7.2 Smc5/6 and rDNA

1.7.2.1 Smc5/6 is required for rDNA segregation

The ribosomal genes in budding yeast are organized into an array of 100-200 identical repeats located in the middle of the right arm of chromosome XII. One of the first evidence of a function of Smc5/6 at the rDNA locus came from a study in budding yeast, in which the authors detected abnormalities in the nucleolar structure in *mms21-11* cells. While in wt cells nucleoli are compact and form a half-moon shape visible in fluorescence microscopy, in *mms21-11* cells nucleoli are spread out and display irregular shape (Zhao and Blobel, 2005). Thus, a functional Smc5/6 complex is required for the proper organization of the ribosomal DNA cluster.

The group of Luis Aragon extensively analyzed the role of Smc5/6 at rDNA (Torres-Rosell et al., 2005; Torres-Rosell et al., 2007a; Torres-Rosell et al., 2007b). In the first study (Torres-Rosell et al., 2005) they observed co-localization between Smc6 and the nucleolar protein Net1 and confirmed by ChIP that Smc6 is enriched at the non-transcribed spacer 1 and 2 (NTS1 and NTS2) of rDNA. By mean of fluorescence microscopy they also observed that nucleolar integrity is compromised in *smc6-9* cells, which display significant rDNA fragmentation. To test if the segregation of the rDNA repeats was compromised in *smc6-9* mutants, several chromosomal tags were inserted at different position along the right arm of chromosome XII. While the tags inserted between the centromere and the rDNA array correctly segregate in *smc6-9* cells, more than half cells missegregate the tags between the rDNA and the telomere, suggesting that *smc6-9* have problems in the disjunction of the rDNA array. Furthermore, *smc6-9* and *smc5-6* cells accumulate X-shaped intermediates by 2D gel analysis at rDNA locus during nocodazole treatment, when cells are arrested in mitosis before anaphase entry. These data suggest that the rDNA segregation defects seen in *smc5-6* mutants are due to the persistence of linkages between sister chromatids at the rDNA locus.

Since condensin complex is involved in the segregation of rDNA array, it was investigated if there could be a common mechanism with Smc5/6. But, since *smc6-9 smc2-8* double mutants present increased thermosensitivity, increased missegregation of chromosomal tags of the rDNA and the localization of condensin at the rDNA is not altered in *smc6-9* cells, it was concluded that the two complexes function independently in modulating rDNA segregation.

1.7.2.2 Delayed replication of rDNA in *smc5-6* cells with normal mitotic entry and intact checkpoint responses

Another study (Torres-Rosell et al., 2007a) reported an increase in replication fork barrier (RFB) signal, recombination and termination structures in *smc6-9* cells during S phase compared to wt at the rDNA. This was apparently not due to increase in origin firing, since wt levels of bubble intermediates were found in the mutant. *smc6-9* cells also show an increase in Y-arc replication structures in nocodazole, meaning that these mutants are still replicating rDNA in metaphase, indicative of a replication delay specific of this locus. This replication delay was confirmed by DNA combing analysis that detected a two fold increase in unreplicated gaps in *smc6-9* cells relative to wt. Moreover, to analyze whether replication is complete before segregation in *smc6* mutants, the authors used Pulse Field Gel Electrophoresis (PFGE), in which incompletely replicated chromosomes do not resolve but remains stuck in the wells. In *smc6-9* cells the amount of chromosome XII containing rDNA that failed to enter the gel after replication and segregation was much greater than that in wt cells. These data suggest that *smc6-9* cells execute anaphase before they finish replication of the rDNA cluster, and this is the reason why they are not delayed in mitotic entry but they show non-disjunction phenotype. Importantly, this mitotic entry before the completion of rDNA replication is not caused by defects in any of all known cellular checkpoint responses, namely the S phase checkpoint, DNA damage

checkpoint and spindle checkpoint. DNA replication intermediates in the rDNA locus are not detected by checkpoints, even if they are fully competent in *smc5-6* mutants.

To decrease the frequency of replication fork collapse, the rDNA locus is replicated unidirectionally in order to reduce the probabilities of collisions between replication and transcriptional machineries. Each rDNA array contains a termination site, called replication fork barrier (RFB), at which the leftward-moving fork is arrested, while the rightward one is not affected, but proceeds until it converges with the leftward. If the polar barrier protein Fob1, which binds to the RFB and ensures unidirectional replication, or Pol1 rRNA gene transcription, which poses a challenge for active replication in the rDNA locus, are inactivated, the chromosome XII nondisjunction phenotype is significantly reduced in *smc6-9.* This means that the delay in rDNA replication in *smc6-9* cells is a consequence of the inability to promote stable fork progression through the rDNA array without a functional Smc5/6 complex due to obstacles such as tightly bound protein-DNA complexes and the high transcription rates. Since the rDNA is a particular genomic locus, which occupies 8 to 12% of the yeast genome, anaphase onset before completion of its replication, even if it is under normal checkpoint surveillance, can be detrimental for genome stability and consequently for proper chromosome segregation.

1.7.2.3 Smc5/6 regulates recombination at the rDNA locus in yeast and at heterochromatic regions in higher eukaryotes

It is known that after DSB generation by ionizing radiation or bleomycin, Rad52 relocalizes to distinct foci. Interestingly, no Rad52 foci form in the nucleolus, despite the role of Rad52 in rDNA recombination, indicating that DSBs in the rDNA locus are not repaired by HR inside the nucleolus. Despite this finding, the nucleolus is proficient in DSBs sensing and processing, since Mre11, Rfa1 and Ddc2 foci are regularly formed in this compartment, meaning that DSBs are recognized by the MRX complex, resected into single stranded DNA and bound by RPA and the checkpoint response is also activated

(Torres-Rosell et al., 2007b). The idea is that DSBs in the rDNA relocalize to an extranucleolar site for repair and thus Rad52 foci form outside the nucleolus.

In mutants of the Smc5/6 complex there is an increased number of spontaneous Rad52 foci in S phase compared to wt cells, primarly in the rDNA compartment. Moreover, the *smc6-9* mutation allows the formation of Rad52 foci inside the nucleolus after a I-SceI-induced DSB, suggesting that Smc5/6 somehow suppresses the formation of Rad52 foci in the rDNA locus. Disruption of Smc5/6 results in a hyperrecombination phenotype at the rDNA array and higher levels of ERCs, dependent on Rad52 and Fob1 activities. These data provide evidence that Smc5/6 excludes Rad52 from the nucleolus suppressing recombinational loss of rDNA repeats. Similarly to what happens in *smc5-6* mutants, a sumoylation-deficient Rad52 mutant, *rad52-K43,44,253R*, accumulate Rad52 foci inside the nucleolus, suggesting that, in addition to Smc5/6, Rad52 sumoylation is also required for efficient extranucleolar focus formation and thereby suppresses rDNA recombination. The additive defective phenotypes of the double mutant *smc6-9 rad52-K43,44,253R* suggest that Smc5/6 and Rad52 sumoylation independently regulate rDNA recombination, in line also with the fact that Rad52 is not sumoylated by Mms21 (Torres-Rosell et al., 2007b).

Recently, a similar mechanism has been described for heterochromatic regions in *Drosophila melanogaster* (Chiolo et al., 2011). Heterochromatin is a specialized domain enriched for highly repetitive sequences, which exacerbate the risk for genome rearrangements in the presence of DBSs, since recombination among repetitive sequences can lead to loss or duplication of genetic information. Heterochromatin in *S. pombe*, flies and mammals is characterized by enrichment of the histone modifications di- and tri-methylation of H3K9 and associated proteins, like HP1a. The authors found that DSBs formed inside heterochromatin are rapidly recognized by resection proteins and checkpoint kinases, but they display a dynamic behavior, since they relocalize to the

HP1a periphery or outside the domain, where Rad51 foci can form. Thus, the recognition and resection of heterochromatin DSBs are spatially and temporally separated from Rad51 foci assembly. Smc5/6 complex is recruited to heterochromatin by HP1a and is required to prevent formation of IR-induced Rad51 foci in this region. The depletion of Smc5/6, similarly to the depletion of HP1a, significantly increases Rad51 foci formation inside heterochromatin and results in the appearance of extended DNA filaments between nuclei that are rescued by blocking HR, suggesting that they arise from aberrant recombination events.

Thus, Smc5/6 plays an important role in preventing aberrant recombination and in ensuring stability of repetitive elements. Smc5/6 may play a structural role and/or may act by mediating sumoylation of relevant targets.

1.7.3 Smc5/6 and telomeres

1.7.3.1 Smc5/6 localizes to telomeres

In the study previously mentioned (Zhao and Blobel, 2005), they observed that the number of telomere foci was increased in *mms21-11* budding yeast cells, suggesting a defect in telomere clustering. While in wt cells there were 2-4 telomere foci, in *mms21-11* their number was increased up to more than 5 in 70% and more than 10 in 9% of cells. They also found that telomere length was modestly increased in the mutant. Moreover, *mms21-11* cells were characterized by an enhanced silencing of a *URA3* reporter gene that was placed in the telomeric region, since cells display a higher fitness compared to wt ones when plated on 5-FOA.

Smc6 co-localizes by fluorescence microscopy with the Rap1 telomeric marker and it is enriched by chromatin immunoprecipitation at telomere sequences. The segregation of telomeric tags was defective in *smc6-9* cells, suggesting that Smc5/6 is required for proper disjunction of telomeres. Furthermore, the deletion of *RIF1* and *RIF2*, which are

responsible of telomere lengthening, causes also an increased sensitivity to temperature of the *smc6-9* mutants, indicating that longer telomeres cause lethality in the absence of a functional Smc5/6 (Torres-Rosell et al., 2005).

In fission yeast, it was shown that Mms21 sumoylates Nse4 specifically during MMS and this modification promotes maximal subtelomeric localization/retention of Nse4 under these DNA damaging conditions. Similar to what happens in MMS, subtelomeric Nse4 foci were detected in HU treated *cds1Δ* cells, and, in addition, Nse4 was sumoylated in *cds1Δ* cells, but not in wt, following HU. The recruitment of Smc5/6 to damaged telomeres might be an important function of Mms21-dependent sumoylation in response to MMS and in checkpoint deficient cells treated with HU, suggesting that replication fork collapse could stimulate Smc5/6 localization to subtelomeric DNA repeats (Pebernard et al., 2008b).

1.7.3.2 Smc5/6 maintains telomere length in ALT cancer cells

Telomeres are repetitive DNA elements that are shortened after every cell division owing to the end-replication problem. Short telomeres result in cellular senescence. Telomerase is the enzyme responsible for synthesis of new telomeric repeats from an RNA template, and it is repressed in normal human somatic cells, while it is transcriptionally upregulated in cancer cells, in order to overcome their limited proliferative potential. But telomerase is not expressed in a subset of tumors, which rely on an alternative mechanism to lengthen telomeres, called alternative lengthening of telomeres (ALT). ALT uses HR between telomeric sequences in order to elongate telomeres, which are localized in promyelocytic leukemia (PML) bodies, called ALT-associated PML bodies (APBs), which are, as a result, the sites of telomere recombination that elongate telomeres allowing unlimited proliferative potential.

The first indication of a possible role of Smc5/6 in ALT was that the complex colocalizes with PML bodies in G2/M specifically in ALT and not in telomerase-positive cells.

Moreover, Smc5/6 localizes to APBs. Knockdown of MMS21, SMC5 or SMC6 resulted in about 75% reduction of telomere recombination, suggesting that the complex is required for telomere sister-chromatid exchange (T-SCE) in ALT cells. In the interfered cells the recruitment of telomeres to PML bodies is blocked, thus inhibiting the formation of APBs, which has been related to progressive telomeres shortening in ALT cells. In MMS21 RNAi cells, a SUMO-ligase-dead mutant of Mms21 is still recruited to PML bodies, but does not restore APB formation, indicating that sumoylation by Mms21 is important for this process. Indeed, MMS21 specifically sumoylates several subunits of the shelterin complex, including Trf1, Trf2 and Rap1, and this sumoylation is required for their recruitment to PML bodies and subsequent APB formation in ALT cells. Finally, knockdown of the Smc5/6 complex results in a progressive shortening of telomeres in these cells, leading to cellular senescence. This study (Potts and Yu, 2007) definitely shows an important role of Smc5/6 complex and its SUMO ligase activity in sumoylation of different shelterin subunits, APB formation and telomere maintenance in ALT cells.

1.7.3.3 Smc5/6 slows senescence in cells lacking telomerase

Budding yeast constitutively expresses telomerase, but the deletion of *TLC1*, which encodes the telomerase RNA template, causes telomere loss leading to senescence. HR slows senescence and enables the emergence of rare telomerase-independent survivors, which indeed maintain their telomere using HR, similarly to what has been reported for ALT human cells. Interestingly, sumoylation was found to slow senescence, since *tlc1Δ uba2-ts10* (Uba2 is a component of the E1 SUMO activating enzyme) senesced faster than the *tlc1Δ* single mutants. Moreover upon loss of telomerase, only the sumoylation defective allele of *MMS21, mms21-sp*, and not *siz1Δ* or *siz2Δ* cells, recapitulated the rapid senescence phenotype of *uba2-ts10* cells. Mms21 is an E3 SUMO ligase required to modulate the rate of senescence likely through targets that remained to be determined. Importantly, *tlc1Δ mms21-sp* cells not only age faster, but, when are near senescent,

accumulate more X-shaped molecules at telomere ends compared to single *tlc1Δ* cells. The same phenotype of faster senescence and X-shaped intermediates accumulation was found in *tlc1Δ smc5-6* and *tlc1Δ smc6-9*. Thus, Smc5/6 complex counteracts the accumulation of telomere recombination intermediate during senescence (Chavez et al., 2010). Furthermore this accelerated senescence might be caused by a higher frequency of telomere breakage events, since in *smc5-6* cells a higher proportion of divergent distal telomeric repeat sequences was observed, suggesting that Smc5/6 presence at telomeres is required for efficient and timely termination of DNA replication and repair to avoid stochastic losses of telomere function (Noel and Wellinger, 2011).

1.8 Smc5/6 in development and disease

The Smc5/6 structurally related cohesin complex has been connected to several human diseases, known as cohesinopathies (reviewed in (Remeseiro et al., 2013)). There are at least three syndromes caused by cohesin dysfunction: Cornelia de Lange (CdLS), Roberts (RBS) and Warsaw Breakage syndromes. CdLS is characterized by both physical and mental developmental problems. Many individuals have heterozygous mutations in the gene encoding the cohesion loader Nipb1, whereas, with less frequency, others show mutations at Smc1, Smc3, Rad21 and Hdac8 loci. RBS patients are characterized by prenatal growth retardation, limb malformations and craniofacial abnormalities. RBS is caused by homozygous mutations in the gene encoding the CoAT Esco2, which is essential for cohesion establishment in pericentric heterochromatin. The last syndrome, Warsaw Breakage, shares common features with RBS and the blood disorder Fanconi anemia and is caused by biallelic mutation in the DDX11 gene, which encodes a DNA helicase.

The budding yeast RecQ helicase Sgs1 has five homologs in human and mouse, known as RECQL1-5, which are extremely important for the maintenance of genome stability,

playing several roles in the repair of DSBs and inter-strand crosslinks (ICLs), in the recovery of stalled or broken replication forks, in preventing the formation of aberrant and recombinogenic DNA structures that arise as intermediate of DNA damage tolerance pathways and in telomere maintenance. Three of these helicases have been associated with autosomal recessive disorders (reviewed in (Singh et al., 2009)). Werner syndrome is associated with defects in Wrn (RECQL2) protein, Bloom syndrome with defects in BLM (RECQL3) and three other disorders with mutations of RECQL4. Werner syndrome (WS) is characterized by premature ageing and elevated risk of cancer. WS cells present many chromosomal aberrations and rearrangements, sensitivity to DNA damaging agents and telomere dysfunction, like increased telomere loss and chromosomal end fusion. Bloom syndrome (BS) is characterized by growth retardation, sunlight sensitivity and predisposition to cancer. BS cells present hypersensitivity to various DNA damaging agents, chromosomal aberrations, high frequency of sister chromatid exchanges (SCE) and persistency of sister chromatid entanglements that impede chromosome segregation and lead to the formation of DNA bridges at anaphase.

Recently, a syndrome caused by mutations in Smc5/6 complex was reported (Payne et al., 2014). Two female patients were identified and they both carried the same heterozygous frameshift mutations in *NSMCE2* locus, which lead to highly depressed levels of full length Mms21. This syndrome is characterized by severe primordial dwarfism with facial dysmorphism, insulin resistant diabetes, fatty liver, hypertriglyceridemia and primary gonadal failure. Both patients have normal karyotypes. Patient derived fibroblasts show high frequency of micronuclei formation, HU-induced nucleoplasmic bridges and spontaneously binucleated cells. These defects are also observed in Bloom syndrome cells, in agreement with the synthetic interaction between *SMC5-6* and *SGS1* in yeast and the shared phenotypes of the respective mutants. Furthermore, Mms21 hypomorphic

patient cells exhibit impairment in BLM foci formation in response to HU replication stress and IR and significant elevation in SCE induced by UV.

The discovery of this syndrome brought to light the fact that the loss of Smc5/6 has similar consequences of the one of cohesin and RECQ helicases. All these proteins have known important and often related functions in DNA damage response and genome stability from yeast to humans and they are all essential for a normal and healthy development of mammalian cells.

2 Material and methods

2.1 Yeast strains and media

2.1.1 Yeast genotypes

The yeast strains (*Saccharomyces cerevisiae*) used in this study were derivatives of W303-1A. Genotypes are shown in Table 2.1.

Strain	Genotype	Source
FY1363	Mata *ade2-1 can1-100 his3-11,-15 leu2-3,112 trp1-1 ura3-1 RAD5+* (W303)	lab collection
FY0090	Mata *his3-delta200 leu2-3, 112 lys2-801 trp1-1 (am) ura3-52* (DF5)	Jentsch lab
HY1358	W303 Mata *esc2Δ::HIS3MX6*	lab collection
HY1465	W303 Mata *sgs1Δ::HIS3MX6*	lab collection
HY1545	W303 Mata *sgs1Δ::HIS3MX6 rad5Δ::HPHMX4*	lab collection
HY1547	W303 Mata *sgs1Δ::HIS3MX6 ubc13Δ::HPHMX4*	lab collection
HY1549	W303 Mata *sgs1Δ::HIS3MX6 mms2Δ::HPHMX4*	lab collection
HY1895	W303 Mata *[pTEF427]*	
HY2508	W303 Mata *G2::NATNT2-MPH1*	this study
HY2721	DF5 Matα *pol32Δ::klTRP1*	lab collection
HY2736	W303 Mata *G2::NATNT2-SMC6*	this study
HY2806	W303 Mata *SMC6-6HIS-3FLAG::KANMX4*	this study
HY2808	W303 Mata *G2::NATNT2-SMC6-6HIS-3FLAG::KANMX4*	this study
HY3153	W303 Mata *G2::NATNT2-SMC5*	this study
HY3156	W303 Mata *SMC5-9PK::HIS3MX6*	this study
HY3158	W303 Mata *G2::NATNT2-SMC6 SMC5-9PK::HIS3MX6*	this study
HY3159	W303 Mata *G2::NATNT2-SMC5-9PK::HIS3MX6*	this study
HY3167	W303 Mata *S::NATNT2-SMC6*	this study
HY3168	W303 Matα *S::NATNT2-SMC6*	this study
HY3170	W303 Mata *S::NATNT2-SMC6-6HIS-3FLAG::KANMX4*	this study
HY3172	W303 Mata *G2::NATNT2-SMC6-6HIS-3FLAG::KANMX4 G2::NATN2-SMC5-9PK::HIS3MX6*	this study
HY3386	W303 Mata *S::NATNT2-SMC6-6HIS-3FLAG::KANMX4 rad51Δ::LEU2*	this study
HY3447	W303 Mata *SMC6-6HIS-3FLAG::KANMX4 SMC5-9PK::HIS3MX6*	this study
HY3611	W303 Mata *rmi1Δ::KANMX4*	lab collection
HY3701	W303 Mata *top2-4 S::NATNT2-SMC6*	this study
HY3702	W303 Matα *top2-4 S::NATNT2-SMC6*	this study
HY3807	W303 Mata *TOP3-6HIS-3FLAG::KANMX4*	this study
HY3817	W303 Mata *S::NATNT2-SMC6 [p427TEF-MPH1]*	this study
HY3819	W303 Mata *G2::NATNT2-SMC6 [p427TEF-MPH1]*	this study
HY3840	W303 Mata *ubc13Δ::HPHMX4*	lab collection

HY3841	W303 Matα *mms2Δ::HPHMX4*	lab collection
HY3876	W303 Mata *[p427TEF-MPH1]*	this study
HY3878	W303 Mata *S::NATNT2-SMC6 [p427TEF]*	this study
HY3880	W303 Mata *G2::NATNT2-SMC6 [p427TEF]*	this study
HY3993	W303 Mata *SMC6-6HIS-3FLAG::KANMX4 [pRS316]*	this study
HY3995	W303 Mata *S::NATNT2-SMC6-6HIS-3FLAG::KANMX4 [pRS316]*	this study
HY3997	W303 Mata *top2-4 SMC6-6HIS-3FLAG::KANMX4 [pRS316]*	this study
HY3999	W303 Mata *top2-4 S::NATNT2-SMC6-6HIS-3FLAG::KANMX4 [pRS316]*	this study
HY4421	W303 Mata *S::NATNT2-SMC6 tof1Δ::HIS3MX6*	this study
HY4422	W303 Mata *S::NATNT2-SMC6 csm3Δ::HPHMX4*	this study
HY4425	W303 Mata *S::NATNT2-SMC6 fob1Δ::HIS3MX6*	this study
HY4896	W303 Mata *ura3::URA3/GPD-TK(7X) G2::NATNT2-SMC6-6HIS-3FLAG::KANMX4 G2::NATNT2-SMC5-9PK-HIS3MX6*	this study
HY4898	W303 Mata *S::NATNT2-MMS21*	this study
HY4899	W303 Matα *S::NATNT2-MMS21*	this study
HY4901	W303 Matα *G2::NATNT2-MMS21*	this study
HY4903	W303 Mata *G2::NATNT2-MMS21-9PK::HISMX6*	this study
HY4904	W303 Matα *S::NATNT2-SMC6 mms2Δ::HPHMX4*	this study
HY4905	W303 Mata *S::NATNT2-SMC6 ubc13Δ::HPHMX4*	this study
HY4906	W303 Mata/α *SMC5-9PK::HIS3MX6/S::NATNT2-SMC5-9PK::HIS3MX6*	this study
HY4909	DF5 Mata *S::NATNT2-SMC6*	this study
HY4910	W303 Mata *sir2Δ::TRP1 [Yep195(URA3)-SMC6]*	this study
HY4912	W303 Mata *sir2Δ::TRP1 S::NATNT2-SMC6-6HIS-3FLAG::KANMX4 [Yep195(URA3)-SMC6]*	this study
HY4914	W303 Mata *sir2Δ::TRP1 S::NATNT2-SMC6-6HIS-3FLAG::KANMX4 rad51Δ::LEU2 [Yep195(URA3)-SMC6]*	this study
HY4915	W303 Mata *S::NATNT2-SMC6 rad5Δ::HPHMX4*	this study
HY4916	W303 Mata *RRM3-10FLAG::KANMX4*	this study
HY5159	W303 Mata *S::NATNT2-RRM3-13MYC::KANMX4*	this study
HY5161	W303 Mata *S::NATNT2-SMC6-6HIS-3FLAG::KANMX4 S::NATNT2-RRM3-13MYC::KANMX4*	this study
HY5162	W303 Mata *S::NATNT2-SMC6-6HIS-3FLAG::KANMX4 S::NATNT2-RRM3-13MYC::KANMX4*	this study
HY5163	W303 Mata/α *MMS21-9PK::HIS3MX6/S::NATNT2-MMS21-9PK::HIS3MX6*	this study
HY5274	W303 Mata *S::NATNT2-SMC6-6HIS-3FLAG::KANMX4 pAHD1-tc3-3HA-RRM3 (NAT)*	this study
HY5277	DF5 Mata *S::NATNT2-SMC6 pol32Δ::klTRP1*	this study
HY5324	W303 Mata/α *SMC5-6HIS-3FLAG::KanMX4/S::NATNT2-SMC5-9PK::HIS3MX6*	this study
FY1002	W303 Matα *rad51Δ::LEU2*	Foiani lab
FY1100	W303 Mata *smc6-9*	Aragon lab
FY1110	W303 Mata *ura3::URA3/GPD-TK(7X)*	Foiani lab
FY1156	W303 Mata *smc6-56-13MYC::HIS3MX6*	Zhao lab
FY1432	W303 Mata *smc6-56-13MYC::KANMX4*	Zhao lab
FY1490	DF5 Mata *ubc13Δ::HPHNT1*	Jentsch lab
FY1534	W303 Mata *smc6-P4-13MYC::KANMX4*	Zhao lab

FY1552	W303 Mata *top2-4*	Nasmyth lab
FY1765	W303 Matα *rrm3Δ::HIS3MX6*	Foiani lab
FY1766	W303 Matα *top3Δ::KANMX4*	Foiani lab

Table 2.1

2.1.2 Media

2.1.2.1 Media for *E. coli*

LB (DIFCO)	1% Bactotryptone
0.5% Yeast extract	
1% NaCl	
pH 7.25	
LB agar	LB + 2% agar (DIFCO)
LB amp	LB + 50 μg/ml ampicillin (Amp)

2.1.2.2 Media for *S. cerevisiae*

YP	1% Yeast extract
2% bactopeptone	
pH 5.4	
YP agar	YP + 2% agar (DIFCO)
YPD	YP + 2% glucose
YPD agar	YPD + 2% agar
SC	0.67% yeast nitrogen base (YNB, DIFCO w/o AA)
	2% glucose
	amino acids as required
SC agar	SC + 2% agar
VB sporulation media	NaAc□3H_2O 1.36%, KCl 0.19%
(+ 1.5% agar)	NaCl 0.12% , $MgSO_4$□7H_2O 0.074%

2.2 Yeast strain construction

2.2.1 *E. coli* transformation

50 μl of fresh chemically competent DH5alpha cells were thawed on ice for approximately 10' prior to the addition of plasmid DNA. Cells are incubated with DNA on ice for 30' and then subjected to a heat shock for 30-45'' at 37° C. After the heat shock the cells are returned to ice for 2'. Finally 950 μl of LB medium are added to the reaction tube. Cell suspension is incubated on a shaker at 37°C for 30' before plating onto LB+Amp plates. Plates are incubated overnight at 37°C.

2.2.2 Plasmid DNA isolation from *E. coli* (mini prep)

Clones picked from individual colonies were used to inoculate 10 ml LB supplemented with 50 μg/ml ampicillin and grown overnight at 37°C. Bacterial cells were transferred to eppendorf tubes and pelleted for 5' at 8000 rpm. Minipreps were performed with Wizard Plus SV Minipreps DNA Purification System (Promega) following the manufacturer's instructions. Plasmids were eluted in 100 μl ddH2O.

2.2.3 *Saccharomyces cerevisiae* transformation

Yeast mutants were constructed by Lithium Acetate-based transformation of yeast cells with the PCR amplification of a gene deletion or tagging cassette (Gietz et al., 1995) (Gietz et al., 1995). Transforming DNA contained a selectable marker flanked by approximately 40 bp of DNA homologous to the upstream and downstream regions of the gene of interest. The primers were designed according to (Longtine et al., 1998; De Antoni and Gallwitz, 2000; Janke et al., 2004; Kotter et al., 2009).

Log-phase cells grown in YPD at 25°C were collected by centrifugation and resuspended in LiAc/TE (Lithium Acetate 0.1M; TE 1X) to a final concentration of $2x10^9$ cells/ml. After 15'-20' at 25°C, $1x10^8$ (50 ml) of LiAc-treated cells were then added to a eppendorf tube containing 3-6 μg of the transforming DNA and 5μl of denatured carrier

DNA (salmon sperm DNA, Sigma). After 10' incubation at RT, 500µl of 40% PEG/LiAc were added and the mix was incubated for other 40' at RT. Cells were then heat-shocked at 42°C for 15', put on the bench for 5'-10' to recover and then centrifuged for 1' at 3000 rpm. Finally, the pellet was re-suspended in distilled water and spread onto selective medium. In case of selection for resistance to antibiotic G418, nourseothricin (NAT), hygromycin (HPH), after the heat shock, the cells are incubated in 3 ml of YPD for about 3 hours at 25°C, before plating on selective plates to allow expression of the resistance gene. The resulting transformant colonies were streaked out to obtain single colonies that were checked for the correct integration by PCR or Western blot (if required).

2.2.4 Crossings

Mutants with multiple mutations (two or more) were often obtained by crossing haploid strains of opposite mating type and by selecting the desired genotype combination from the product of meiosis. *MATα* and *MATa* strains were grown on individual YPD plates O/N, then mixed and incubated at 28°C for 4-6 hours in order to allow opposite sex recognition and mating. Cells were then analyzed at the microscope and zygotes were selected with the help of the micromanipulator (Singer). Diploid colonies derived from zygote clonal division were allowed to grow for 2 days and then patched on VB sporulation media to induce meiosis. After 3-5 days a sufficient number of tetrads containing 4 haploid spores were dissected at the micromanipulator and incubated at permissive temperature until colony appearance. Genotype and correct allele segregation was checked by markers resistance and, if necessary, PCR.

2.2.5 Yeast genomic DNA isolation

Independent colonies of yeast were grown to stationary phase in YPD at 28°C. Cells were harvested and the genomic DNA was isolated using Mr. Gentle kit (Takara) or Yeast DNA Extraction kit (Thermo Scientific) following manifacturer's instructions.

2.3 Robot-assisted genetic screens

The manipulation of deletion mutant array (DMA) and generation of a double mutant collection was performed with a robotic station (VersarrayTM colony arrayer & picker, Biorad) as described in (Tong et al., 2004; Tong and Boone, 2006).

2.3.1 Synthetic genetic array (SGA)

1. Query strain was grown in 5 ml YPD O/N and the liquid culture was then pin-spotted on a 768 format plate and incubated O/N at 30°C
2. Mating was performed by pin-replica-plating the query plates and the YKO plates on the same medium.
3. Zygotes were pin-replica-plated on double selective medium (G418 and NAT) to allow only the survival of the diploids.
4. Sporulation was obtained by pin-replica-plating diploids on VB medium
5. *MATa* haploid progeny was selected on SD – His/Arg/Lys + canavanine (two consecutive rounds of selection)
6. *MATa* double mutants were obtained by consecutive pin-replica on G418 plates followed by G418+NAT plates
7. Synthetic lethality was scored as the absence of colonies growing on double selective medium

2.4 Cells growth, synchronization, drugs treatment and conditional depletions

Unless otherwise indicated, yeast cells were grown at 25ºC in YPD medium supplemented with Adenine 50 μg/ml (YPDA) or YPA+Glucose pH 7.4 specifically when treated with nocodazole. Cells were synchronized in different cell-cycle phases by using α-factor or nocodazole (both from Sigma).

2.4.1 Arrest in G1 phase

The pheromone α-factor is produced by Mat α cells in order to induce cellular fusion with the opposite mating. Mat a cells sense the pheromone and induce mating genes that in turn lead to morphological alterations and cell-cycle arrest in G1. Exponentially growing cells were therefore treated with 3-5 μg/ml of α-factor for 2-2.5 hours with a second addition of the hormone of half of the initial amount after 1 hour from the first treatment and when >95% of cells showed the characteristic morphology, they were considered synchronized. If required by the protocol cells were then released in a medium without α-factor after 1 washing in YP medium.

2.4.2 Arrest in G2/M phase

Nocodazole is a microtubules poisoning agent that causes their depolymerization throughout the cell cycle. In G2, it causes the activation of the spindle checkpoint and the consequent cell cycle arrest in pro-metaphase. Cells were therefore treated with 10-20 μg/ml of nocodazole dissolved in DMSO (1% total) for about 3 hours. When >95% of cells displayed the characteristic G2 morphology they were considered synchronized. If required by the protocol, cells were then released in a medium without nocodazole after 1 washing in YP medium containing 1% DMSO.

2.4.3 MMS and HU treatment

Methylmethane sulfonate (MMS) was used at 0.033% in 2D gel experiments and at the indicated concentration for spot assay. Hydroxiurea (HU) was used at 200 mM in ChIP-on-chip and BrdU-ChIP-on-chip experiments.

2.4.4 Regulation of conditionally mutant genes

Temperature sensitive alleles were inactivated by incubating cells at the restrictive temperature (usually 37°C).

To deplete target mRNA using tetracycline as translational repressor, tetracycline

(nzytech) was added at a final concentration of 0.6 mM. When long kinetics were done, half of the initial amount of the antibiotic was added 3 hours after the release to maintain efficient mRNA degradation.

2.5 Protein based procedures

2.5.1 TCA protein extraction

The yeast protein extraction was performed with Trichloroacetic acid (TCA) method as described by (Foiani et al., 2000; Reid and Schatz, 1982). 10 ml of cells at the concentration of $1*10^7$ cells/ml are harvested, resuspended in 2 ml of TCA 20% and transferred in 2 ml eppendorf tube. The pellet is resuspended in 200 µl of TCA 20% and an equal volume of acid-washed glass beads (425-600 µm, Sigma-Aldrich) is added. Cells are broken by continuous vortexing for 3'-5'. 400 µl of TCA 5% is added to have a final concentration of 10% of TCA. The lysate is then transferred to a new 1.5 ml tube and centrifuged for 10' at 3000rpm at RT. The pellet is resuspend in 100 µl Laemmly Buffer 1X (2X Laemmli Buffer: 4% SDS, 20% glycerol, 10% 2-mercaptoethanol, 0.004% bromphenol blue, 0.125 M Tris HCl pH6.8). The pH is neutralized with 50 µl of Tris Base 1M. The protein extract is boiled for 3' and centrifuged for 10' at 3000 rpm at RT. The supernatant is collected and analyzed by SDS-PAGE.

2.5.2 SDS polyacrylamide gel electrophoresis (SDS-PAGE) and Western blotting

The proteins were separated according to their molecular weight by polyacrylamide gel electrophoresis (PAGE) under denaturing conditions. The gel was composed of 7.5% or 10% polyacrylamide and 0.13% bisacrylamide and run in SDS-PAGE running buffer (Glicine 2 M, Tris 0.25 M, SDS 0.02 M, pH 8.3) through which an electric field was applied.

Proteins were transferred in western transfer tanks to nitrocellulose (Protran, Whatman

0.45 mm) in 1X Western Transfer buffer (1% glycine, 0.02 M Tris base, 20% methanol) at 30 volts ON at 4ºC. Ponceau staining was used to roughly reveal the amount of protein transferred onto the filters. Membranes were blocked for 1 h in 4% milk/ TBS 1X (50 mM Tris-HCl pH 7.5, 150 mM NaCl). After blocking, membranes were incubated with the primary antibody for 2 hours at RT or ON at 4ºC, followed by 3 x 10' washes in TBS 1X and then incubated with the horseradish peroxidase-conjugated secondary antibody diluted in milk/TBS 1X for 1 h. After incubation with the secondary antibody, the membrane was washed 3 times for 10' each in TBS 1X and the bound secondary antibody was revealed using ECL kit (Amersham). Membranes were then exposed to photographic films and developed.

The antibodies used for western blots are the monoclonal anti-FLAG M2 from SIGMA (F1804), the monoclonal anti-PK SV5-Pk1 from AbD Serotech, the 22C5 monoclonal antibody from Invitrogen (A6457) for Pgk1, the policlonal Clb2 (y-180) antibody from Santa Cruz Biotechnology, the mouse monoclonal anti-MYC (9E10), the mouse monoclonal anti-HA (12CA5).

2.6 Cell based procedures

2.6.1 FACS (Fluorescence activated cell sorter) analysis

0.5-2 x10^7 cells were fixed with 70% ethanol. Cells were treated with 2 mg/ml RNAse A (Sigma) in Tris-HCl 50 mM pH 7.5 for at least 1hour at 37˚C. Cells were then stained with Propidium Iodide (Sigma) 50 µg/ml in FACS Buffer solution (180 mM Tris-HCl pH 7.5; 190 mM NaCl; 70 mM $MgCl_2$). A 1:10 dilution in Tris-HCl 50mM pH 7.5 was sonicated for 6'' and analyzed in Becton Dickinson FACScan for FL2H fluorescence.

Alternatively, after RNase A treatment, cells were treated with Proteinase K (Roche) 1mg/ml for 30' at 50˚C. Cells were than resuspended in Tris-HCl 50 mM pH 7.5. A 1:10

dilution in sytox green staining solution (1 μM sytox green in Tris-HCl 50 mM pH 7.5), sonicated for 6'' and analyzed in Becton Dickinson FACScan for FL1H fluorescence.

2.6.2 Spot assay

Stationary phase grown cells were counted and 10 fold serial dilutions were spotted onto YPDA, YPDA containing HU or MMS at the indicated concentrations, SC or 5-FOA plates. The plates were then incubated for 2-4 days at the indicated temperatures and scanned.

5-FOA plates (200 ml):

1) 4 gr of Agar are dissolved in 100 ml of water and then autoclaved.

2) Prepare a mix with:

- 1,4 gr YNB
- 200 mg FOA (1 g/L)
- 10 mg Ura (50 mg/L)
- 8 ml Glucose 50%
- 2 ml Ade 5 mg/ml
- 2 ml His 5 mg/ml
- 2 ml Trp 5 mg/ml
- 2 ml Leu 5 mg/ml

3) Add water to 100 ml final volume and let this mix to dissolve.

4) Then filter it and warm at 65°C.

5) Put together agar+water and the mix containing FOA and Ura (final 200 ml) and pour the plates (10).

2.6.3 DAPI staining

10^7 cells were fixed with 1 ml of EtOH 70% for 30'. Cells were than washed twice with PBS 1X (137 mM NaCl, 10 mM Na_2HPO_4, 1.76 mM KH_2PO_4, 2.7 mM KCl, pH 7.4) and stored at 4˚C. Cells were pelleted, resuspended in 100 μl of DAPI 0.5 μg/ml and analyzed

using Hoest filter.

2.6.4 ChIP-on-chip

The ChIP-on-chip technique uses the DNA obtained by chromatin immunoprecipitation (ChIP) and PCR amplification as a probe for hybridization to DNA chips, allowing the detection of protein binding to chromosomal DNA at a resolution of 300 bp. Protein-DNA complexes are crosslinked by formaldehyde treatment, chromatin is then sheared by sonication to obtain suitable protein-DNA fragments and immunoprecipitation is carried out with specific antibodies. Two fractions are obtained: IP, enriched in the protein of interest, and SUP, which contains non-immunoprecipitated DNA and is used as a hybridization control. Crosslink is reversed, samples are treated with proteinase K and RNase to extract DNA. DNA fractions are amplified by tagged-random PCR, DNAse digested and labeled with biotin. Enriched and non-enriched DNA pools are probed to independent chips and, after staining, washing and scanning, signal intensities of each locus for IP and SUP hybridized arrays are compared, providing a measurement of the protein-DNA association along the entire genome.

A scheme of the ChIP-on-chip protocol is reported in Figure 2.1, modified from (Katou et al., 2006).

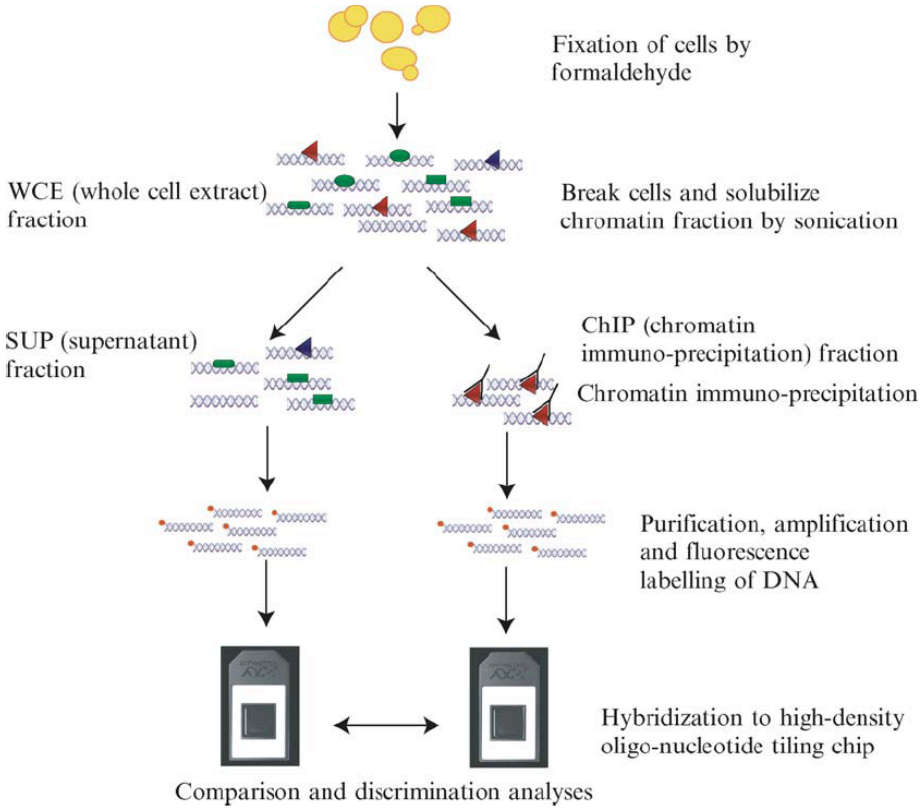

Figure 2.1 Schematic representation of ChIP-on-chip protocol in yeast.

S.cerevisiae oligonucleotide microarrays were provided by Affymetrix (*S.cerevisiae* Tiling 1.0R, P/N 900645). Proteins ChIP-chip analysis were carried out as described (Bermejo et al., 2009b), employing anti-Flag monoclonal antibody M2 (Sigma-Aldrich) and anti-PK SV5-Pk1 antibody (AbD Serotec). ChIP-on-chip experiment were performed after HU 200 mM or Nocodazole 20 µg/ml treatment, to analyze, respectively, chromatin enrichment of a given protein in S phase or in G2/M. Analysis of the data was performed using TAS (Affymetrix) and MAT software.

Solutions

PBS 1X

TBS 1X

TE 1X: 10 mM Tris-HCl pH 8.0, 1 mM EDTA

Laemmli Buffer 2X

PBS/BSA: PBS 1X containing 5 mg/ml Bovine Serum Albumin

Lysis Buffer: Hepes-KOH pH 7.5 50 mM, NaCl 140 mM, EDTA 1 mM, Triton-X100 1%, Na-deoxycholate 0.1% (autoclaved)

Wash Buffer: Tris-HCl pH 8.0 10 mM, LiCl 250 mM, NP-40 0.5%, Na-deoxycholate 0.5%, EDTA 1 mM (autoclaved)

Elution Buffer: Tris-HCl pH 8.0 50 mM, EDTA10 mM, SDS 1%

TE -1% SDS: Tris-HCl pH 8.0 10 mM, EDTA1 mM, SDS 1%

10X One-Phor-All-Buffer: Tris-Acetate pH7.5 100 mM, Mg-Acetate 100 mM, K-Acetate 500 mM

Magnetic beads preparation (Protein A)

1. Transfer 60 µl of magnetic beads (Dynabeads, Invitrogen) in a 1.7-ml prelubricated Costar tube

2. Place the tube in a magnetic grid and aspirate the supernatant with a vacuum pump.

3. Wash beads twice as follows with 0.5 ml of ice cold PBS/BSA

4. Resuspend the beads in 60 µl of PBS/BSA and add 20 µg of anti-Flag monoclonal antibody M2 or anti-PK SV5 antibody

5. Incubate with rotation overnight at 4°C

6. Immediately before use, remove the antibody containing solution; wash twice with ice-cold PBS/BSA and resupend in 60 µl of PBS/BSA (15 µl of magnetic beads are added to each 0.4 ml Lysis Buffer aliquot)

Chromatin extracts preparation and immunoprecipitation

1. Collect 100 ml of culture at the concentration of $1*10^7$ cells/ml

2. Transfer the culture into two 50-ml centrifuge tubes containing formaldehyde to a 1% final concentration

3. Incubate at room temperature for 30 minutes gently shaking by rotation

4. Wash cells twice with 20 ml of ice-cold TBS 1X; after the last washing step discard the supernatant and carefully remove the remaining liquid with a vacuum pump

5. Resuspend each pellet in 0.8 ml of Lysis Buffer supplemented with 1 mM PMSF (Phenylmethanesulphonyl fluoride) and antiproteolytic cocktail (Complete protease inhibitor tablets, Roche) immediately before use

6. Transfer 0.4 ml Lysis Buffer aliquots into 2-mL O-ring screw-cap tubes add glass beads (Sigma) up to 1 mm below the buffer's meniscus (approximately 1 ml of beads)

7. Break cells with a multibeads shocker (Yasui-kikai, Osaka, Japan) using the following pattern: 60 min total time (1 min shaking / 1 min pause) at 2500 rpm and 4 °C

Breakage time can be extended if broken cells are not over 90% of the total (cell breakage can be assessed by analyzing a small aliquot of the lysate by phase contrast microscopy)

8. Recover the cell lysate

9. Centrifuge the extracts at 13400 g for 1 min at 4°C. Add a 5 µl aliquot of the soluble fraction to 5 µl of 2X Laemmli Buffer for Western blot analysis of IP efficiency (Western blot detection of this fraction indicates the proportion of protein that is not associated to chromatin after the formaldehyde crosslink)

10. Discard the supernatant containing the soluble protein fraction and add 0.45 ml of Lysis Buffer supplemented to 1 mM PMSF and 1X Antiproteolytic Cocktail) without resuspending the pellet

11. Shear chromatin by applying 5 sonication cycles of 15 sec at 1.5 tune; after each sonication cycle, pellet the chromatin by centrifuging at 2300 g for 1 min at 4 °C

12. After the final sonication cycle, centrifuge the sheared DNA at 16000 g for 5 min at 4°C and transfer the supernatant to a new 1.7-ml prelubricated tube.

Add a 5 µl aliquot of this Whole Cell Extract (WCE) to 5 µl of 2X Laemmli Buffer for Western blot analysis

13. Add previously washed antibody-bound magnetic beads (15 µl per tube) and incubate on a rotating wheel at 4°C ON

Beads washing and crosslink reversal

1. Place beads-containing tubes in a magnetic grid and wait until the beads attach to the magnet leaving a clear supernatant.

2. Transfer 5 µl of the supernatant to a 1.5 ml microcentrifuge tube to be used as hybridization control (SUP)

3. Transfer another 5 µl to a tube containing 5 µl of 2X Laemmli Buffer for Western blot analysis of IP efficiency.

4. Wash the beads as follows:

a. twice with 1 ml of ice cold Lysis Buffer (without antiproteolytics)

b. twice with 1 ml of ice cold Lysis Buffer supplemented with 360mM NaCl

c. twice with 1 ml of ice cold Wash Buffer

d. once with 1 ml of ice cold TE 1X pH 8

5. Remove the TE 1X with a micropipette in order to avoid beads aspiration and centrifuge the beads at 800 g for 3 min at 4 °C

6. Add 40 µl of Elution Buffer to each tube and incubate at 65 °C for 10 min

7. Centrifuge the tubes for 1 min at 16000 g at RT

8. Place the tubes back in the magnetic grid and transfer 5 µl in a tube containing 5 ml of 2X Laemmli Buffer

9. For the Western blot analysis of IP efficiency boil the samples at 95 °C for 30 min prior to SDS-PAGE

10. Transfer the remaining IP fractions (35-40 µl) to new 1.5-ml microcentrifuge tubes containing 4 volumes (140-160 µl) of TE-1% SDS

11. Add 95 µl of TE-1% SDS to the SUP fraction (collected on step 2)

12. Incubate overnight at 65 °C in order to reverse the crosslink

DNA purification

1. Consolidate the samples by pulse-spinning and add 25 µl of TE to the IP sample containing 175 µl

2. Add:

- 89.5 µl of TE, 3 µl of glycogen (20 mg/ml) and 7.5 µl of Proteinase K (50 mg/ml) to the IP samples
- 44.75 µl of TE, 1.5 µl of glycogen (20 mg/ml) and 3.75 µl of Proteinase K (50 mg/ml) to the SUP sample

3. Mix, without vortexing, and incubate at 37 °C for 2 hours

4. Pulse-spin to consolidate the samples and add:

- 12 µl of a 5M NaCl stock to the IP samples
- 6 µl of a 5M NaCl stock to the SUP samples

5. Extract twice by adding an equal volume of phenol/chlorophorm/isoamylalcohol pH 8.0 (300 µl for the IP samples and 150 µl for SUP samples)

6. Vortex and spin at 13400 g for 5 min at RT.

7. Add 2 volumes of cold 100% ethanol (600 µl for the IP samples and 300 µl for the SUP samples), vortex and incubate at -20 °C for at least 20 min (can be extended up to ON)

8. Centrifuge at 13400 g for 10 minutes at 4 °C

9. Discard the supernatant using a Gilson pipette and wash with 1 ml of cold 80% ethanol

10. Centrifuge at 13400 g for 10 minutes at 4 °C

11. Discard the supernatant and spin again; discard the remaining ethanol with a gel loading tip and let the pellet air-dry

12. Resuspend the pellet in 30 µl of TE containing 10 mg of RNase A (stock 10 mg/ml)

13. Incubate 1h at 37 °C

14. Consolidate the samples by pulse spinning

15. Pool two 30 µl IP samples together to obtain two 60 µl samples and purify the IP/SUP DNA using a PCR purification kit following the manufacturer's instructions (QIAquick PCR purification kit, QIAGEN)

16. Elute the DNA with 50 µl of EB buffer

17. Pool the two 50 µl IP samples together and precipitate the DNA by adding:

- 5 µl of 3M Sodium Acetate, 2 µl of glycogen (20 mg/ml) to the IP SAMPLE
- 2.5 µl of 3M Sodium Acetate, 1 µl of glycogen (20 mg/ml) to the SUP SAMPLE

18. Add 2.5 volumes of cold 100% ethanol (267.5 µl to the IP samples and 133.75 µl to the SUP samples)

19. Incubate at -20 °C for at least 20 min (can be extended up to ON)

20. Centrifuge at 13400 g for 10 minutes at 4 °C

21. Discard supernatant using a Gilson pipette and wash with 0.5 ml of cold 70% ethanol

22. Centrifuge at 13400 g for 10 minutes at 4° C

23. Discard the supernatant using a Gilson pipette and spin again; discard the remaining ethanol with a gel loading tip

24. Leave 5' at 37° C and resuspend the pellet in 10 µl of bidistilled water

25. Vortex then pulse-spin for three times to recover the precipitate

<u>DNA amplification</u>

1. Use WGA2 GenomePlex Complete Genome Amplification (WGA) Kit (Sigma) and follow the manufacturer's instructions from the *Library Preparation* step on:

a) Add 2 µl of 1X Library preparation Buffer to each sample

b) Add 1 µl of Library stabilization solution

c) Vortex thoroughly, consolidate by centrifugation and place in thermal cycler at 95° C for 2 minutes

d) Cool the sample on ice, consolidate the sample by centrifugation and return to ice

e) Add 1 µl Library Preparation Enzyme, vortex thoroughly and centrifuge briefly

f) Place the sample in a thermal cycler and incubate as follows:

16° C for 20 minutes

24° C for 20 minutes

37° C for 20 minutes

75° C for 5 minutes

4° C hold

g) Centrifuge briefly the samples and amplify them immediately or store at -20° C

2. Amplification step

A master mix may be prepared by adding the following reagents:

Nuclease-free water:	48.5 µl
10X Amplification Master Mix:	7.5 µl
Reaction from step g):	14.0 µl
WGA DNA Polymerase:	5.0 µl

Vortex thoroughly, centrifuge briefly, and begin thermocycling.

Initial Denaturation: 95° C for 3 minutes

Perform 14 cycles as follows:

Denature: 94° C for 15 seconds

Anneal/Extend: 65° C for 5 minutes

After cycling is complete, maintain the reactions at 4°C or store at -20°C

- Pulse-spin the samples

- Check the amplified DNA by loading a 2.5 µl aliquot of the reaction in a 1.2% agarose gel; a smear ranging from 100-1000 bp should be observed.
- Concentrate the DNA with YM30 Microcon cartridges (Millipore):

Add to the sample 400 µl of bidistilled water

Centrifuge at 14000g for 8 min

discard the eluted material and add 500 µl of bidistilled water

Centrifuge at 14000g for 8 min

Check the concentrate volume, that should be less than 41.75 µl

Collect the concentrate centrifuging at 1000g for 3'

Arrange the concentrate volume up to 41.75 µl

- Measure the DNA concentrations by spectrometry at 260 nm (using a Nanodrop)

DNAse digestion

1. Prepare a DNAse reaction mix as follows (for 13 samples):

ddH_2O	14.8 µl
10X One-Phor-All-Buffer plus	2 µl
25mM $CoCl_2$	1.2 µl
DNAse I 1U/ml (Invitrogen)	2 µl

2. Add to each sample:

10X One-Phor-All-Buffer plus	4.85 µl
25mM $CoCl_2$	2.9 µl
DNAse I reaction mix	1.5 µl

3. Vortex, pulse-spin and incubate at 37° C for 30''; then transfer the samples at to 95°C for 15' (in a thermocycler)

DNA labeling

1. Spin the samples and transfer them into new 1.5ml-microcentrifuge tubes

2. Add:

5µl of TdT reaction buffer

1µl Biotin-N11-ddATP (Perkin)

1µl terminal transferase (Roche)

3. Vortex, pulse-spin and incubate at 37° C for 1 hour

Hybridization and analysis of the data

Hybridization, washing, staining, and scanning were performed according to the manufacturer's instructions (Affymetrix).

Primary data analyses were carried out using the Affymetrix microarray Suite version 5.0 software to obtain hybridization intensity, fold change value, change p value and detection of p value for each locus.

Evaluation of the significance of protein cluster distributions within the different genomic areas and protein-binding correlations was performed by confrontation to the model of the null hypothesis distribution generated by a Montecarlo-like simulation. The significance of the overlap between proteins clusters was evaluated as in (Bermejo et al., 2009a; Gonzalez-Huici et al., 2014).

2.6.5 BrdU-ChIP-on-chip

Yeast cells are engineered to incorporate a thymidine analog, 5-bromo-2'-deoxyuridine (BrdU), into synthetized DNA. These cells are grown in media containing BrdU allowing them to incorporate it into replicating DNA, then genomic DNA is isolated and BrdU labeled DNA is immunoprecipitated. This DNA is amplified by PCR, labeled with a fluorophore, and cohybridized along with a reference sample onto DNA microarrays. The

data are then normalized and regions with BrdU incorporation are identified genome wide.

BrdU-ChIP-on-chip was performed as in (Fachinetti et al., 2010), employing the anti-BrdU antibody MBL M1-11-3.

1) Grow the cells o/n at 25°C in 150 ml SC–URA medium up to $1x10^7$ cells/ml.

Day 1: DNA extraction and beads preparation

1) Synchronize the cells in 150 ml SC-URA medium with α-Factor at 25° C.

2) Release cells from G1 arrest into YPDA medium containing

HU 200 mM

BrdU 200 mg/ml.

Culture for the desired time at 23° C (to better maintain synchronization), keeping cultures in the dark

3) Mix 150 ml of culture with 1,5 mL of cold Na-Azide 10% and keep on ice for at least 5 min.

-Final Azide concentration is 0.1%

4) Centrifuge the culture using the Beckman centrifuge and the JA-14 rotor:

5000 rpm, 5 min at 4°C and discard the supernatant

5) Resuspend the pellet in 20ml of cold and sterilized TE 1X

6) Centrifuge the culture at 3220 g, 5 min at 4°C

discard the supernatant and carefully remove the remaining liquid with a vacuum pump

- *At this point the dried pellet can be stored at -20° C*

7) Genomic DNA extraction was performed according to the QIAGEN Genomic DNA Handbook.

a. Resuspend cell pellet in 50 ml Falcon tube with 5 ml of spheroplasting buffer (1 M

sorbitol, 100 mM EDTA pH 8.0, 0.1% β –mercaptoethanol).

b. Place the cell suspension at 30°C until spheroplasts are visible under microscope

c. Discard the supernatant and re-suspend the pellet in 5 ml of G2 buffer of the QUIAGEN kit.

d. Add 100 µl of RNase (10 mg/ml) and incubate the tube for 30 min at 37°C

e. Add 100 µl of Proteinase K (20 mg/ml) and incubate for 1 hour at 37°C

f. Collect the supernatant by centrifugation at 5000 rpm, 4°C, for 5 min

g. Equilibrate the Genomic tip 100/G with 4 ml of QBT

h. Gently mix the supernatant with 5 ml of QBT and apply it to the equilibrated Genomic tip 100/G.

i. Wash 2 times the columns with 7.5 ml of QC

j. Elute the DNA into an isopropanol-containing corex tube with 5ml of QF pre-warmed at 50°C

k. Centrifuge for 10 min at 8100 rpm RT in a proper swing out rotor

l. Wash the pellet with 1 ml ethanol 70%

m. Centrifuge for 5min at 8100 rpm RT

n. Let the corex containing the pellet to air-dry

o. Add 250 µl of Tris pH 8 10 mM and let the pellet resupending ON at 4°C

8) Protein A Magnetic Beads preparation, for each 150 ml culture:

a) Take 20 µl of dynabeads for each IP and put in a Costar prelubricated tube

b) Wash the beads two times with 1 ml of PBS 1X, 5 mg/ml BSA, 0.1% Tween20

c) Resuspend in 20 µl of PBS, 5mg/ml BSA, 0.1% Tween20; add 4 µg of anti-BrdU antibody

d) Incubate the beads ON at 4°C, rotating

Day 2: chromatin shearing and BrdU immunoprecipitation

1) Shear the BrDU containing DNA by sonication to a length of 200-1000bp

Using the Bandelin UW2070 sonicator you can use the following parameters:

Power: 20%

20 seconds/pulse

6 pulses

After each sonication cycle, pellet the chromatin by centrifuging at 2300xg for 1 min. at 4°.

2) Quantify the DNA

The average amount of genomic DNA should range from 50 to 200ng/mL

3) Centrifuge for 5 min at 3000 rpm at 4°C

4) Normalisation: Depending of the quantification, use the same quantity of DNA for all your conditions: for example, fix that you will work with 2* 13 µg of DNA in total for each one of your conditions. Do the appropriate dilution to have two tubes of 1.5 ml containing 100 µl of the DNA solution of the fixed concentration.

5) Wash the antibody-beads complex two times with 1 ml of PBS 1, 5 mg/mL BSA, 0,1% Tween20

6) Resuspend the antibody-beads complex in 20 µl of PBS 1X, 5 mg/ml BSA, 0.1% Tween20

7) Divide the antibody-beads complex in two Costar prelubricated tubes, 10 µl per tube

8) Denaturate the DNA at 100°C for 10 min and immediately put on ice

9) Add rapidly to each tube:

100 µl of ice cold 2x PBS

200 µl of ice cold PBS, 2% BSA, 0,2% Tween20

10) Add the DNA solution from each tube to the 10 µl antibody-beads complex and incubate o/n at 4°C, rotating.

Day 3: beads washes and DNA purification

1) Place beads containing tubes in a magnetic grid. Wait until the beads attach to the magnet leaving a clear supernatant.

2) Collect 2.5 µl +2.5 µl of supernatant from each precipitation tube and put into a new eppendorf tube with 45 µl of Elution Buffer 1X (Sup fraction); keep R.T.

3) Wash the beads as follows:

- 2X with 1 ml of ice cold Lysis buffer

- 2X with 1 ml of ice cold Lysis buffer +500 mM NaCl

(add 72 µL of NaCl 5M to 1 ml lysis buffer)

- 2X with 1 ml of ice cold Washing buffer

- 1X with 1 ml of ice cold TE 1X pH8

4) Place on the magnetic grid;

Remove the TE with a micropipette to avoid beads aspiration

Centrifuge 3 min at 800 g 4°C

Place the tubes back in the magnetic grid and remove thoroughly the remaining liquid with a vacuum pump.

5) Resuspend the beads in 50 µl of elution buffer;

incubate at 65°C for 10 min mixing 3 times during the incubation

6) Centrifuge 1 min at 16000 g at RT

7) Place the tubes back in the magnetic grid and transfer the eluted material into new tubes

8) Add to the IP and to the SUP:

49 µl of TE 1X

1 ml of Proteinase K (Stock 50 mg/mL)

The final concentration of the prot. K is 0.5 mg/ml

9) Mix, without vortexing, and incubate at 37°C for 1h.

10) Purify DNA by Qiagen PCR purification Kit. Elute with 50 µL of EB buffer

11) Pool the two identical IP samples together and precipitate the DNA adding:

5 µl of 3M Sodium Acetate, 1 µl glycogen to the IP samples

2.5 µl of 3M Sodium Acetate, 0.5 µl glycogen to the SUP samples

12) Add 2.5 volumes of cold 100% ethanol:

265 µl to the IP samples

132,5 µl to the SUP samples

13) Incubate at -20 °C for at least 20 min. or O.N.

14) Centrifuge at ≥ 13400 g for 10 minutes at 4 °C.

15) Discard supernatant using a Gilson pipette and wash with 0.5 ml of cold 70% ethanol.

16) Centrifuge at ≥ 13400 g for 10 minutes at 4° C.

17) Discard the supernatant using a Gilson pipette and spin again; discard the remaining ethanol with a gel loading tip.

18) Leave 5' at 37° C. Resuspend the pellet in 10 µl of ddH_20

19) Vortex then pulse-spin for three times to recover the precipitate

20) Proceed as for ChIP on chip with WGA PCR amplification.

2.6.6 CTAB DNA extraction and 2D gel electrophoresis

2.6.6.1 Yeast DNA extraction with CTAB

DNA CTAB extraction was performed as described in (Branzei et al., 2006; Liberi et al., 2005; Lopes et al., 2001).

Materials and Solutions

- Sodium azide 10%, store at 4°C.
- 10 mg/ml Zymolyase stock (1000U/ml).
- Spheroplasting buffer: 1M sorbitol, 100 mM EDTA pH 8.0, 0.1% β-mercaptoethanol.

- Solution I: 2% w/v CTAB (FLUKA-cetyltrimethylammonium bromide), 1.4 M NaCl,
- 100 mM Tris HCl pH 7.6, 25 mM EDTA pH 8.0
- 10 mg/ml RNase (DNase free)
- 20 mg/ml Proteinase K
- 24:1 Chloroform/isoamylalcohol
- Corex glass tubes
- Solution II: 1% w/v CTAB, 50mM Tris HCl pH 7.6, 10mM EDTA
- Solution III: 1.4 M NaCl, 10mM Tris HCl pH 7.6, 1mM EDTA
- Isopropanol
- 70% Ethanol
- 10 mM Tris-HCl pH 8.0

Procedure

1. Block samples with 0.1% sodium azide (final concentration).

2. Collect samples by centrifugation at 6000-8000 rpm (JA-14 Beckman tubes), 5-10 min, at 4°C, washed once with 20ml cold water.

3. Transfer cells in 50 ml Falcon tube, re-suspend in 5 ml of spheroplasting buffer and incubate for 20-30 minutes at 30°C

4. Collect spheroplasts by centrifugation at 4000 rpm (in Falcon tubes) for 10 min at 4°C;

5. Resuspend spheroplasts in 2 ml of cold water and sub sequentially add 2.5 ml of Solution I and 200 µl of 10 mg/ml RNA-se; gently mix the suspension and place it at 37°C with for 15 min.

6. Add 200 µl of 20 mg/ml Proteinase K and incubate for further 1.5 hours at 50°C. If cell clamps are still visible, add 100 µl more of Proteinase K and incubate overnight at 30°C

7. Separate the solution by centrifugation at around 3500 g for 10 min at room

temperature. Supernatant and pellet are processed separately as indicated below.

Supernatant:

1. Transfer the supernatant into a 15 ml Falcon tube and add 2.5 ml Chloroform/isoamylalcohol 24:1.

2. Mix vigorously 6 times and separate the two phases by centrifugation at 3500 g for 10 min.

3. Carefully transfer the clear upper phase into a Corex glass tube with a pipette and add two volumes (10 ml) of Solution II. Note that at this step the prolonged incubation (1-2 hours) with Solution II might help DNA precipitation in the next step.

4. Separate the solution by centrifugation at 8500 rpm for 10 min in a Beckman JS 13.1 swing out rotor, discard the supernatant and resuspend the pellet in 2.5 ml of Solution III. Briefly incubate at 37°C to dissolve of the pellet.

Pellet:

1. Energetically resuspend the pellet into 2 ml of Solution III and incubate 1 hour at 50°C.

2. Transfer the solution into a 15 ml Falcon tube and extract with 1 ml of Chloroform/isoamylalcohol 24:1. Separate the two phases by centrifugation at 3500g for 10 min at full speed in an appropriate centrifuge.

3. Carefully transfer the clear upper phase (Solution III) into the Corex glass tube containing Solution III obtained from the treatment of the supernatant (see treatment of "supernatant" step 4).

4. Precipitate the DNA with 1 volume (10 ml) of isopropanol and centrifuge at 8500 rpm for 10 min in a Beckman JS 13.1 swing out rotor.

5. Wash the pellet with 2 ml of ethanol 70%. After centrifugation, carefully remove the ethanol with a pipette as much as possible and dissolve the DNA into 250 µl of 10mM Tris-HCl pH 8. Genomic DNA preparations are stored at 4° C.

2.6.6.2 In-vivo psoralen crosslinking of the DNA

Psoralen efficiently intercalates in the double strand DNA and upon irradiation with ultraviolet (UV) light (366 nm) forms covalent crosslinks between pyrimidines of opposite strands. Psoralen derivatives easily penetrate the membranes of living cells and Trimethylpsoralen (TMP) is the most commonly used for in vivo crosslinking of DNA (Wellinger and Sogo, 1998).

Material and solutions:

- Psoralen solution: 0.2 mg/ml Trioxalen (SIGMA) in 100% Ethanol. Keep in the dark. Dissolve by stirring overnight at 4°C. Store at -20°C.
- 6 well plates (FALCON)
- UV stratalinker (Stratagene), 365 nm and 265 nm UV bulbs

Procedure:

1. 2 x 10^9 cells (200 ml from a 1 x 10^7 cells/ml culture) were collected.
2. Block cells by treating with sodium azide (0.1% final) and 5 min or more on ice.
3. Pellet the cells and wash with 20 ml of ice-cold water.
4. Re-suspend in 5 ml of ice-cold water and transfer in a 6 well plate (1sample/well)
5. Keep the 6 well dish always on ice while performing psoralen-crosslinking.
6. Add 300 µl of psoralen solution, mix well and incubate for 5 minutes (on ice)
7. Mix again within the 5 minutes and irradiate for 10 minutes (on ice) in a Stratalinker (Stratagene) with 365 nm UV bulbs, at a distance of 2-3 centimeters from the bulbs.
8. Repeat steps 6-7 for three more times. (Cover with aluminum wrap during incubation with psoralen to keep samples as much as possible in the dark).
9. Transfer cells in falcon tubes and wash the dish with 5 ml of ice-cold water to collect all cells
10. Pellet the cells and proceed with DNA extraction.

Before blotting, revert the crosslinking by irradiating the gel for 10 minutes with 265 nm UV lamps in a Stratalinker (Stratagene). It's not necessary to place the gels very close to the UV bulbs.

2.6.6.3 Analysis of replication intermediates by two-dimensional agarose gel electrophoresis (2D gel)

Replication of a DNA fragment generates a variety of structures that differ from each other by mass and shape. For instance, passively replicated DNA assumes a characteristic "Y" shape due to the unwinding of a single double helix in two newly replicated templates. When the DNA fragment contains an origin of replication, the two fork molecules are bound in a "bubble" like structures that enlarges with the progression of replication and results in two linear DNA molecules when forks proceed outside the fragment. Recombination intermediates that link two newly replicated DNA molecules assume instead an "X" shape due to the presence of a physical link between them.

Neutral-neutral two-dimensional agarose gel electrophoresis (2D gel) technique allows separation and identification of branched DNA molecules according to their mass and shape complexity (Bell and Byers, 1983; Bell and Byers, 1983). This technique further developed by Brewer and Fangman (Brewer and Fangman, 1987) has been used to map origins of DNA replication in yeast chromosomes and to study replication and recombination related DNA structures in many organisms.

The principle on which the method is based consists on the fact that differences in shape can affect, under specific conditions, the electrophoretic mobility of DNA molecules of equal mass. Restriction fragments are therefore separated through a first dimension gel, in conditions that emphasize the mass differences and minimize the contribution of shape to the mobility (low agarose concentration, low voltage, no ethidium bromide). Subsequently, each sample lane is cut out and separated by the second dimension gel, where DNA runs orthogonally with respect to the first dimension gel. The second gel, on

the contrary, is run under conditions that maximize the contribution of the shape to the mobility by means of a delay of complex structures during migration (high agarose concentration, high voltage and in the presence of ethidium bromide).

As a result of the consecutive electrophoretic runs, each DNA structure assumes in the two dimensional area a specific position dictated by the unique combination of mass and shape. Moreover, molecules of the same nature (e.g. replication forks), undergo transitions that define specific continuous patterns, the most often encountered arcs been confirmed by electron microscopy (Kuzminov et al., 1997; Kuzminov et al., 1997). The migration patterns of the major DNA structures arising during replication origin firing, replication fork progression, pausing and recombination are depicted in the following scheme (Figure 2.2).

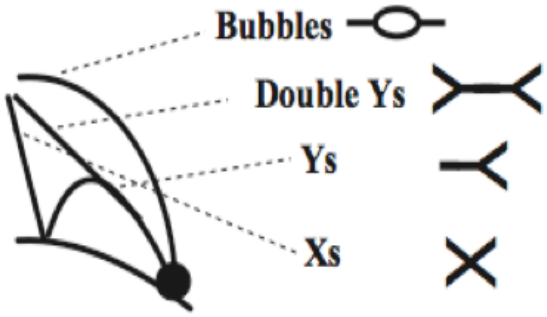

Figure 2.2 Schematic representation of the replication and repair intermediates analyzed by 2D gel electrophoresis. In the scheme the signals corresponding to bubbles, Y-arcs, double Y-arcs and X shaped molecules are indicated. Adapted from (Branzei et al., 2008).

2D gel electrophoresis was performed as described in (Branzei et al., 2006; Branzei et al., 2008).

Digestion of DNA:

1. Digest 10-20 µg of genomic DNA in 150 µl final volume containing:

- 1X BSA

- 1X enzyme buffer
- 100-120 units of each restriction enzyme (half of the amount is added after 30 min of incubation at 37°C).

2. Digest for 6h to overnight at 37ºC.

3. Add 1/8V(19 µl) KAc 2.5 M pH=6 (autoclaved) and 1V (169 µl) of Isopropanol 100% at RT

4. Invert tube delicately

5. Cfg. a 14000rpm for 10 min at RT

6. Wash with 0.5ml Ethanol 75%

7. Discard supernatant, fast spin and remove the remaining supernatant with a yellow tip. Resuspend in 20 µl TE 1X autoclaved. Leave from 1-2 hours at 30°C to resuspend with gentle shaking.

Digestions for 2D gel analysis were done using the following enzymes purchased from NEB BioLabs:

- NcoI: ARS305
- HindIII and PstI: TER302
- EcoRI: TER704

1st dimension electrophoresis:

1. Pour 0.35% agarose gel (Low EEO agarose, without EtBr in 500 ml TBE1X*)* at 4°C.

2. Add 5 µl of loading dye 20X to the digested DNA that is dissolved in 20 µl of TE. Load the DNA leaving one free lane between each sample.

3. Run gels at 50V at room temperature (15-24 hours, depending on the size of the fragment of interest).

2nd dimension electrophoresis:

1. Stain gel in 500 ml of TBE 1X containing 15 µl EtBr 10 mg/ml in a plastic tray for about 30'. Using the 1Kb marker as reference, cut the gel in order to keep only the fragment(s) of interest. Then cut between the lanes in order to obtain individual slices for each sample.

2. Arrange the slices in a new tray allowing 10-12 cm of space for the second dimension migration.

3. Pour the second dimension gel at room temperature (0.9% low EEO agarose, 1X TBE, 15 µl EtBr) and wait 30 min for complete solidification.

4. For each gel prepare 2 L of cold TBE 1X supplemented with 60 µl EtBr.

5. Run the electrophoresis at 4°C with the following settings: 180V, max 140 mA, 7-9h (time depends on the size of the fragment of interest)

Southern blot:

1. Transfer gels to glass trays and treat as follows with agitation:

- HCl 0.25 N (1 x 7min)
- Denaturing solution (0.5 M NaOH, 1.5 M NaCl) (1 x 20 min)
- Blot#2 (1 M ammonium acetate, 0.02 M NaOH; prepared fresh) (1 x 20min)

2. Equilibrate genescreen membrane in SSC 10x.

3. Build southern blot transfer with the following order: 3M paper, gel, genescreen membrane, wet 3M paper, dry 3M paper, towels transfer and 1kg weight on the top.

4. At the end of the transfer dry the membranes with clean 3 M paper and crosslink the DNA by UV irradiation (autocrosslinking program, with 265 nm UV lamps on *Stratalinker*).

Oligonucleotides used to amplify the probes by PCR

ARS305

ARS305F: CTCCGTTTTTAGCCCCCCGTG

ARS305R: GATTGAGGCCACAGCAAGACCG

TER302

TER302Fw: GAAGGTTCAACATCAATTGATTGATTCTGCCGCCATGATC

TER302Rv: GCTTCCCTAGAACCTTCTTATGTTTTACATGCGCTGGGTA

TER704

TER704Fw: TGTGCACATCTTGCCCATTA

TER704Rv: GCCTCTATCACTGCAAAGTG

Hybridization of the filters:

1. Add 30 ml of Perfecthyb plus solution (Sigma) to the tubes and warm-up at 65°C for 30 min.

2. Wash filter with 10X SCC, then position them in the hybridization tube Incubate at 65°C for at least 1 hour, until probe is ready.

3. Prepare the radioactive probe using prime-a-gene labelling kit (Promega). Boil the DNA with water for 10min before adding the rest of the reagents.

- 50 ng of DNA
- 30.4 ml H_20
- 10 ml Buffer
- 2 ml BSA
- 0.7 ml of dATP, dTTP, dGTP solutions
- 3-5 units of Klenow DNA polymerase
- 50 μcurie of radioactive a-dCTP

Incubate at RT for at least 1 hour to allow incorporation of the radioactive nucleotides in the DNA fragments.

4. Clean DNA from unbounded dCTP using the G50 column (1st centrifuge 3000 rpm 1', change tube, add reaction, wait 1-2' and spin again).

5. Boil the labeled DNA (the flow through) and ssDNA for 10 min and add them to the hybridization tube.

6. Incubate the tubes at 65°C for at least 6 h in constant rotation prior to washing.

Washing of the filters:

1. Prepare for each tube 500ml *Washing Solution I* and 1000 ml *Washing Solution II*

Washing solution I (65°C)		Washing Solution II (42°C)	
SSC 2x	50ml SSC 20x	SSC 0.1x	5ml SSC 20x
SDS 1%	25ml SDS 20%	SDS 0.1%	5ml SDS 20%
Final volume	500ml H_2O	Final volume	1000ml H_2O

2. Wash the filters in the following order:

50 ml *Wash Sol. I* at 65°C in tube	10 min, tube rotation
450 ml *Wash Sol. I* at 65°C in tube	15 min with agitation
500 ml *Wash Sol. II* at 42°C in a tray	15 min with agitation
500 ml *Wash Sol. II* a 42°C in a tray	15 min with agitation

3. Dry the filters with 3M paper, cover with saran wrap and expose to a storage phosphor screen in an appropriate cassette.

Re-probing method:

- Boil a solution of 0.1xSSC, 1% SDS
- Add it to the filter and agitate for 15-20 min at 65°C
- Wash filter with water

2.6.6.4 Quantification of replication intermediates

Quantification of X-shaped intermediate signals was performed using the Image Quant software (GE Healthcare) as in (Branzei et al., 2008; Vanoli et al., 2010). For each time point, areas corresponding to the monomer spot (M), the X-spike signal and a region without any replication intermediates as background reference were selected and the signal intensities (SI) in percentage of each signal were obtained. The values for the X and monomer were corrected by subtracting from the SI value the background value after the latter was multiplied for the ratio between the dimension of the area for the intermediate of interest and for background. Thus, the values for X and M were calculated in the following way:

$$X = SI(Xs) - \frac{SI(backgroud) * A(Xs)}{A(background)}$$

$$M = SI(M) - \frac{SI(backgroud) * A(M)}{A(background)}$$

The relative signal intensity for the X was then determined by dividing the value for X with the sum of the total signals (the sum of the X and monomer values).

$$Spike = \frac{X}{X + M}$$

2.6.7 Pulse Field Gel Electrophoresis (PFGE)

Pulse Field Gel Electrophoresis (PFGE) is a technique that allows the separation of large DNA molecules, like entire chromosomes. Differently from standard gel electrophoresis, the electric field applied periodically changes direction during the run. PFGE was carried out as described in (Branzei et al., 2004).

Solutions and Materials

- 1% Low Melting Point (LMP) agarose (SeaKem Gold Agarose, Lonza) in 0.125 M EDTA pH 8.0 at 50°C.
- Ice cold 50 mM EDTA pH 8.0
- 10 mg/ml Zymolyase stock (1000 U/ml)
- 20% Sarkosyl stock at RT
- 20 mg/ml Proteinase K stock
- 10 mg/ml RNAse stock
- SCE solution: 1 M Sorbitol, 0.1 M Sodium citrate, 0.06 M EDTA pH 8.0
- Solution I: SCE, 0.2% β-mercapto ethanol, 1 mg/ml Zymolyase (100 U/ml)
- Solution II: 0.5 M EDTA pH 8.0, 1% Sarkosyl, RNAse 100 µl/ml
- 1X TE pH 8.0
- Plugs molds from Bio-Rad
- Pulse Filed Certified Agarose (Bio-Rad), ultra pure DNA grade agarose
- 5X TBE

DNA isolation in agarose plugs

1. Take 25 ml of 1 x 10^7 cells/ml and add Sodium Azide to a final concentration of 0.1%. Put immediately in ice and leave until all the time points are collected.

2. Spin down cells in 50 ml falcon tube by centrifugation at 4000 rpm for 5' at 4°C.

3. Resuspend cells in ice with 1 ml of cold 50 mM EDTA pH 8.0 and transfer them in 1.5 ml eppendorf tube.

4. Spin down cells by centrifugation at 14000 rpm for 3' at 4°C.

5. Wash one more time with 1ml of cold 50 mM EDTA pH 8.0.

6. Spin down cells by centrifugation at 14000 rpm for 3' at 4°C and be sure to remove all the EDTA with a pipette.

7. Leave the pellet in ice (it can be stored ON).

8. Melt 1% LMP agar and store in a waterbath at 50°C.

9. Prepare the plugs covering the bottom with a tape.

10. Resuspend the cells in Solution I 50 µl for each plugs; β-mercapto ethanol and Zymolyase are freshly added to SCE solution. If you have started from a 25 ml yeast colture, you need 5ml (5 x 10^7 cells) for each plug, so you are going to make 5 plugs and you resuspend the pellet in 250 µl of Solution I. If you have started with a different concentration of cells, in this step you can adjust the concentration so that you will have 5 x 10^7 cells for plugs.

11. Pre-warm each sample in a thermoblock at 50°C for about 1' and then add an equal volume of 50°C molten LMP agarose and mix quickly and gently with a pipette. This step needs to be done very quickly, in order to avoid to cool down the agarose and make it solidify while you are pipetting it.

12. Fill plugs mold with cells/agarose mix (approximately 90 µl per plug).

13. Leave the molds at RT for 20' and then put them at 4°C for 10' in order to allow blocks to solidify.

14. Eject plugs in a 15 ml falcon tube and cover them with Solution I, generally you can calculate around 0.5 ml for each plug (2.5 ml if you have 5 plugs).

15. Leave at 37°C for 1 h in a waterbath. This step can be extended leaving the plugs in Solution I ON.

16. Gently remove the Solution I without damaging the plugs, wash the plugs with abundant volume (5-10 ml) of 0.5 M EDTA pH 8.0 and remove it immediately. You can use a vacuum pump with a tip in order to remove well without touching the plugs.

17. Resuspend the plugs with Solution II, you can still calculate 0.5ml for each plug.

18. Incubate at 37°C for 60'-90'.

19. Add Proteinase K to a final concentration of 1 mg/ml.

20. Leave ON at 37°C.

21. Discard gently the Solution II and wash 3 times with 5 ml of 1X TE pH 8.0 directly in the falcon tube. It is important to wash well because you need to get rid of all the detergent and of the cells debris that might interfere with the run. You can use a vacuum pump with a tip to remove well the washes.

21. Transfer the plugs in a new 15 ml falcon tube, add 10 ml of 1X TE pH 8.0 and leave them on a rotating orizontal wheel for 1 h at the minimum speed.

22. Equilibrate the plug that you want to analyze for 2 h in the running buffer of the gel (0.5X TBE) in the orizontal wheel in a 1.5 ml eppendorf tube. Leave the other 4 plugs in the 15 ml falcon tube with 1X TE at 4°C, where they can be stored for several months.

Run conditions

1. Agarose gel from Bio-Rad 0.9% in 200ml of 0.5X TBE at 65°C (without Ethidium bromide)

2. Running buffer 0.5X TBE 2.5 L 10°C

3. Run condition (20 h total, 10°C):

6 V/cm, 10 h, 60 sec pulse, angle 120°

6 V/cm, 10 h, 90 sec pulse, angle 120°

4. Ethidium bromide staining 1:20000 in 0.5X TBE in agitation for 30'

5. Take a picture of chromosomes after staining

Use the comb with just one tooth so that you will have one big well, if you do not have the comb with one tooth you can tape the comb with multiple teeth in order to have just one big tooth. Put the plugs in the only well using a spatula; try to put the plugs at the same distance between each other. Seal the plugs in place using the agarose gel 0.9% of the run.

Eventually, gels are subjected to Southern Blot and hybridized using specifically genomic probes. Probes used recognized TER302 and TER603 (Fachinetti et al., 2010).

Oligonuleotides used to amplify the probes by PCR

TER603

TER603Fw: GAATGCCCGAGCCCTAAAAA

TER603Rv: ATGTGAGCCATCTGGAAAGG

2.6.8 Plasmid assay

Plasmid assay is a technique that allows the analysis of the topological status of an episomal plasmid. This assay was performed as described in (Baxter and Diffley, 2008; Kegel et al., 2011) with some variations.

<u>DNA extraction</u>

CTAB DNA extraction is carried out as described for 2D gel electrophoresis.

Run conditions

25 µg of genomic DNA is loaded in a 0.8% TBE 0.5X gel in the presence of 0.5 µg/ml of EtBr. The run of DNA is carried out at 50 V at RT for 30 hours.

Southern blot

Southern blot is performed as described for 2D gel electrophoresis. A probe recognizing the AMP locus of pRS316 plasmid was used.

Oligonucleotides used to amplify the probe by PCR

AmpF: GACGCTCAGTGGAACGAAAACTCACG

AmpR: GGAGGACCGAAGGAGCTAACCGC

2.6.8 Molecular combing

Molecular combing is a method to stretch DNA molecules on silanized glass coverslips and allows the analysis of the activation of replication origins and the progression of replication forks at the level of single DNA molecules, after the incorporation of thymidine analogs, like BrdU and EdU, in newly synthesized DNA. This assay tells about variability of replication profiles in single cells.

Molecular combing experiments have been performed in collaboration with the lab of Philippe Pasero at the Institute of Human Genetics in Montpellier. A detailed protocol of the technique is described in (Bianco et al., 2012).

3 Results

3.1. Limiting expression of Smc5/6 complex subunits to G2/M does not affect cell proliferation and DNA damage tolerance

3.1.1 Endogenous promoters of *SMC5, SMC6* and *MMS21* can be substituted with a promoter containing regulatory elements of Clb2 without affecting cell viability

To understand the essential functions of Smc5/6 complex, we asked first if they are manifested throughout the cell cycle or are specific to S or G2/M phases of the cell cycle. We applied two different tags, namely the G2-tag and the S-tag (see below), to genes encoding crucial components of the complex to restrict their expression either in G2/M or in S phase, respectively.

We began by applying the G2-tag to the three key subunits Smc5, Smc6 and the SUMO ligase Mms21. The G2-tag takes advantage of regulatory elements of the mitotic B-type cyclin Clb2 (Karras and Jentsch, 2010): Clb2 is expressed in the G2/M phase of the cell cycle and it is downregulated at the end of mitosis and in G1, being ubiquitylated by APC (Anaphase Promoting Complex) and degraded by the 26S proteasome. The G2-tag consists of the promoter of Clb2 and the sequence encoding for the first 180 aminoacids, which carry the degrons (D-, KEN1- and KEN2- boxes), a mutation in the nuclear export signal NES sequence (L26A) that prevents the nuclear export and a Clb2-derived antibody epitope (Figure 3.1). When introduced upstream of the open reading frame of the target gene, this tag allows in principle restricted expression of the tagged protein to G2/M.

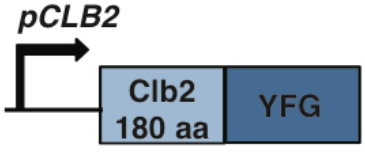

Figure 3.1 The G2-tag. Schematic representation of the G2-tag system, with the promoter of the G2/M cyclin Clb2 and the N-terminal region of the protein located at the 5' UTR of Your Favorite Gene (YFG).

Since restricted expression to G2/M of the genes encoding Smc5/6 subunits could potentially result in lethality, due to possible essential functions of the complex in S phase, we transformed wild-type (wt) diploid cells with the G2-tag constructs *G2-SMC5, G2-SMC6* and *G2-MMS21* to obtain the corresponding three heterozygous mutants, *SMC5/G2-SMC5*, *SMC6/G2-SMC6* and *MMS21/G2-MMS21*. We then recovered the haploid single mutants by tetrad dissection. In all cases, cells in which Smc5-6 components were restricted to G2/M were characterized by normal fitness and proliferation speed (Figure 3.2a).

To verify that the applied G2 tag was functional –that is, the expression of each subunit was indeed confined to G2/M, we checked by western blot the corresponding proteins at different points during cell cycle. To this purpose, we further tagged C-terminally the G2-Smc5 and G2-Mms21 variants with a PK epitope and G2-Smc6 with Flag. We then synchronized the three different cell types, G2-Smc5-PK, G2-Smc6-Flag and G2-Mms21-PK, in G1 with α-factor and released them in media for 90 min taking samples for FACS analysis and TCA extraction every 10 min. As it can be observed from the time course experiments in Figure 3.2b, all three subunits of the Smc5/6 complex were absent in G1 and in early S phase and started to be expressed concurrently with Clb2 at 50-60 min post release, indicating that the expression of each G2-tagged variant is correctly restricted to G2/M.

a

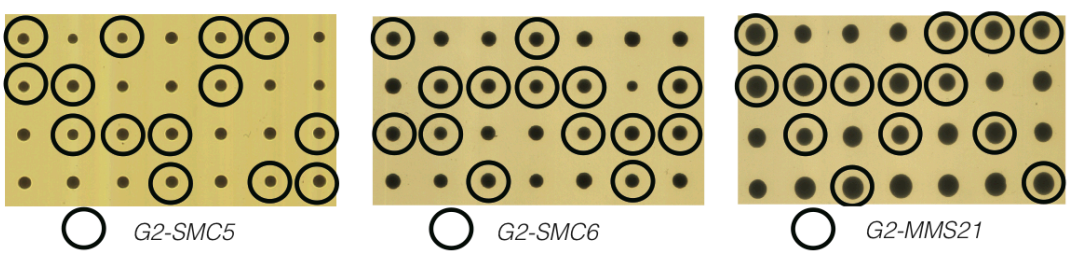

b

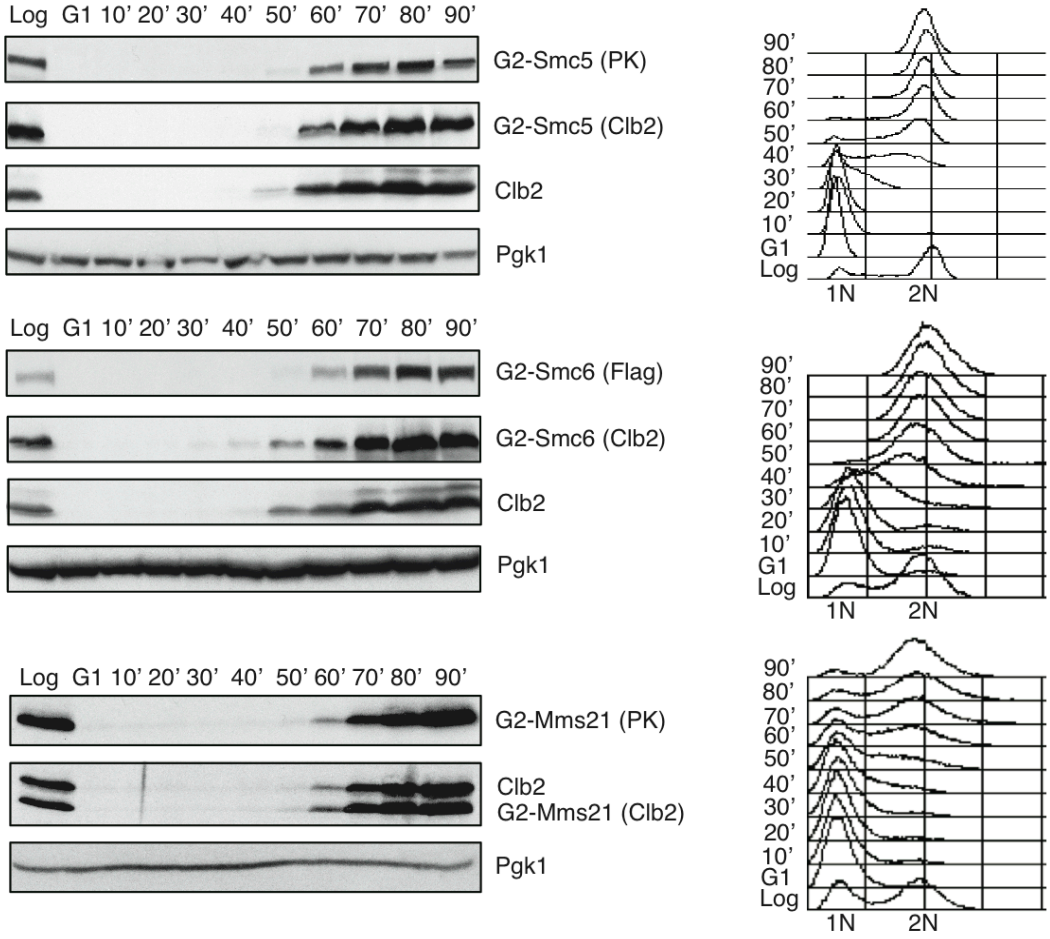

Figure 3.2 *G2-SMC5/6* haploid cells are viable. a) Plates with tetrad dissections of the diploids *SMC5/G2-SMC5, SMC6/G2-SMC6* and *MMS21/G2-MMS21* were grown for 3 days at 28°C. Black circles indicate the haploid single mutants *G2-SMC5, G2-SMC6, G2-MMS21*. b) G2-Smc5-PK, G2-Smc6-Flag and G2-Mms21-PK cells were synchronized in G1 and released in YPDA for 90 min. Samples for TCA protein extraction and FACS analysis were collected every 10 min after the release. Western blots were performed using anti-PK (G2-Smc5, G2-Mms21), anti-Flag (G2-Smc6), anti-Clb2 (G2-Smc5, G2-Smc6, G2-Mms21, Clb2) and anti-Pgk1 (used as a loading control). FACS plots of the collected samples are shown on the right.

We conclude that the G2-tag is functional for Smc5, Smc6 and Mms21 and cells that lack any of these components in S phase grow normally and do not show prominent proliferation or cell cycle progression problems.

3.1.2 *G2-SMC5 G2-SMC6* double mutants cells are viable and sustain Smc5/6 functions

To address the possibility that homodimers of Smc5 or Smc6 proteins would form in S phase and substitute functionally the heterodimer Smc5-Smc6, we constructed *G2-SMC5 G2-SMC6* cells by crossing *G2-SMC5-PK* with *G2-SMC6-FLAG* cells and recovering the double mutants by tetrad dissection. *G2-SMC5-PK G2-SMC6-FLAG* cells were viable with a fitness resembling the one of wt cells (Figure 3.3a). To verify once again the restricted expression of the G2-tagged Smc5 and Smc6 variants, we synchronized *G2-SMC5 G2-SMC6* cells in G1 and released in YPDA in the presence of nocodazole for 120 min, taking FACS and protein samples every 15 min. Western blotting was again used to monitor the expression of G2-Smc5-PK, G2-Smc6-Flag and Clb2 at various time points. In *G2-SMC5 G2-SMC6* cells, Smc5-6 variants were correctly restricted to G2/M: both proteins became detectable at 60-70 minutes upon release from G1 arrest, coincidentally with Clb2 (Figure 3.3b). These data indicate that absence of both Smc5 and Smc6, and consequently lack of the entire Smc5-6 complex in early S phase is not detrimental for cell viability and growth.

a

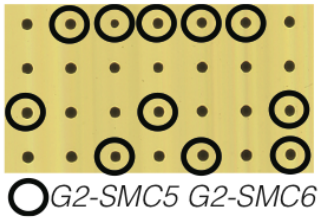

b

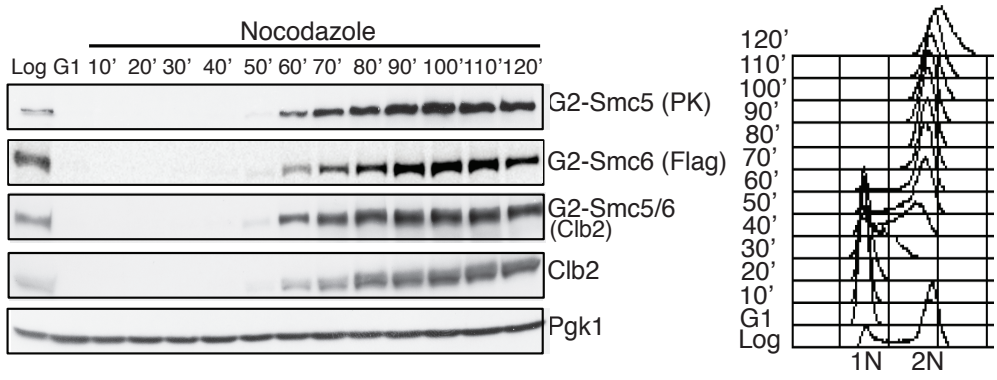

Figure 3.3 *G2-SMC5 G2-SMC6* cells are viable. a) Diploids *SMC5/G2-SMC5 SMC6/G2-SMC6* were dissected on YPDA plates and haploid cells scanned after 3 days. Black circles indicate the double mutants *G2-SMC5 G2-SMC6.* b) *G2-SMC5-PK G2-SMC6-FLAG* cells were arrested in G1 and released in nocodazole 20 μg/ml for 2 h. Samples for TCA protein extraction and FACS analysis were collected every 10 min after the release. Western blots were done using anti-PK (G2-Smc5), anti-Flag (G2-Smc6), anti-Clb2 (G2-Smc5, G2-Smc6, Clb2) and anti-Pgk1 (loading control). FACS analysis of the samples is shown on the right.

To monitor the initiation of replication and origin firing, we performed BrdU ChIP-on-chip experiment in wt and *G2-SMC5-PK G2-SMC6-FLAG* cells. Strains were arrested in G1 and released in HU 200 mM for 45 min at 23°C. We checked by western blotting that at the time point collected (45 min) no expression of G2-Smc5-PK and G2-Smc6-Flag was detected (Figure 3.4). The BrdU incorporation efficiency between wt and the mutant was comparable, with highly statistical significant overlap between the genomic profiles (p= 2.10E-237) as it is shown in Figure 3.4, which reports chromosome III maps of BrdU ChIP-on-chip. This result indicates that in the absence of a functional Smc5/6 complex in early S phase, origin firing and replication initiation are not affected.

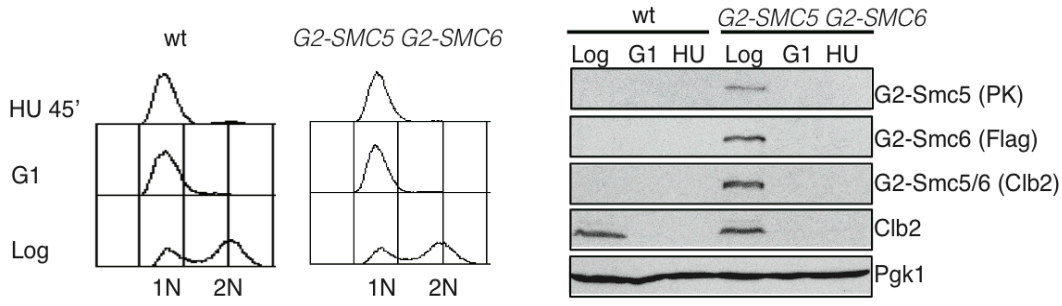

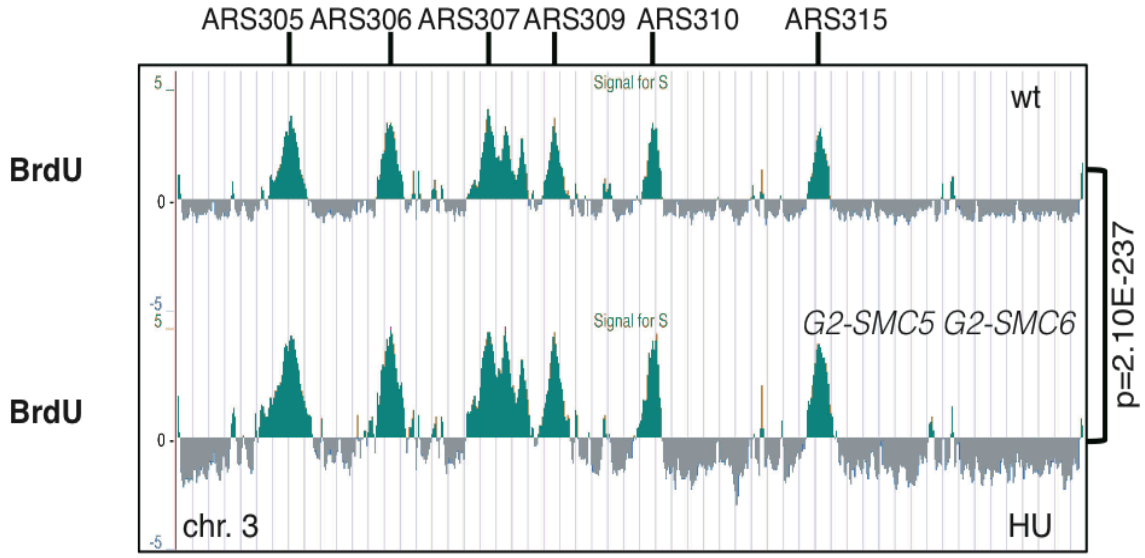

Figure 3.4 Origin firing efficiency is not decreased in *G2-SMC5 G2-SMC6* cells. Wt and *G2-SMC5-PK G2-SMC6-FLAG* cells were synchronized in G1 and released in HU 200 mM for 45'. Samples for FACS analysis, protein extraction and BrdU-ChIP-on-chip were collected. Western blots were done using anti-PK (G2-Smc5), anti-Flag (G2-Smc6), anti-Clb2 (G2-Smc5, G2-Smc6, Clb2) and anti-Pgk1. Chromosome III of the BrdU-ChIP-on-chip binding profile of wt and mutant is reported, with the p value of the significance of the genome wide clusters overlap indicated.

To test replication fork speed of individual forks in the absence of Smc5-6, we performed molecular combing experiments to monitor the progression of replication forks at the level of single DNA molecules. BrdU incorporating wt and *G2-SMC5-PK G2-SMC6-FLAG* strains were transformed with a plasmid encoding hENT1, which facilitates the entrance in the cell of thymidine analogs, and were analyzed for molecular combing in several conditions. We note that the molecular combing experiments presented here were performed in Philippe Pasero's lab in Montpellier by Armelle Lengronne and Axel Delamarre. For these experiments, either asynchronously growing cells were treated with EdU for 10 min and 20 min or cells were arrested in G1 and released in EdU containing media supplemented with HU 200 mM (90 min). In all analyzed conditions the length of the replicated tract was very similar between the two strains (Figure 3.5), suggesting that Smc5/6 is not required for the progression of replication forks in early/mid S phase.

a

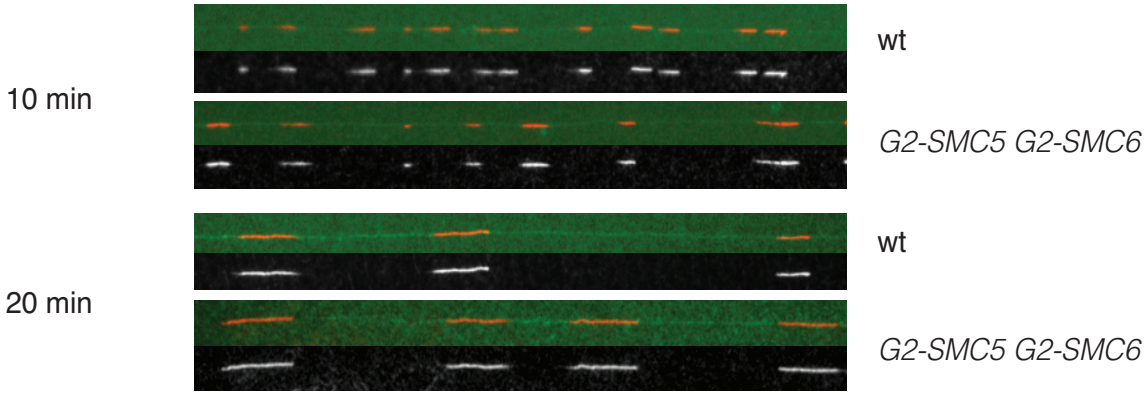
10 min
wt
G2-SMC5 G2-SMC6
20 min
wt
G2-SMC5 G2-SMC6

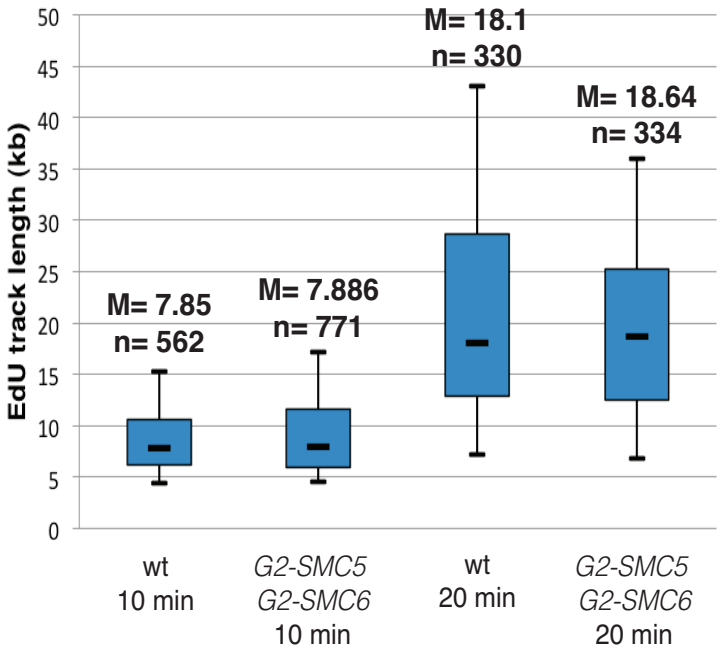
EdU track length (kb)
50
45
40
35
30
25
20
15
10
5
0
M= 7.85
n= 562
M= 7.886
n= 771
M= 18.1
n= 330
M= 18.64
n= 334
wt
10 min
G2-SMC5
G2-SMC6
10 min
wt
20 min
G2-SMC5
G2-SMC6
20 min

b

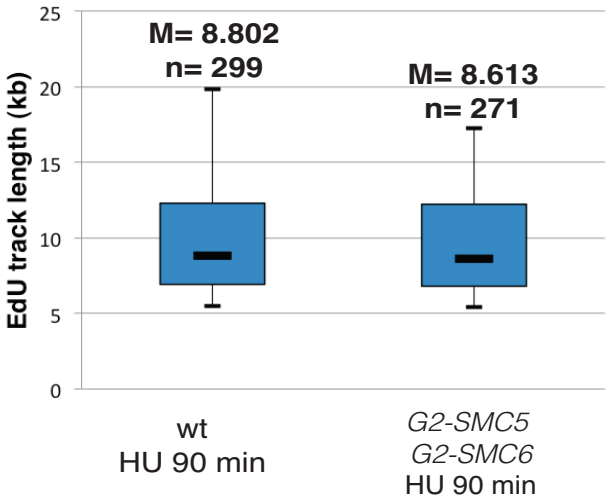

Figure 3.5 Replication fork progression in S phase is not affected in *G2-SMC5 G2-SMC6* cells. a) Wt and *G2-SMC5 G2-SMC6* cells were analyzed using the molecular combing technique. Asynchronous growing cells in YNB –Leu were treated at 0 min with EdU 50 μM and samples were collected at 10 min and at 20 min in unperturbed S phase. Examples of forks are reported, with DNA stained with the green fluorescent dye YOYO-1 and EdU tracks stained in red. The box and whiskers plots report the median as the black line, the 25 and the 75 percentiles as the box and the 10 and the 90 percentiles as the whiskers. M indicates the value of the median and n the number of the EdU tracks counted. b) wt and *G2-SMC5 G2-SMC6* cells were arrested in G1 and released in media containing HU 200 mM and EdU 400 μg/ml for 90 min. Box and whiskers plots as described above.

Since the association of Smc5/6 to chromosome is integral for its functions (Jeppsson et al., 2014a; Kegel et al., 2011; Lindroos et al., 2006), we performed ChIP-on-chip studies of G2-Smc5-PK and G2-Smc6-Flag and we compared them with the binding of the wt proteins. The double tagged strains, *SMC5-PK SMC6-FLAG* and *G2-SMC5-PK G2-SMC6-FLAG*, were synchronized in G1 and released in nocodazole for 180 min. Samples were collected at G2/M and processed for ChIP-on-chip analysis for the PK and the FLAG tagged wild-type or G2-tagged variants. As already reported for Smc6, Smc5-PK and Smc6-Flag have multiple binding sites in G2/M, including centromeres, pericentromeric regions and chromosome arms. Similarly, G2-Smc5-PK and G2-Smc6-Flag bind to the

same genomic regions. The genome-wide p values of the clusters overlap between all the relevant pairs considered (Smc5 vs Smc6, Smc5 vs G2-Smc5, Smc6 vs G2-Smc6, G2-Smc5 vs G2-Smc6) were highly significant, indicating that all the proteins analyzed share similar/identical binding sites on chromosomes. A snapshot of chromosome 3 is reported with the p values derived from genome-wide cluster analysis indicated on the right (Figure 3.6). Thus, Smc5 and Smc6, even if are not expressed in S phase, are able to bind DNA in G2/M and their loading in S phase is not a pre-condition for their recruitment to chromatin.

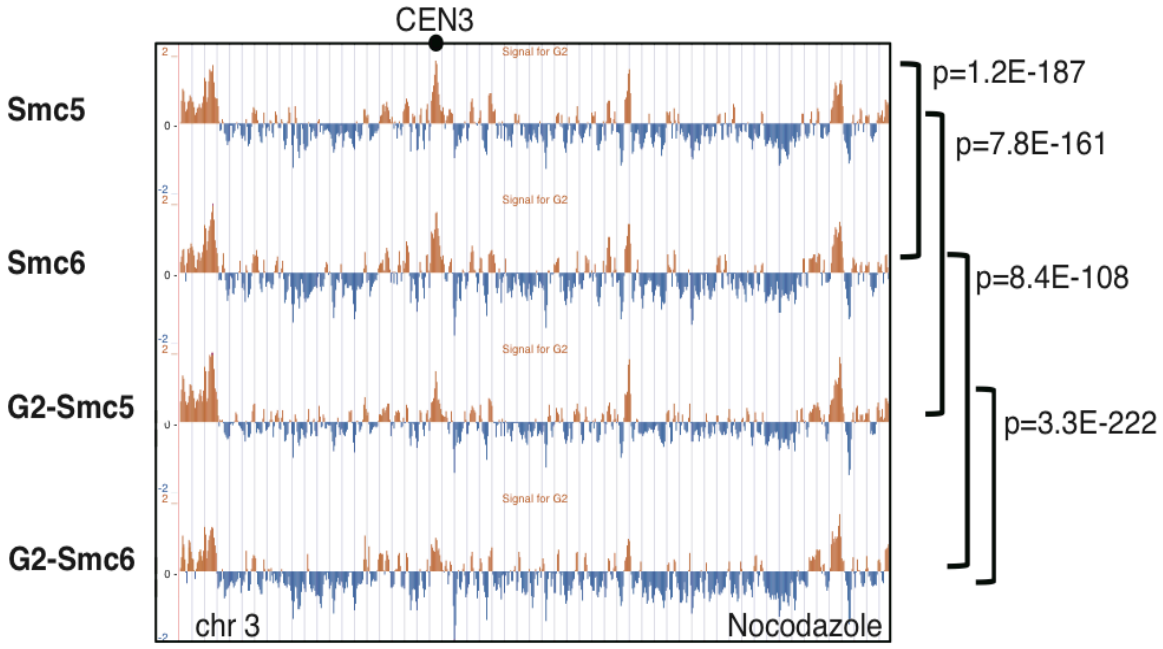

Figure 3.6 Chromatin binding profile of Smc5/6 and G2-Smc5/6 in G2/M. *SMC5-PK SMC6-FLAG* and *G2-SMC5-PK G2-SMC6-FLAG* cells were synchronized in G1 and released in nocodazole 20 µg/ml for 3 hours when samples were collected for ChIP-on-chip analysis of Smc5-PK, Smc6-Flag, G2-Smc5-PK and G2-Smc6-Flag. Chromosome III is reported as an example and p values of the genome wide overlap between clusters of relevant pairs are indicated.

When we analyzed carefully the chromosomal association of wt Smc5/6 and G2-Smc5/6 in G2/M synchronized cells, we noticed that, even if the genome-wide clusters significantly overlapped between all the proteins, as mentioned above, some differences could be observed between the association to short and long chromosomes. In the model proposed in

(Jeppsson et al., 2014a; Kegel et al., 2011), the frequency of binding of Smc6 increases with the length of the chromosomes and is triggered by the number of SCIs. We were able to reproduce this analysis, since in our experimental conditions the frequency of binding, calculated as the number of peaks per kb, of Smc5-PK and Smc6-Flag increases significantly for longer chromosomes (12, 14, 16) compared to shorter ones (1, 3, 9). In Figure 3.7 it can be noticed that the number of peaks of Smc5 and Smc6 per kb on short chromosomes is between ~0.8-0.9, while on longer chromosomes is almost doubled being ~0.17-0.19. Remarkably, G2-Smc5-PK and G2-Smc6-Flag have almost the same number of peaks per kb as the wt proteins on shorter chromosomes (~0.8-0.9), but not on longer ones, where is significantly less, ~0.11-0.13. Thus, G2-Smc5-PK and G2-Smc6-Flag, despite the significant genome-wide overlap, do not bind to longer chromosomes with the same frequency of wt proteins. This result is in line with the model proposed, since if SCIs trigger the binding of Smc5/6 during replication in order to release topological stress mainly on long chromosomes (which have more SCIs compared to shorter ones), in *G2-SMC5 G2-SMC6* the complex is largely absent in S phase and is not triggered to all the sites of replication stress. Our results also suggest that Smc5/6's recruitment to SCIs is not crucial for completing replication and fork speed.

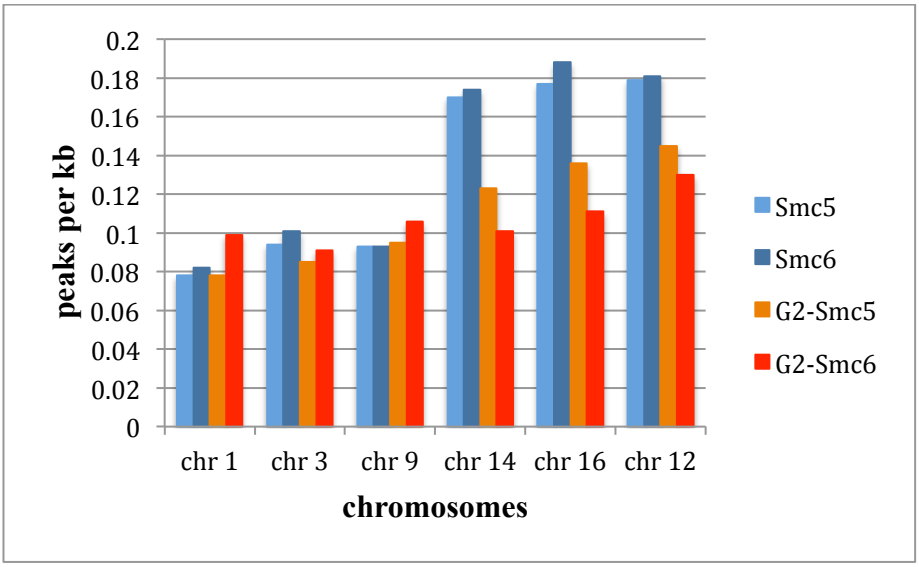

Figure 3.7 Number of peaks per kb of Smc5/6 and G2-Smc5/6 on some short (1, 3, 9) and long (14, 16, 12) chromosomes. For each chromosome analyzed, the number of peaks per kb was counted and divided for the length of the chromosome.

Smc5/6 is known to bind early origins of replication in S phase in the presence of HU (Bustard et al., 2012; Jeppsson et al., 2014a). We asked if Smc5 can bind DNA in S phase when Smc6 is not expressed, by analyzing the ChIP-on-chip profile of Smc5-PK in wt versus *G2-SMC6* cells early in S phase in the presence of HU. Consistent with previous results, we found that 68.5% of the early/middle origins were enriched for Smc5 in wt cells. By contrast, we observed very few binding clusters of Smc5 in *G2-SMC6* background, with a total coverage on the genome of about 1% and only 5.58% early/middle ARS bound by the protein (Figure 3.8). Thus, we conclude that Smc5/6 acts as a compulsory heterodimer and, in the absence of the partner Smc5-6 subunit, the other one does not bind DNA.

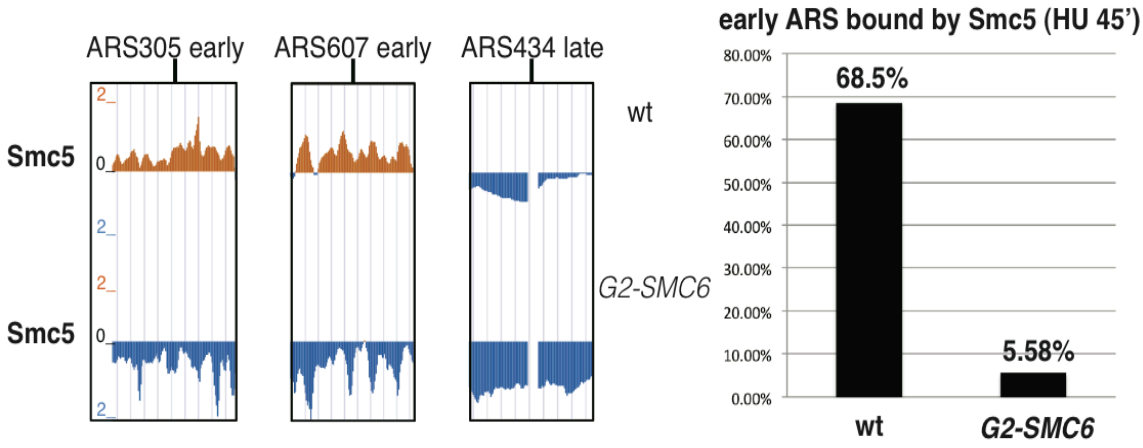

Figure 3.8 Smc5 does not bind to origins of replication in HU treated *G2-SMC6* cells. Wt and *G2-SMC6* cells were arrested in G1 and released in HU 200 mM for 45 min when samples for ChIP-on-chip analysis of Smc5-PK were collected . The binding of Smc5-PK in wt and *G2-SMC6* at two early origins of replication (*ARS305, ARS607*) and at one late origin (*ARS434*) is shown. In wt cells Smc5 binds to most (68.5%) of early ARS, while in *G2-SMC6* cells it binds to very few of them (5.58%).

Conversely, we tested if Smc5-PK is able to bind chromosomes equally in wt and *G2-SMC6* cells in G2/M. ChIP-on-chip was performed after G1 release in media containing nocodazole, with samples being collected at 3 h post-release when the cells were in G2/M. Smc5 binding profile was very similar in wt and *G2-SMC6* cells, with a highly significant overlap between genome-wide clusters (p=2.50E-240). Chromosome V is shown as example (Figure 3.9). In *G2-SMC6* cells in S phase G2-Smc6 is not expressed and Smc5 is not able to bind DNA, but in G2/M, when G2-Smc6 is expressed and binds DNA, also wt Smc5 is recruited equally well to chromosome arms and centromeres. Thus, even when Smc5-6 is loaded onto chromatin postreplicatively (such as in *G2-SMC6*, *G2-SMC5 G2-SMC6* cells), there is no delay in cellular proliferation or replication fork speed.

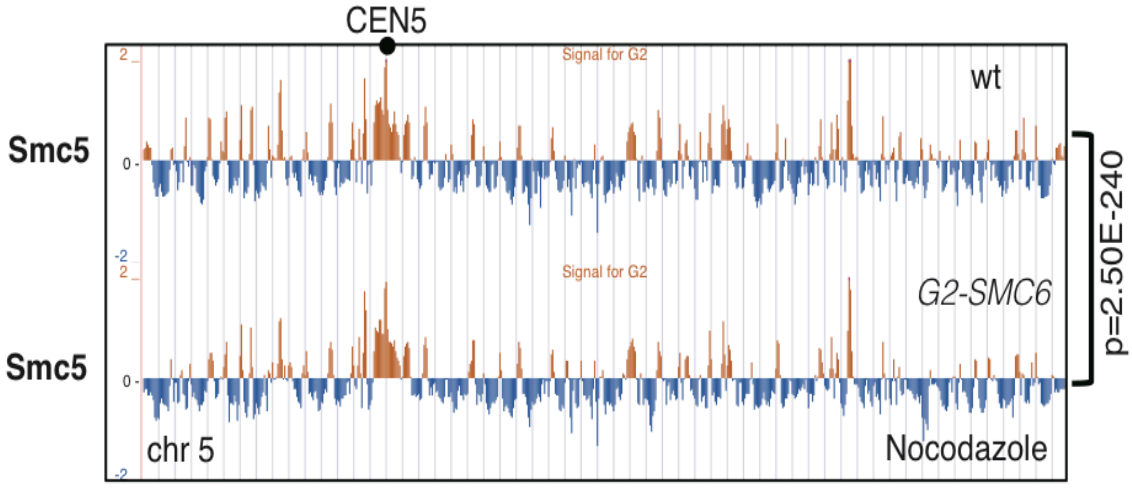

Figure 3.9 Smc5 is loaded after replication in *G2-SMC6* cells. Wt and *G2-SMC6* cells were synchronized in G1 and released in nocodazole 20 µg/ml for 3 h when samples were collected for ChIP-on-chip analysis of Smc5-PK. Chromosome V is shown as example and p value of the genome-wide overlap between clusters of significance is reported on the right.

3.1.3 *G2-SMC5/6* cells are proficient in DNA damage tolerance

Since *smc5-6* mutants are defective in DNA damage tolerance and sensitive to DNA damaging agents, we asked if the postreplicative expression of the Smc5/6 could negatively

affect the DNA repair capability of the cells. By spot assay all the mutants tested, that is *G2-SMC5*, *G2-SMC6*, *G2-MMS21* and *G2-SMC5 G2-SMC6*, are not sensitive to MMS (Figure 3.10), differently from *smc6-56* and *smc6-P4* that are used as positive controls (Chen et al., 2009; Onoda et al., 2004). Therefore, *G2-SMC5/6* cells are proficient in DNA damage tolerance even if the complex is supplied postreplicatively.

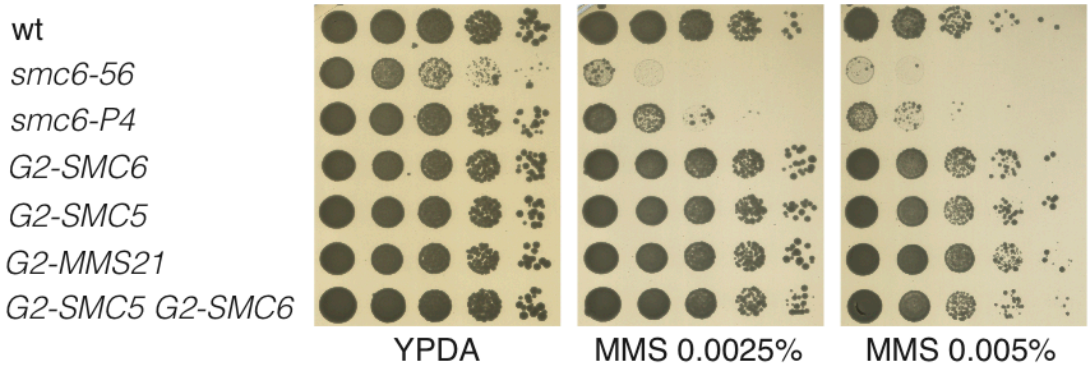

Figure 3.10 *G2-SMC5/6* cells are not sensitive to MMS. Ten fold dilutions of the strains indicated were plated on YPDA and on MMS plates at the indicated concentrations. *smc6-56* and *smc6-P4* were used as positive controls. Plates were incubated at 25°C and scanned after 3 days.

Previous studies showed that *smc5-6* mutants accumulate recombination X-shaped intermediates formed in the context of error-free DDT during replication of damaged templates (Branzei et al., 2006; Chen et al., 2009; Choi et al., 2010; Sollier et al., 2009). To address if *G2-SMC6* cells are defective in X-shaped intermediate metabolism, we arrested wt and *G2-SMC6* in G1 and then released them in the presence of MMS 0.033% for 3 hours, taking several time points for FACS analysis and 2D gel electrophoresis. We monitored replication/recombination intermediates arising at an early origin of replication on chromosome III, *ARS305* (Figure 3.11a). Replication and repair intermediates (bubble, Y-arc and X-spike) can be observed after southern blot of *ARS305* 30 min after release from G1 arrest, they start to decline at 60 min and they are completely absent from the region at 120 min due to resolution or migration to flanking regions (Figure 3.11b). Similar kinetics of X-molecule formation and disappearance were observed in wt and *G2-SMC6.*

Thus post-replicative Smc6 is proficient in X-molecule metabolism and DNA damage tolerance.

a

b

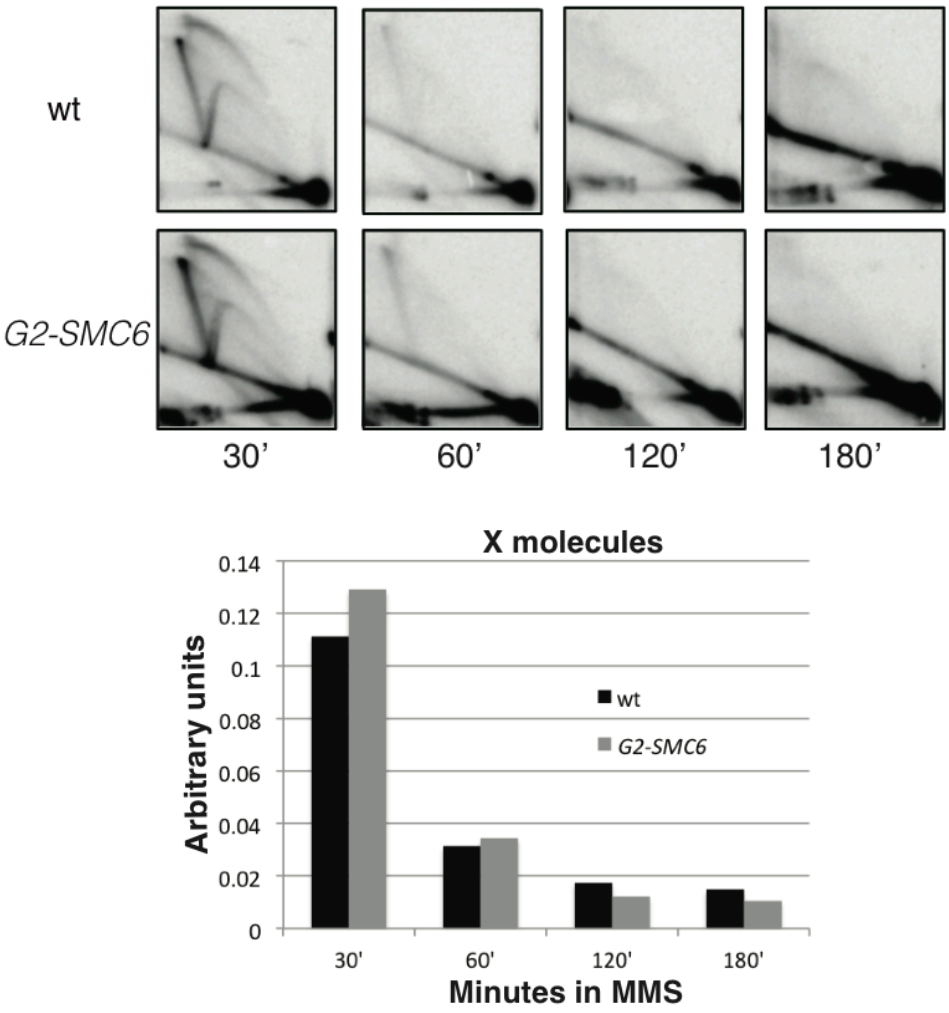

Figure 3.11 *G2-SMC6* cells are not defective in X molecules resolution. a) Schematic representation of the digestion used for 2D gel analysis of *ARS305*. NcoI is used as restriction enzyme and the resulted fragment is 5 kb long. b) Wt and *G2-SMC6* cells were synchronized in G1 at 25°C and released in MMS 0.033% at 30°C. Samples for FACS analysis and CTAB extraction were collected at the indicated time points for 3 hours. Quantification of the X spike signal versus monomer spot is reported.

Finally, to analyze the response of single replication forks encountering DNA damage, we performed molecular combing experiments in wt and *G2-SMC5-PK G2-SMC6-FLAG* cells. Cells were arrested in G1 and released in media containing EdU and MMS for 30 min. As it is shown in the graph below, the track lengths between the two strains showed a very similar distribution (Figure 3.12), suggesting that Smc5/6 is not required for progression of early S phase replication forks during DNA damage treatment.

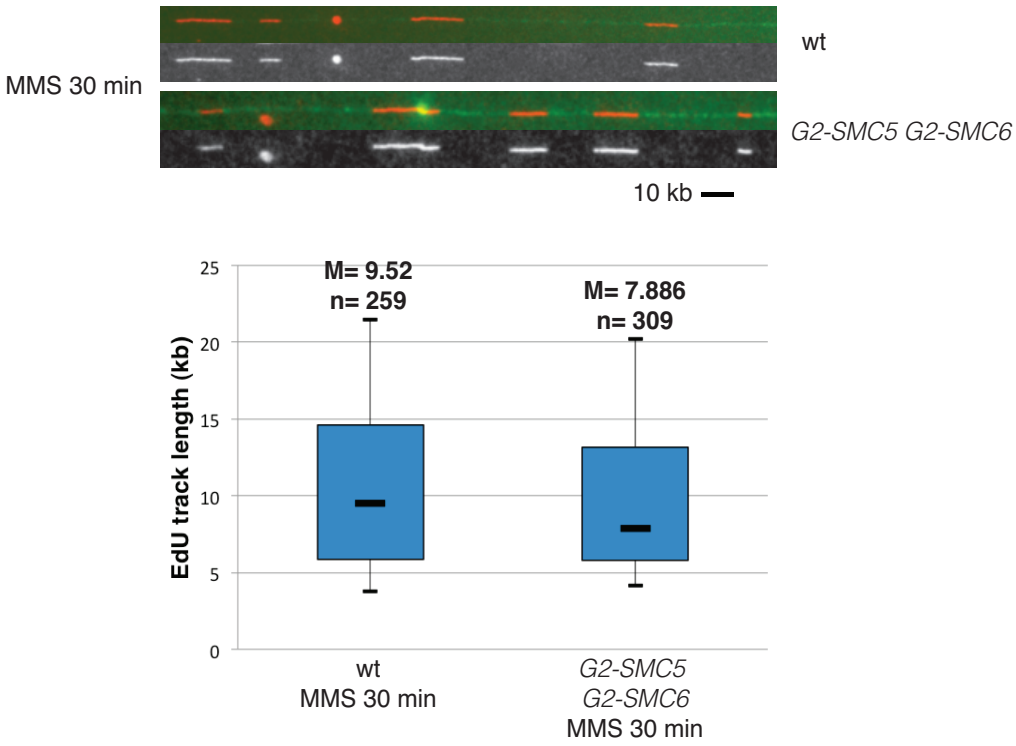

Figure 3.12 Replication fork progression in MMS is not affected in *G2-SMC5 G2-SMC6*. Wt and *G2-SMC5 G2-SMC6* cells were grown in YNB – Leu, arrested in G1 and released in media containing MMS 0.033% for 30 min when samples were collected for molecular combing analysis. Examples of forks are reported, with DNA stained with the green fluorescent dye YOYO-1 and EdU tracks stained in red. The box and whiskers plots report the median as the black line, the 25 and the 75 percentiles as the box and the 10 and the 90 percentiles as the whiskers. M indicates the value of the median and n the number of the EdU tracks counted.

3.2 Smc5/6 exerts its essential functions in G2/M

3.2.1 *S-SMC5* cells are lethal

We next tested whether the essential functions of Smc5/6 may be instead manifested in G2/M. To this end, we applied the so called S-tag (Hombauer et al., 2011). The S-tag works similarly to the G2-tag, but it contains the promoter and the sequence that code for the first N-terminal 195 aminoacids of Clb6 (Figure 3.13), a cyclin expressed during the S phase of the cell cycle, then ubiquitylated by the multisubunit ubiquitin ligase SCF complex and degraded by the 26S proteasome in G2. The endogenous promoter of the target gene is substituted by this construct, which allows for gene expression to be induced specifically in S phase, and then degradation of the tagged protein in G2/M.

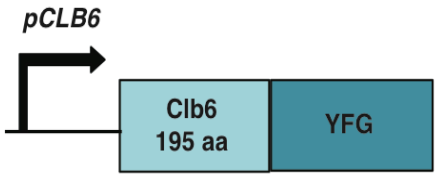

Figure 3.13 The S-tag. The S-tag, composed of the promoter of Clb6 and the nucleotides encoding the first 195 aminoacids of the protein, is put at the 5' UTR of Your Favorite Gene (YFG).

As we did for the G2-tag, we first transformed diploid cells in order to obtain heterozygous cells for the mutation introduced. We started applying the S-tag to *SMC5* locus and we obtained the diploid *SMC5/S-SMC5*, which we then dissected to recover haploid *S-SMC5* cells. Remarkably, S-SMC5 cells were dead (Figure 3.14a).

To examine if lethality was due to lack of SMC5 expression by the S-tag introduced, we C-terminally tagged both SMC5 alleles in the heterozygous diploid with the PK tag. We synchronized those diploid cells in G2/M, released them in the presence of HU 200 mM, allowing arrest in S phase, and then released again in nocodazole for 120 min so that we

could monitor the behavior of the S-tagged protein. We found that S-Smc5-PK is present in S phase and correctly downregulated in G2/M (Figure 3.14b).

a

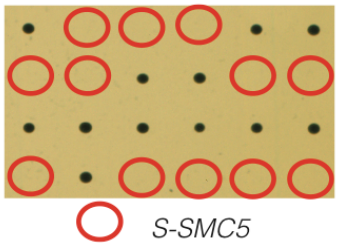

b

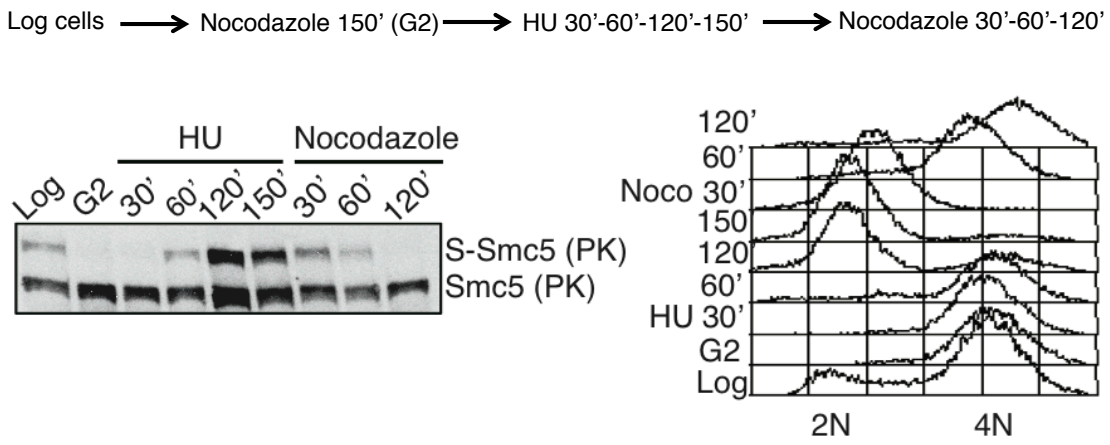

Figure 3.14 *S-SMC5* cells are lethal. a) Tetrads from diploids *SMC5/S-SMC5* were dissected and plates were incubated at 28°C for 3 days. Red circles indicate where haploid *S-SMC5* cells are, based on genetic segregation of markers. b) Diploid *SMC5-PK/S-SMC5-PK* were arrested with nocodazole, released in media containing 200 mM of HU for 150 min and then released from the HU-induced arrest in media containing nocodazole for additional 2 h. Samples for FACS and protein analysis were collected at the indicated time points. Western blot was done using anti-PK.

To verify that S-Smc5 variant is functional in the time window in which it is expressed, we performed ChIP-on-chip analysis in diploid cells. We first swapped the PK C-terminal tag of one isoform with Flag, in order to perform ChIP-on-chip of both variants, one tagged with PK (S-Smc5) and one with Flag (Smc5). Diploid cells Smc5-Flag/S-Smc5-PK were synchronized in G2/M and released in HU 200 mM for 130 min, when cells were in mid-S phase. Remarkably, both Smc5 and S-Smc5 variants bound to the same chromosomal

regions and with similar efficiencies. A snapshot of chromosome 3 with the genome-wide p value of the clusters overlap is reported in Figure 3.15.

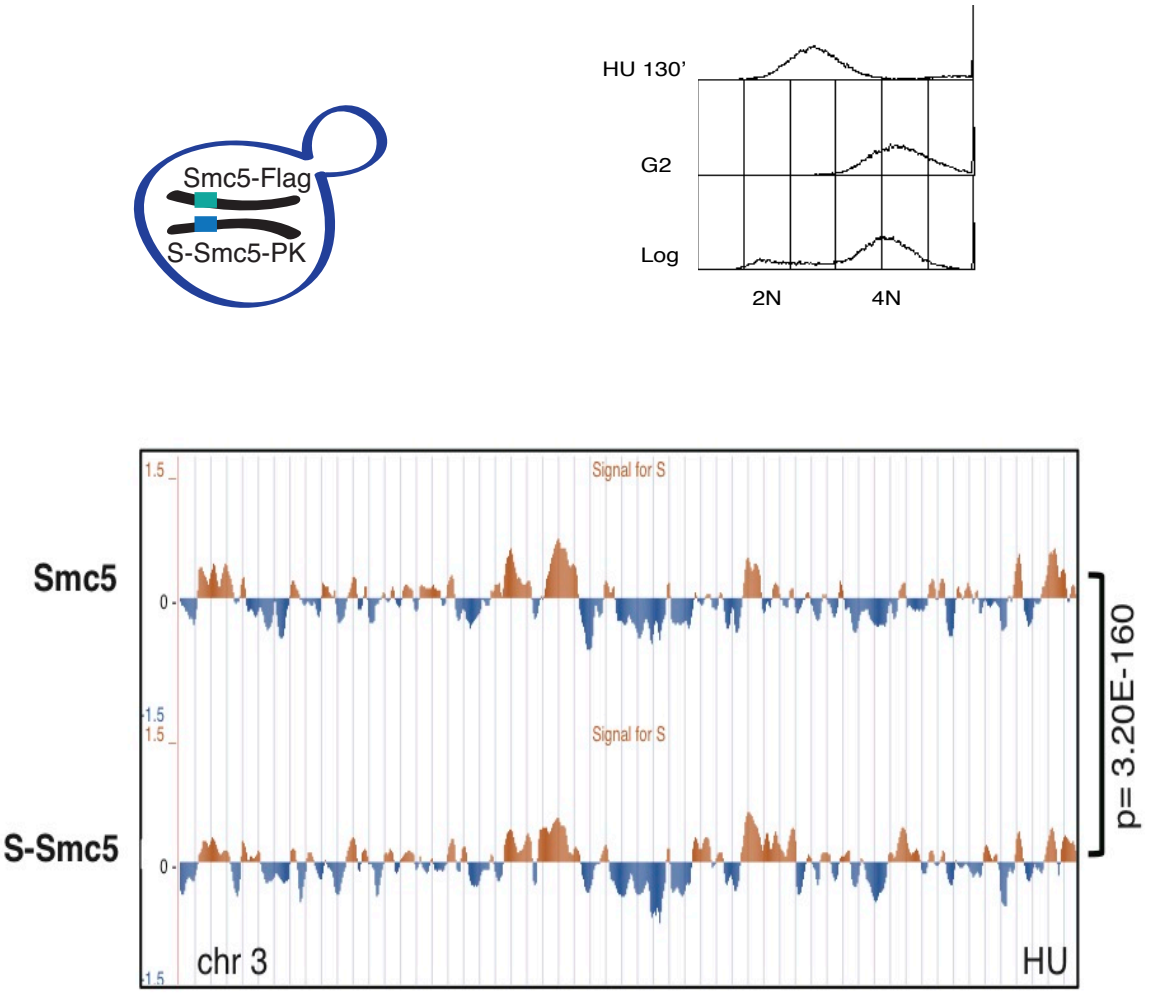

Figure 3.15 Smc5 and S-Smc5 bind similarly to chromatin in S phase. Diploid cells Smc5-Flag/S-Smc5-PK were synchronized in G2/M with nocodazole and released in the presence of HU 200 mM for 130'. Samples were collected in mid-S phase for ChIP-on-chip analysis of Smc5-Flag and S-Smc5-PK. A snapshot of chromosome 3 is reported with the p value indicating the significance of genome-wide clusters overlap.

Thus, S-Smc5-PK is present and functional in the heterozygous diploid, but cannot sustain cell viability in haploid cells, likely because of essential functions of Smc5-6 postreplicatively.

3.2.2 *S-MMS21* cells are sick and show phenotype of catastrophic mitosis

To corroborate the above interpretation, we applied then the S-tag to other components of the Smc5-6 complex. We transformed diploid cells with *S-MMS21* construct and we obtained the heterozygous *MMS21/S-MMS21*. Haploid single mutant *S-MMS21* cells recovered by tetrad dissection were characterized by poor growth (Figure 3.16a). The size of *S-MMS21* cells was very small compared to wt, meaning that these mutants, even if viable, are strongly delayed in the cell cycle progression. Since it is not possible to properly synchronize haploid *S-MMS21* cells in G1, we decided to perform western blot of Mms21-PK and S-Mms21-PK in the heterozygous diploid, with the same kinetic described above for the diploid Smc5-PK/S-Smc5-PK. S-Mms21-PK is also correctly regulated throughout the cell cycle, being degraded in G2/M and expressed mainly in S phase (Figure 3.16b).

a

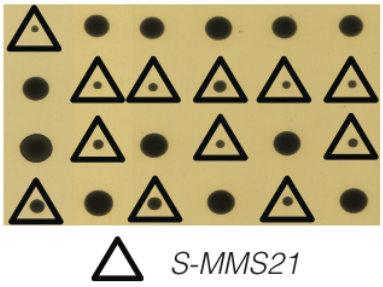

b

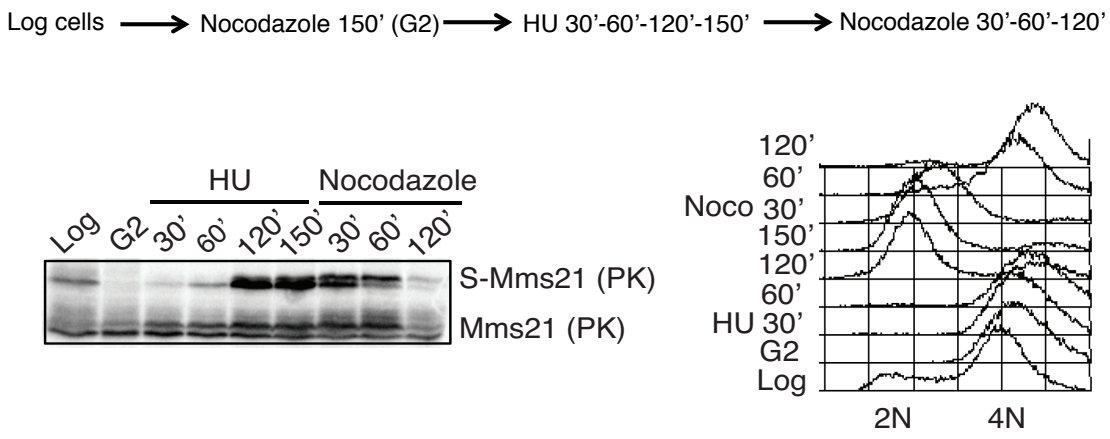

Figure 3.16 *S-MMS21* cells are sick. a) Tetrads from diploids *MMS21/S-MMS21* were dissected and plates were incubated at 28°C for 3 days. Black triangles indicate haploid *S-MMS21* cells. b) Diploid *MMS21-PK/S-MMS21-PK* were synchronized in G2/M with nocodazole, released in media containing 200 mM HU for 150 min and then released again in nocodazole for additional 2 h. Samples for FACS and western blot analysis were collected at the indicated time points. Western blot was done using anti-PK.

Since we noted aberrant cell shape and morphology of S-MMS21 cells, we decided to analyze chromosomal DNA of these cells by DAPI staining. To analyze cells in G2/M without using nocodazole and, at the same time, to allow them to reach G2 synchronously, we arrested wt and *S-MMS21* cells first in S phase using HU and then released them in YPDA medium for 100 min to let them reach G2/M. Cells were then fixed and analyzed for nuclei conformation using DAPI staining. We found evidences of catastrophic mitosis, with extensive nuclei and chromosome fragmentation, in *S-MMS21* cells (72%) compared to wt. *S-MMS21* mutants also showed higher percentage of cells in anaphase compared to wt (27.5% versus 10.6%), suggesting that they have problems in chromosome segregation and they are delayed in mitosis (Figure 3.17). Similar phenotypes were reported for Smc5/6 depleted cells in fission yeast and in mammals (Gallego-Paez et al., 2014; Harvey et al., 2004).

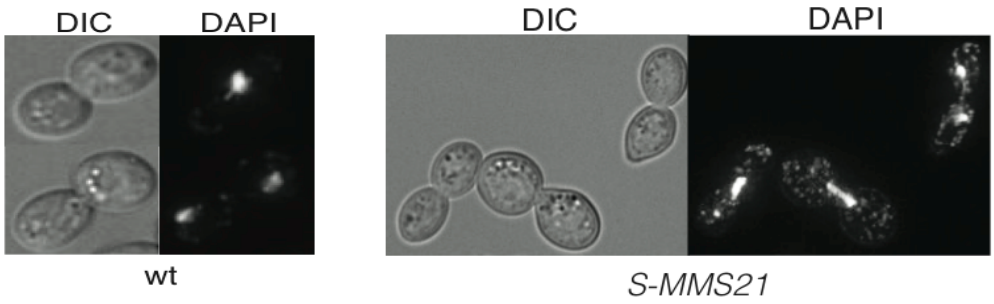

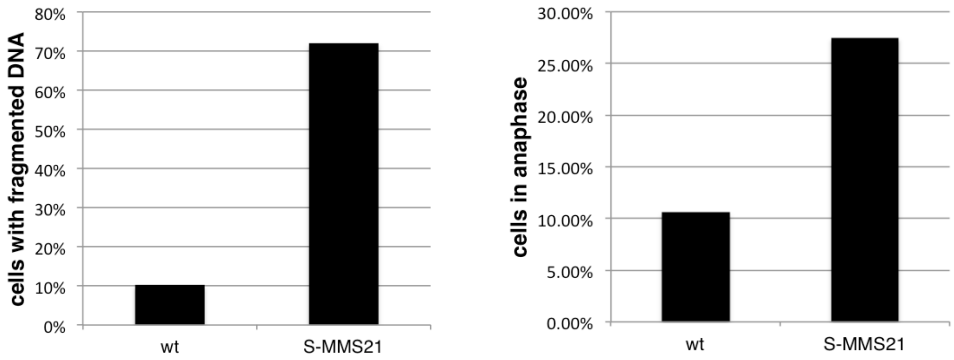

Figure 3.17 *S-MMS21* cells are characterized by catastrophic mitosis. Wt and *S-MMS21* cells were collected in mitosis at 100 min in YPDA medium after the release from an HU arrest, fixed and DAPI stained. Representative images of mitotic cells are reported for both strains. Quantifications, derived from two independent experiments, indicate the mean of the percentage of cells with fragmented DNA and the mean of the percentage of cells in anaphase.

3.2.3 *S-SMC6* cells are viable, but defective in DNA damage tolerance

When we sporulated heterozygous diploids *SMC6/S-SMC6* we observed that haploid *S-SMC6* cells are viable (Figure 3.18a). Following tetrad dissection *S-SMC6* cells grew as well as wt, and doubling time measurements revealed a slower proliferation, of about 15 min, in comparison to wt, as it is revealed in the growth curves in Figure 3.18b.

a

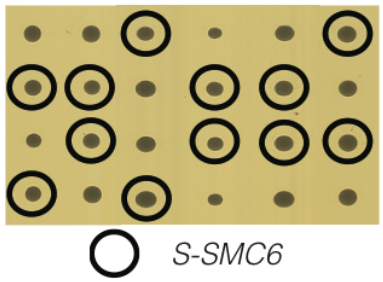

b

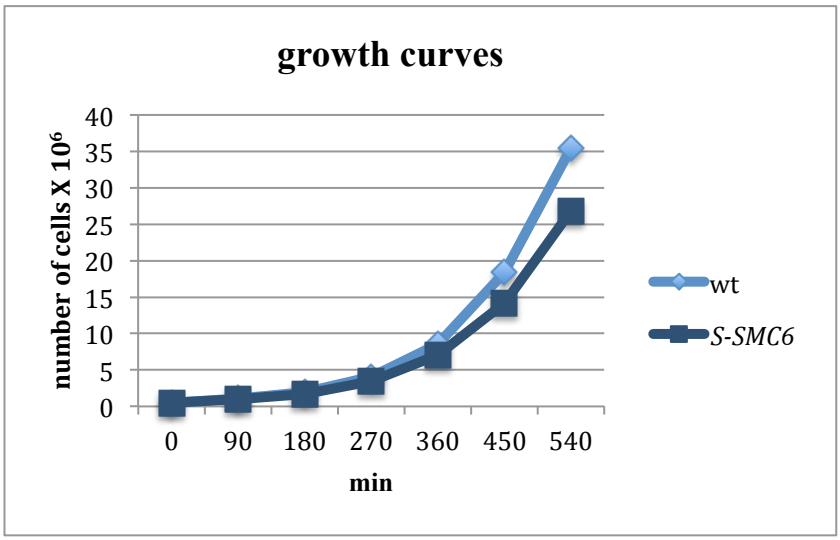

Figure 3.18 Growth curve of wt and *S-SMC6* cells. a) Tetrads from diploids *SMC6/S-SMC6* were dissected and incubated at 28°C for 3 days. Black circles indicate haploid *S-SMC6* cells. b) Wt and *S-SMC6* cells were grown overnight, diluted at a concentration of 5 X 10^5 cells/ml and then counted every 90 min for 9 h. The average cellular concentration calculated for two independent clones for each genotype is reported in the graph.

To examine the S-tag functionality, *S-SMC6* cells were arrested in G1 and released in nocodazole for 3 h, while collecting samples at various intervals. S-Smc6-Flag is present and most abundant in S phase and, while it starts being degraded in G2/M, low amounts of S-Smc6 protein could still be detected in G2/M (Figure 3.19). We suspect that such low amounts of Smc5-6 may suffice to sustain cell viability. We favor this scenario, that is, of slightly different efficiencies in S-tagged protein degradation in G2/M to explain the differential effects on viability between *S-SMC5, S-MMS21* and *S-SMC6* cells, rather than invoking functions for Smc5 that are performed out of the context of the Smc5-6 complex.

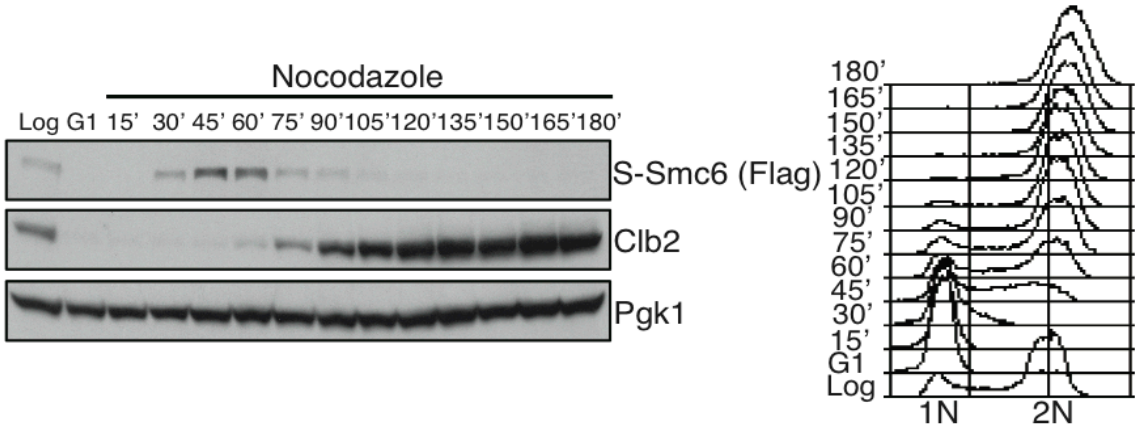

Figure 3.19 Cell cycle expression of S-Smc6-Flag. b) *S-SMC6-FLAG* cells were synchronized in G1 and released in media containing nocodazole 20 µg/ml for 3 h. Samples for Western blots and FACS were collected every 15 min. Western blots were done using anti-Flag (S-Smc6), anti-Clb2 (Clb2) and anti-Pgk1.

If the above interpretation is correct and *S-SMC6* cells are viable because the low amounts of Smc5-6 can sustain viability, a prediction would be that further impairment of Smc5/6 function in G2/M in *S-SMC6* cells would be detrimental to growth. We crossed *S-SMC6* with *S-MMS21*, and indeed the double mutant was dead. In addition, the C-terminal tagging of Smc5 in *S-SMC6-FLAG* cells ended up in very slow growing cells, indicating that *S-SMC6-FLAG* cells are very sensitive to any other destabilizing modifications of the complex (Figure 3.20).

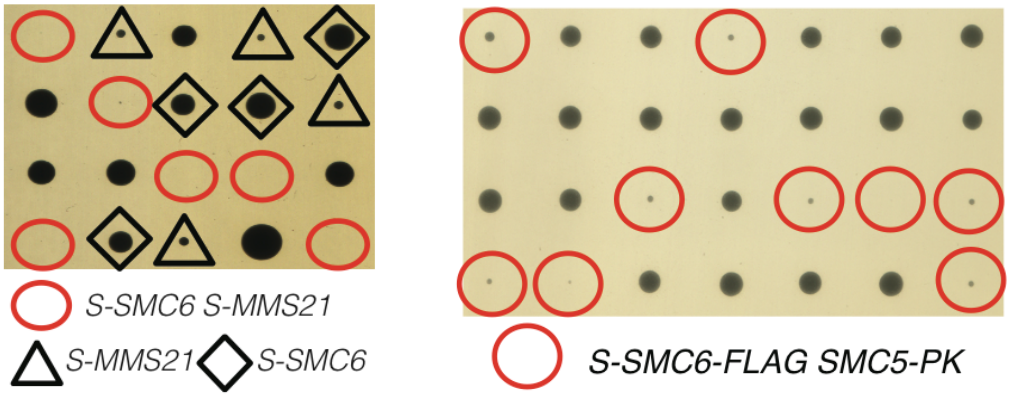

Figure 3.20 *S-SMC6* cells are sensitive to destabilizing mutations in the Smc5-6 complex. Diploids *SMC6/S-SMC6 MMS21/S-MMS21* and diploids *SMC6/S-SMC6-FLAG SMC5/SMC5-PK* were dissected and

plates incubated for 3 days at 28°C. Red circles mark lethal/very sick double mutants, *S-SMC6 S-MMS21* and *S-SMC6-FLAG SMC5-PK*.

Since *S-SMC6* cells are viable, we planned to use them to study the molecular mechanisms underlining the essential functions of the complex in G2/M. First, we examined that indeed the S-Smc6 variant is functional in the time window in which it is primarily expressed (S phase). We performed ChIP-on-chip of Smc6-Flag and S-Smc6-Flag in HU 200 mM 60 min after G1 release. The chromosome binding profile of the two proteins in S phase was very similar with p value of the overlap between the genome-wide clusters highly significant (p=1.3E-155). S-Smc6 was indeed able to bind the same genomic regions of wt Smc6 in HU synchronized cells, and was enriched to a large fraction of the early origins of replication (Figure 3.21). Thus, S-Smc6 is likely functional in S phase.

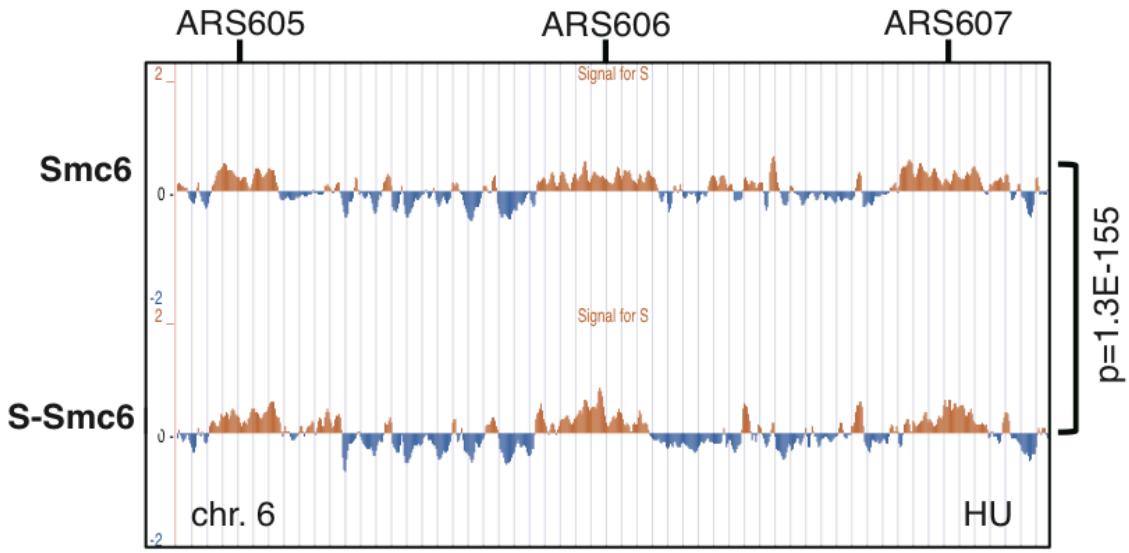

Figure 3.21 Smc6 and S-Smc6 bind to early ARS in S phase. *SMC6-FLAG* and *S-SMC6-FLAG* cells were synchronized in G1 and released in media containing HU 200 mM for 60 min when samples were collected for ChIP-on-chip analysis of Smc6-Flag and S-Smc6-Flag. A snapshot of chromosome 6 early origins (*ARS605, ARS606, ARS607*) is shown; p value indicates the significance of the genome wide overlap between the clusters of binding of Smc6 and S-Smc6.

Next, we examined the MMS sensitivity of the S-tagged *smc5-6* mutants. Differently from the G2-tagged alleles, and similarly to previously characterized *smc6* mutants (*smc6-56*, *smc6-P4*, *smc6-9*), *S-MMS21* and *S-SMC6* cells were hypersensitive to MMS (Figure 3.22), suggesting that limiting amounts/absence of Smc5/6 proteins in G2/M interfere with DNA damage tolerance in these cells.

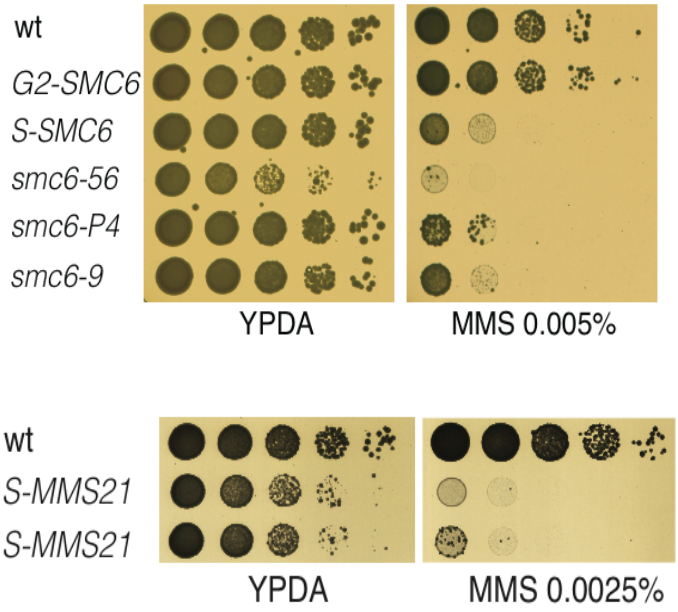

Figure 3.22 *S-SMC6* and *S-MMS21* cells are sensitive to MMS. Ten fold dilutions of the indicated strains were plated on YPDA and on MMS plates at the indicated concentrations. Plates were scanned after 3 days at 25°C. *smc6-56, smc6-P4* and *smc6-9* were used as positive controls.

We further analyzed whether X molecules accumulate in *S-SMC6* cells, similarly to other *smc6* mutants previously characterized. Wild-type, *S-SMC6* and *smc6-56* cells were synchronized in G1 and released in the presence of MMS 0.033% for 240 min. As soon as S-Smc6 levels start to decline during replication in the presence of MMS (180-240 min), X shaped molecules began to accumulate (Figure 3.23). Thus Smc5/6 is needed in late S/G2 to prevent the accumulation of cruciform structures forming during replication in the presence of DNA damage.

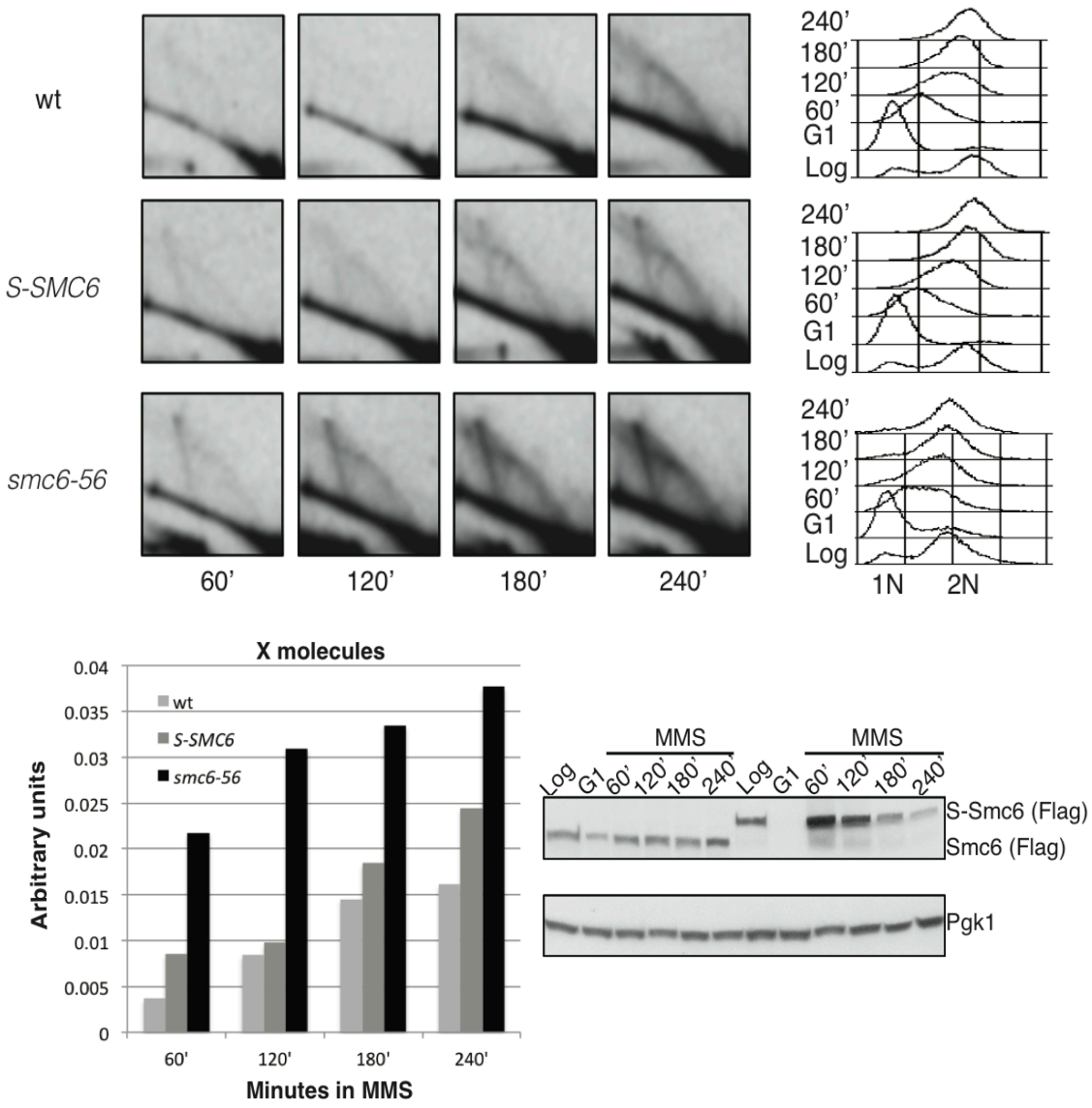

Figure 3.23 *S-SMC6* cells accumulate X-shaped structures during replication in the presence of DNA damage. Wt, *S-SMC6* and *smc6-56* cells were arrested in G1 at 25°C and released in MMS 0.033% at 30°C for 4 hours. Samples for FACS, TCA protein extraction and CTAB extraction were collected every hour. Quantification of the X spike accumulation in the three strains is reported. Western blots were done using anti-Flag (Smc6 and S-Smc6) and anti-Pgk1.

3.2.4 Mph1 helicase is toxic in *S-SMC5* and *S-SMC6* cells

Since it has been shown that there are several connections between the Smc5/6 complex and the DNA helicase Mph1 (Chen et al., 2009; Xue et al., 2014), we analyzed the effects of deleting or overexpressing *MPH1* gene in the S-tag mutants.

As *mph1Δ* is able to rescue the lethality of *smc6Δ* and *mms21Δ* cells (Chen et al., 2009), similarly, the deletion of *MPH1* and the helicase-dead mutant are able to individually rescue the lethality of *S-SMC5* cells; furthermore, a *G2-MPH1* allele does not rescue the lethality of *S-SMC5* (Figure 3.24a). Thus, Mph1 helicase exerts a toxic action, largely postreplicatively in unperturbed condition that must be controlled/counteracted by the Smc5/6 complex in G2/M. In addition, we overexpressed *MPH1* in wt, *G2-SMC6* and *S-SMC6* cells, by the use of the p427TEF vector with 2 micron origin of replication that allows propagation of the plasmid in yeast at high copy numbers. Overexpression of *MPH1* negatively affected *S-SMC6* viability in unperturbed conditions and strongly aggravated *S-SMC6* sensitivity to MMS, making cells almost dead even at very low concentrations of drug (MMS 0.0005%) (Figure 3.24b). We noted that overexpression of *MPH1* results in partial toxicity also in wt and *G2-SMC6* cells, suggesting that the Mph1 helicase has to be tightly controlled in its expression in order to limit unscheduled toxic functions, which might be, at least partly, related to its replication fork regression activity (Xue et al., 2014). While so far this toxic activity was envisaged to happen at stalled forks, our experiments with G2-tagged proteins suggest that such action may be relevant only to those forks persisting in G2/M, at late replicating zones or at forks formed during recombination repair in G2/M.

a

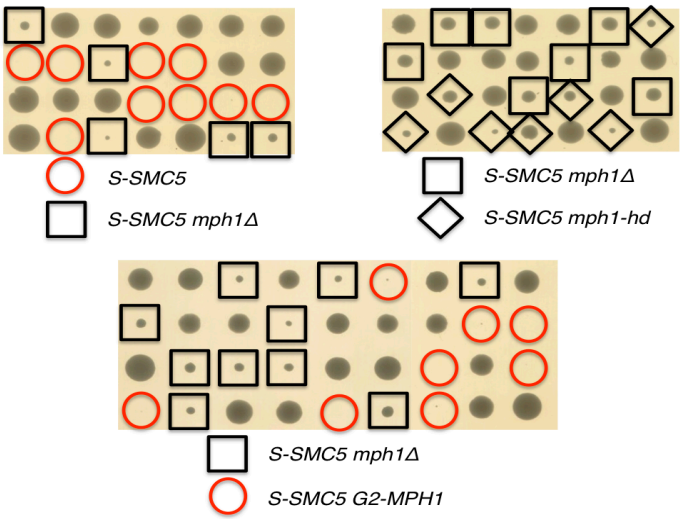

b

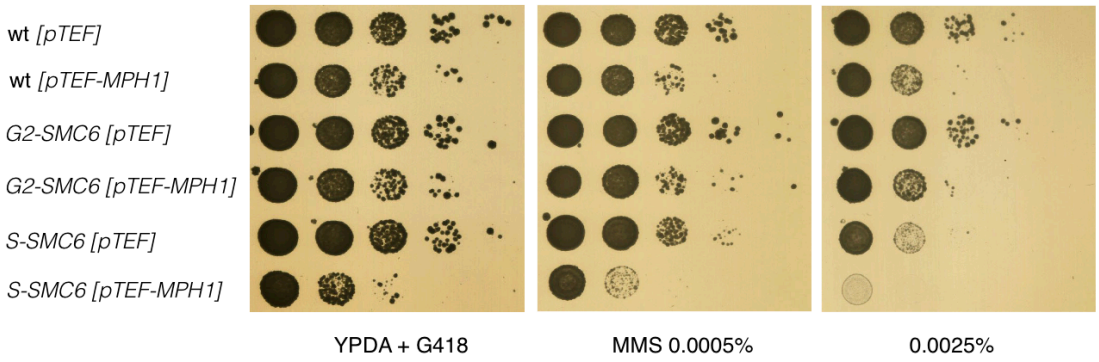

Figure 3.24 Deletion of *MPH1* has alleviatory effects on *S-SMC5* and *S-SMC6* phenotypes. a) Diploids *SMC5/S-SMC5 MPH1/mph1Δ, SMC5/S-SMC5 mph1Δ/mph1-hd, SMC5/S-SMC5 mph1Δ/G2-MPH1* were dissected, plates were incubated at 28°C for 3 days and scanned. Red circles indicate lethal haploids *S-SMC5* and *S-SMC5 G2-MPH1*, while black squares indicate viable haploids *S-SMC5 mph1Δ* and black diamonds viable *S-SMC5 mph1-hd.* b) Ten fold dilutions of the indicated strains were plated on YPDA+G418 and on MMS+G418 plates. Spot assays were incubated for 3 days and scanned.

3.3 Genetic pathways required for viability in *S-SMC6* cells

The phenotypes described so far identify *S-SMC6* as a unique hypomorphic allele caused by attenuated Smc6 levels and functions specifically in G2/M. To gather information on the essential roles of Smc5/6 manifested in G2/M, we screened for synthetic sick/lethal interactors with *S-SMC6* using a robot-assisted synthetic genetic array (SGA) screen between *S-SMC6* and the yeast library knockout (Figure 3.25).

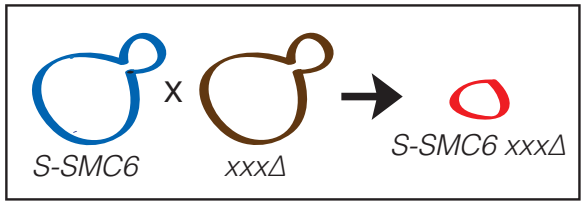

Figure 3.25 Schematic representation of SGA. *S-SMC6* mutants were crossed with the yeast non-essential genes library KO (*xxxΔ* indicates each of the non-essential genes of the library). Lethal/sick interactions were analyzed and validated in W303 background.

The mutations resulting in synthetic interactions were then manually validated by classical genetics methods, yeast cross and tetrad dissection analysis using a different yeast background, W303, which was used for most of the experiments described here. In addition, we crossed *S-SMC6* with temperature-sensitive alleles of several essential genes, which are not present in the library, or knockout mutations that were not identified in the screen but that were interesting to examine as they affect known pathways of DNA metabolism.

After a careful analysis, we found that mutations in cohesin (*scc1-73*), condensin (*smc2-8*) and replication factors involved in sister chromatid cohesion (*ctf4Δ*) did not negatively affect *S-SMC6* growth, and neither did mutation in the replication or damage checkpoint (*rad53-K227A*, *rad9Δ*, *ddc1Δ*). Thus, Smc5/6's deficient function in G2/M does not prominently impact on sister chromatid cohesion and condensation, nor does require a fully functional damage checkpoint.

Among the synthetic sick interactions identified by the SGA screen we found the members of the Rad6 pathway Bre1, which is a ubiquitin ligase that forms a heterodimer with Rad6, and Lge1, which has been identified as a Rad6-Bre1 associated protein. Rad6, Bre1, and Lge1 are important for various histone modifications, but also for correct timing and amplitude of cyclin gene expression (Zimmermann et al., 2011). They promote transcription of *CLN1*, *CLN2*, *CLB5*, *CLB6*. We speculate that the synthetic interaction found between *S-SMC6* and *bre1Δ* and *lge1Δ* is due to the inability of the double mutant to activate the transcription of *CLB6*, and consequently also *S-SMC6*, which is essential for viability. As a result *S-SMC6 bre1Δ* and *S-SMC6 lge1Δ* likely die due to altered expression of *S-SMC6*.

The other mutations we found to be synthetic lethal/sick with *S-SMC6*, but not with *G2-SMC6,* were divided in the following groups:

- *SGS1-TOP3-RMI1*

- *ESC2*
- *RRM3*

Each group is described separately in the following sections.

3.4. Smc5/6 deficient function in G2/M is compensated by the Sgs1-Top3-Rmi1 dissolvase

3.4.1 *S-SMC6,* but not *G2-SMC6*, is lethal when combined with *sgs1Δ*, *top3Δ*, *rmi1Δ*

The first group of mutants displaying synthetic sickness/lethality with *S-SMC6* consisted of the Sgs1-Top3-Rmi1 (STR) complex. We used *G2-SMC6* to examine if the synthetic interaction with *sgs1Δ* is specific for the Smc5-6 functions manifested in G2/M, and found that double mutants *G2-SMC6 sgs1Δ* are viable and as fit as wt cells. *S-SMC6* mutants required for viability also the other two members of the STR complex, being lethal in combination with *top3Δ* and very sick with *rmi1Δ* (Figure 3.26).

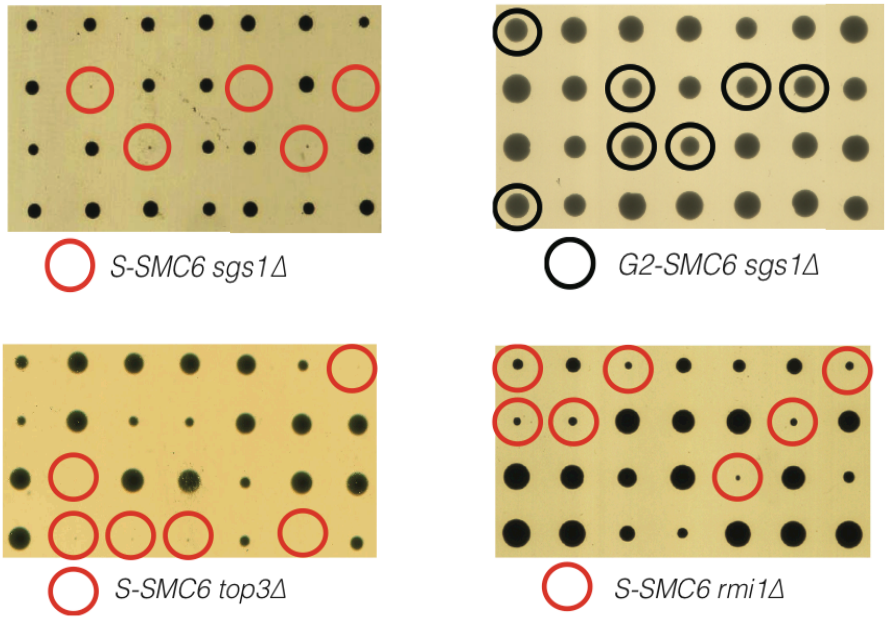

Figure 3.26 *S-SMC6* is synthetic lethal/sick with *sgs1Δ, top3Δ, rmi1Δ*. Tetrads from diploids *SMC6/S-SMC6 SGS1/sgs1Δ, SMC6/G2-SMC6 SGS1/sgs1Δ, SMC6/S-SMC6 TOP3/top3Δ*, *SMC6/S-SMC6 RMI1/rmi1Δ* were dissected, plates were incubated at 28°C and scanned after 3 days. Red circles indicate sick/lethal

haploids *S-SMC6 sgs1Δ*, *S-SMC6 top3Δ, S-SMC6 rmi1Δ,* while black circles indicate viable haploids *G2-SMC6 sgs1Δ.*

From the genetics data it appeared likely that Smc5/6 and Sgs1-Top3 would function on similar substrates specifically in G2/M. We performed ChIP-on-chip of Top3-Flag in nocodazole-arrested cells after G1 release and we compared the chromosome binding profile with the one of Smc5-PK and Smc6-Flag in the same experimental conditions. Statistical analysis of the genome-wide clusters indicated significant p values of overlap both between Smc5 and Top3 (p= 6E-76) and Smc6 and Top3 (p= 1.6E-50) (Figure 3.27). Therefore we conclude that both complexes earmark the same chromosomal regions in G2/M.

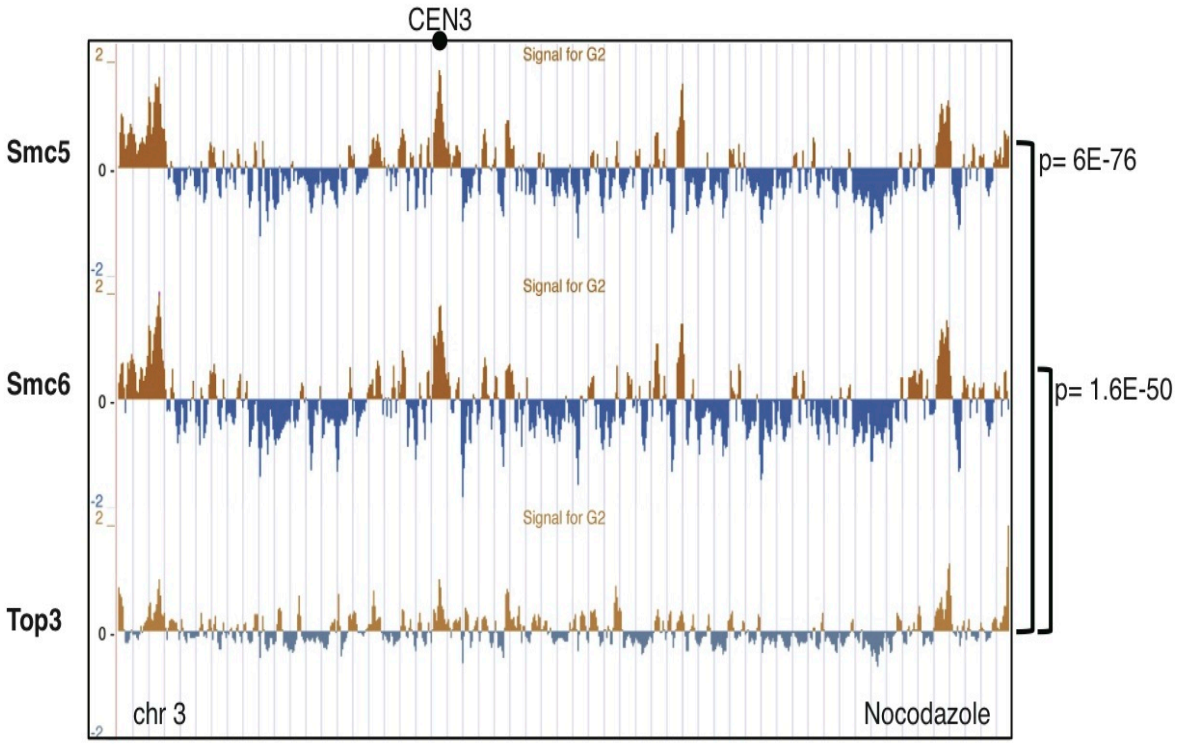

Figure 3.27 Smc5, Smc6 and Top3 co-localize in G2/M. *SMC5-PK, SMC6-FLAG* and *TOP3-FLAG* cells were arrested in G1 and then released in media containing nocodazole 20 µg/ml for 3 hours when samples for ChIP-on-chip were collected. Chromosome 3 is shown as example and p values of the genome-wide significance of the clusters overlap are reported on the right.

3.4.2 *S-SMC6* is sick in combination with *pol32Δ*

Deletion of *POL32*, which encodes a nonessential subunit of the replicative polymerase δ, induces replication stress in cells, causing a G2/M delay accompanied by damage checkpoint activation at 25ºC-30ºC or even a terminal G2/M arrest at low temperatures (non-permissive for growth of *pol32Δ* cells). *POL32* deletion also triggers the PCNA polyubiquitylation, which is toxic in these cells (Karras and Jentsch, 2010), likely due to a concomitant requirement for Pol32 and Pol δ for the error-free branch of DDT mediated by PCNA polyubiquitylation (Branzei et al., 2008; Vanoli et al., 2010). Moreover, Pol32 is required for break-induced recombination (BIR)-mediated genome duplications in budding yeast and in human replication stress models (Costantino et al., 2014; Lydeard et al., 2007; Putnam et al., 2009).

Because *pol32Δ sgs1Δ* combination is synthetic lethal (Karras et al., 2013), and we found that, similarly to *pol32Δ sgs1Δ,* the *S-SMC6 sgs1Δ* lethality is also rescued by mutations in error-free DDT that abolish PCNA polyubiquitylation (see below), we decided to further probe if *S-SMC6* causes a similar situation to that caused by *sgs1Δ* mutation, by examining its genetic interactions with *pol32Δ*. Since the phenotypes seen for *pol32Δ* has been characterized in the DF5 background, we made the *S-SMC6* allele in DF5. We than crossed *S-SMC6* with *pol32Δ* and we recovered by tetrad dissection very sick *S-SMC6 pol32Δ* double mutant cells (Figure 3.28). This result suggests that in *pol32Δ*, Smc5/6 is required for viability. While this finding draws a further line of similarities between Smc5/6 and Sgs1, the result can be also read as to suggest that in conditions of limited Sgs1 or Smc5-6 function, cells are addicted to pathways such as BIR and associated genome duplications, mediated by Pol32, to complete replication and promote DNA repair. As the latter are an important feature of cancer and other human disorders, the results indicate Smc5-6 as a

potential important suppressor of such genomic instability. Current efforts are aimed at analyzing whether genomic duplications are indeed increased in *smc5-6* mutants.

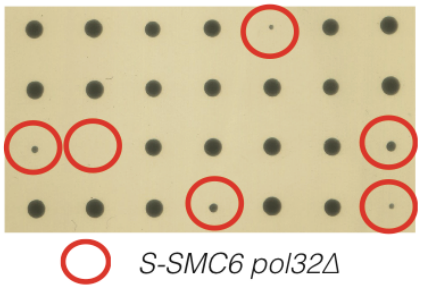

Figure 3.28 *S-SMC6* is synthetic sick with *pol32Δ*. Tetrads from diploids *SMC6/S-SMC6 POL32/pol32Δ* were dissected, plates were incubated at 30°C and scanned after 3 days. Red circles indicate sick/lethal *S-SMC6 pol32Δ* haploid cells.

3.4.3 Rad51 and Rad5 pathways mediate *S-SMC6 sgs1Δ* and *S-SMC6 pol32Δ* sickness/lethality

As described in the Introduction, both Sgs1-Top3-Rmi1 and Smc5/6 play a role in processing recombination intermediates arising during damage-bypass replication and formed via the actions of Rad18-Rad5- and Mms2-Ubc13-mediated PCNA polyubiquitylation in cooperation with Rad51 (Branzei et al., 2006; Branzei et al., 2008; Sollier et al., 2009). We found that *rad51Δ*, as well as *rad5Δ*, *mms2Δ* and *ubc13Δ* mutations rescued the synthetic lethality of *S-SMC6 sgs1Δ* (Figure 3.29a). In line with these data, also the synthetic fitness defect of *S-SMC6 pol32Δ* was partially rescued by *ubc13Δ* (Figure 3.29b). Moreover, the MMS damage sensitivity of *S-SMC6* revealed by spot assay was suppressed by individual deletions in *RAD51*, *MMS2* and *UBC13* (Figure 3.29c).

a

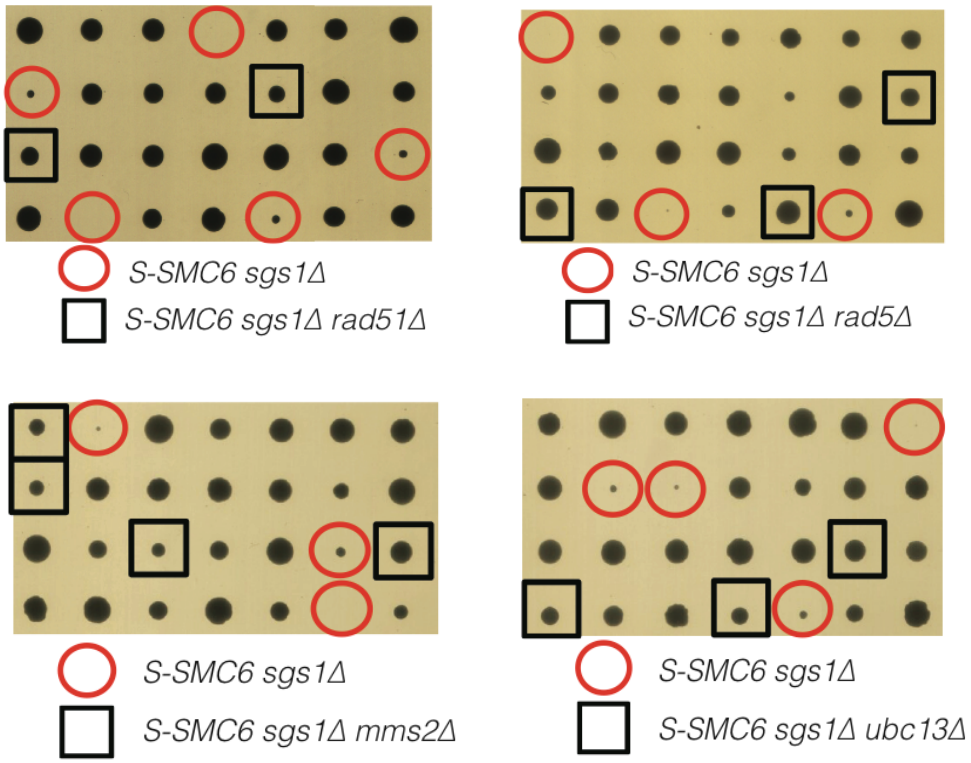
S-SMC6 sgs1Δ
S-SMC6 sgs1Δ rad51Δ
S-SMC6 sgs1Δ
S-SMC6 sgs1Δ rad5Δ
S-SMC6 sgs1Δ
S-SMC6 sgs1Δ mms2Δ
S-SMC6 sgs1Δ
S-SMC6 sgs1Δ ubc13Δ

b

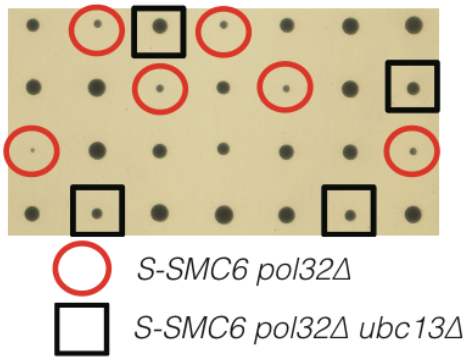
S-SMC6 pol32Δ
S-SMC6 pol32Δ ubc13Δ

c

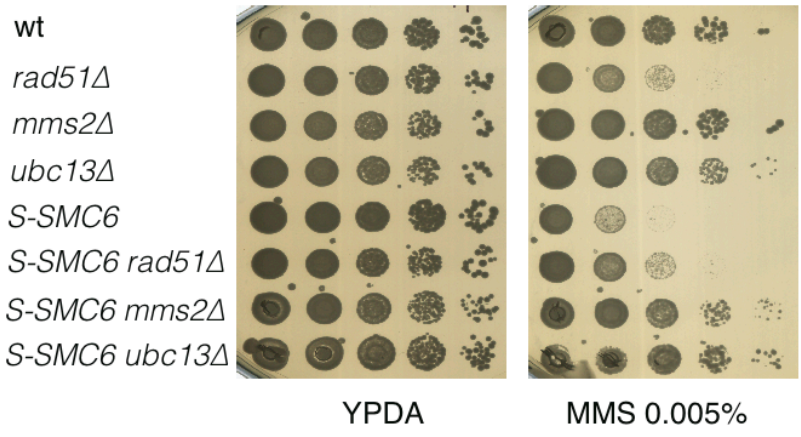
wt
rad51Δ
mms2Δ
ubc13Δ
S-SMC6
S-SMC6 rad51Δ
S-SMC6 mms2Δ
S-SMC6 ubc13Δ
YPDA
MMS 0.005%

Figure 3.29 Rad51 and Rad5 pathways dependent *S-SMC6 sgs1Δ* lethality and *S-SMC6* MMS sensitivity. a) Tetrads from diploids *SMC6/S-SMC6 SGS1/sgs1Δ RAD51/rad51Δ, SMC6/S-SMC6 SGS1/sgs1Δ RAD5/rad5Δ, SMC6/S-SMC6 SGS1/sgs1Δ MMS2/mms2Δ, SMC6/S-SMC6 SGS1/sgs1Δ UBC13/ubc13Δ* were dissected, plates were incubated at 28°C and scanned after 3 days. Red circles indicate sick/lethal haploids *S-SMC6 sgs1Δ*, while black squares indicate viable triple mutants *S-SMC6 sgs1Δ rad51Δ, S-SMC6 sgs1Δ rad5Δ, S-SMC6 sgs1Δ mms2Δ, S-SMC6 sgs1Δ ubc13Δ*. b) Tetrads from diploids *SMC6/S-SMC6 POL32/pol32Δ UBC13/ubc13Δ w*ere dissected, plates were incubated at 30°C and scanned after 3 days. Red circles indicate sick/lethal haploids *S-SMC6 pol32Δ,* while black squares indicate viable triple mutants *S-SMC6 pol32Δ ubc13Δ*. c) Ten fold dilutions of the indicated strains were plated on YPDA and on MMS 0.005% plates. Spot assays were incubated for 3 days and scanned.

Thus, these results indicate that Smc5/6 acts jointly with the Sgs1-Top3-Rmi1 complex to resolve chromatin structures arising during unperturbed replication via the action of Rad51 and PCNA polyubiquitylation.

3.5 Smc5/6 deficient function in G2/M needs compensation by silencing functions

The second class of synthetic lethal interactors was defined by *ESC2*. We verified that also in this case the interaction was specific for the absence of Smc5/6 in G2/M, as the double mutant *G2-SMC6 esc2Δ* was viable and as fit as wt cells (Figure 3.30).

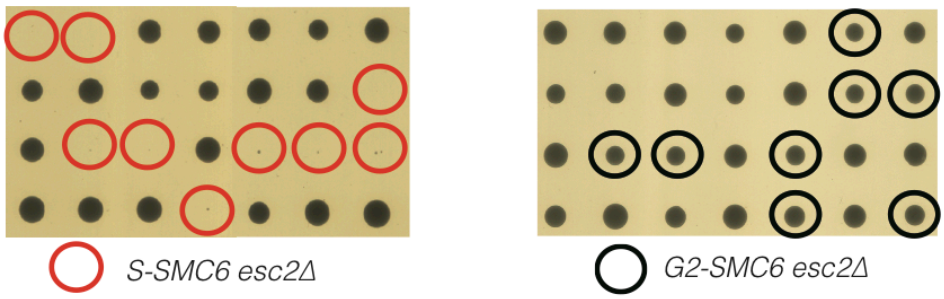

Figure 3.30 *S-SMC6* is lethal with *esc2Δ*. Tetrads from diploids *SMC6/S-SMC6 ESC2/esc2Δ* and *SMC6/G2-SMC6 ESC2/esc2Δ* were dissected, plates were incubated at 28°C and scanned after 3 days. Red circles indicate sick/lethal haploids *S-SMC6 esc2Δ*, while black circles indicate viable haploids *G2-SMC6 esc2Δ*.

Esc2 has an important role in regulating recombination, by counteracting the accumulation of Rad51- and Rad5/Mms2/Ubc13-dependent X molecules forming during replication of damaged templates (Choi et al., 2010; Sollier et al., 2009). However, differently from the situation of *S-SMC6 sgs1Δ* cells, deletion of *RAD51* only weakly suppressed *S-SMC6 esc2Δ* lethality, whereas *RAD5* deletion did not suppressed at all, keeping the triple mutant *S-SMC6 esc2Δ rad5Δ* lethal (Figure 3.31). Notwithstanding similar functions between Sgs1 and Esc2 in the error-free damage-bypass process, these results suggest that the requirement for Esc2 when Smc5/6 function is deficient in G2/M reflects Esc2's role in a pathway different from the one of Sgs1-Top3-Rmi1.

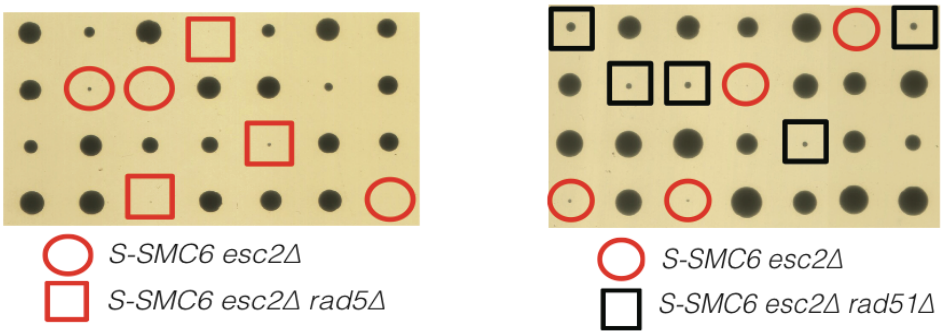

Figure 3.31 *S-SMC6 esc2Δ* lethality is not rescued by *rad5Δ* and mildly by *rad51Δ*. Tetrads from diploids *SMC6/S-SMC6 ESC2/esc2Δ RAD5/rad5Δ* and *SMC6/S-SMC6 ESC2/esc2Δ RAD51/rad51Δ* were dissected, plates were incubated at 28°C and scanned after 3 days. Red circles indicate lethal haploids *S-SMC6 esc2Δ,* red squares lethal triple mutants *S-SMC6 esc2Δ rad5Δ*, black squares viable slow growing triple mutants *S-SMC6 esc2Δ rad51Δ*.

Esc2 is also required for the establishment and maintenance of silencing of regions such telomeric and ribosomal DNA (Yu et al., 2010). Since both Smc5/6 and Esc2 are enriched at heterochromatic regions, we asked if the requirement for Esc2 in *S-SMC6* cells reflects a

need for enhanced silencing functions. Sir2 is a NAD^+ dependent histone deacetylase required for heterochromatin silencing maintenance at different genomic loci, including *HML, HMR* and telomeres as part of the SIR complex (together with Sir3 and Sir4), and at rDNA repeats as part of the RENT complex (together with Net1 and Cdc14) (reviewed in (Wierman and Smith, 2013)). We decided to examine if *S-SMC6 sir2Δ* double mutant recapitulated *SMC6 esc2Δ* phenotypes. Since *sir2Δ* cells neither mate nor sporulate we proceeded as following. We transformed wt, *S-SMC6* and *S-SMC6 rad51Δ* cells with a plasmid derived from YEplac195 vector, which carries the *URA3* marker and in which *SMC6* was cloned. The resulting strains were deleted for *SIR2* by transformation. Finally, *SMC6*-plasmid covered strains, *sir2Δ [SMC6-URA]*, *sir2Δ S-SMC6 [SMC6-URA]* and *sir2Δ S-SMC6 rad51Δ [SMC6-URA],* were plated on 5-FOA to expel the *[SMC6-URA]* plasmid. Remarkably, *S-SMC6 sir2Δ* cells were dead, while the triple mutant *S-SMC6 sir2Δ rad51Δ* was as fit as *sir2Δ* (Figure 3.32).

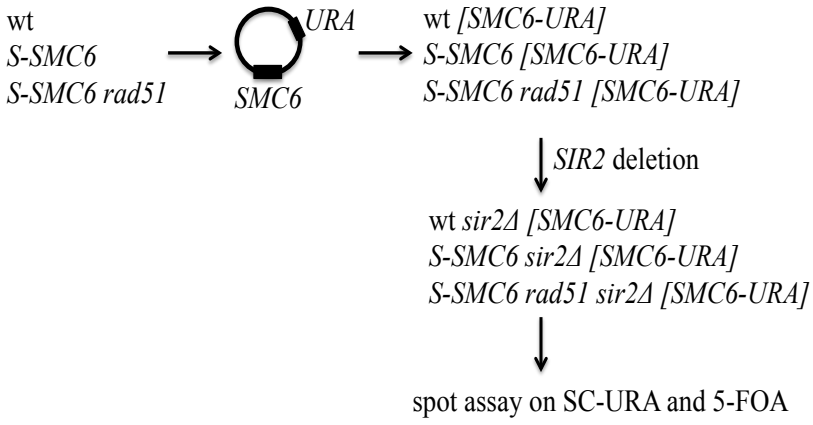

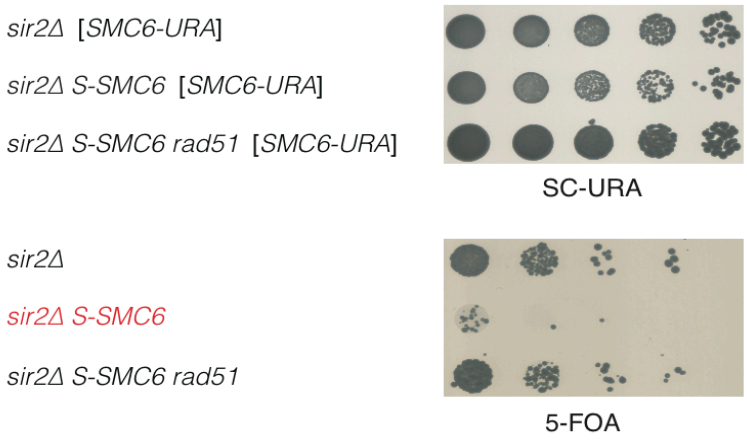

Figure 3.32 Rad51 dependent lethality of *S-SMC6 sir2Δ*. A scheme of the experimental procedure is reported. *sir2Δ [SMC6-URA], sir2Δ S-SMC6 [SMC6-URA], sir2Δ S-SMC6 rad51Δ [SMC6-URA]* were plated on SC-URA (control plates) and on 5-FOA, where cells loose the plasmid *[SMC6-URA]*. Plates were incubated at 28°C and scanned after 3 days.

Thus, when Smc5/6 function is deficient in G2/M, silencing functions are more needed for viability, likely because Smc5/6 plays itself a role in this process or because more substrates requiring heterochromatinization emerge. When silencing is defective, recombination becomes de-repressed, creating potentially more substrates for Smc5-6.

3.6 Smc5/6 facilitates replication through natural pausing elements and site-specific RFBs

3.6.1 *S-SMC6 rrm3Δ* lethality is alleviated by mutations in Rad51, the pausing complex Tof1-Csm3 and the RFB-enhancer Fob1

The third class of mutants that were sick/lethal in combination with *S-SMC6*, but not with *G2-SMC6*, was represented by the DNA helicase-encoding gene *RRM3* (Figure 3.33). Among the double mutants *S-SMC6 rrm3Δ* analyzed by tetrad dissection, 64/87 (73.56%) were found to be lethal, while 23/87 (26.44%) were synthetic sick.

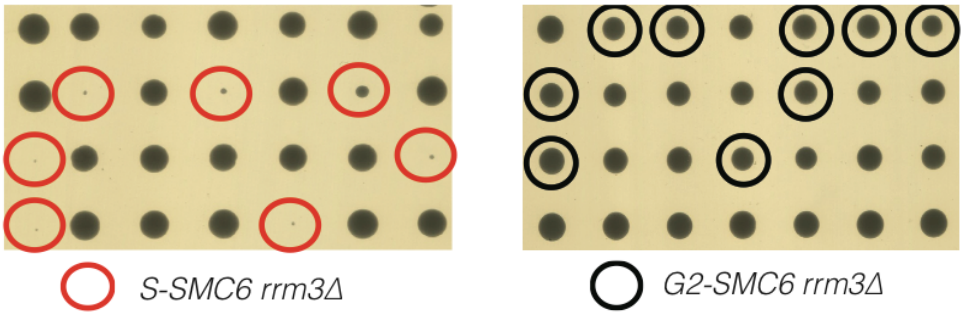

Figure 3.33 *S-SMC6* is sick/lethal with *rrm3Δ*. Tetrads from diploids *SMC6/S-SMC6 RRM3/rrm3Δ* and *SMC6/G2-SMC6 RRM3/rrm3Δ* were dissected, plates were incubated at 28°C and scanned after 3 days. Red

circles indicate sick/lethal haploids *S-SMC6 rrm3Δ*, while black circles indicate viable haploids *G2-SMC6 rrm3Δ*.

S-SMC6 rrm3Δ growth defects were not suppressed by *rad5Δ*, but *rad51Δ* had alleviatory effects (Figure 3.34), indicating that toxic recombination is taking place in the double mutants *S-SMC6 rrm3Δ*.

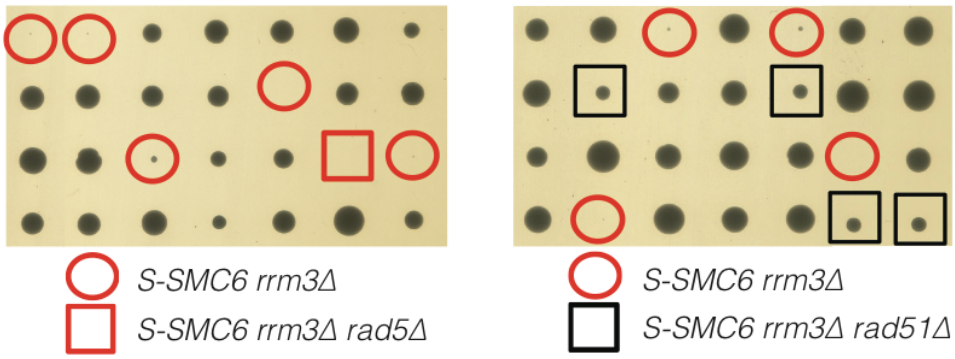

Figure 3.34 *rad51Δ*, but not *rad5Δ*, rescues *S-SMC6 rrm3Δ* lethality. Tetrads from diploids *SMC6/S-SMC6 RRM3/rrm3Δ RAD5/rad5Δ* and *SMC6/S-SMC6 RRM3/rrm3Δ RAD51/rad51Δ* were dissected, plates were incubated at 28°C and scanned after 3 days. Red circles indicate sick/lethal haploids *S-SMC6 rrm3Δ*, red squares lethal triple mutants *S-SMC6 rrm3Δ rad5Δ*, black squares viable triple *S-SMC6 rrm3Δ rad51Δ*.

Rrm3 is a 5' to 3' DNA helicase needed for replication fork progression past non-histone protein-DNA complexes. *RRM3* was identified because its absence increases recombination at the rDNA locus and greatly exacerbates the stalling of replication forks and the accumulation of converged forks at the rDNA replication fork barriers (RFBs). These defects in rDNA replication are associated with rDNA breakage and increased recombination associated with rDNA circles generation (Ivessa et al., 2000). Rrm3 also facilitates replication of subtelomeric and telomeric DNA (Ivessa et al., 2002). It was estimated that Rrm3 is needed for normal fork progression at about 1,400 descrete loci in the *S. cerevisiae* genome. These sites include centromeres, tRNA genes, inactive replication origins and the silent mating type loci, besides rDNA and telomeres (Ivessa et

al., 2003). The function of this helicase is likely to remove tightly bound proteins from the DNA in order to assist replication, avoiding stalling and subsequent fork breakage. At the rDNA locus Rrm3 might act as a "sweepase" by transiently displacing a fraction of the RFB-bound protein Fob1, reducing fork arrest at this region. Fob1 protein binds directly to the rDNA RFBs and has a potent polar activity, through which it arrests only the forks that enter the rDNA transcription units in the 3' to 5' direction (Mohanty and Bastia, 2004). The polar RFBs thus ensure unidirectional replication throughout the rDNA repeats. Tof1 and Csm3 are replisome components required for restraining the progression of stalled forks promoting fork pausing at the natural RFBs of rDNA and at RNA polymerase III transcription-induced fork stalling caused by head-on collisions between replication and transcription machineries. If *S-SMC6 rrm3Δ* lethality is due to an excessive pausing of replication forks, the ablation of Tof1, Csm3 or Fob1, which are needed for efficient pausing, should rescue the lethal phenotype. Remarkably, we found that the sickness/lethality of *S-SMC6 rrm3Δ* was rescued by individual deletions of *TOF1, CSM3* and *FOB1* (Figure 3.35).

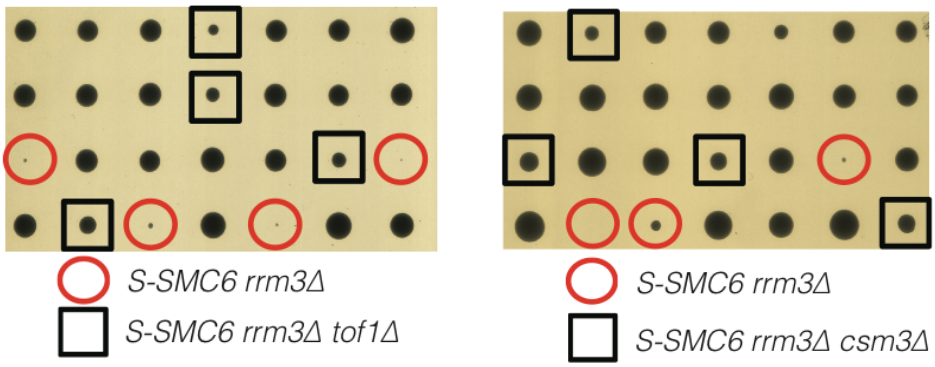

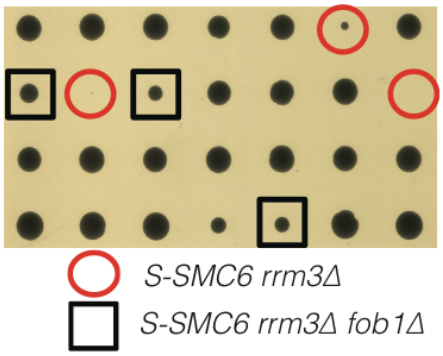

Figure 3.35 *S-SMC6 rrm3Δ* lethality depends on the pausing complex Tof1-Csm3 and Fob1. Tetrads from diploids *SMC6/S-SMC6 RRM3/rrm3Δ TOF1/tof1Δ, SMC6/S-SMC6 RRM3/rrm3Δ CSM3/csm3Δ* and *SMC6/S-SMC6 RRM3/rrm3Δ FOB1/fob1Δ* were dissected, plates were incubated at 28°C and scanned after 3 days. Red circles indicate sick/lethal haploids *S-SMC6 rrm3Δ*, black squares viable triple *S-SMC6 rrm3Δ tof1Δ, S-SMC6 rrm3Δ csm3Δ, S-SMC6 rrm3Δ fob1Δ.*

These genetic data suggest that in the double mutant *S-SMC6 rrm3Δ* prolonged pausing is deleterious, likely leading to failure in completing the replication of those loci and causing cells to rely on recombination to replicate them. We suspect that problems in replicating RFB-containing regions underlie the silencing defects of *smc5-6* mutants and provide an explanation for the reliance that *S-SMC6* cells manifest for other silencing pathways.

3.6.2 Conditional depletion of both *SMC6* and *RRM3* leads to mitotic delay and failure

To examine when *S-SMC6 rrm3Δ* cells die, we established conditional alleles of *RRM3*. We first applied the S- and G2-tags also to *RRM3*. The *G2-RRM3* tag was leaky (data not shown), while the *S-RRM3* tag efficiently restricted the expression of Rrm3 in S phase (Figure 3.36a). We then crossed the resulting *S-RRM3* with *S-SMC6*. *S-SMC6 S-RRM3* cells are slow growing (Figure 3.36b), suggesting that Smc6 and Rrm3 mutually require each other's functions in G2/M.

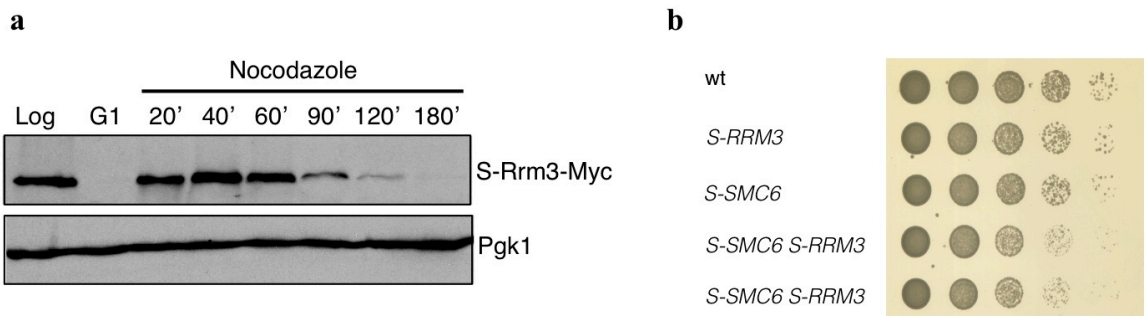

Figure 3.36 *S-SMC6 S-RRM3* are mildly slow growth. a) S-Rrm3-Myc cells were synchronized in G1 and released in the presence of nocodazole 20 µg/ml. Samples were collected at the indicated time points for Western blots anti-Myc and anti-Pgk1. b) Ten fold dilutions of the indicated strains were plated on YPDA. Plates were incubated at 25°C and scanned after 3 days.

We then applied a tetracycline-induced translational conditional system to *RRM3*. This system introduces aptamers in the 5'UTRs of the target gene, which are then bound by tetracycline, which prevents the translation of the target mRNA, causing the conditional depletion of the resulting protein. We established a double mutant *S-SMC6 Tc-RRM3*. We verified that after a G1 arrest and release in the presence of nocodazole and tetracycline both the proteins, S-Smc6-Flag and Tc-HA-Rrm3, get degraded, as detected by Western blotting (Figure 3.37).

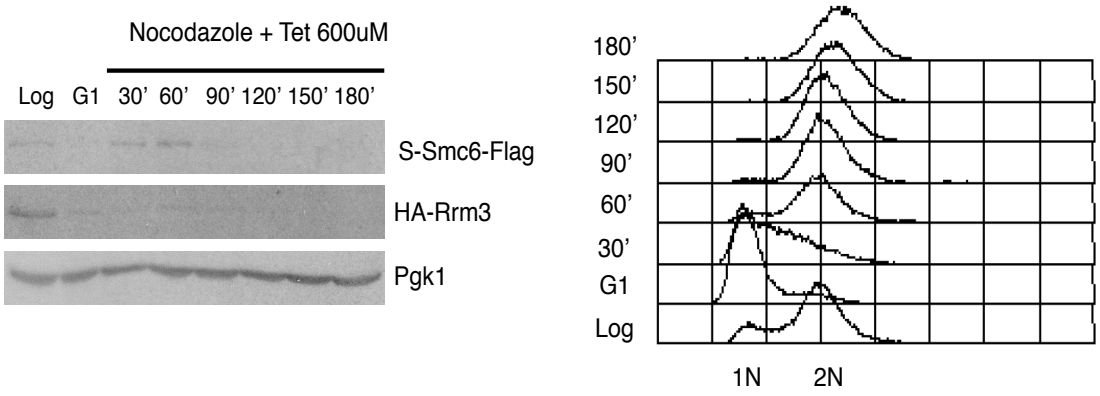

Figure 3.37 *S-SMC6 TC-RRM3.* *S-SMC6-FLAG TC-HA-RRM3* cells were synchronized in G1 and released in the presence of nocodazole 20 µg/ml and tetracycline 600 µM for 3 h. Samples were collected every 30 min for Western blot and FACS analysis. Anti-Flag, anti-HA and anti-Pgk1 antibodies were used.

We then divided G1-synchronized cells in media containing or not tetracycline and collected samples for cell cycle analysis up to 8 hours. Without tetracycline, cells proceed normally through the cell cycle, while in the presence of the antibiotic, and thus in the absence of Rrm3 protein, *S-SMC6 Tc-RRM3* showed a prolonged G2/M or mitotic arrest. At 6-8 hours post-release, *S-SMC6* cells depleted for Rrm3 showed populations of cells in sub-G1 (less then 1N DNA content) or with more then 2N DNA, indicative of aberrant cell division and chromosome segregation (Figure 3.38). Thus, in the absence of Smc6 and Rrm3 in G2/M, cells experience problems in mitosis, which likely underlie the observed lethality of *S-SMC6 rrm3* cells.

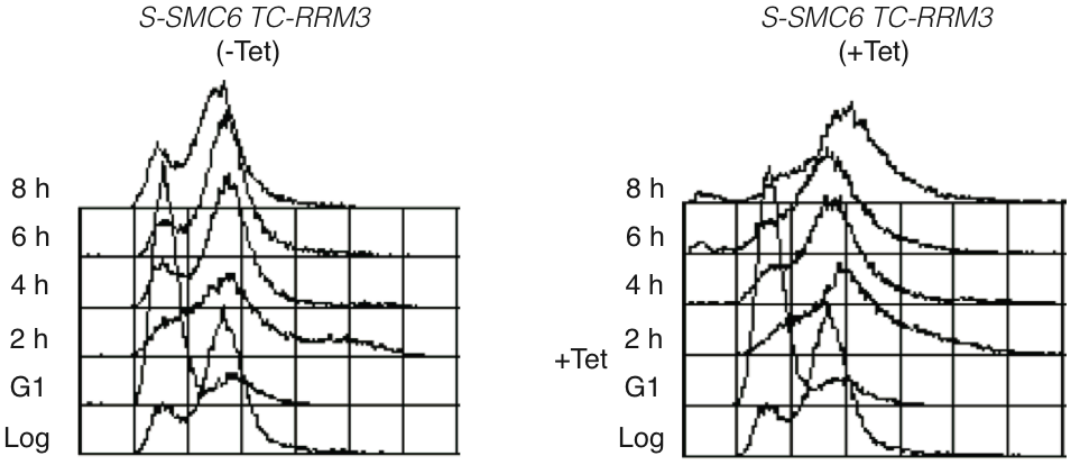

Figure 3.38 *S-SMC6 TC-RRM3* cells experience mitotic problems. *S-SMC6 TC-RRM3* cells were synchronized in G1 and released in YPDA without tetracycline or with tetracycline 600 μM for 8 hours. Samples for FACS analysis were collected every two hours.

3.6.3 Smc5/6 is enriched at natural pausing elements and site-specific RFBs

Given the genetic interactions described above, we decided to investigate possible functional connections between Smc5/6 and Rrm3 in G2/M. We performed ChIP-on-chip of Rrm3-Flag in nocodazole-arrested cells after release from G1 and compared the chromatin clusters with the ones of Smc5 and Smc6 under the same experimental conditions. We found a statistically significant overlap between the clusters of the three

proteins (Smc5 and Rrm3 p=4.5E-82; Smc6 and Rrm3 p=1.3E-78). Chromosome 3 for Smc5-PK, Smc6-Flag and Rrm3-Flag is shown in Figure 3.39.

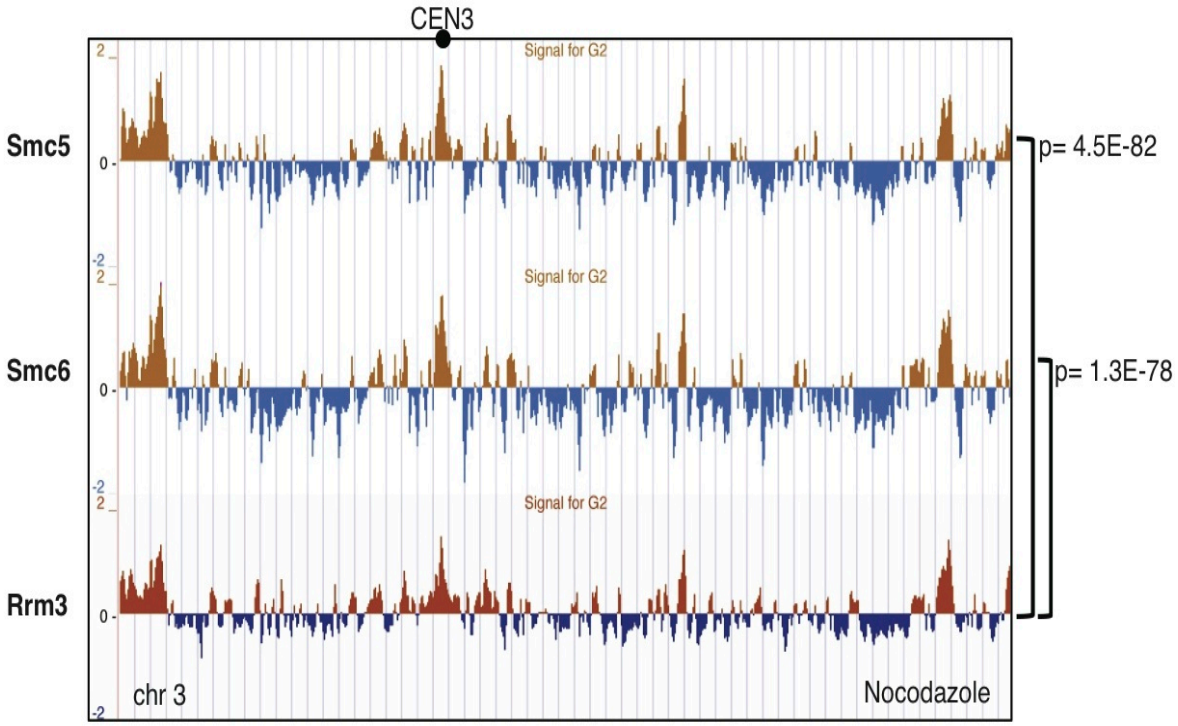

Figure 3.39 Smc5, Smc6 and Rrm3 co-localize in G2/M. *SMC5-PK*, *SMC6-FLAG* and *RRM3-FLAG* cells were synchronized in G1 and released in nocodazole 20 µg/ml for 3 hours when samples for ChIP-on-chip were collected. Chromosome 3 is shown as example and p values of the significance of the genome wide clusters overlap are reported on the right.

Careful analysis indicated that Smc5 and Smc6, similarly to what was already shown for Rrm3, are significantly enriched in G2/M at natural pausing sites, such as centromeres, tRNA genes and the *HML* locus on chromosome III (Figure 3.40a) (Deshpande and Newlon, 1996; Greenfeder and Newlon, 1992; Wang et al., 2001).

Besides the above-mentioned functions, Rrm3 plays a role in promoting fork passage through site-specific RFBs where replication termination occurs, also called TERs (Fachinetti et al., 2010). There are 71 TER regions, of about 5 kb in length, often located between two early origins of replication. Almost all these TERs contain elements that are known to pause/stall replication forks, such as CENs, tRNA genes, Ty retrotrasposones and

transcription clusters defined by PolII- and PolIII- dependent pausing sites. By ChIP-on-chip Smc5 binds to 57/71 (80%) and Smc6 to 56/71 (79%) of these TER sites in G2/M. 53 TERs were shared by both Smc5 and Smc6 and the small difference observed between the two proteins is likely due to technical reason rather than to real biological differences. By our analysis Rrm3 binds to 58/71 (81.70%) TERs. 66% of TERs are bound by Smc5, Smc6 and Rrm3 (Figure 3.40b).

a

CEN	increase	p value
Smc5	24.39	6.10E-39
Smc6	17.99	5.80E-21
Rrm3	35.87	4.10E-65

tRNA	increase	p value
Smc5	11.36	9.40E-86
Smc6	4.05	3.50E-09
Rrm3	10.58	9.60E-52

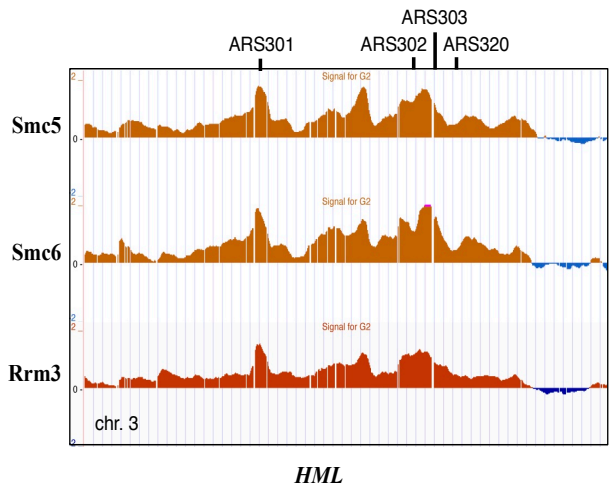

b

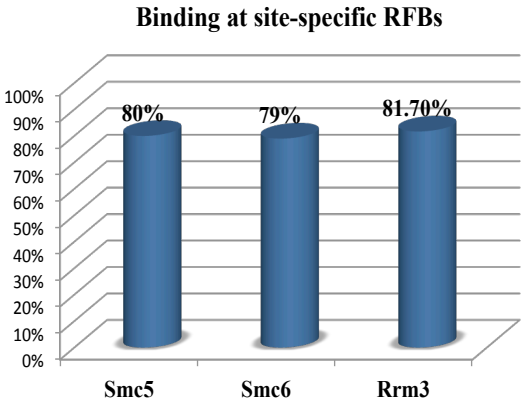

Figure 3.40 Smc5/6 and Rrm3 are enriched at natural pausing elements and site-specific RFBs. a) Smc5, Smc6 and Rrm3 are enriched by ChIP-on-chip in G2/M at the natural pausing elements CENs and tRNAs. The fold increase experimentally found at these genomic regions relative to the expected one and the p value of the significance of the binding are reported in the tables. Smc5, Smc6 and Rrm3 are enriched at the mating type locus *HML* by ChIP-on-chip. Replication fork pause sites were found near *HML,* which is the transcriptionally silent mating-type locus located on chromosome III. Fork pausing sites were mapped to the silent origins of replication that constitute the *HML* ARS cluster (*ARS302-ARS303-ARS320*) and *ARS301* (Wang et al., 2001). b) Smc5/6 and Rrm3 bind to a significant number of site-specific RFBs (Fachinetti et al., 2010) in G2/M.

We performed the same analyses for G2-Smc5-PK and G2-Smc6-Flag. Both the G2 isoforms are significantly enriched at natural pausing elements (CENs, tRNA genes, *HML* locus) and at site-specific TERs (Figure 3.41) in nocodazole synchronized cells. These data reveal that Smc5/6 can be recruited in late S/G2/M after the bulk of replication at these specific genomic loci, likely assisting replication fork passage and completion.

a

CEN	fold increase	p value
G2-Smc5	27.45	3.00E-40
G2-Smc6	18.52	2.40E-16

tRNA	fold increase	p value
G2-Smc5	8.79	8.40E-42
G2-Smc6	4.81	5.60E-10

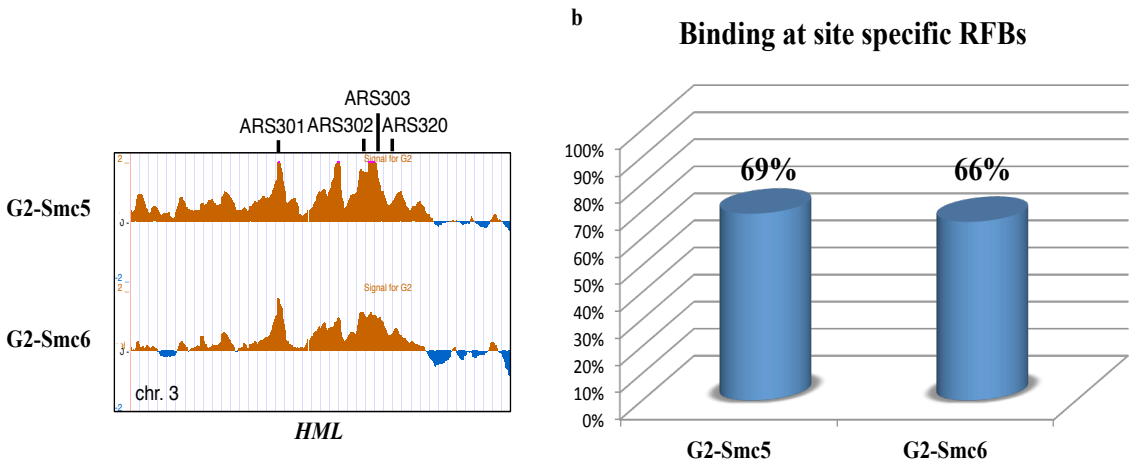

Figure 3.41 G2-Smc5 and G2-Smc6 are enriched at natural pausing elements and site-specific RFBs. a) G2-Smc5 and G2-Smc6 are enriched by ChIP-on-chip in G2/M at the natural pausing elements CENs and tRNAs. The fold increase experimentally found at these genomic regions relative to the expected one and the p value of the significance of the binding are reported in the tables. G2-Smc5 and G2-Smc6 are enriched at the mating type locus *HML* by ChIP-on-chip. b) G2-Smc5 and G2-Smc6 bind to a significant number of site-specific RFBs (Fachinetti et al., 2010) in G2/M.

3.6.4 Chromosome fragility in *S-MMS21* cells is associated with breakage at RFBs in G2/M

Since *S-MMS21* cells are very slow growing and show signs of nuclei and chromosome fragmentation (see Fig. 3.17), we decided to investigate if this was associated with increased chromosome fragility at some of the RFBs found to be bound by the Smc5-6 complex.

We synchronized wt and *S-MMS21* cells in G2/M with nocodazole and released them in the presence of α-factor. We took samples for Pulse-Field Gel Electrophoresis (PFGE) in G2/M-arrested cells, as well as 60 and 150 min after release from the nocodazole block in media containing α-factor to stop the dividing cells in the subsequent G1. Gels were than hybridized with several RFBs enriched for Smc5/6 in G2/M. We observed a smear for the chromosomes analyzed, chr. III and VI, specifically in *S-MMS21* cells, indicating the presence of chromosome breakage (Figure 3.42). These results support the notion that RFBs are prone to fragility when Smc5/6 function is impaired in G2/M.

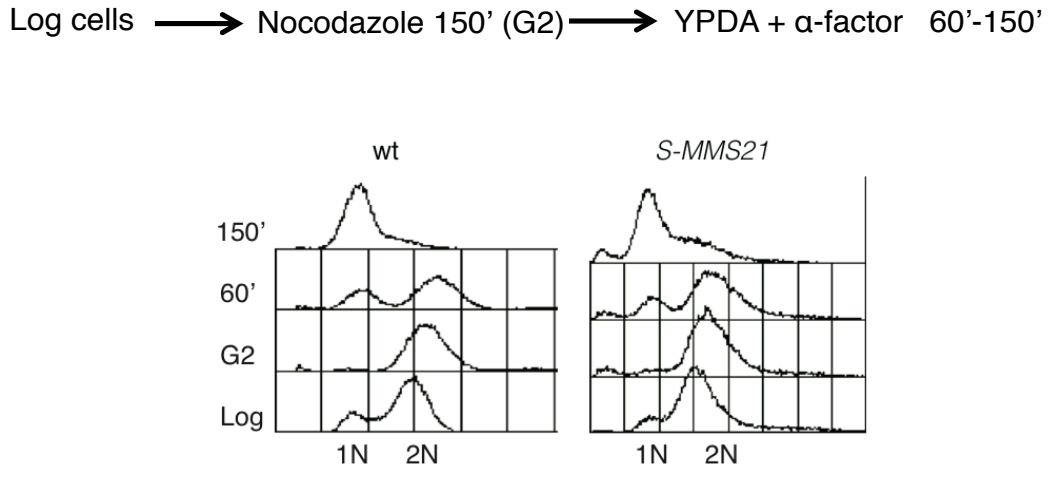

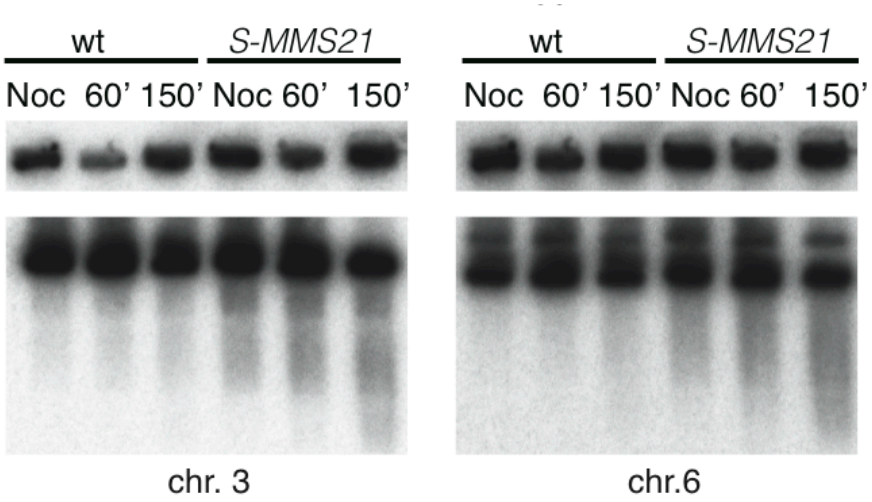

Figure 3.42 *S-MMS21* cells show chromosome breaks at site-specific RFBs. Wt and *S-MMS21* cells were arrested in nocodazole 10 μg/ml and released in the presence of α-factor 5 μg/ml for 150 min. Samples were collected in G2/M and at 60 min and 150 min during α-factor treatment and then analyzed for PFGE. FACS analysis and Southern blot with probes recognizing site-specific RFBs on chr. 3 (*TER302*) and chr. 6 (*TER603*) are shown.

3.6.5 Smc5/6 is not involved in the decatenation of mitotic chromosomes

Top2 is a topoisomerase of class II that has been involved in several chromosome processes, including mitotic chromosome decatenation and replication termination (Baxter and Diffley, 2008; Baxter et al., 2011; Fachinetti et al., 2010). Top2 binds to a significant number of site-specific RFBs by ChIP-on-chip and *top2-1* mutants show inability to properly resolved structures that arise during replication termination. Since Smc5/6 binds to many RFBs, we investigated its genetic interaction with Top2. We found that *S-SMC6* decreases the semipermissive temperature of *top2-4* allele, making the double mutant *S-SMC6 top2-4* growing slower than *top2-4* already at 30°C (Figure 3.43).

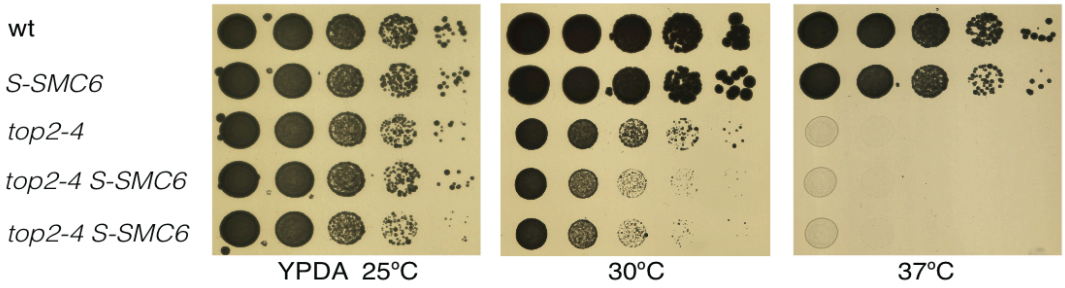

Figure 3.43 *S-SMC6* is synthetic sick with *top2-4*. Ten fold dilutions of the indicated strains were plated on YPDA and incubated at permessive (25°C), semipermessive (30°C) and restrictive (37°C) temperatures for *top2-4*. Plates were scanned after 3 days.

Since one of the main functions of Top2 is to decatenate mitotic chromosomes (Baxter et al., 2011), we considered the possibility that also Smc5/6 may have a similar function, since its binding to DNA has been recently connected to topological changes during DNA synthesis (Kegel et al., 2011). Subsequently, by this taken, the sickness of *S-SMC6 top2-4* could be explained as an aberrant accumulation of supercoiled molecules during replication. To examine this hypothesis, we transformed wt, *top2-4*, *S-SMC6* and *S-SMC6 top2-4* cells with the pRS316 plasmid and we followed its catenated status by electrophoresis and southern blot. We synchronized cells in G1, released them in the presence of nocodazole for 180 min at 37°C and collected samples for DNA extraction. We found that *S-SMC6* is not defective in the decatenation of the episomal plasmid and does not aggravate the phenotype observed for *top2-4* single mutant (Figure 3.44). From these data we can exclude that the sickness of *S-SMC6 top2-4* is due to problems in decatenation.

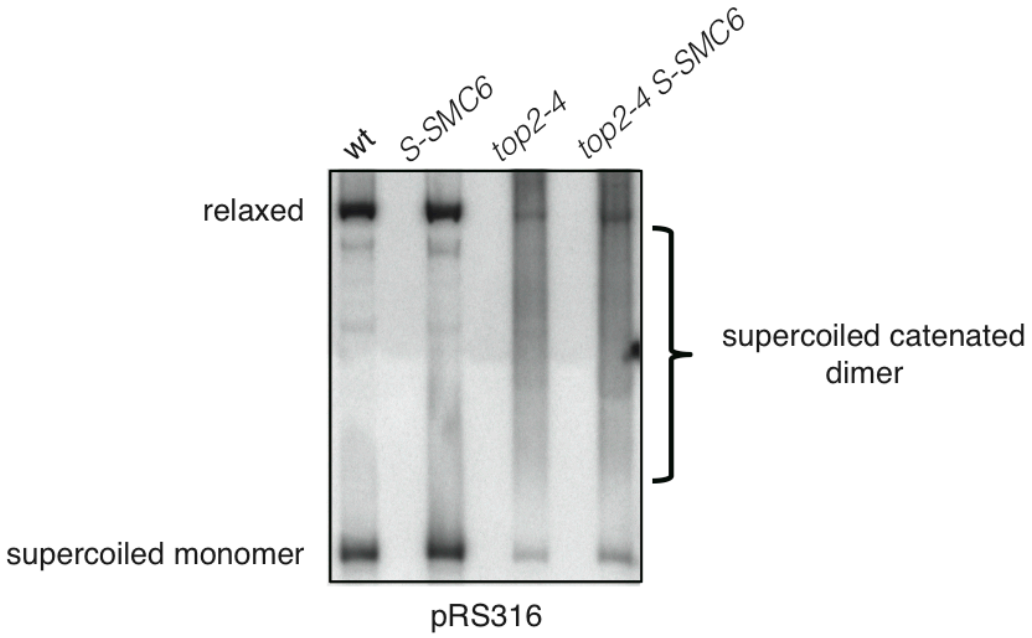

Figure 3.44 *S-SMC6* is not defective in DNA decatenation in G2/M. Wt, *S-SMC6*, *top2-4* and *top2-4 S-SMC6* cells were arrested in G1 at the permessive temperature of 25°C and released in nocodazole 15 µg/ml at the restrictive temperature of 37°C. Samples for plasmid assay were collected after three hours when cells reached the G2/M phase of the cell cycle. Suothern blot was done using a probe recognizing the AMP region of the plasmid pRS316.

3.6.6 Smc5/6 enables resolution of replication termination structures facilitating fork converging

Smc5/6 mutants' synthetic interactions with proteins involved in replication termination and fork fusion (Rrm3 and Top2), the significant enrichment of the complex at natural pausing elements and site-specific RFBs, and the structural similarity between recombination intermediates and DNA structures arising during replication termination (Branzei et al., 2006), suggested that Smc5/6 might have an additional role in facilitating replication completion at such RFB- or natural pausing sites-containing regions.

We investigated the involvement of Smc5/6 in late steps of replication by 2D gel analysis of genomic regions containing RFBs. We began by analyzing a chromosomal region between two early origins of replication, *ARS306* and *ARS307*, called *TER302*, where collisions between transcription and replication occur (Deshpande and Newlon, 1996;

Fachinetti et al., 2010) and Smc5/6 clusters are observed in G2/M. *TER302* is a region of about 5 kb characterized by the presence of a tRNA and a LTR-containing Ty element, two genomic features that are known to pause replication forks and to which Smc5-6 is generally enriched (Figure 3.45).

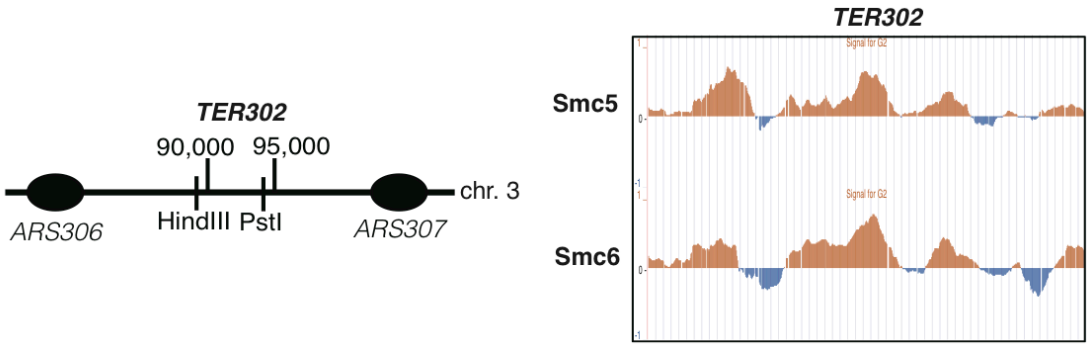

Figure 3.45 Smc5/6 is enriched at *TER302* in G2/M. Schematic representation of the localization of *TER302* on chromosome 3 between the two early origins of replication *ARS306* and *ARS307*. The restriction enzymes used for 2D gel analysis of the region (HindIII and PstI) are indicated. Binding of Smc5-PK and Smc6-Flag by ChIP-on-chip at *TER302* in G2/M is shown.

We decided to investigate replication fork progression in wt and in the temperature sensitive *smc6-56* mutant, first in S phase and then in late S/G2. We synchronized cells in G1 at the permessive temperature of 25°C and released in YPDA medium at the restrictive temperature of 37°C taking samples for FACS and 2D gel analysis every 10 min and up to 50 min in order to monitor early S phase progression. Replication of the *TER302* region initiated normally in *smc6-56* mutants as assessed by the appearance of Y-arc fork structure in the region with the same kinetic observed for wt cells (Figure 3.46).

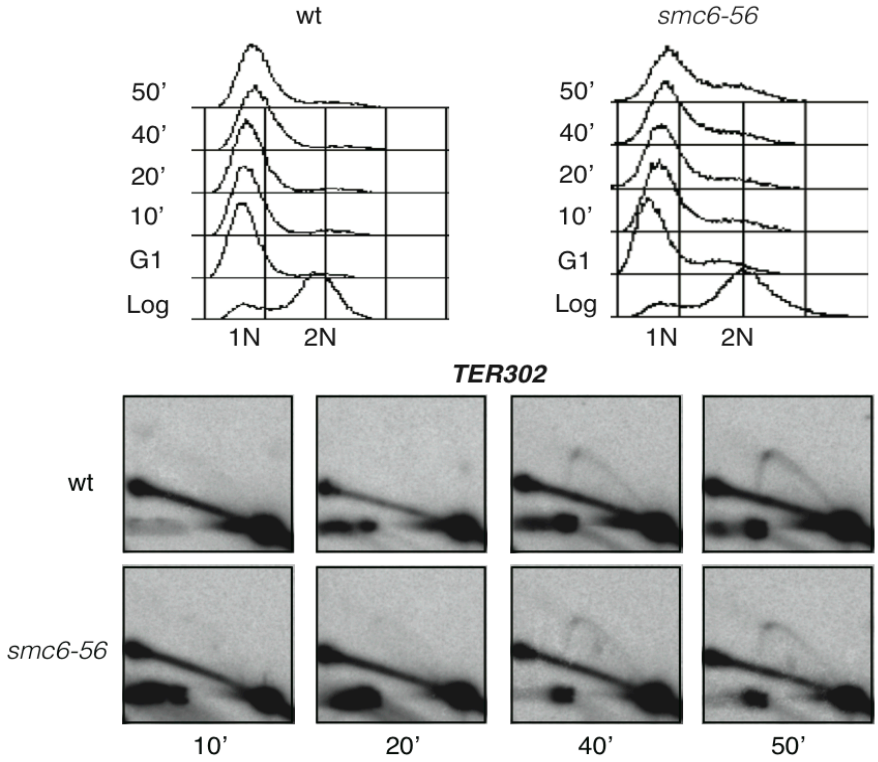

Figure 3.46 Replication fork progression in S phase is not defective in *smc6-56*. Wt and *smc6-56* cells were synchronized in G1 at 25°C and released in YPDA at the restrictive temperature of 37°C for 50 min. Samples for 2D gel analysis were collected at the indicated time point after release. FACS analysis and southern blot of *TER302* are shown.

To monitor late replication, we arrested wt and *smc6-56* in G1 at 25°C and then released them in nocodazole at 37°C for 180 min taking samples for FACS and 2D gel analysis at various time points. In wt both Y-arc and X-shaped like structures disappeared within 90 min, while they persisted and accumulated in *smc6-56* until late G2/M (Figure 3.47). This result suggests that in the absence of a functional Smc5/6 complex there is a prolonged pausing and a persistence of chromosome entanglements that resembles termination or recombination structures, in G2/M.

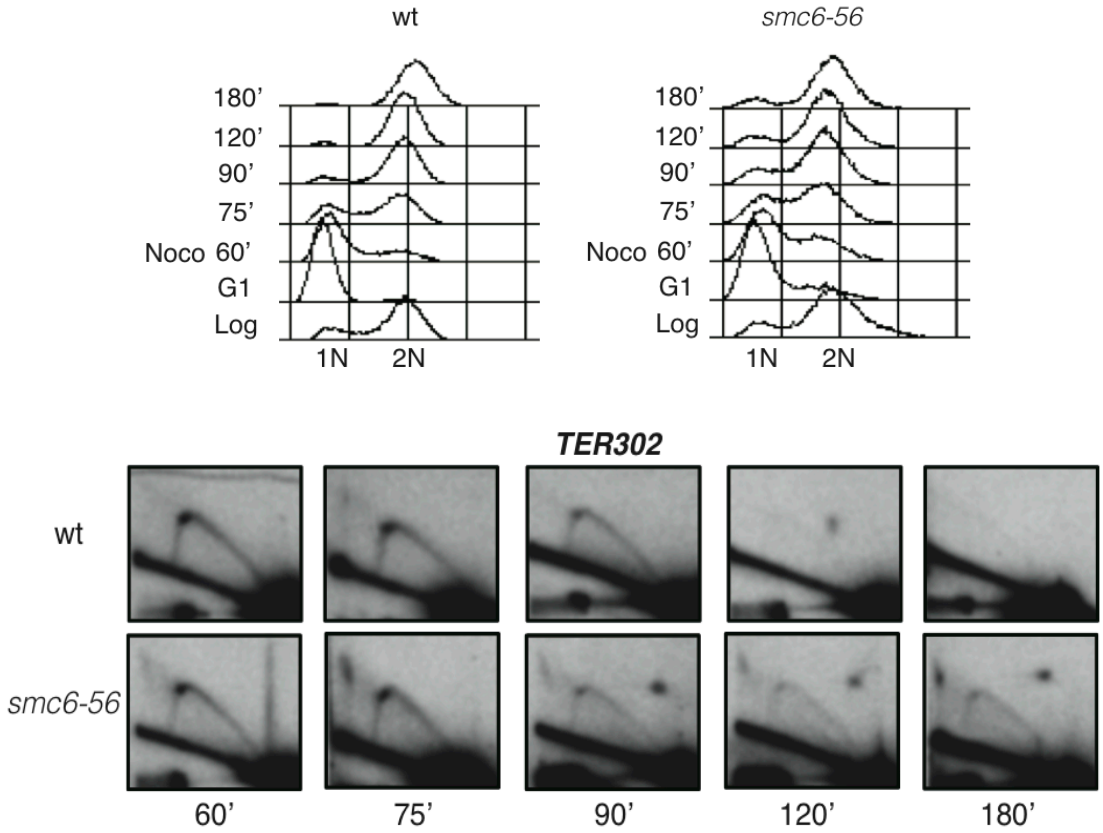

Figure 3.47 Termination/recombination structures accumulate in *smc6-56* at *TER302*. Wt and *smc6-56* cells were synchronized in G1 at 25°C and released in nocodazole 15 µg/ml at 37°C for 3 h. Samples for 2D gel analysis were collected at the indicated time points. FACS analysis and southern blot of *TER302* are shown.

We obtained qualitatively similar results, with X-shaped resembling structures accumulating in *smc6-56* cells late in G2/M, for another RFB analyzed enriched for Smc5/6, *TER704*, which contains CEN7 as pausing element (Figure 3.48) (Fachinetti et al., 2010).

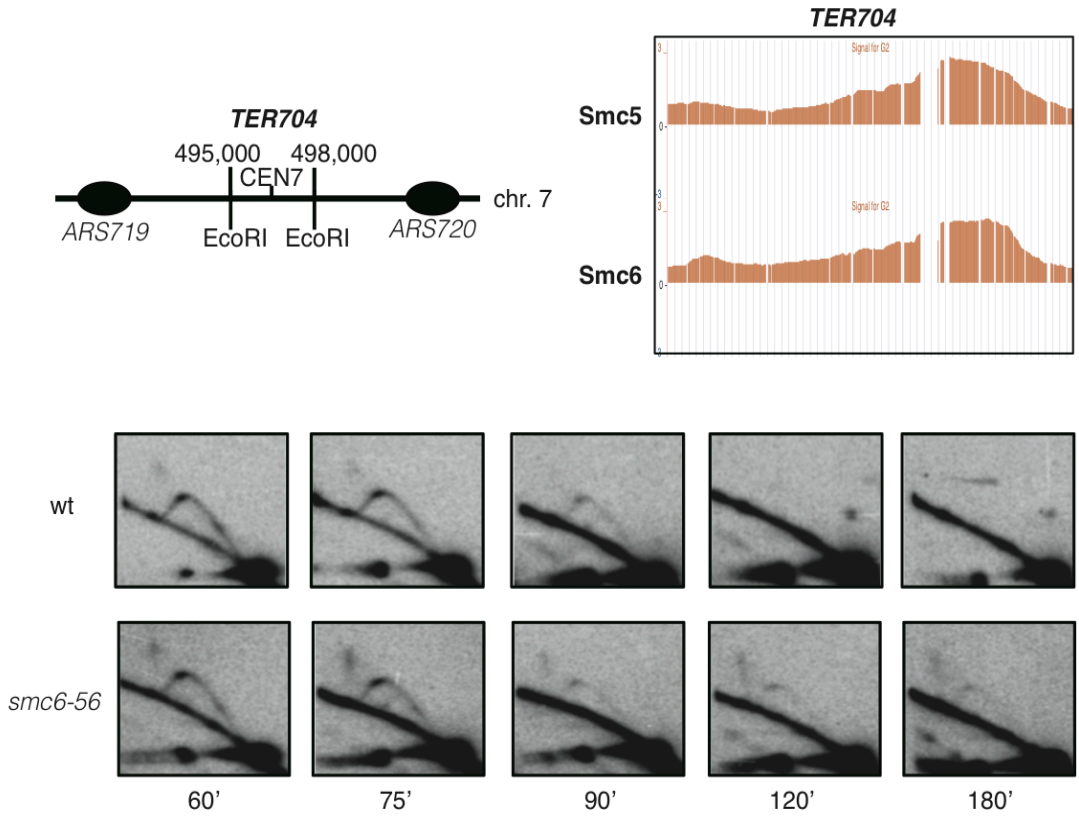

Figure 3.48 Termination/recombination structures accumulate in *smc6-56* at *TER704*. Schematic representation of the localization of *TER704* on chromosome 7 between the two early origins of replication *ARS719* and *ARS720*. The restriction enzyme used for 2D gel analysis of the region (EcoRI) is indicated. Binding of Smc5-PK and Smc6-Flag by ChIP-on-chip at *TER704* in G2/M is shown. 2D gel analysis was done in the same conditions of 2D gel in figure 3.47. Southern blot of *TER704* is reported.

In *smc6-56* cells replication forks of which at least one is stalled at a RFB are not able to terminate properly, but rather pause for prolonged times giving rise to X shaped structures as well as Y structures. Thus, Smc5/6 is required for efficient replication at such RFB-containing regions.

4 Discussion

4.1 Essential functions of Smc5/6 manifested in the late S and G2/M phases of the cell cycle

The structural maintenance of chromosome (SMC) proteins constitute the cores of three SMC complexes involved in fundamental aspects of chromosome metabolism. Two of these complexes, cohesin and condensin, are crucial for chromosome cohesion and condensation, respectively, in addition to playing other roles in DNA metabolism related processes such as transcription and DNA repair (Jeppsson et al., 2014b; Wu and Yu, 2012). The third complex, Smc5/6, was described to have key roles during DNA damage tolerance and repair, but its essential functions in chromosome metabolism remain elusive (Kegel and Sjogren, 2010). Smc5/6 was placed by epistasis analysis in the HR pathway of repair (Onoda et al., 2004; Stephan et al., 2011), but since in budding yeast HR genes are not essential, while Smc5/6 is, it follows that Smc5/6 must have functions outside of HR. Moreover, Smc6 knockout mouse is embryonic lethal (Ju et al., 2013) and individuals with mutations in Mms21 are affected by a very severe growth syndrome (Payne et al., 2014). We hypothesized that the complex has important functions during unperturbed or non-damaging conditions. The aim of this study was to uncover such fundamental chromosome metabolism processes to which *S. cerevisiae* Smc5/6 participates.

First, we asked when in the cell cycle the essential functions of Smc5/6 are manifested. We used recently developed cell cycle conditional systems, the G2-tag (Karras and Jentsch, 2010) and the S-tag (Hombauer et al., 2011), which restrict the expression of a given protein in G2/M and in S phase, respectively. We applied these tags to the core subunits of the complex, Smc5 and Smc6, and to the SUMO ligase, Mms21. From our data it is clear that the expression of one or more subunits of Smc5/6 only in late S/G2/M does not affect

cell viability and cell cycle progression (Figures 3.2, 3.3). The G2-Smc5/6 proteins are fully capable to bind to chromatin postreplicatively, in G2/M (Figure 3.6). Moreover, we demonstrate that in the absence of the partner, the other Smc5/6 subunit is not recruited to chromatin in S-phase; this does not negatively affect replication either in population studies or at the level of single replication forks. This was an unexpected result. Previous studies showed that Smc5/6 is loaded in S phase, during replication, and the binding of the complex in G2/M was presumed to be a consequence of this earlier loading and functions of the complex in S phase (Lindroos et al., 2006). Smc5/6 was also proposed to drive topological transitions during replication, reducing the accumulation of sister chromatid intertwinings (SCIs) that are originated by the rotation of the fork, thereby driving fork rotation and removing the superhelical tension ahead of the replication machinery (Kegel et al., 2011). Smc5/6's binding to origins of replication in HU treated cells and its mediated stabilization of the replisome (Bustard et al., 2012) may imply that Smc5/6 promotes fork rotation during both unperturbed or replication stress situations. Our results confirm that Smc5/6 binds to origins of replication in HU-treated cells. However, our data suggest that such binding does not significantly affect replication fork speed, at least early during replication, in both undamaged or replication stress conditions. In this regard, we found that in *G2-SMC6* cells, Smc5 does not bind to origins of replication in HU-treated cells (Figure 3.8), but it is loaded postreplicatively in G2/M at the same genomic regions bound by Smc5/6 when its partner is expressed (Figure 3.9), without affecting cell viability or growth. When both Smc5 and Smc6 were restricted to G2/M, again the binding of the complex containing the two variants G2-Smc5/G2-Smc6 was normal and efficient (Figure 3.6), and no deleterious consequences on S phase speed or replication fork progression were observed (Figures 3.4, 3.5). These results make it unlikely that Smc5/6 is essential for fork rotation during replication. Furthermore, *G2-SMC5/6* cells were not sensitive to MMS and did not accumulate SCJs during replication in the presence of DNA damage,

suggesting that, even if supplied in late S/G2/M, the complex is fully capable to deal with damage induced in early S phase (Figures 3.10, 3.11). Previous reports showed that the error-free branch of post-replication repair or DDT is active on MMS and UV lesions even if is expressed only after S phase (Daigaku et al., 2010; Karras and Jentsch, 2010), although the Rad5 pathway also plays important roles early in S phase (Gonzalez-Huici et al., 2014; Karras et al., 2013; Ortiz-Bazan et al., 2014). Based on genetic tests, Smc5/6 was proposed to be another member of the error-free bypass of lesions and thus, it is not surprising that its functions in DDT are manifested efficiently even when restricted to G2/M.

We then applied the S-tag to the same three subunits of the complex. *S-SMC5* cells were lethal, *S-MMS21* were very sick, while *S-SMC6* were viable, but defective in damage tolerance (Figures 3.14, 3.16, 3.18, 3.22, 3.23). Thus, the data do indicate that Smc5 and Mms21 play crucial roles in G2/M in unperturbed conditions. However, the difference observed for the three S-tagged Smc5/6 subunits was somewhat puzzling. Smc5 and its interacting partner Mms21 might have additional functions in G2/M, not shared with Smc6, which make them indispensable for growth. But since Smc5 and Smc6 are structurally almost identical, are part of the same complex, and bind to the same genomic regions as observed by ChIP-on-chip in both S and G2/M phases of the cell cycle, independent functions for these different components of the Smc5/6 complex are difficult to predict. Rather, we suspect that technical issues are most likely to explain these apparent incongruities. These S-tags are located at the N-terminal of the tagged proteins and function first to induce the expression in S phase of the modified alleles and then later in G2/M to induce the degradation of the tagged proteins. However, especially the efficiency of the latter process is likely to vary from protein to protein, even if they are part of the same complex. The S-tag might work better for some proteins and might even not work at all for others, depending on the folding and the conformation of the polypeptides. Thus, we

believe that the restriction of S-Smc5 is tight and leads to smooth degradation of the protein in G2/M (as also confirmed by Western blotting in the heterozygous diploid, Figure 3.14), it is a bit less tight for Mms21 and even less stringent for Smc6. Indeed, looking carefully at western blots of S-Smc6 variant throughout the cell cycle, it is clear that a small percentage of the protein can be detected in G2/M (Figure 3.19). This may be enough to provide for viability. It was shown that reduction of the cohesin complex to less than 13% of wild-type levels did not affect cellular viability, but reduced the DNA repair proficiency of cells (Heidinger-Pauli et al., 2010). A similar scenario can be envisaged for Smc5/6. However, thanks to the low amounts of S-Smc6 present in G2/M, the S-tagged *smc6* allele gave us the opportunity to proceed further and ask what pathways of chromosome metabolism are sensitive to such low amounts of Smc5/6 in G2/M.

4.2 Smc5/6 function in G2/M affects three main pathways of DNA metabolism

Since all the combinations of G2-Smc5/6 are compatible with life and sustain normal Smc5/6 functions, while the S-Smc5/6 combinations result in lethality/sickness and in impairment of Smc5/6 functions, we deducted that the essential roles of the complex are likely to be executed in the G2/M phase of the cell cycle. We found that *S-MMS21* and *S-SMC6* behave as loss of function alleles of Smc5/6 in G2/M and used them as tools to investigate further the crucial functions of the complex. We conducted a robot-assisted genetic screen between *S-SMC6* and the yeast library knock-out. From the screen, three main pathways emerged to be synthetic sick/lethal in combination with *S-SMC6,* but not with *G2-SMC6*, implying that mutations in those pathways specifically sensitize cells to limiting amounts of Smc5/6 complex in G2/M.

The first pathway comprises the STR complex genes, *SGS1*, *TOP3* and *RMI1* (Figure 3.26). A synthetic interaction in DNA damaging conditions between *smc5-6* and *sgs1-top3* was already reported by our lab (Sollier et al., 2009), but our new findings enabled us to restrict this interaction specifically to G2/M for what regards Smc5/6 requirement in *sgs1Δ* cells. Remarkably, we found that *S-SMC6 sgs1Δ* lethality is completely rescued by deleting genes of the Rad5 error-free pathway (*RAD5, MMS2, UBC13*) as well as HR (*RAD51*) (Figure 3.29). To our knowledge, this is the first time that Rad5 pathway is shown to be responsible for generating recombination substrates in unperturbed conditions. At least two possible mutually non-exclusive explanations for these genetic data are possible. The first scenario places Smc5/6 upstream and as counteracting the Rad5-pathway responsible for producing recombination-substrates that need to be resolved later via the action of the STR complex. In the absence of STR, this excessive amount of unresolved chromatin structures results in lethality. So far we do not have indications that Smc5/6 would counteract the action of the Rad5 pathway as assessed by the levels of PCNA polyubiquitylation that appear to be normal in *smc6* mutants (data not shown). However, whether Rad5 localization to chromatin as observed by ChIP-on-chip or Rad5 foci are influenced by Smc5/6 are experiments that have not been addressed and deserve further future consideration.

On the other hand, Smc5/6 may play a role in resolving Rad5-dependent structures, jointly with the STR complex, a proposal already previously discussed in the context of recombination-mediated DDT intermediates induced by genotoxic stress (Bermudez-Lopez et al., 2010; Branzei et al., 2006; Branzei et al., 2008; Sollier et al., 2009). That postreplicative Smc5/6 may affect a similar step with Sgs1 in what regards the error-free DDT was also supported by the fact that *pol32Δ* mutants require both postreplicative Smc6 and Sgs1 for viability, and both these synthetic interactions are alleviated by mutations in factors required for PCNA polyubiquitylation (Karras and Jentsch, 2010) (figure 3.29). If

Smc5-6 affects the same resolution step as the STR complex (Figure 4.1), then *S-SMC6 sgs1 Δ* cells are synthetic lethal because the two key players in resolving or dissolving such Rad5-dependent structures are absent. This scenario would predict that a large number of unresolved structures arising during normal proliferation would accumulate in the double mutant, likely causing problems in chromosome segregation and lethality. This hypothesis is supported by the fact that *S-MMS21* cells show problems in chromosome segregation and aberrant mitoses (Figure 3.17), and it can be further probed.

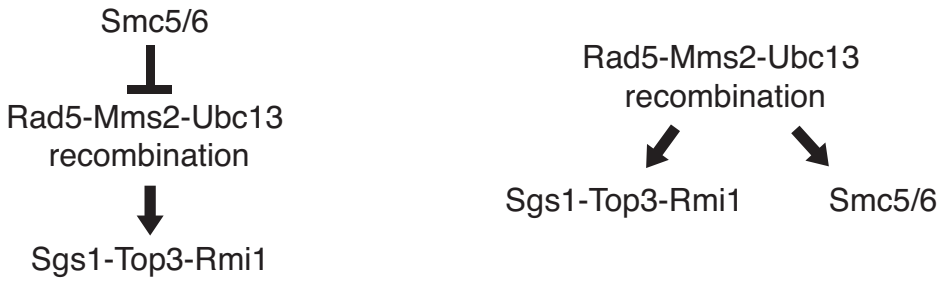

Figure 4.1 Smc5/6 and STR complex possible functions and interplays.

Using conditional *sgs1* and *top3* alleles established in the lab, *Tc-SGS1* and *Tc-TOP3-AID*, now we have established double mutants with *S-SMC6* and we plan to examine the progression through G2/M and in the next cell cycle of these mutants when Sgs1 or Top3 are conditionally inactivated. Alternate to the STR pathway of dissolution, a resolution pathway involving Mus81-Mms4 was shown to act in G2/M in resolving late and persistent cruciform structures (Szakal and Branzei, 2013). Either the action of Mus81-Mms4 is not sufficient in the absence of both Smc5/6 and STR, or its action might require Smc5/6 functionality. This latter possibility is significant as Smc5/6 and Mus81-Mms4 appear to be connected physically via Slx4 and Rtt107 scaffold proteins (Gritenaite et al., 2014), and possibly via Esc2. In this case, one may expect that *sgs1Δ mms4Δ* synthetic lethality would also be rescued by *rad5Δ*, *ubc13Δ, mms2Δ* mutations. This to our

knowledge was not so far reported and we are currently investigating this scenario. On the other hand, Smc5/6 might function together with Mus81-Mms4 only on a subset of structures formed via Rad5 action, whereas Mus81 may have in its repertoire many other recombination substrates that do not necessarily require Rad5 for their formation, but only Rad51. In this latter scenario, *sgs1Δ mms4Δ* synthetic lethality would be suppressed by *rad51Δ* (as it is well known and reported (Szakal and Branzei, 2013)), but not by *rad5Δ*, and Smc5/6 might act as a specific co-factor for Mus81 and Sgs1 on such Rad5-dependent structures only.

The co-localization between Smc5/6 and Top3 clusters in G2/M observed by ChIP-on-chip also supports the idea that both Smc5/6 and the STR complex function together or in parallel, on similar substrates and at nearby genomic regions. Whether and how these localizations are influenced by Rad5 functionality remains to be investigated by future studies. Recently, our lab published a systematic analysis of the recombination structures accumulating in *sgs1Δ* cells under MMS conditions using a combination of 2D gel electrophoresis and electron microscopy (EM) (Giannattasio et al., 2014). To what extent these structures are similar to the ones accumulating in *smc5-6* mutants during replication in the presence of MMS is currently under investigation in the lab. Moreover, using double mutants between conditional *sgs1, top3* alleles and *S-SMC6* we will attempt to identify when in the cell cycle cells lacking in both STR and Smc5/6 activities are dying, and after collecting samples for genomic DNA at those time points we will examine the presence or enrichment of recombination-like structures by 2D gel and eventually their molecular architecture by EM. These directions, together with the genetic approaches described above, will likely bring new insights on the connections between Smc5/6 and STR, as well as on Smc5/6's role in recombination intermediate formation and resolution.

The second class of factors found to be synthetic lethal with *S-SMC6* comprises Esc2 (Figure 3.30). *esc2Δ* cells, similarly to *smc5-6* and *sgs1Δ* cells, accumulate recombination-dependent SCJs following replication in the presence of MMS (Sollier et al., 2009; Mankouri et al., 2009). Initially we thought that the lethality of *S-SMC6 esc2Δ* was due, as for *S-SMC6 sgs1Δ*, to an excessive accumulation of such structures, even in unperturbed conditions. But surprisingly, we found that deletion of *RAD5* does not rescue the lethality, while loss of Rad51 does so, but the fitness of the triple mutants, *S-SMC6 esc2Δ rad51Δ* was still not at wt levels (Figure 3.31). These results reveal that the lethality of *S-SMC6 esc2Δ* is not driven by an aberrant accumulation of Rad5- and PCNA polyubiquitylation-dependent chromatin structures. Esc2 is also known to cooperate with Mms21 sumoylation activity in suppressing genome duplications (Albuquerque et al., 2013), and thereby the lethality can be caused by a severe loss of sumoylated targets that are required for genome stability. If that is the case, the synthetic lethality of *S-SMC6 S-MMS21* (Figure 3.20) should have the same genetic requirements as *S-SMC6 esc2Δ*, a topic that we plan to examine. However, Esc2 has an additional important role in maintaining efficient telomeric and rDNA silencing and it interacts with Sir2 (Yu et al., 2010), which is the main histone deacetylase in yeast involved in transcriptional silencing. We found that *S-SMC6* is synthetic lethal with *sir2Δ* and this lethality is rescued by deleting the key player of homologous recombination, Rad51 (Figure 3.32). In the absence of appropriate silencing, without Esc2 or Sir2, rDNA and telomeres might become more susceptible to unrestrained recombination. Thus, Smc5/6 may play an important role in suppressing recombination at heterochromatin and silent loci in which repetitive regions are likely organized. On the other hand, Smc5/6 might promote replication or silencing of such regions, jointly with Esc2 and Sir2, and as a result, aberrant recombination at such loci would be prevented. This hypothesis is in line with previous reports in which Smc5/6 was found to regulate and prevent recombination after DSBs induction in the yeast rDNA (Torres-Rosell et al.,

2007b) and in *Drosophila melanogaster* heterochromatin (Chiolo et al., 2011), and with the fact that in the absence of a functional Smc5/6 complex, aberrant recombination foci start to accumulate in heterochromatic regions. While during error-free template switching Smc5/6 functions downstream of recombination machinery to resolve SCJs, at silenced and heterochromatic regions, Smc5/6 seems to play an additional role, directly or indirectly, in preventing recombination. A model of the above mentioned mechanism is shown in Figure 4.2. Our view is that via its ability to promote replication at such repetitive loci, Smc5/6 facilitates silencing associated with replication and as a result recombination is less needed to promote replication of such genomic regions.

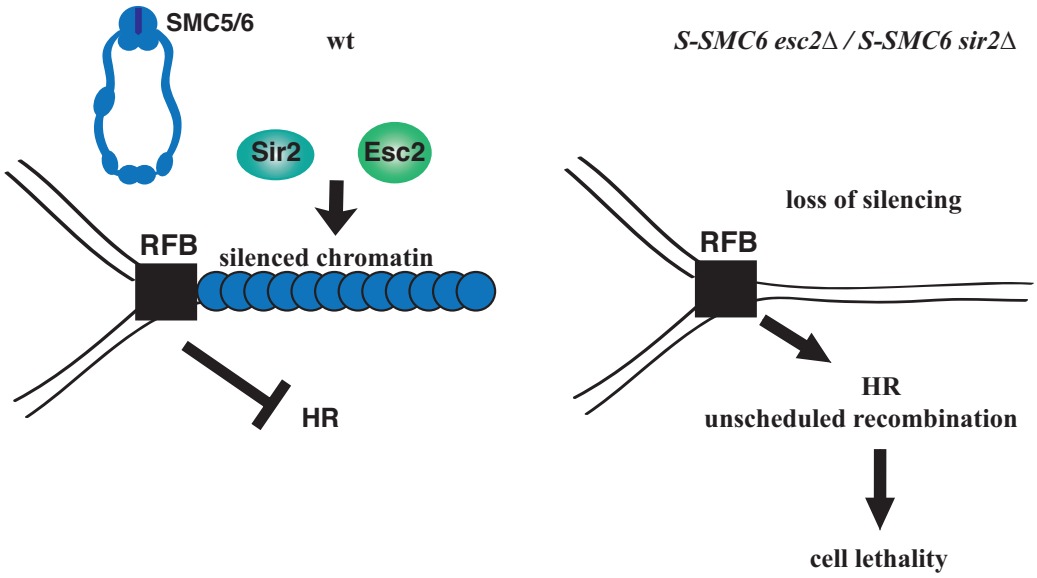

Figure 4.2 Smc5/6 promotes replication at repetitive silent loci/heterochomatin.

The third class of factors shown to be synthetic sick/lethal with *S-SMC6*, and not with *G2-SMC6*, was defined by the Rrm3 helicase (Figure 3.33). We found, by ChIP-on-chip analysis, that Smc5/6 and Rrm3 colocalize in G2/M at natural pausing elements, including CENs, tRNA genes and *HML* locus, and at site-specific RFBs, also known as TER sites, where replication forks are prone to stall (Figures 3.39, 3.40). Rrm3 is known to facilitate fork progression through non-histone protein-DNA complexes (Ivessa et al., 2003) and its

activity is counteracted by the pausing complex Tof1-Csm3 and the RFB protein Fob1 (Mohanty et al., 2006). At natural pausing elements and at RFBs, an excessive or prolonged pausing of the replication fork in the double mutant *S-SMC6 rrm3Δ* can lead to its collapse and subsequent engagement of homologous recombination in order to rescue the broken fork and to restart replication. At these specific genomic loci, such as the rDNA, which is physiologically silenced and contains several RFBs (one for each of the 150-200 repeats), Smc5/6 might be involved in mediating silencing and replication completion, thereby preventing unscheduled recombination. Smc5/6 could work in parallel or together with Rrm3 in facilitating the passage of replication fork at pausing sites. Thus, in the absence of these factors unscheduled recombination events are elicited (Figure 4.3). Indeed, deletions of *RAD51* or pausing genes (*TOF1, CSM3, FOB1*) make cells independent from Smc5/6 and Rrm3 for replicating through RFBs, allowing a partial rescue of *S-SMC6 rrm3Δ* lethality (Figures 3.34, 3.35).

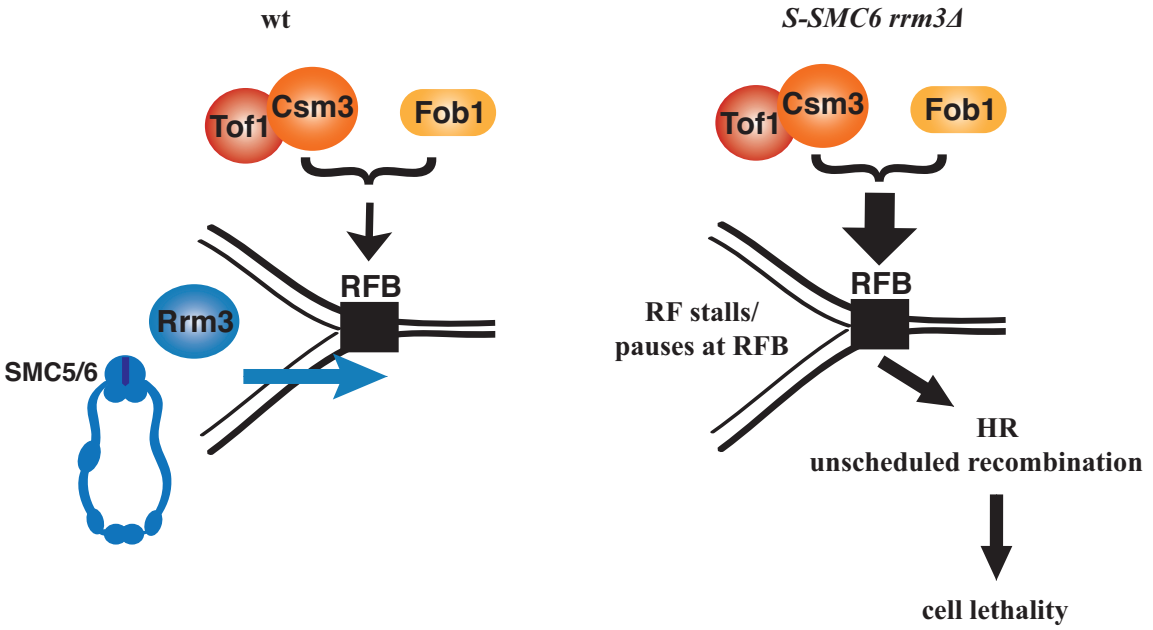

Figure 4.3 Smc5/6 and Rrm3 bind to natural pausing elements and site-specific RFBs facilitating replication completion, thereby preventing unscheduled recombination.

Smc5/6 seems to be crucial in late steps of replication and indeed we found problems in replication completion at some TER/RFB sites in *smc5-6* mutants (Figures 3.47, 3.48). Since replication termination junctions structurally resembles the X-shaped molecules that from during DNA damage tolerance template switching (Branzei et al., 2006), Smc5/6 may facilitate resolution of chromatin entanglements that arise at site-specific RFBs, possibly functioning jointly with Rrm3 and Top2 (Fachinetti et al., 2010).

Interestingly, natural pausing elements and RFBs, at which Smc5/6 and Rrm3 are enriched, were found to resemble fragile sites. Genome wide study of γ-H2A localization by ChIP-on-chip in yeast identified tRNA genes, LTRs, DNA replication origins, telomeres and mating type locus as the main binding sites for the phosphorylated histone (Szilard et al., 2010). Thus, γ-sites are not distributed randomly throughout the genome, but are concentrated at these specific loci, which are indeed characterized by intrinsic fragility and are prone to breakage. Furthermore, deletion of *RRM3* leads to an increase in γ-H2A accumulation at most γ-sites. In a recent study (Song et al., 2014) a genome-wide high resolution mapping of chromosomes identified as fragile sites sequences that slow or pause DNA replication forks. These include Rrm3-binding sites, TERs, tRNA genes, LTRs, CENs, highly transcribed genes, inverted repeats and DNA sequences capable of secondary structures. Since these sites are fragile, they are breakpoints that can induce fork breakage, DSBs and recombination. The role of Smc5/6 might be structural, proving a protective function of these genomic loci in order to allow passage of replication fork and in facilitating replication completion, avoiding fork collapse and recombination in unperturbed conditions, during normal DNA synthesis. In the absence of a functional complex in G2, and of Rrm3, these sites become more prone to breakage, DSBs are formed, unrestrained recombination is induced and finally cells die in G2/M because of problems in chromosome segregation and mitosis. Using PFGE, we indeed found evidence

of increased breakage and fragmentation at site-specific RFBs in *S-MMS21* cells in metaphase and after chromosome segregation (Figure 3.42).

It was noted in previous studies that also yeast DNA origins of replication are prone to fragility and are categorized as γ-sites (Raveendranathan et al., 2006; Szilard et al., 2010). Recently in B lymphocytes, early replicating fragile sites (ERFSs) have been identified as sites of spontaneous DNA lesions that drive genome instability (Barlow et al., 2013). These ERFSs are early replicating and co-localize with highly expressed gene clusters and repetitive sequences, such as DNA transposons, tRNA elements, LINE and SINE. Smc5 was found to bind and mark these ERFSs, together with other repair proteins, BRCA1 and RPA. Since in budding yeast, Smc5/6 binds early ARS regions in HU-treated cells, it was proposed that Smc5/6 travels with the replisome and rescues stalled replication forks (Bustard et al., 2012). Besides these possible functions, we would like to propose that Smc5/6 binding to ARS regions falls in the same category to its binding to other at risk elements in the budding yeast and human genome, potentially providing structural protection and allowing replication fork passage without breakage.

Smc5/6 can be a guardian of genome stability by binding fragile sites, structurally organizing them and allowing passage of replication fork and replication completion, facilitating the epigenetic modifications coupled with the replication of such loci. This may play an important role in restricting DSBs formation and unrestrained recombination associated with GCRs. We propose that this function of Smc5/6 is crucial in the late stages of genomic duplication and G2/M, when replication of such natural pausing elements occurs.

4.3 Conclusions

In *S. cerevisiae*, Smc5/6 function in G2/M at the late stages of genome replication is essential for cellular proliferation. Our results uncover three fundamental aspects of the complex, summarized in Figure 4.4. On one hand Smc5/6 plays a topological role affecting the formation or resolution of Rad5-dependent chromatin structures later engaged by the STR complex. Second, Smc5/6 facilitates an epigenetic pathway that ensures silencing of certain loci such as those including repetitive DNA, while preventing unscheduled recombination at those regions. Third, Smc5/6 has an anti-fragility function at natural pausing sites, facilitating replication through site-specific RFBs and preventing their breakage in mitosis during chromosome segregation.

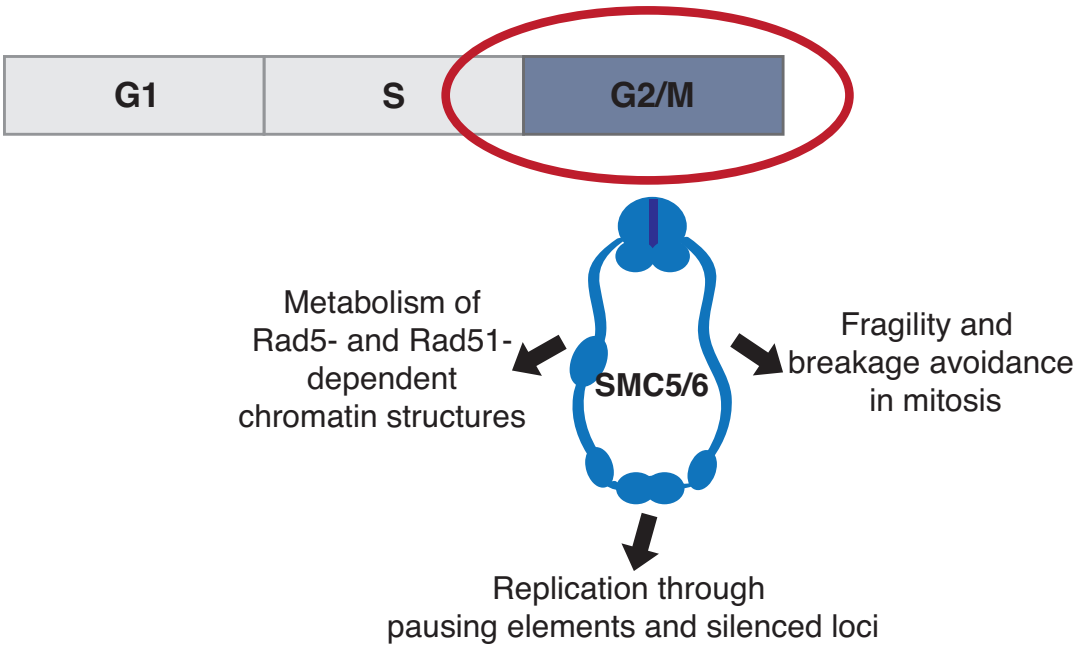

Figure 4.4 Smc5/6 essential functions in G2/M.

In higher eukaryotes Smc5/6 might have similar crucial roles in maintaining genome stability, since KO mouse for Smc6 are embryonic lethal (Ju et al., 2013). Correlations between Smc5/6 and the tumor suppressor gene BRCA1 binding loci have been also reported at ERFSs in B lymphocites (Barlow et al., 2013). Recently, BRCA1 was described to control homologous recombination at stalled mammalian replication forks

(Willis et al., 2014), a function we have revealed for budding yeast Smc5/6 complex at natural pausing sites and at regions at which silencing is coupled with DNA replication. Based on these findings, we propose that Smc5/6 acts as a tumor suppressor, playing fundamental roles in regulating genome stability and in preventing oncogenic transformation. The recently identified individuals with mutations in Smc5/6 display severe dwarfism and insulin resistant diabetes (Payne et al., 2014), proving the importance of the complex for development in humans. The mechanisms underlying these drastic phenotypes are not known, but they might involve the structural activity of the complex as well as the sumoylation of important human targets. It is still unknown if these syndromes are associated with higher incidence of cancer, as it is for BLM syndromes (Singh et al., 2009).

In conclusion, these new findings provide interesting leads for future works on the influence of Smc5/6 complex in genome maintenance in normal and in cancer cells.

5 Appendix 1

The role of Hcs1 helicase in DNA damage tolerance

5.1 Introduction

During all chromosome metabolism processes, highly specialized DNA helicases utilize the energy derived from ATP hydrolysis to unwind duplex DNA or RNA-DNA duplexes. Several DNA helicases have been characterized with roles in replication, repair or transcription. Hcs1 is a hexameric helicase and shares 25% of sequence homology with DnaB, which is the major helicase at the origin of replication *OriC* of *E. coli*. Hcs1 is a non essential Polα/Primase interacting factor, it has a 5' to 3' polarity of movement and its activity is stimulated by the single strand binding protein RPA (Biswas et al., 1997a; Biswas et al., 1997b).

Besides its biochemical characterization, very little is known about Hcs1 functions *in vivo*. To date, there is only a genetic report in yeast in which *HCS1* deletion was shown to slightly suppress *rad5Δ* mutation in the duplication-mediated GCRs assay (Putnam et al., 2010). However, its roles in DNA replication and associated processes, such as DNA damage tolerance, Polα-mediated repriming and chromatin metabolism processes coupled with replication, such as silencing and cohesion, remain unknown.

The aim of our study was to characterize Hcs1 functions in the above-mentioned DNA metabolism pathways.

5.2 Material and methods

Transformations, spot assays, 2D gel electrophoresis and ChIP-on-chip were performed as described in the main Material and methods section. The *Delitto perfetto* methodology to introduce point mutations in Hcs1 ORF was conducted as described in (Storici and Resnick, 2006).

The list of yeast strains used in this section is reported in table 5.1.

Strain	Genotype	Source
FY1363	Mata *ade2-1 can1-100 his3-11,-15 leu2-3,112 trp1-1 ura3-1 RAD5+* (W303)	lab collection
HY0137	W303 Mata *rad5Δ::HPHMX4*	lab collection
HY0733	W303 Mata *rad18Δ::HPHMX4*	lab collection
HY1465	W303 Mata *sgs1Δ::HIS3MX6*	lab collection
HY1532	W303 Matα *hcs1Δ::TRP1*	this study
HY1635	W303 Mata *rad5Δ::HPHMX4 hcs1Δ::TRP1*	this study
HY1691	W303 Mata *sgs1Δ::HIS3MX6 hcs1Δ::TRP1*	this study
HY2018	W303 Mata *PGAL1-3HA-HIS3MX6-HCS1*	this study
HY2019	W303 Mata *PGAL1-3HA-HIS3MX6-HCS1*	this study
HY2025	W303 Mata *hcs1Δ::TRP1*	this study
HY2031	W303 Mata *rad18Δ::HPHMX4 hcs1Δ::TRP1*	this study
HY2059	W303 Mata *POL1-6HIS-3FLAG::KANMX4*	this study
HY2061	W303 Mata *hcs1Δ::TRP1 POL1-6HIS-3FLAG::KANMX4*	this study
HY2065	W303 Mata *rad5DE681,2AA hcs1Δ::TRP1*	this study
HY2101	W303 Mata *rad51Δ::LEU2 hcs1Δ::TRP1*	this study
HY2162	W303 Mata *RAD5-6HIS-3FLAG::KANMX4*	this study
HY2164	W303 Mata *hcs1Δ::TRP1 RAD5-6HIS-3FLAG::KANMX4*	this study
HY2571	W303 Matα *hcs1GK234,5AA*	this study
HY2902	W303 Matα *rad5Δ::HPHMX4 hcs1GK234,5AA*	this study
FY1002	W303 Matα *rad51Δ::LEU2*	Foiani lab
FY1427	W303 Mata *rad5DE681,2AA*	Xiaolan lab

Table 5.1

5.3 Results

5.3.1 *HCS1* deletion confers resistance to DNA damaging and replication stress agents

We started our analysis by characterizing the phenotypes associated with the deletion of *HCS1* gene by spot assay. Surprisingly, *hcs1Δ* cells were resistant to DNA damaging agents, such as the alkylating drugs MMS and Nitrogen Mustard (NM), and to replication stress induced by HU (Figure 5.1). These resistances were remarkable, being observed even at very high concentrations of drugs.

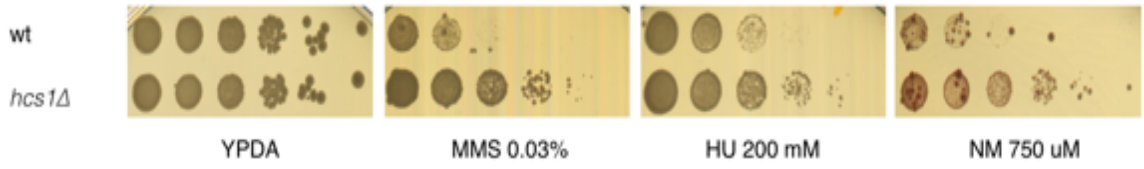

Figure 5.1 *hcs1Δ* cells are resistant to MMS, HU and NM. Ten fold dilutions of wt and *hcs1Δ* cells were plated on YPDA, MMS 0.03%, HU 200 mM and NM 750 µM. Plates were incubated at 28°C and scanned after 3 days.

5.3.2 *hcs1Δ* resistance to DNA damaging and replication stress agents depends on Rad5-Rad18 and Rad51 pathways

The previous set of data suggests that in the absence of Hcs1, cells are more resistant to a variety of damages and stresses, possibly because Hcs1 counteracts some DDT pathways or branches that otherwise would account for replication stress tolerance. This possible role is substantiated by the fact that overexpression of *HCS1* acted in the opposite manner to make cells slow growing and enhance their damage sensitivity (Figure 5.2).

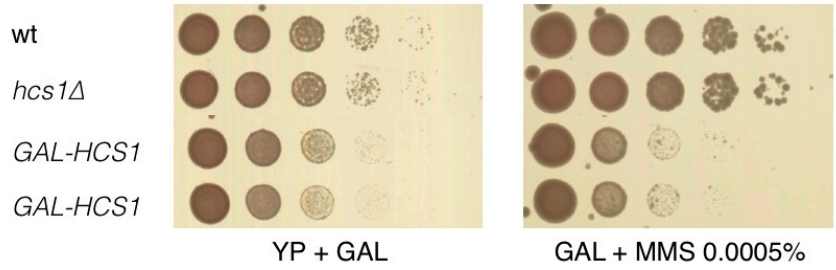

Figure 5.2 Overexpression of Hcs1 affects growth and damage sensitivity. Ten fold dilutions of the indicated strains were plated on YP+Raffinose 2%+Galactose 2% without or with MMS at the concentration of 0.0005%. Plates were incubated at 28°C and scanned after 3 days.

We examined whether the *hcs1Δ* resistance to such drugs depends on some well-established DDT factors. While most combinations tested led to an intermediate damage sensitivity phenotype between the sensitive mutant analyzed and the resistant *hcs1Δ* (examples include *srs2Δ*, *mph1Δ*), we found that deletions of genes belonging to the error-free pathway of damage tolerance, *RAD5* and *RAD18*, as well as *CTF4* (a component of the Polα/Primase complex connecting Polα/Primase to the replicative helicase), completely abolished *hcs1Δ's* resistance to MMS and HU (Figure 5.3). Remarkably, the double mutants *ctf4Δ hcs1Δ* and *rad5Δ hcs1Δ* were as sensitive as the single *ctf4Δ* and *rad5Δ*, suggesting an epistasis between *RAD5, CTF4* and *HCS1*, while the double mutant *rad18Δ hcs1Δ* was much more sensitive than *rad18Δ*. As *rad18Δ* is defective in both Rad5-dependent and translesion synthesis polymerase-mediated bypass, we further tested if the resistance of *hcs1Δ* was dependent on *REV3,* which encodes the catalytic subunit of polymerase zeta, but the double mutant *hcs1Δ rev3Δ* was resistant as the single *hcs1Δ* (data not shown). Other epistasis tests with strains in which all translesion synthesis polymerases are deleted as well as mutagenesis assays will be performed to clarify the relationship between Hcs1 and the two main branches of DDT.

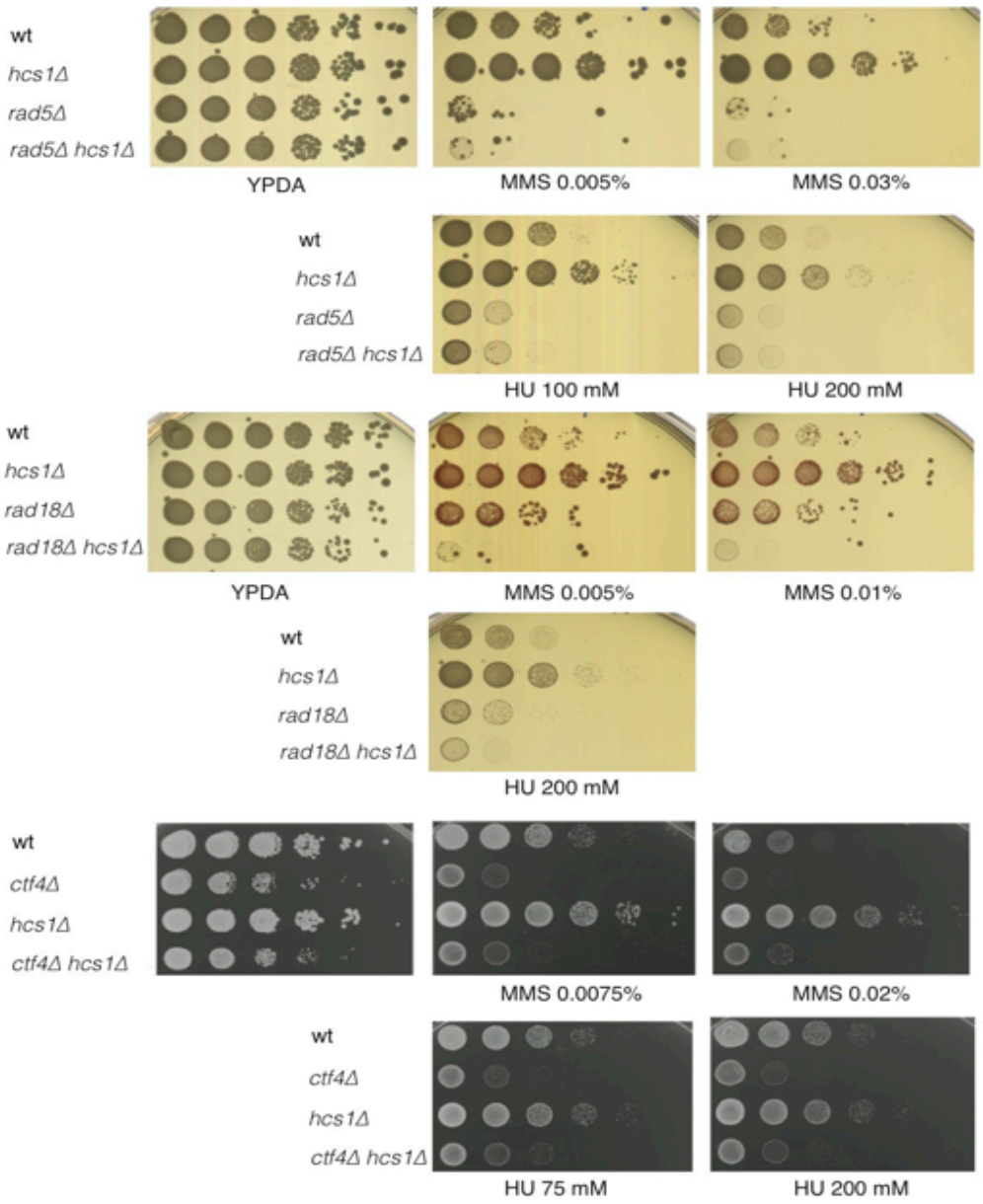

Figure 5.3 Rad5-Rad18 and Ctf4 dependent *hcs1Δ* resistance to MMS and HU. Ten fold dilutions of the indicated strains were plated on several concentrations of MMS and HU, plates were incubated at 28°C and scanned after 3 days.

Furthermore, also an allele of *RAD5* defective in both helicase activity as well as in PCNA polyubiquitination (Ball et al., 2014; Choi et al, submitted collaboration manuscript), *rad5-D681A, E682A* (*rad5-hd, helicase dead*), totally abrogates *hcs1Δ* resistance to MMS and HU, indicating that one of these activities of Rad5 is responsible for the increased viability and altered DDT response of *hcs1Δ* cells (Figure 5.4).

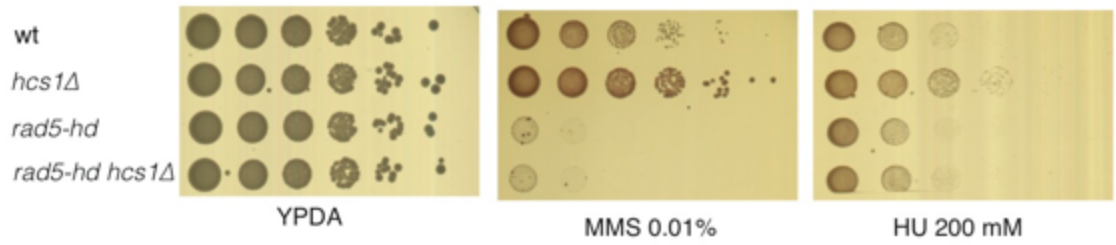

Figure 5.4 *rad5-hd* totally abrogates *hcs1Δ* resistance to MMS and HU. Ten fold dilutions of the indicated strains were plated on on YPDA, MMS 0.01% and HU 200 mM, plates were incubated at 28°C and scanned after 3 days.

The *hcs1Δ* resistance was completely suppressed also by deleting other genes belonging to HR and error-free template switching, such as *RAD51* and *SGS1* (Figure 5.5).

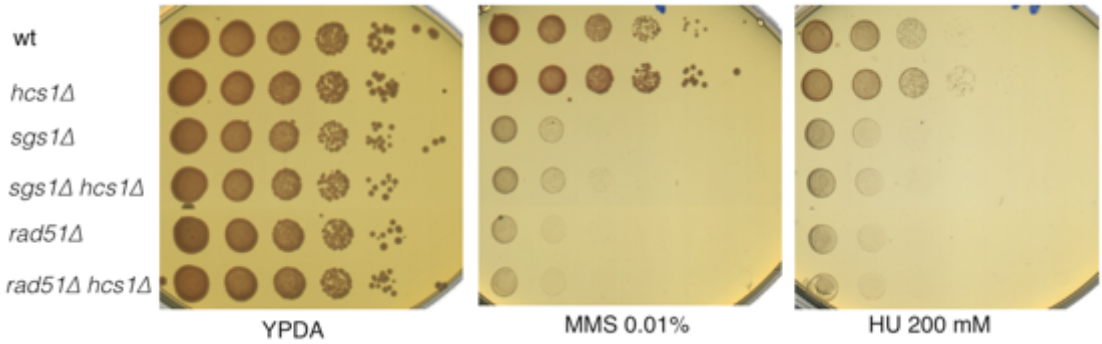

Figure 5.5 Rad51 and Sgs1 dependent *hcs1Δ* resistance to MMS and HU. Ten fold dilutions of the indicated strains were plated on YPDA, MMS 0.01% and HU 200 mM, plates were incubated at 28°C and scanned after 3 days.

The resistance of *hcs1Δ* to NM showed the same genetic dependencies to *RAD5, RAD18, RAD51,* but, differently from MMS and HU, *rad5-hd* mutation did not suppress it, indicating that the resistance to NM damage does not rely on the helicase or PCNA polyubiquitination-dependent functions (Figure 5.6).

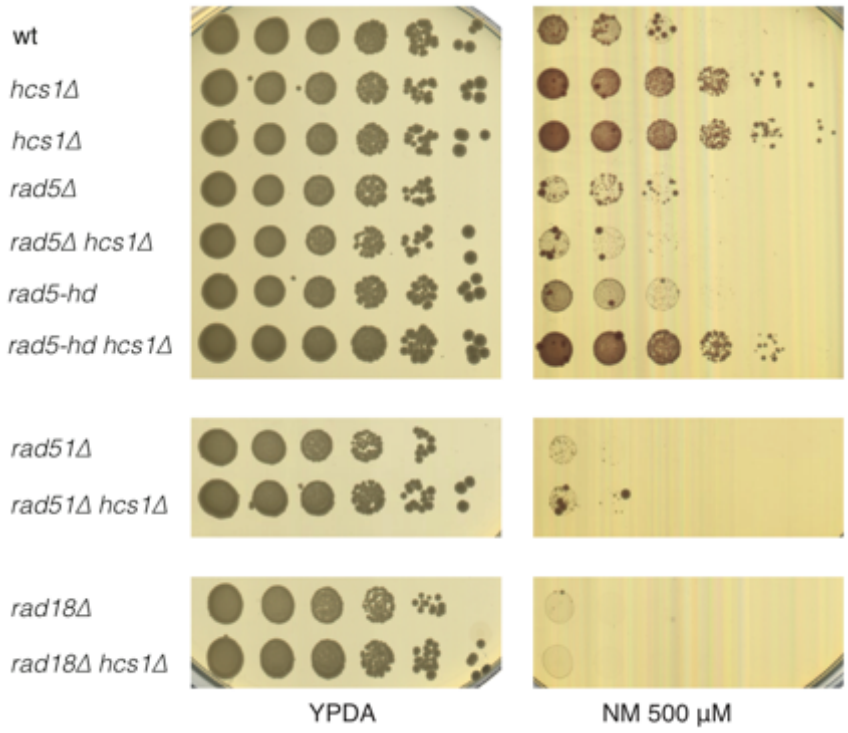

Figure 5.6 Genetic dependencies of *hcs1Δ* resistance to NM. Ten fold dilutions of the indicated strains were plated on YPDA and NM 500 µM, plates were incubated at 28°C and scanned after 3 days.

5.3.3 Loss of Hcs1 helicase activity results in partial resistance to MMS and NM

Hcs1 is a DNA helicase with a Walker A motif, which contains a lysine residue essential for ATP binding and is characterized by a glycine rich loop preceded by a β strand and followed by an α helix.

Hcs1 Walker A is the following:

229-GPPGTGKT-236

The glycine (G) 234 and the lysine (K) 235 were both mutated to Alanine by *Delitto Perfetto* and we called the resulting allele *hcs1-hd (helicase dead)*.

We tested the sensitivity to MMS, NM and HU by spot assay and we found that *hcs1-hd* is partially resistant to MMS and NM, showing an intermediate phenotype between wt cells and *hcs1Δ*. The partial resistance of *hcs1-hd* was still dependent on Rad5 (Figure 5.7).

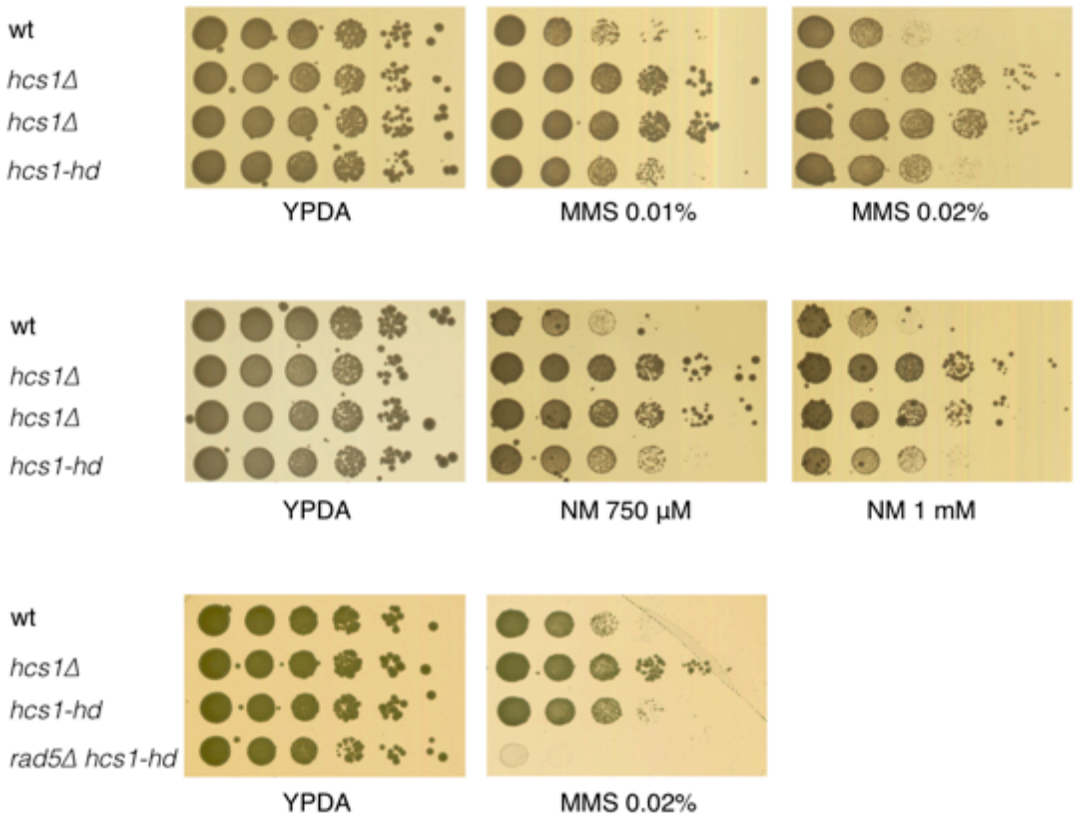

Figure 5.7 *hcs1-hd* is partially resistant to MMS and NM. Ten fold dilutions of the indicated strains were plated on YPDA, MMS and NM, plates were incubated at 28°C and scanned after 3 days.

5.3.4 Hcs1 influences the recruitment of replication and DNA damage tolerance factors to chromatin

Hcs1 is a Polα/Primase-interacting factor and we asked if it is required for the appropriate binding of the catalytic subunit Pol1 to chromatin during replication stress. We performed ChIP-on-chip of Pol1-Flag in wt and *hcs1Δ* cells after 60 min of HU treatment from a G1 release. We found that in the absence of Hcs1, the binding of Pol1 to chromatin at early ARS is severely affected, with a significant reduction in the number of clusters compared to wt. This result suggests that the helicase is required for proper binding of the Polymerase α to S phase replication forks and/or stalled forks (Figure 5.8). However, how this result relates to the increased resistance of *hcs1Δ* cells to HU is not clear and will need to be investigated. An interesting possibility that we plan to examine is that upon prolonged stalling, in *hcs1Δ*, Polα/Primase is aberrantly removed from chromatin, being

possibly degraded. This may make the space for other types of abnormal replication-fork restart that rely on mutagenic pathways or specific recombination pathways, such as BIR. BIR depends on specialized factors such as Ctf4 and Rad51, but Ctf4 binding did not appear to be affected in *hcs1Δ* (data not shown). These results will be reproduced, as they open also the possibility of understanding how BIR is regulated at the fork. Moreover, as in *hcs1Δ* cells, BIR-associated with genomic duplications is increased, our results may reveal what factors are needed for such aberrant events.

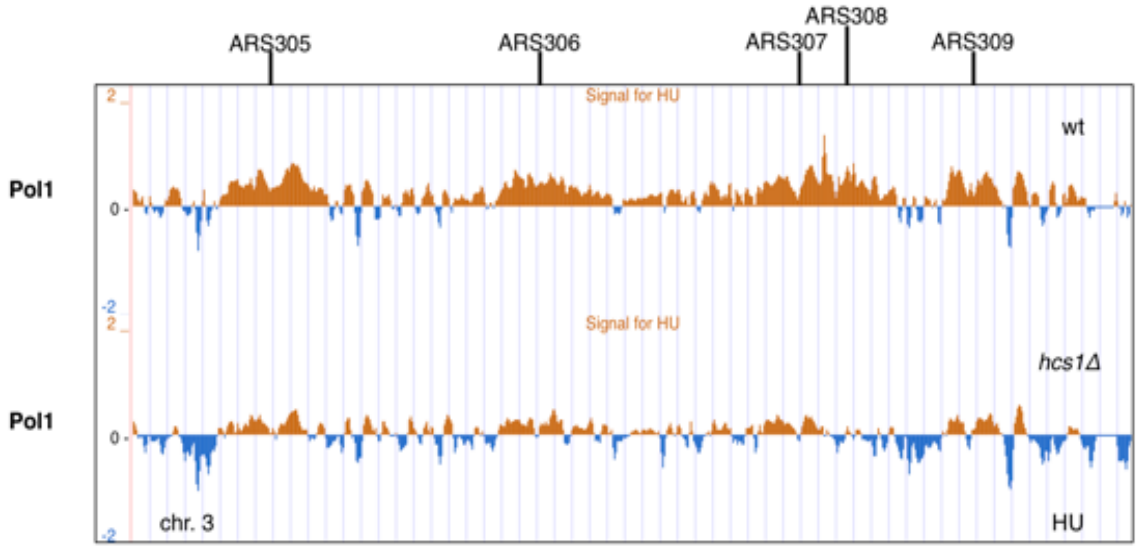

Figure 5.8 Pol1 integral binding to chromatin requires Hcs1. Wt and *hcs1Δ* cells were synchronized in G1 and released in HU 200 mM for 60' when samples for ChIP-on-chip of Pol1-Flag were collected. A snapshot of early origins of replication on chromosome 3 (*ARS305, ARS306, ARS307, ARS308, ARS309*) is shown as example.

We asked if Hcs1 regulates the recruitment to chromatin of other factors that mediate error-free damage tolerance by recombination. To this purpose, we analyzed the binding of Rad51 and Rad5 in HU-treated wt and *hcs1Δ* cells. The results of Rad51 ChIP-on-chip were not yet reproduced possibly due to the background of antibody. Concomitantly with repeating the experiment, we will also try to re-examine Rad51 binding using N-terminal tagged Rad51. With regard to Rad5 binding, we found that Rad5 binds to several regions on chomosomes, such as early origins of replication and centromeres (generally close to

origins of replication). The overall binding profile of Rad5 and enrichment to early origins of replication was not dramatically affected in the absence of Hcs1, but the number of peaks of Rad5 was reduced by 1/4 (36.57% was the genome-wide coverage of Rad5 peaks in wt cells, while 27.63% in *hcs1Δ*) and several Rad5 clusters were altered in the mutant (Figure 5.9).

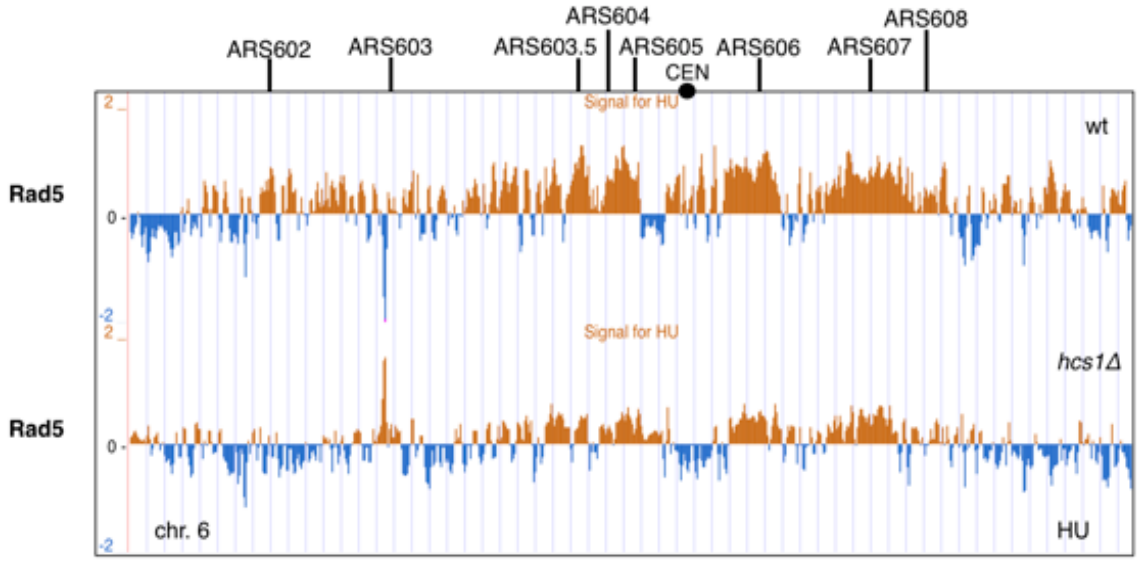

Figure 5.9 Rad5 binding in HU is partially altered in the absence of Hcs1. Wt and *hcs1Δ* cells were synchronized in G1 and released in HU 200 mM for 90' when samples for ChIP-on-chip of Rad5-Flag were collected. Chromosome 6 is shown as example.

5.4 Discussion

Hcs1 is an RPA-stimulated DNA helicase that physically interacts with Polα/Primase. In spite of its conservation, very little is known about how Hcs1 influences replication. Although this work is still far from being complete, we are encouraged in continuing it by our identification of new replication-associated functions influenced by Hcs1. A clear and unusual phenotype is the high resistance of the deletion mutant to several DNA damaging and replication stress agents, making *hcs1Δ* a "super yeast strain", more fit than wt cells under several conditions. One possible explanation for these phenotypes is a toxic role of

Hcs1, partially through its helicase domain. This function of Hcs1 might be induced by DNA damage, allowing cells to survive better the damage.

Since it is unlikely that evolution has retained one protein with only toxic functions for the cells, it is possible that Hcs1 has also important roles during unperturbed replication, within the replisome, and other functions in the presence of damage. Hcs1 might restrain some DDT/ repair activities following genotoxic stress or might negatively influence in some other way the transcription or turn-over of such DDT factors. Interestingly, Slx5/Slx8 (and human RNF4) are now known to mediate Ubiquitin-dependent degradation of SUMOylated relisome components or other repair factors and a genetic interaction between *slx5Δ* and *hcs1Δ* has been reported (Collins et al., 2007). One future direction of our research will be to uncover these functions of Hcs1 in unperturbed and DNA damaging conditions. On one hand, our lab aims at identifying SUMOylated targets upon replication stress and the ones that get degraded in an Slx5/Slx8-dependent manner using SILAC approaches (I. Psakye and D. Branzei). As this assay is set-up, we can focus on identified repair/DDT factors and examine their abundance in *hcs1Δ* as well as functional interactions with *hcs1Δ*. ChIP-on-chip of tagged Hcs1 will tell us if the protein binds to DNA and understanding its chromosomal localization may help in uncover its functions. Moreover, S-tagged and G2-tagged Hcs1 (if functional) might also help in understanding when Hcs1's functions in preventing genomic duplications and in modulating DNA damage tolerance pathways are executed.

DNA damage tolerance allows cells to bypass lesions on DNA and to finish replication without blocking the progression of the fork. Many factors of the error-prone and error-free pathways have been elucidated to date (Branzei, 2011). The resistance of *hcs1Δ* cells to MMS, HU and NM is completely dependent on the error-free pathway of DDT and on recombination. Thus, in the absence of Hcs1, the higher fitness of cells during damage might be explained with the inability to form unscheduled replication intermediates

without the helicase or with the formation of substrates which facilitate the tolerance and/or repair of lesions, which absolutely require the activities of Rad5, both its helicase and its ubiquitin ligase functions, and of Rad51.

From our limited ChIP-on-chip analysis, we found reproducibly that Hcs1 plays a role in the chromatin localization of replication and damage tolerance factors, such as Polα/Primase and Rad5. Without Hcs1 cells are more fit than wt in HU and Pol1 and Rad5 bind less to chromatin and some of the binding is altered during replication stress. One possible explanation is that Hcs1 stabilizes these proteins, and in its absence, fork restart pathways are activated abnormally (that is, differently from wt cells to promote damage tolerance). Hcs1 might represent a new regulatory mechanism via which these important activities are modulated. Interestingly, these factors (Primase, Rad5) also appear to be SUMOylated in response to replication stress (Albuquerque et al., 2013). As Hcs1 function was genetically linked to the one of Slx5/Slx8 (Collins et al., 2007), we also plan to examine the functional interactions between Hcs1 and Rad5, Pol1/Ctf4-variants in which the proteins are fused to a SUMO protease (Ulp) domain causing the fused variant and the associated proteins to be de-SUMOylated. As controls, variants containing fusions to a catalytically dead domain of Ulp will be used. With these constructs being now established and in use in the lab (B. Szakal and D. Branzei, unpublished results), there is high expectancy that new understanding on Hcs1 genetic interaction with these pathways will be illuminated.

6 Appendix 2

During my PhD I worked on an other project related to the Smc5/6 complex in collaboration with Dr. Jennifer A. Cobb, Department of Biochemistry and Molecular Biology, Southern Alberta Cancer Research Institute, University of Calgary, Calgary, Alberta T2N 4N1, Canada. This work was published in The Journal of Biological Chemistry, 2012, 287:11374-11383.

Title

During Replication Stress, Non-Smc Element 5 (Nse5) Is Required for Smc5/6 Protein Complex Functionality at Stalled Forks

Abstract

The Smc5/6 complex belongs to the SMC (structural maintenance of chromosomes) family, which also includes cohesin and condensin. In Saccharomyces cerevisiae, the Smc5/6 complex contains six essential non-Smc elements, Nse1–6. Very little is known about how these additional elements contribute to com- plex function except for Nse2/Mms21, which is an E3 small ubiquitin-like modifier (SUMO) ligase important for Smc5 sumoylation. Characterization of two temperature-sensitive mutants, *nse5-ts1* and *nse5-ts2*, demonstrated the importance of Nse5 within the Smc5/6 complex for its stability and func- tionality at forks during hydroxyurea-induced replication stress. Both *NSE5* alleles showed a marked reduction in Smc5 sumoylation to levels lower than those observed with *mms21-11*, a mutant of Mms21 that is deficient in SUMO ligase activity. However, a phenotypic comparison of *nse5-ts1* and *nse5-ts2* revealed a separation of importance between Smc5 sumoylation and the function of the Smc5/6 complex during replication. Only cells carrying the *nse5-ts1* allele exhibited defects such as dissociation

of the replisome from stalled forks, formation of fork-associated homologous recombination intermediates, and hydroxyurea sensitivity that is additive with *mms21-11*. These defects are attributed to a failure in Smc5/6 localization to forks in *nse5-ts1* cells. Overall, these data support the premise that Nse5 is important for vital interactions between components within the Smc5/6 complex, and for its functionality during replication stress.

The manuscript is given in attachment to the thesis.

During my PhD I worked on a project of the lab aiming at elucidating the role of DNA bending in DNA damage tolerance. This work was published in EMBO Journal, 2014, 33: 327-40.

Title

DNA bending facilitates the error-free DNA damage tolerance pathway and upholds genome integrity

Abstract

DNA replication is sensitive to damage in the template. To bypass lesions and complete replication, cells activate recombination- mediated (error-free) and translesion synthesis-mediated (error- prone) DNA damage tolerance pathways. Crucial for error-free DNA damage tolerance is template switching, which depends on the formation and resolution of damage-bypass intermediates consist- ing of sister chromatid junctions. Here we show that a chromatin architectural pathway involving the high mobility group box pro- tein Hmo1 channels replication-associated lesions into the error- free DNA damage tolerance

pathway mediated by Rad5 and PCNA polyubiquitylation, while preventing mutagenic bypass and toxic recombination. In the process of template switching, Hmo1 also promotes sister chromatid junction formation predominantly dur- ing replication. Its C-terminal tail, implicated in chromatin bend- ing, facilitates the formation of catenations/hemicatenations and mediates the roles of Hmo1 in DNA damage tolerance pathway choice and sister chromatid junction formation. Together, the results suggest that replication-associated topological changes involving the molecular DNA bender, Hmo1, set the stage for dedi- cated repair reactions that limit errors during replication and impact on genome stability.

The manuscript is given in attachment to the thesis.

7 References

Albuquerque, C.P., Wang, G., Lee, N.S., Kolodner, R.D., Putnam, C.D., and Zhou, H. (2013). Distinct SUMO ligases cooperate with Esc2 and Slx5 to suppress duplication-mediated genome rearrangements. PLoS Genet *9*, e1003670.

Almedawar, S., Colomina, N., Bermudez-Lopez, M., Pocino-Merino, I., and Torres-Rosell, J. (2012). A SUMO-dependent step during establishment of sister chromatid cohesion. Curr Biol *22*, 1576-1581.

Andrews, E.A., Palecek, J., Sergeant, J., Taylor, E., Lehmann, A.R., and Watts, F.Z. (2005). Nse2, a component of the Smc5-6 complex, is a SUMO ligase required for the response to DNA damage. Mol Cell Biol *25*, 185-196.

Ball, L.G., Xu, X., Blackwell, S., Hanna, M.D., Lambrecht, A.D., and Xiao, W. (2014). The Rad5 helicase activity is dispensable for error-free DNA post-replication repair. DNA Repair (Amst) *16*, 74-83.

Barlow, J.H., Faryabi, R.B., Callen, E., Wong, N., Malhowski, A., Chen, H.T., Gutierrez-Cruz, G., Sun, H.W., McKinnon, P., Wright, G.*, et al.* (2013). Identification of early replicating fragile sites that contribute to genome instability. Cell *152*, 620-632.

Bavner, A., Matthews, J., Sanyal, S., Gustafsson, J.A., and Treuter, E. (2005). EID3 is a novel EID family member and an inhibitor of CBP-dependent co-activation. Nucleic Acids Res *33*, 3561-3569.

Baxter, J., and Diffley, J.F. (2008). Topoisomerase II inactivation prevents the completion of DNA replication in budding yeast. Mol Cell *30*, 790-802.

Baxter, J., Sen, N., Martinez, V.L., De Carandini, M.E., Schvartzman, J.B., Diffley, J.F., and Aragon, L. (2011). Positive supercoiling of mitotic DNA drives decatenation by topoisomerase II in eukaryotes. Science *331*, 1328-1332.

Behlke-Steinert, S., Touat-Todeschini, L., Skoufias, D.A., and Margolis, R.L. (2009). SMC5 and MMS21 are required for chromosome cohesion and mitotic progression. Cell Cycle *8*, 2211-2218.

Bell, L., and Byers, B. (1983). Separation of branched from linear DNA by two-dimensional gel electrophoresis. Anal Biochem *130*, 527-535.

Bergink, S., and Jentsch, S. (2009). Principles of ubiquitin and SUMO modifications in DNA repair. Nature *458*, 461-467.

Bermejo, R., Capra, T., Gonzalez-Huici, V., Fachinetti, D., Cocito, A., Natoli, G., Katou, Y., Mori, H., Kurokawa, K., Shirahige, K.*, et al.* (2009a). Genome-organizing factors Top2 and Hmo1 prevent chromosome fragility at sites of S phase transcription. Cell *138*, 870-884.

Bermejo, R., Katou, Y.M., Shirahige, K., and Foiani, M. (2009b). ChIP-on-chip analysis of DNA topoisomerases. Methods Mol Biol *582*, 103-118.

Bermudez-Lopez, M., Ceschia, A., de Piccoli, G., Colomina, N., Pasero, P., Aragon, L., and Torres-Rosell, J. (2010). The Smc5/6 complex is required for dissolution of DNA-mediated sister chromatid linkages. Nucleic Acids Res *38*, 6502-6512.

Bhalla, N., Biggins, S., and Murray, A.W. (2002). Mutation of YCS4, a budding yeast condensin subunit, affects mitotic and nonmitotic chromosome behavior. Mol Biol Cell *13*, 632-645.

Bianco, J.N., Poli, J., Saksouk, J., Bacal, J., Silva, M.J., Yoshida, K., Lin, Y.L., Tourriere, H., Lengronne, A., and Pasero, P. (2012). Analysis of DNA replication profiles in budding yeast and mammalian cells using DNA combing. Methods *57*, 149-157.

Biswas, E.E., Fricke, W.M., Chen, P.H., and Biswas, S.B. (1997a). Yeast DNA helicase A: cloning, expression, purification, and enzymatic characterization. Biochemistry *36*, 13277-13284.

Biswas, S.B., Chen, P.H., and Biswas, E.E. (1997b). Purification and characterization of DNA polymerase alpha-associated replication protein A-dependent yeast DNA helicase A. Biochemistry *36*, 13270-13276.

Boddy, M.N., Shanahan, P., McDonald, W.H., Lopez-Girona, A., Noguchi, E., Yates, I.J., and Russell, P. (2003). Replication checkpoint kinase Cds1 regulates recombinational repair protein Rad60. Mol Cell Biol *23*, 5939-5946.

Branzei, D. (2011). Ubiquitin family modifications and template switching. FEBS Lett *585*, 2810-2817.

Branzei, D., and Foiani, M. (2008). Regulation of DNA repair throughout the cell cycle. Nat Rev Mol Cell Biol *9*, 297-308.

Branzei, D., and Foiani, M. (2010). Maintaining genome stability at the replication fork. Nat Rev Mol Cell Biol *11*, 208-19.

Branzei, D., Seki, M., and Enomoto, T. (2004). Rad18/Rad5/Mms2-mediated polyubiquitination of PCNA is implicated in replication completion during replication stress. Genes Cells *9*, 1031-1042.

Branzei, D., Sollier, J., Liberi, G., Zhao, X., Maeda, D., Seki, M., Enomoto, T., Ohta, K., and Foiani, M. (2006). Ubc9- and mms21-mediated sumoylation counteracts recombinogenic events at damaged replication forks. Cell *127*, 509-522.

Branzei, D., Vanoli, F., and Foiani, M. (2008). SUMOylation regulates Rad18-mediated template switch. Nature *456*, 915-920.

Brewer, B.J., and Fangman, W.L. (1987). The localization of replication origins on ARS plasmids in S. cerevisiae. Cell *51*, 463-471.

Bustard, D.E., Menolfi, D., Jeppsson, K., Ball, L.G., Dewey, S.C., Shirahige, K., Sjogren, C., Branzei, D., and Cobb, J.A. (2012). During replication stress, non-SMC element 5 (NSE5) is required for Smc5/6 protein complex functionality at stalled forks. J Biol Chem *287*, 11374-11383.

Chavez, A., Agrawal, V., and Johnson, F.B. (2011). Homologous recombination-dependent rescue of deficiency in the structural maintenance of chromosomes (Smc) 5/6 complex. J Biol Chem *286*, 5119-5125.

Chavez, A., George, V., Agrawal, V., and Johnson, F.B. (2010). Sumoylation and the structural maintenance of chromosomes (Smc) 5/6 complex slow senescence through recombination intermediate resolution. J Biol Chem *285*, 11922-11930.

Chen, Y.H., Choi, K., Szakal, B., Arenz, J., Duan, X., Ye, H., Branzei, D., and Zhao, X. (2009). Interplay between the Smc5/6 complex and the Mph1 helicase in recombinational repair. Proc Natl Acad Sci U S A *106*, 21252-21257.

Chiolo, I., Minoda, A., Colmenares, S.U., Polyzos, A., Costes, S.V., and Karpen, G.H. (2011). Double-strand breaks in heterochromatin move outside of a dynamic HP1a domain to complete recombinational repair. Cell *144*, 732-744.

Choi, K., Szakal, B., Chen, Y.H., Branzei, D., and Zhao, X. (2010). The Smc5/6 complex and Esc2 influence multiple replication-associated recombination processes in Saccharomyces cerevisiae. Mol Biol Cell *21*, 2306-2314.

Ciosk, R., Shirayama, M., Shevchenko, A., Tanaka, T., Toth, A., and Nasmyth, K. (2000). Cohesin's binding to chromosomes depends on a separate complex consisting of Scc2 and Scc4 proteins. Mol Cell *5*, 243-254.

Coelho, P.A., Queiroz-Machado, J., and Sunkel, C.E. (2003). Condensin-dependent localisation of topoisomerase II to an axial chromosomal structure is required for sister chromatid resolution during mitosis. J Cell Sci *116*, 4763-4776.

Collins, S.R., Miller, K.M., Maas, N.L., Roguev, A., Fillingham, J., Chu, C.S., Schuldiner, M., Gebbia, M., Recht, J., Shales, M.*, et al.* (2007). Functional dissection of protein complexes involved in yeast chromosome biology using a genetic interaction map. Nature *446*, 806-810.

Costantino, L., Sotiriou, S.K., Rantala, J.K., Magin, S., Mladenov, E., Helleday, T., Haber, J.E., Iliakis, G., Kallioniemi, O.P., and Halazonetis, T.D. (2014). Break-induced replication repair of damaged forks induces genomic duplications in human cells. Science *343*, 88-91.

D'Ambrosio, C., Schmidt, C.K., Katou, Y., Kelly, G., Itoh, T., Shirahige, K., and Uhlmann, F. (2008). Identification of cis-acting sites for condensin loading onto budding yeast chromosomes. Genes Dev *22*, 2215-2227.

Daigaku, Y., Davies, A.A., and Ulrich, H.D. (2010). Ubiquitin-dependent DNA damage bypass is separable from genome replication. Nature *465*, 951-955.

De Antoni, A., and Gallwitz, D. (2000). A novel multi-purpose cassette for repeated integrative epitope tagging of genes in Saccharomyces cerevisiae. Gene *246*, 179-185.

De Piccoli, G., Cortes-Ledesma, F., Ira, G., Torres-Rosell, J., Uhle, S., Farmer, S., Hwang, J.Y., Machin, F., Ceschia, A., McAleenan, A.*, et al.* (2006). Smc5-Smc6 mediate DNA double-strand-break repair by promoting sister-chromatid recombination. Nat Cell Biol *8*, 1032-1034.

Deshpande, A.M., and Newlon, C.S. (1996). DNA replication fork pause sites dependent on transcription. Science *272*, 1030-1033.

Doyle, J.M., Gao, J., Wang, J., Yang, M., and Potts, P.R. (2010). MAGE-RING protein complexes comprise a family of E3 ubiquitin ligases. Mol Cell *39*, 963-974.

Duan, X., Sarangi, P., Liu, X., Rangi, G.K., Zhao, X., and Ye, H. (2009a). Structural and functional insights into the roles of the Mms21 subunit of the Smc5/6 complex. Mol Cell *35*, 657-668.

Duan, X., Yang, Y., Chen, Y.H., Arenz, J., Rangi, G.K., Zhao, X., and Ye, H. (2009b). Architecture of the Smc5/6 Complex of Saccharomyces cerevisiae Reveals a Unique Interaction between the Nse5-6 Subcomplex and the Hinge Regions of Smc5 and Smc6. J Biol Chem *284*, 8507-8515.

Fachinetti, D., Bermejo, R., Cocito, A., Minardi, S., Katou, Y., Kanoh, Y., Shirahige, K., Azvolinsky, A., Zakian, V.A., and Foiani, M. (2010). Replication termination at eukaryotic chromosomes is mediated by Top2 and occurs at genomic loci containing pausing elements. Mol Cell *39*, 595-605.

Feng, Y., Gao, J., and Yang, M. (2011). When MAGE meets RING: insights into biological functions of MAGE proteins. Protein Cell *2*, 7-12.

Foiani, M., Pellicioli, A., Lopes, M., Lucca, C., Ferrari, M., Liberi, G., Muzi Falconi, M., and Plevani, P. (2000). DNA damage checkpoints and DNA replication controls in Saccharomyces cerevisiae. Mutat Res *451*, 187-196.

Fousteri, M.I., and Lehmann, A.R. (2000). A novel SMC protein complex in Schizosaccharomyces pombe contains the Rad18 DNA repair protein. Embo J *19*, 1691-1702.

Gallego-Paez, L.M., Tanaka, H., Bando, M., Takahashi, M., Nozaki, N., Nakato, R., Shirahige, K., and Hirota, T. (2014). Smc5/6-mediated regulation of replication progression contributes to chromosome assembly during mitosis in human cells. Mol Biol Cell *25*, 302-317.

Gandhi, R., Gillespie, P.J., and Hirano, T. (2006). Human Wapl is a cohesin-binding protein that promotes sister-chromatid resolution in mitotic prophase. Curr Biol *16*, 2406-2417.

Giannattasio, M., Zwicky, K., Follonier, C., Foiani, M., Lopes, M., and Branzei, D. (2014). Visualization of recombination-mediated damage bypass by template switching. Nat Struct Mol Biol.

Gietz, R.D., Schiestl, R.H., Willems, A.R., and Woods, R.A. (1995). Studies on the transformation of intact yeast cells by the LiAc/SS-DNA/PEG procedure. Yeast *11*, 355-360.

Gonzalez-Huici, V., Szakal, B., Urulangodi, M., Psakhye, I., Castellucci, F., Menolfi, D., Rajakumara, E., Fumasoni, M., Bermejo, R., Jentsch, S.*, et al.* (2014). DNA bending facilitates the error-free DNA damage tolerance pathway and upholds genome integrity. Embo J *33*, 327-340.

Graumann, P.L., and Knust, T., (2009). Dynamics of the bacterial SMC complex and SMC-like proteins involved in DNA repair. Chromosome Research *17*, 265-275

Greenfeder, S.A., and Newlon, C.S. (1992). Replication forks pause at yeast centromeres. Mol Cell Biol *12*, 4056-4066.

Gritenaite, D., Princz, L.N., Szakal, B., Bantele, S.C., Wendeler, L., Schilbach, S., Habermann, B.H., Matos, J., Lisby, M., Branzei, D.*, et al.* (2014). A cell cycle-regulated Slx4-Dpb11 complex promotes the resolution of DNA repair intermediates linked to stalled replication. Genes Dev *28*, 1604-1619.

Haeusler, R.A., Pratt-Hyatt, M., Good, P.D., Gipson, T.A., and Engelke, D.R. (2008). Clustering of yeast tRNA genes is mediated by specific association of condensin with tRNA gene transcription complexes. Genes Dev *22*, 2204-2214.

Harvey, S.H., Sheedy, D.M., Cuddihy, A.R., and O'Connell, M.J. (2004). Coordination of DNA damage responses via the Smc5/Smc6 complex. Mol Cell Biol *24*, 662-674.

Hauf, S., Roitinger, E., Koch, B., Dittrich, C.M., Mechtler, K., and Peters, J.M. (2005). Dissociation of cohesin from chromosome arms and loss of arm cohesion during early mitosis depends on phosphorylation of SA2. PLoS Biol *3*, e69.

Heidinger-Pauli, J.M., Mert, O., Davenport, C., Guacci, V., and Koshland, D. (2010). Systematic reduction of cohesin differentially affects chromosome segregation, condensation, and DNA repair. Curr Biol *20*, 957-963.

Heidinger-Pauli, J.M., Unal, E., and Koshland, D. (2009). Distinct targets of the Eco1 acetyltransferase modulate cohesion in S phase and in response to DNA damage. Mol Cell *34*, 311-321.

Hirano, T. (2006). At the heart of the chromosome: SMC proteins in action. Nat Rev Mol Cell Biol *7*, 311-322.

Hoege, C., Pfander, B., Moldovan, G.L., Pyrowolakis, G., and Jentsch, S. (2002). RAD6-dependent DNA repair is linked to modification of PCNA by ubiquitin and SUMO. Nature *419*, 135-141.

Hombauer, H., Srivatsan, A., Putnam, C.D., and Kolodner, R.D. (2011). Mismatch repair, but not heteroduplex rejection, is temporally coupled to DNA replication. Science *334*, 1713-1716.

Hwang, J.Y., Smith, S., Ceschia, A., Torres-Rosell, J., Aragon, L., and Myung, K. (2008). Smc5-Smc6 complex suppresses gross chromosomal rearrangements mediated by break-induced replications. DNA Repair (Amst) *7*, 1426-1436.

Irmisch, A., Ampatzidou, E., Mizuno, K., O'Connell, M.J., and Murray, J.M. (2009). Smc5/6 maintains stalled replication forks in a recombination-competent conformation. Embo J *28*, 144-155.

Ivessa, A.S., Lenzmeier, B.A., Bessler, J.B., Goudsouzian, L.K., Schnakenberg, S.L., and Zakian, V.A. (2003). The Saccharomyces cerevisiae helicase Rrm3p facilitates replication past nonhistone protein-DNA complexes. Mol Cell *12*, 1525-1536.

Ivessa, A.S., Zhou, J.Q., Schulz, V.P., Monson, E.K., and Zakian, V.A. (2002). Saccharomyces Rrm3p, a 5' to 3' DNA helicase that promotes replication fork progression through telomeric and subtelomeric DNA. Genes Dev *16*, 1383-1396.

Ivessa, A.S., Zhou, J.Q., and Zakian, V.A. (2000). The Saccharomyces Pif1p DNA helicase and the highly related Rrm3p have opposite effects on replication fork progression in ribosomal DNA. Cell *100*, 479-489.

Janke, C., Magiera, M.M., Rathfelder, N., Taxis, C., Reber, S., Maekawa, H., Moreno-Borchart, A., Doenges, G., Schwob, E., Schiebel, E.*, et al.* (2004). A versatile toolbox for

PCR-based tagging of yeast genes: new fluorescent proteins, more markers and promoter substitution cassettes. Yeast *21*, 947-962.

Jeppsson, K., Carlborg, K.K., Nakato, R., Berta, D.G., Lilienthal, I., Kanno, T., Lindqvist, A., Brink, M.C., Dantuma, N.P., Katou, Y.*, et al.* (2014a). The chromosomal association of the smc5/6 complex depends on cohesion and predicts the level of sister chromatid entanglement. PLoS Genet *10*, e1004680.

Jeppsson, K., Kanno, T., Shirahige, K., and Sjogren, C. (2014b). The maintenance of chromosome structure: positioning and functioning of SMC complexes. Nat Rev Mol Cell Biol *15*, 601-614.

Ju, L., Wing, J., Taylor, E., Brandt, R., Slijepcevic, P., Horsch, M., Rathkolb, B., Racz, I., Becker, L., Hans, W.*, et al.* (2013). SMC6 is an essential gene in mice, but a hypomorphic mutant in the ATPase domain has a mild phenotype with a range of subtle abnormalities. DNA Repair (Amst) *12*, 356-366.

Kagey, M.H., Newman, J.J., Bilodeau, S., Zhan, Y., Orlando, D.A., van Berkum, N.L., Ebmeier, C.C., Goossens, J., Rahl, P.B., Levine, S.S.*, et al.* (2010). Mediator and cohesin connect gene expression and chromatin architecture. Nature *467*, 430-435.

Kannouche, P.L., Wing, J., and Lehmann, A.R. (2004). Interaction of human DNA polymerase eta with monoubiquitinated PCNA: a possible mechanism for the polymerase switch in response to DNA damage. Mol Cell *14*, 491-500.

Karras, G.I., Fumasoni, M., Sienski, G., Vanoli, F., Branzei, D., and Jentsch, S. (2013). Noncanonical role of the 9-1-1 clamp in the error-free DNA damage tolerance pathway. Mol Cell *49*, 536-546.

Karras, G.I., and Jentsch, S. (2010). The RAD6 DNA damage tolerance pathway operates uncoupled from the replication fork and is functional beyond S phase. Cell *141*, 255-267.

Katou, Y., Kaneshiro, K., Aburatani, H., and Shirahige, K. (2006). Genomic approach for the understanding of dynamic aspect of chromosome behavior. Methods Enzymol *409*, 389-410.

Kegel, A., Betts-Lindroos, H., Kanno, T., Jeppsson, K., Strom, L., Katou, Y., Itoh, T., Shirahige, K., and Sjogren, C. (2011). Chromosome length influences replication-induced topological stress. Nature *471*, 392-396.

Kegel, A., and Sjogren, C. (2010). The Smc5/6 complex: more than repair? Cold Spring Harb Symp Quant Biol *75*, 179-187.

Kim, J.S., Krasieva, T.B., LaMorte, V., Taylor, A.M., and Yokomori, K. (2002). Specific recruitment of human cohesin to laser-induced DNA damage. J Biol Chem *277*, 45149-45153.

Kitajima, T.S., Sakuno, T., Ishiguro, K., Iemura, S., Natsume, T., Kawashima, S.A., and Watanabe, Y. (2006). Shugoshin collaborates with protein phosphatase 2A to protect cohesin. Nature *441*, 46-52.

Kliszczak, M., Stephan, A.K., Flanagan, A.M., and Morrison, C.G. (2012). SUMO ligase activity of vertebrate Mms21/Nse2 is required for efficient DNA repair but not for Smc5/6 complex stability. DNA Repair (Amst) *11*, 799-810.

Kotter, P., Weigand, J.E., Meyer, B., Entian, K.D., and Suess, B. (2009). A fast and efficient translational control system for conditional expression of yeast genes. Nucleic Acids Res *37*, e120.

Kuzminov, A., Schabtach, E., and Stahl, F.W. (1997). Study of plasmid replication in Escherichia coli with a combination of 2D gel electrophoresis and electron microscopy. J Mol Biol *268*, 1-7.

Lee, K.M., Nizza, S., Hayes, T., Bass, K.L., Irmisch, A., Murray, J.M., and O'Connell, M.J. (2007). Brc1-mediated rescue of Smc5/6 deficiency: requirement for multiple nucleases and a novel Rad18 function. Genetics *175*, 1585-1595.

Lehmann, A.R., Walicka, M., Griffiths, D.J., Murray, J.M., Watts, F.Z., McCready, S., and Carr, A.M. (1995). The rad18 gene of Schizosaccharomyces pombe defines a new subgroup of the SMC superfamily involved in DNA repair. Mol Cell Biol *15*, 7067-7080.

Lengronne, A., Katou, Y., Mori, S., Yokobayashi, S., Kelly, G.P., Itoh, T., Watanabe, Y., Shirahige, K., and Uhlmann, F. (2004). Cohesin relocation from sites of chromosomal loading to places of convergent transcription. Nature *430*, 573-578.

Leung, G.P., Lee, L., Schmidt, T.I., Shirahige, K., and Kobor, M.S. (2011). Rtt107 is required for recruitment of the SMC5/6 complex to DNA double strand breaks. J Biol Chem *286*, 26250-26257.

Li, X., Zhuo, R., Tiong, S., Di Cara, F., King-Jones, K., Hughes, S.C., Campbell, S.D., and Wevrick, R. (2013). The Smc5/Smc6/MAGE complex confers resistance to caffeine and genotoxic stress in Drosophila melanogaster. PLoS One *8*, e59866.

Liberi, G., Maffioletti, G., Lucca, C., Chiolo, I., Baryshnikova, A., Cotta-Ramusino, C., Lopes, M., Pellicioli, A., Haber, J.E., and Foiani, M. (2005). Rad51-dependent DNA structures accumulate at damaged replication forks in sgs1 mutants defective in the yeast ortholog of BLM RecQ helicase. Genes Dev *19*, 339-350.

Lindow, J.C., Kuwano, M., Moriya, S., and Grossman, A.D. (2002). Subcellular localization of the Bacillus subtilis structural maintenance of chromosomes (SMC) protein. Mol Microbiol *46*, 997-1009.

Lindroos, H.B., Strom, L., Itoh, T., Katou, Y., Shirahige, K., and Sjogren, C. (2006). Chromosomal association of the Smc5/6 complex reveals that it functions in differently regulated pathways. Mol Cell *22*, 755-767.

Longtine, M.S., McKenzie, A., 3rd, Demarini, D.J., Shah, N.G., Wach, A., Brachat, A., Philippsen, P., and Pringle, J.R. (1998). Additional modules for versatile and economical PCR-based gene deletion and modification in Saccharomyces cerevisiae. Yeast *14*, 953-961.

Lopes, M., Cotta-Ramusino, C., Pellicioli, A., Liberi, G., Plevani, P., Muzi-Falconi, M., Newlon, C.S., and Foiani, M. (2001). The DNA replication checkpoint response stabilizes stalled replication forks. Nature *412*, 557-561.

Losada, A., and Hirano, T. (2005). Dynamic molecular linkers of the genome: the first decade of SMC proteins. Genes Dev *19*, 1269-1287.

Lydeard, J.R., Jain, S., Yamaguchi, M., and Haber, J.E. (2007). Break-induced replication and telomerase-independent telomere maintenance require Pol32. Nature *448*, 820-823.

Mankouri, H.W., Ngo, H.P., and Hickson, I.D. (2009). Esc2 and Sgs1 act in functionally distinct branches of the homologous recombination repair pathway in Saccharomyces cerevisiae. Mol Biol Cell *20*, 1683-1694.

Mascarenhas, J., Sanchez, H., Tadesse, S., Kidane, D., Krisnamurthy, M., Alonso, J.C., and Graumann, P.L. (2006). Bacillus subtilis SbcC protein plays an important role in DNA inter-strand cross-link repair. BMC Mol Biol *7*, 20.

McAleenan, A., Cordon-Preciado, V., Clemente-Blanco, A., Liu, I.C., Sen, N., Leonard, J., Jarmuz, A., and Aragon, L. (2012). SUMOylation of the alpha-kleisin subunit of cohesin is required for DNA damage-induced cohesion. Curr Biol *22*, 1564-1575.

Misulovin, Z., Schwartz, Y.B., Li, X.Y., Kahn, T.G., Gause, M., MacArthur, S., Fay, J.C., Eisen, M.B., Pirrotta, V., Biggin, M.D.*, et al.* (2008). Association of cohesin and Nipped-B with transcriptionally active regions of the Drosophila melanogaster genome. Chromosoma *117*, 89-102.

Mohanty, B.K., Bairwa, N.K., and Bastia, D. (2006). The Tof1p-Csm3p protein complex counteracts the Rrm3p helicase to control replication termination of Saccharomyces cerevisiae. Proc Natl Acad Sci U S A *103*, 897-902.

Mohanty, B.K., and Bastia, D. (2004). Binding of the replication terminator protein Fob1p to the Ter sites of yeast causes polar fork arrest. J Biol Chem *279*, 1932-1941.

Noel, J.F., and Wellinger, R.J. (2011). Abrupt telomere losses and reduced end-resection can explain accelerated senescence of Smc5/6 mutants lacking telomerase. DNA Repair (Amst) *10*, 271-282.

Ono, T., Losada, A., Hirano, M., Myers, M.P., Neuwald, A.F., and Hirano, T. (2003). Differential contributions of condensin I and condensin II to mitotic chromosome architecture in vertebrate cells. Cell *115*, 109-121.

Onoda, F., Takeda, M., Seki, M., Maeda, D., Tajima, J., Ui, A., Yagi, H., and Enomoto, T. (2004). SMC6 is required for MMS-induced interchromosomal and sister chromatid recombinations in Saccharomyces cerevisiae. DNA Repair (Amst) *3*, 429-439.

Ortiz-Bazan, M.A., Gallo-Fernandez, M., Saugar, I., Jimenez-Martin, A., Vazquez, M.V., and Tercero, J.A. (2014). Rad5 Plays a Major Role in the Cellular Response to DNA Damage during Chromosome Replication. Cell Rep.

Outwin, E.A., Irmisch, A., Murray, J.M., and O'Connell, M.J. (2009). Smc5-Smc6-dependent removal of cohesin from mitotic chromosomes. Mol Cell Biol *29*, 4363-4375.

Palecek, J., Vidot, S., Feng, M., Doherty, A.J., and Lehmann, A.R. (2006). The Smc5-Smc6 DNA repair complex. bridging of the Smc5-Smc6 heads by the KLEISIN, Nse4, and non-Kleisin subunits. J Biol Chem *281*, 36952-36959.

Payne, F., Colnaghi, R., Rocha, N., Seth, A., Harris, J., Carpenter, G., Bottomley, W.E., Wheeler, E., Wong, S., Saudek, V.*, et al.* (2014). Hypomorphism in human NSMCE2 linked to primordial dwarfism and insulin resistance. J Clin Invest *124*, 4028-4038.

Pebernard, S., Perry, J.J., Tainer, J.A., and Boddy, M.N. (2008a). Nse1 RING-like domain supports functions of the Smc5-Smc6 holocomplex in genome stability. Mol Biol Cell *19*, 4099-4109.

Pebernard, S., Schaffer, L., Campbell, D., Head, S.R., and Boddy, M.N. (2008b). Localization of Smc5/6 to centromeres and telomeres requires heterochromatin and SUMO, respectively. Embo J *27*, 3011-3023.

Pebernard, S., Wohlschlegel, J., McDonald, W.H., Yates, J.R., 3rd, and Boddy, M.N. (2006). The Nse5-Nse6 dimer mediates DNA repair roles of the Smc5-Smc6 complex. Mol Cell Biol *26*, 1617-1630.

Petrushenko, Z.M., Lai, C.H., Rai, R., and Rybenkov, V.V. (2006). DNA reshaping by MukB. Right-handed knotting, left-handed supercoiling. J Biol Chem *281*, 4606-4615.

Potts, P.R. (2009). The Yin and Yang of the MMS21-SMC5/6 SUMO ligase complex in homologous recombination. DNA Repair (Amst) *8*, 499-506.

Potts, P.R., Porteus, M.H., and Yu, H. (2006). Human SMC5/6 complex promotes sister chromatid homologous recombination by recruiting the SMC1/3 cohesin complex to double-strand breaks. Embo J *25*, 3377-3388.

Potts, P.R., and Yu, H. (2005). Human MMS21/NSE2 is a SUMO ligase required for DNA repair. Mol Cell Biol *25*, 7021-7032.

Potts, P.R., and Yu, H. (2007). The SMC5/6 complex maintains telomere length in ALT cancer cells through SUMOylation of telomere-binding proteins. Nat Struct Mol Biol *14*, 581-590.

Prakash, R., Satory, D., Dray, E., Papusha, A., Scheller, J., Kramer, W., Krejci, L., Klein, H., Haber, J.E., Sung, P.*, et al.* (2009). Yeast Mph1 helicase dissociates Rad51-made D-loops: implications for crossover control in mitotic recombination. Genes Dev *23*, 67-79.

Putnam, C.D., Hayes, T.K., and Kolodner, R.D. (2009). Specific pathways prevent duplication-mediated genome rearrangements. Nature *460*, 984-989.

Putnam, C.D., Hayes, T.K., and Kolodner, R.D. (2010). Post-replication repair suppresses duplication-mediated genome instability. PLoS Genet *6*, e1000933.

Raveendranathan, M., Chattopadhyay, S., Bolon, Y.T., Haworth, J., Clarke, D.J., and Bielinsky, A.K. (2006). Genome-wide replication profiles of S-phase checkpoint mutants reveal fragile sites in yeast. Embo J *25*, 3627-3639.

Reid, G.A., and Schatz, G. (1982). Import of proteins into mitochondria. Yeast cells grown in the presence of carbonyl cyanide m-chlorophenylhydrazone accumulate massive amounts of some mitochondrial precursor polypeptides. J Biol Chem *257*, 13056-13061.

Remeseiro, S., Cuadrado, A., and Losada, A. (2013). Cohesin in development and disease. Development *140*, 3715-3718.

Riedel, C.G., Katis, V.L., Katou, Y., Mori, S., Itoh, T., Helmhart, W., Galova, M., Petronczki, M., Gregan, J., Cetin, B.*, et al.* (2006). Protein phosphatase 2A protects centromeric sister chromatid cohesion during meiosis I. Nature *441*, 53-61.

Rolef Ben-Shahar, T., Heeger, S., Lehane, C., East, P., Flynn, H., Skehel, M., and Uhlmann, F. (2008). Eco1-dependent cohesin acetylation during establishment of sister chromatid cohesion. Science *321*, 563-566.

Roy, M.A., and D'Amours, D. (2011). DNA-binding properties of Smc6, a core component of the Smc5-6 DNA repair complex. Biochem Biophys Res Commun *416*, 80-85.

Roy, M.A., Siddiqui, N., and D'Amours, D. (2011). Dynamic and selective DNA-binding activity of Smc5, a core component of the Smc5-Smc6 complex. Cell Cycle *10*, 690-700.

Sergeant, J., Taylor, E., Palecek, J., Fousteri, M., Andrews, E.A., Sweeney, S., Shinagawa, H., Watts, F.Z., and Lehmann, A.R. (2005). Composition and architecture of the Schizosaccharomyces pombe Rad18 (Smc5-6) complex. Mol Cell Biol *25*, 172-184.

Sheedy, D.M., Dimitrova, D., Rankin, J.K., Bass, K.L., Lee, K.M., Tapia-Alveal, C., Harvey, S.H., Murray, J.M., and O'Connell, M.J. (2005). Brc1-mediated DNA repair and damage tolerance. Genetics *171*, 457-468.

Singh, D.K., Ahn, B., and Bohr, V.A. (2009). Roles of RECQ helicases in recombination based DNA repair, genomic stability and aging. Biogerontology *10*, 235-252.

Sogo, J.M., Lopes, M., and Foiani, M. (2002). Fork reversal and ssDNA accumulation at stalled replication forks owing to checkpoint defects. Science *297*, 599-602.

Sollier, J., Driscoll, R., Castellucci, F., Foiani, M., Jackson, S.P., and Branzei, D. (2009). The Saccharomyces cerevisiae Esc2 and Smc5-6 proteins promote sister chromatid junction-mediated intra-S repair. Mol Biol Cell *20*, 1671-1682.

Song, W., Dominska, M., Greenwell, P.W., and Petes, T.D. (2014). Genome-wide high-resolution mapping of chromosome fragile sites in Saccharomyces cerevisiae. Proc Natl Acad Sci U S A *111*, E2210-2218.

Stelter, P., and Ulrich, H.D. (2003). Control of spontaneous and damage-induced mutagenesis by SUMO and ubiquitin conjugation. Nature *425*, 188-191.

Stephan, A.K., Kliszczak, M., Dodson, H., Cooley, C., and Morrison, C.G. (2011). Roles of vertebrate Smc5 in sister chromatid cohesion and homologous recombinational repair. Mol Cell Biol *31*, 1369-1381.

Storici, F., and Resnick, M.A. (2006). The delitto perfetto approach to in vivo site-directed mutagenesis and chromosome rearrangements with synthetic oligonucleotides in yeast. Methods Enzymol *409*, 329-345.

Strom, L., Karlsson, C., Lindroos, H.B., Wedahl, S., Katou, Y., Shirahige, K., and Sjogren, C. (2007). Postreplicative formation of cohesion is required for repair and induced by a single DNA break. Science *317*, 242-245.

Szakal, B., and Branzei, D. (2013). Premature Cdk1/Cdc5/Mus81 pathway activation induces aberrant replication and deleterious crossover. Embo J *32*, 1155-1167.

Szilard, R.K., Jacques, P.E., Laramee, L., Cheng, B., Galicia, S., Bataille, A.R., Yeung, M., Mendez, M., Bergeron, M., Robert, F.*, et al.* (2010). Systematic identification of fragile sites via genome-wide location analysis of gamma-H2AX. Nat Struct Mol Biol *17*, 299-305.

Tapia-Alveal, C., Lin, S.J., Yeoh, A., Jabado, O.J., and O'Connell, M.J. (2014). H2A.Z-dependent regulation of cohesin dynamics on chromosome arms. Mol Cell Biol *34*, 2092-2104.

Taylor, E.M., Copsey, A.C., Hudson, J.J., Vidot, S., and Lehmann, A.R. (2008). Identification of the proteins, including MAGEG1, that make up the human SMC5-6 protein complex. Mol Cell Biol *28*, 1197-1206.

Tong, A.H., and Boone, C. (2006). Synthetic genetic array analysis in Saccharomyces cerevisiae. Methods Mol Biol *313*, 171-192.

Tong, A.H., Lesage, G., Bader, G.D., Ding, H., Xu, H., Xin, X., Young, J., Berriz, G.F., Brost, R.L., Chang, M.*, et al.* (2004). Global mapping of the yeast genetic interaction network. Science *303*, 808-813.

Torres-Rosell, J., De Piccoli, G., Cordon-Preciado, V., Farmer, S., Jarmuz, A., Machin, F., Pasero, P., Lisby, M., Haber, J.E., and Aragon, L. (2007a). Anaphase onset before complete DNA replication with intact checkpoint responses. Science *315*, 1411-1415.

Torres-Rosell, J., Machin, F., Farmer, S., Jarmuz, A., Eydmann, T., Dalgaard, J.Z., and Aragon, L. (2005). SMC5 and SMC6 genes are required for the segregation of repetitive chromosome regions. Nat Cell Biol *7*, 412-419.

Torres-Rosell, J., Sunjevaric, I., De Piccoli, G., Sacher, M., Eckert-Boulet, N., Reid, R., Jentsch, S., Rothstein, R., Aragon, L., and Lisby, M. (2007b). The Smc5-Smc6 complex and SUMO modification of Rad52 regulates recombinational repair at the ribosomal gene locus. Nat Cell Biol *9*, 923-931.

Tsang, C.K., Wei, Y., and Zheng, X.F. (2007). Compacting DNA during the interphase: condensin maintains rDNA integrity. Cell Cycle *6*, 2213-2218.

Uhlmann, F., Lottspeich, F., and Nasmyth, K. (1999). Sister-chromatid separation at anaphase onset is promoted by cleavage of the cohesin subunit Scc1. Nature *400*, 37-42.

Uhlmann, F., Wernic, D., Poupart, M.A., Koonin, E.V., and Nasmyth, K. (2000). Cleavage of cohesin by the CD clan protease separin triggers anaphase in yeast. Cell *103*, 375-386.

Unal, E., Heidinger-Pauli, J.M., Kim, W., Guacci, V., Onn, I., Gygi, S.P., and Koshland, D.E. (2008). A molecular determinant for the establishment of sister chromatid cohesion. Science *321*, 566-569.

Unal, E., Heidinger-Pauli, J.M., and Koshland, D. (2007). DNA double-strand breaks trigger genome-wide sister-chromatid cohesion through Eco1 (Ctf7). Science *317*, 245-248.

Vanoli, F., Fumasoni, M., Szakal, B., Maloisel, L., and Branzei, D. (2010). Replication and recombination factors contributing to recombination-dependent bypass of DNA lesions by template switch. PLoS Genet *6*, e1001205.

Volkov, A., Mascarenhas, J., Andrei-Selmer, C., Ulrich, H.D., and Graumann, P.L. (2003). A prokaryotic condensin/cohesin-like complex can actively compact chromosomes from a single position on the nucleoid and binds to DNA as a ring-like structure. Mol Cell Biol *23*, 5638-5650.

Wang, Y., Vujcic, M., and Kowalski, D. (2001). DNA replication forks pause at silent origins near the HML locus in budding yeast. Mol Cell Biol *21*, 4938-4948.

Wellinger, R.E., and Sogo, J.M. (1998). In vivo mapping of nucleosomes using psoralen-DNA crosslinking and primer extension. Nucleic Acids Res *26*, 1544-1545.

Wierman, M.B., and Smith, J.S. (2013). Yeast sirtuins and the regulation of aging. FEMS Yeast Res.

Willis, N.A., Chandramouly, G., Huang, B., Kwok, A., Follonier, C., Deng, C., and Scully, R. (2014). BRCA1 controls homologous recombination at Tus/Ter-stalled mammalian replication forks. Nature *510*, 556-559.

Wolters, S., Ermolaeva, M.A., Bickel, J.S., Fingerhut, J.M., Khanikar, J., Chan, R.C., and Schumacher, B. (2014). Loss of Caenorhabditis elegans BRCA1 promotes genome stability during replication in smc-5 mutants. Genetics *196*, 985-999.

Wu, N., Kong, X., Ji, Z., Zeng, W., Potts, P.R., Yokomori, K., and Yu, H. (2012). Scc1 sumoylation by Mms21 promotes sister chromatid recombination through counteracting Wapl. Genes Dev *26*, 1473-1485.

Wu, N., and Yu, H. (2012). The Smc complexes in DNA damage response. Cell Biosci *2*, 5.

Xue, X., Choi, K., Bonner, J., Chiba, T., Kwon, Y., Xu, Y., Sanchez, H., Wyman, C., Niu, H., Zhao, X., and Sung, P. (2014) Restriction of Replication Fork Regression Activities by a Conserved SMC complex. Mol Cell *56*, 436-445.

Yong-Gonzales, V., Hang, L.E., Castellucci, F., Branzei, D., and Zhao, X. (2012). The Smc5-Smc6 complex regulates recombination at centromeric regions and affects kinetochore protein sumoylation during normal growth. PLoS One *7*, e51540.

Yu, Q., Kuzmiak, H., Olsen, L., Kulkarni, A., Fink, E., Zou, Y., and Bi, X. (2010). Saccharomyces cerevisiae Esc2p interacts with Sir2p through a small ubiquitin-like modifier (SUMO)-binding motif and regulates transcriptionally silent chromatin in a locus-dependent manner. J Biol Chem *285*, 7525-7536.

Zhao, X., and Blobel, G. (2005). A SUMO ligase is part of a nuclear multiprotein complex that affects DNA repair and chromosomal organization. Proc Natl Acad Sci U S A *102*, 4777-4782.

Zimmermann, C., Chymkowitch, P., Eldholm, V., Putnam, C. D., Lindvall, J. M., Omerzu, M., Bjørås, M., Kolodner, R. D., and Enserink, J. M. (2011). A chemical-genetic screen to unravel the genetic network of *CDC28/CDK1* links ubiquitin and Rad6-Bre1 to cell cycle progression. Proc Nat Acad Sci U S A *108*, 18748-53.

DNA and Chromosomes:

During Replication Stress, Non-Smc Element 5 (Nse5) Is Required for Smc5/6 Protein Complex Functionality at Stalled Forks

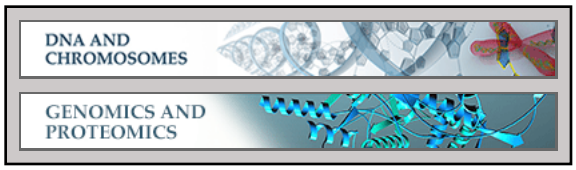

Denise E. Bustard, Demis Menolfi, Kristian Jeppsson, Lindsay G. Ball, Sidney Carter Dewey, Katsuhiko Shirahige, Camilla Sjögren, Dana Branzei and Jennifer A. Cobb

J. Biol. Chem. 2012, 287:11374-11383.
doi: 10.1074/jbc.M111.336263 originally published online February 2, 2012

THE JOURNAL OF BIOLOGICAL CHEMISTRY VOL. 287, NO. 14, pp. 11374–11383, March 30, 2012

During Replication Stress, Non-Smc Element 5 (Nse5) Is Required for Smc5/6 Protein Complex Functionality at Stalled Forks*[S]

Received for publication, December 22, 2011, and in revised form, February 1, 2012 Published, JBC Papers in Press, February 2, 2012, DOI 10.1074/jbc.M111.336263

Denise E. Bustard[‡], Demis Menolfi[§¶], Kristian Jeppsson[‖], Lindsay G. Ball[‡], Sidney Carter Dewey[‖], Katsuhiko Shirahige[**], Camilla Sjögren[‖], Dana Branzei[§], and Jennifer A. Cobb[‡1]

From the [‡]Department of Biochemistry and Molecular Biology, Southern Alberta Cancer Research Institute, University of Calgary, Calgary, Alberta T2N 4N1, Canada, the [§]Istituto FIRC di Oncologia Molecolare (IFOM), 20139 Milan, Italy, the [¶]Università degli Studi di Milano, 20122 Milan, Italy, the [‖]Department of Cell and Molecular Biology, Karolinska Institutet, 171 77 Stockholm, Sweden, and the [**]Laboratory of Genome Structure and Function, Center for Epigenetic Disease, Institute of Molecular and Cellular Biosciences, The University of Tokyo, Bunkyo-ku, Tokyo 113-0032, Japan

Background: The Smc5/6 complex has six non-SMC elements, including Nse5.
Results: Utilizing two mutants of *NSE5*, we separated Smc5 sumoylation from Smc5/6 complex function.
Conclusion: Nse5 integrity is important for Smc5/6 complex stability, which in turn is essential for localization of the complex to stalled forks.
Significance: Our results provide the first *in vivo* characterization of Nse5 for Smc5/6 complex function.

The Smc5/6 complex belongs to the SMC (structural maintenance of chromosomes) family, which also includes cohesin and condensin. In *Saccharomyces cerevisiae*, the Smc5/6 complex contains six essential non-Smc elements, Nse1–6. Very little is known about how these additional elements contribute to complex function except for Nse2/Mms21, which is an E3 small ubiquitin-like modifier (SUMO) ligase important for Smc5 sumoylation. Characterization of two temperature-sensitive mutants, *nse5*-ts1 and *nse5*-ts2, demonstrated the importance of Nse5 within the Smc5/6 complex for its stability and functionality at forks during hydroxyurea-induced replication stress. Both *NSE5* alleles showed a marked reduction in Smc5 sumoylation to levels lower than those observed with *mms21-11*, a mutant of Mms21 that is deficient in SUMO ligase activity. However, a phenotypic comparison of *nse5*-ts1 and *nse5*-ts2 revealed a separation of importance between Smc5 sumoylation and the function of the Smc5/6 complex during replication. Only cells carrying the *nse5*-ts1 allele exhibited defects such as dissociation of the replisome from stalled forks, formation of fork-associated homologous recombination intermediates, and hydroxyurea sensitivity that is additive with *mms21-11*. These defects are attributed to a failure in Smc5/6 localization to forks in *nse5*-ts1 cells. Overall, these data support the premise that Nse5 is important for vital interactions between components within the Smc5/6 complex, and for its functionality during replication stress.

The SMC (structural maintenance of chromosomes) family of proteins controls chromosomal organization throughout the cell cycle. The Smc5/6 complex is a member of the SMC complex family, which also includes cohesin and condensin (1–3). The Smc5/6 complex is recruited to DNA damage and is enriched at rDNA repeats (4–6). Upon treatment with the damaging agent methyl methanesulfonate (MMS),[2] the complex promotes the resolution of hemicatenane-like recombination DNA intermediates that form at replication forks. These intermediates are visualized as X-shaped structures by two-dimensional gel electrophoresis (7–9). A proposed function of the Smc5/6 complex is to give structural organization to collapsed forks, promoting their processing and preserving genome stability (2, 10).

In *Schizosaccharomyces pombe*, the Smc5/6 complex is recruited to stalled replication forks and is proposed to play a role during hydroxyurea (HU)-induced replication fork stalling by maintaining fork conformation, allowing the loading of homologous recombination (HR) factors Rad52 and replication protein A (11, 12). In budding yeast, recruitment of the Smc5/6 complex has been detected only at HU-stalled replication forks in checkpoint-deficient cells, where stalling leads to fork collapse (4). Moreover, to date, the visualization of recombination intermediates by two-dimensional gel electrophoresis in Smc5/6-deficient cells has been limited to either cells that have been treated with MMS or cells in which replication forks have collapsed (9, 12). Nonetheless, many Smc5/6 hypomorphic alleles

* This work was supported by grants from the Alberta Heritage Foundation for Medical Research (AHFMR), Alberta Cancer Board Grant 23575, and Canadian Institutes of Health Research Grant MOP-82736 (to J. A. C.); Associazione Italiana per la Ricerca sul Cancro (AIRC) Grant IG 10637 and European Research Council (ERC) Grant REPSUBREP242928 (to D. B.); and the European Research Council, the Swedish Research Council, the Swedish Cancer Society, Vinnova, and the Swedish Foundation for Strategic Research (SSF) (to C. S.).
[S] This article contains supplemental Figs. S1–S6, Tables S1 and S2, Text S1, and Datasets S1–S4.
[1] To whom correspondence should be addressed: Dept. of Biochemistry and Molecular Biology, Southern Alberta Cancer Research Institute, University of Calgary, 3330 Hospital Dr. NW, Calgary, Alberta T2N 4N1, Canada. E-mail: jcobb@ucalgary.ca.

[2] The abbreviations used are: MMS, methyl methanesulfonate; HU, hydroxyurea; HR, homologous recombination; SUMO, small ubiquitin-like modifier; Ni-NTA, nickel-nitrilotriacetic acid; qPCR, quantitative real-time PCR.

are very sensitive to the drug HU, which suggests that the complex also has a fundamental role when forks stall prior to collapse (11–18).

In addition to the two SMC components Smc5 and Smc6, the complex has six non-Smc elements, Nse1–6. The Mms21 (Nse2) component of the Smc5/6 complex is an E3 small ubiquitin-like modifier (SUMO) ligase (19–21). Deletion of the SUMO ligase domain, as in the *mms21-11* mutant allele, results in cellular sensitivity to MMS and HU, suggesting that the complex might regulate targets involved in damage tolerance or replication through sumoylation. Indeed, Mms21 contains an SP-RING-like domain and facilitates the SUMO modification of repair proteins, including Yku70 and Smc5 (19); however, deletion of the SUMO ligase domain dramatically reduces but does not eliminate Smc5 sumoylation (19). This could be due to redundancy with other E3 ligases such as Siz1 and Siz2 (22, 23) or, alternatively, could be due to ligase-independent SUMO conjugation by the E2-conjugating enzyme Ubc9 (24). The essential function of Mms21 is not its E3 ligase activity because *mms21-11* mutant cells, lacking ligase activity, grow well in the absence of DNA-damaging agents. By contrast, the full disruption of Mms21 is lethal (19, 20, 25).

The Nse1, Nse3, and Nse4 components form a trimeric subcomplex at the head and adjacent region of Smc5 (26). Little is known about the Nse5 and Nse6 subunits, except, like the other components, they are essential in *Saccharomyces cerevisiae*. Important to this study, high-throughput two-hybrid screens identified SUMO and Ubc9 as binding partners of Nse5 (27); however, to the best of our knowledge, this has not been verified, and the involvement of Nse5 in sumoylation or replication has never been reported.

In this study, we characterized two hypomorphic Nse5 alleles, *nse5*-ts1 (28) and *nse5*-ts2, which were generated by PCR-based mutagenesis and identified by reduced growth at 37 °C. Both alleles have a dramatic reduction in Smc5 sumoylation. The *nse5*-ts1 allele exhibits replication defects that become additive when combined with the E3 ligase mutant *mms21-11*. In contrast to *nse5*-ts1, however, there are no detectable replication defects in *nse5*-ts2 mutants. Our results support a role for the Smc5/6 complex in preventing fork collapse during stalls in replication and suggest that Smc5/6 complex integrity, which is compromised in *nse5*-ts1 cells, rather than Smc5 sumoylation, is critical for recovery from HU-induced replication stress.

EXPERIMENTAL PROCEDURES

Yeast Strains, Plasmids, Primers, and Antibodies—Yeast strains are listed in supplemental Table S1. All experiments were performed at 25 °C unless indicated otherwise. For yeast two-hybrid analysis, the *NSE5* genes were cloned into a pEG202-derived bait plasmid (29), creating Nse5-LexA fusion proteins under the control of a galactose-inducible promoter. *SMT3* was cloned into pJG4-6-derived prey vectors (29), creating a B42-activating domain fusion protein under the control of a galactose-inducible promoter. Inserting a stop codon after amino acid 96 created the Smt3ΔGG mutant. All constructs were confirmed by sequencing, and protein expression was confirmed by Western blot analysis with anti-LexA (2-12) and anti-HA (F7) antibodies (Santa Cruz Biotechnology).

Detection of Sumoylated Proteins—Nickel-nitrilotriacetic acid (Ni-NTA) purification of His_8-Smt3 was performed as described by Wohlschlegel *et al.* (30) with the following changes. Pellets of 2×10^9 cells were treated with *N*-ethylmaleimide (Sigma) to preserve sumoylation. Proteins were immunoprecipitated with Ni-NTA (Qiagen) overnight at 4 °C, followed by washing three times with 6 M guanidine hydrochloride, 100 mM NaH_2PO_4 (pH 8), and 0.05% Tween 20 and five times with 8 M urea, 100 mM NaH_2PO_4 (pH 6.3), and 0.05% Tween 20. Beads were resuspended in SDS loading buffer, boiled, and run on 4–20% gradient gels (Bio-Rad).

Two-dimensional Gel Electrophoresis—Samples were psoralen cross-linked, and the purification of DNA intermediates, the two-dimensional gel procedure, and the quantification of replication intermediates were carried out as described previously (31). A complete description of the quantification is provided in supplemental Text S1. The DNA samples were digested with NcoI and analyzed with probes recognizing *ARS305*. Each experiment was performed independently at least twice with qualitatively identical results. Representative results are shown in the figures.

Chromatin Immunoprecipitation—ChIP/quantitative real-time PCR (qPCR) was performed as described previously (32–34). DNA quantification by real-time PCR was performed on an ABI 7900 sequence detector system at the Southern Alberta Cancer Research Institute. The -fold enrichment represents recovery at the origin sites relative to a late replicating non-origin site as determined by BrdU incorporation.

BrdU/IP-chip and ChIP-chip—BrdU/IP-chip and ChIP-chip experiments were performed as described previously (4, 35) 60 min after release from the mating pheromone α-factor into 0.2 M HU at 25 °C with the following modifications. For FLAG-Smc6 ChIP, 150 ml of culture (A_{600} = 0.8–1.0) was used. Cells were lysed using a 6870 Freezer/Mill (SPEX). Anti-FLAG® monoclonal antibody M2 (F1804, Sigma) was used, and the recovered DNA was hybridized to *S. cerevisiae* tiling arrays from Affymetrix® at the Bioinformatics and Expression Analysis Core Facility of Karolinska Institutet. Analysis and map making were performed as described previously (36). Complete maps are included in supplemental Data Sets S1–S4.

Two-hybrid Analysis—Constructs were transformed into JC1280. For drop assays, strains were grown in the absence of glucose and plated on medium containing 2% galactose and lacking His and Trp (to select for plasmids) and additionally Leu (to measure expression from *lexAop6-LEU2*). Liquid culture yeast two-hybrid assays were also performed in strain JC1280, which was additionally transformed with the *lacZ* reporter plasmid pSH18034. Protein-protein interactions were detected by quantitative β-galactosidase activity for permeabilized cells and represent the averages of three independent experiments, with error bars indicating S.D. (37).

Co-immunoprecipitation Assays—Cells containing HA-tagged Nse6 and Myc-tagged Smc5 were grown at 25 °C to log phase before cells were lysed with glass beads in lysis buffer (50 mM HEPES, 140 mM NaCl, 1 mM EDTA, and 1% Triton X-100). Protein extracts were applied to anti-Myc antibody-coupled

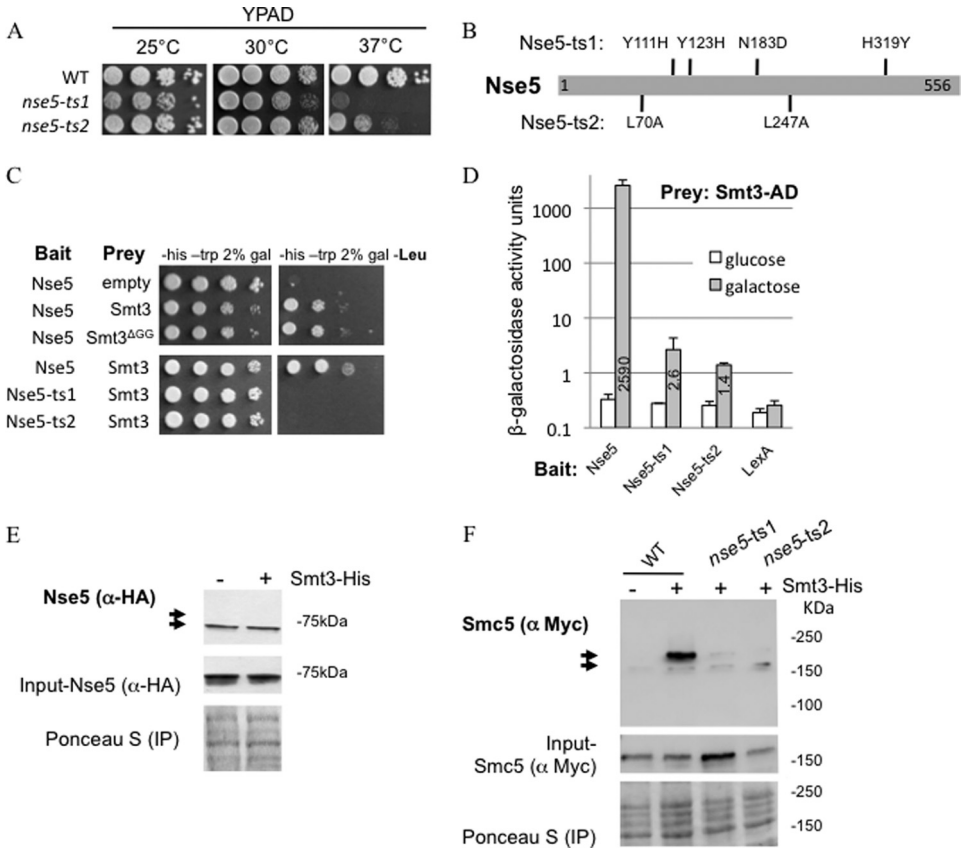

FIGURE 1. **Nse5 temperature-sensitive alleles *nse5*-ts1 and *nse5*-ts2 are unable to interact with SUMO and are defective in Smc5 sumoylation.** *A*, drop assays on YPAD (yeast extract, peptone, adenine, and dextrose) were performed with exponentially growing cultures for which 1:10 serial dilutions were performed, and plates were incubated at 25, 30, or 37 °C to compare WT (JC470), *nse5*-ts1 (JC1361), and *nse5*-ts2 (JC1833) cells. *B*, sequencing of *nse5*-ts1 revealed four point mutations, Y111H, Y123H, N183D, and H319Y, whereas sequencing of *nse5*-ts2 revealed two point mutations, L70A and L247A. *C* and *D*, yeast two-hybrid analysis (described under "Experimental Procedures") demonstrated that Nse5, but not Nse5-ts1 or Nse5-ts2, interacted with both WT Smt3 and Smt3ΔGG, a truncation that cannot be conjugated to target proteins. *E*, Nse5 does not appear to be a target of SUMO modification. Sumoylated proteins were purified from cells expressing endogenously HA-tagged Nse5 with (JC1960) or without (JC1355) His_8-tagged Smt3. Proteins were isolated by Ni-NTA affinity purification of His-Smt3 as described previously (30). Western blotting with anti-HA antibody failed to show a higher mobility shift band corresponding to sumoylated Nse5. *F*, *nse5*-ts1 and *nse5*-ts2 cells are deficient in Smc5 sumoylation. Sumoylated proteins were purified from cells expressing endogenously Myc-tagged Smc5 and His_8-tagged Smt3. Proteins were isolated by Ni-NTA affinity purification of His-Smt3 as described previously (30). Western blotting with anti-Myc antibody allowed visualization of sumoylated Smc5 in WT cells (JC1157), but not *nse5*-ts1 (JC1156) or *nse5*-ts2 (JC1884) cells or cells lacking the Smt3 tag (JC720). *IP*, immunoprecipitation.

Dynabeads (Invitrogen) and immunoprecipitated for 2 h at 4 °C. Following immunoprecipitation, samples were split and washed by shaking at 1400 rpm for 5 min once in lysis buffer and twice in wash buffer (100 mM Tris (pH 8), 0.5% Nonidet P-40, 1 mM EDTA, and either 300 mM or 1 M NaCl). Beads were resuspended in SDS loading buffer and run on 8% SDS-polyacrylamide gels, followed by Western blotting with anti-HA (F7) and anti-Myc (9E10) antibodies.

RESULTS

Nse5 Interacts with SUMO and Is Required for Smc5 Sumoylation—We sought to characterize Nse5 within the Smc5/6 complex by utilizing two temperature-sensitive alleles, *nse5*-ts1 and *nse5*-ts2 (Ref. 28 and this study). Both alleles exhibited normal growth at 25 °C; however, *nse5*-ts1 cells were inviable at 37 °C, and *nse5*-ts2 cells were extremely slow growing (Fig. 1*A*). (Unless stated otherwise, all experiments hereafter were performed at 25 °C.) DNA sequencing revealed that *nse5*-ts1 included four point mutations, Y111H, Y123H, N183D, and H319Y, and that *nse5*-ts2 had two, L70A and L247A (Fig. 1*B*).

A high-throughput screen previously reported SUMO to be a binding partner of Nse5 (27). Consistent with this, we confirmed that Nse5 interacted with SUMO (Smt3) in yeast two-hybrid analysis (Fig. 1, *C* and *D*). To determine whether this interaction represents the sumoylation of Nse5, we performed a Ni-NTA pulldown assay of His-tagged Smt3 in cells carrying HA-tagged Nse5 (30). Western blot analysis with anti-HA antibody indicated that no high-mobility band shifts representing SUMO-modified Nse5 were present (Fig. 1*E*, *lower arrow* indicating the unmodified form), suggesting that Nse5 is not a target of sumoylation. Furthermore, Nse5 interacted with a mutant form of SUMO that cannot be conjugated to target proteins, Smt3ΔGG (Fig. 1*C*), which indicates that Nse5 associates with SUMO via noncovalent interactions. Strikingly, we observed a significant reduction in the association between Nse5 and SUMO for both Nse5-ts1 and Nse5-ts2 (Fig. 1, *C* and *D*) despite being overexpressed at similar levels to the wild type (supplemental Fig. S1).

The localization of Mms21 on the coiled-coil arm of Smc5 is adjacent to the Nse5/Nse6-binding site at the hinge domain of the complex (25, 26), and this led us to question whether Nse5

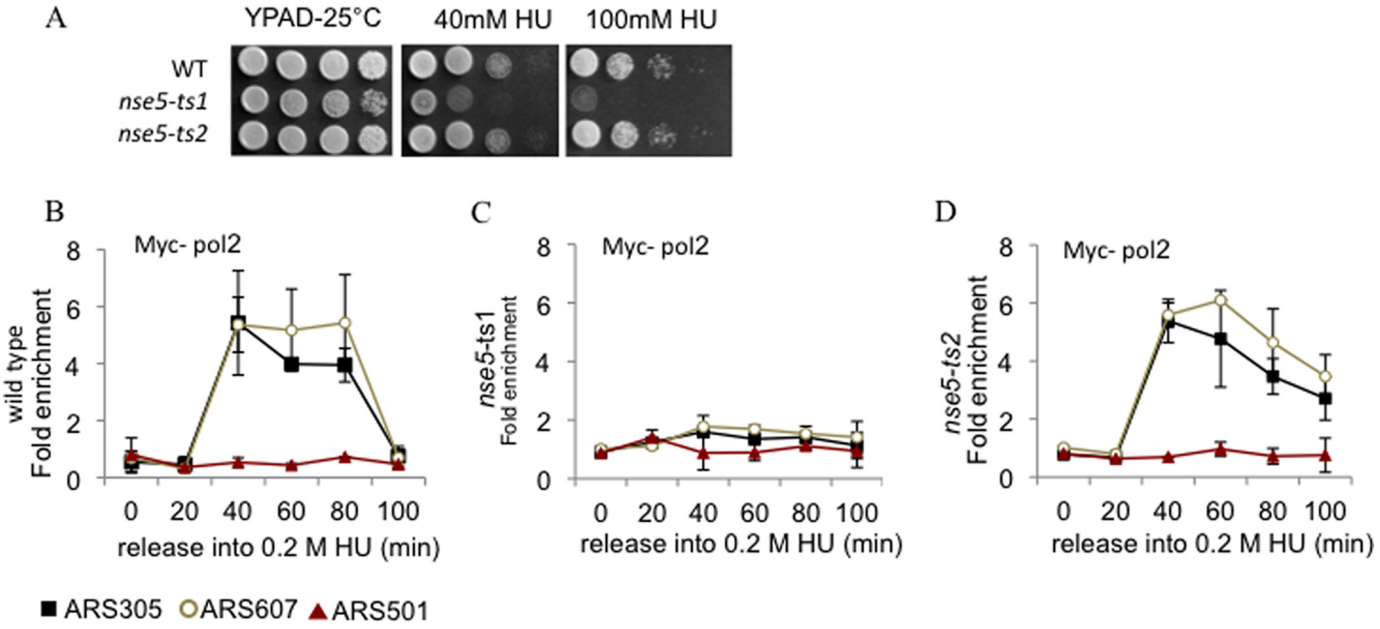

FIGURE 2. ***nse5*-ts1 cells display replisome instability during HU-induced replication stress.** *A*, drop assays (1:10 serial dilutions) with exponentially growing cultures were performed on YPAD ± medium containing the indicated concentrations of HU for WT (JC470), *nse5*-ts1 (JC1361), and *nse5*-ts2 (JC1833) cells at 25 °C. *B–D*, ChIP with anti-Myc antibody 9E10 was performed 25 °C on the following cells released from α-factor into YPAD + 0.2 M HU for Myc-Pol2: WT (JC1805), *nse5*-ts1 (JC1471), and *nse5*-ts2 (JC1914) cells. Genomic regions amplified in the ChIP analysis correspond to early-firing origins *ARS305* and *ARS607* and late-firing origin *ARS501* as described previously (32, 34).

could play a role in facilitating Mms21-dependent sumoylation of Smc5. To investigate this, we performed Ni-NTA pulldown assays of His-tagged Smt3 in cells carrying Myc-tagged Smc5 in wild-type and mutant cells, followed by Western blot analysis with anti-Myc antibody (30). Similar to previous reports (19), Smc5 sumoylation was readily detected in wild-type cells (Fig. 1*F*); however, there was a marked decrease in the sumoylation of Smc5 in the *nse5*-ts1 and *nse5*-ts2 mutants (Fig. 1*F*).

During Replication Stress, Defects Are Observed in nse5-ts1 Cells—Previous reports have demonstrated that hypomorphic alleles of Smc5/6 components are very sensitive to HU, indicating that the complex likely has a fundamental role when forks stall (11–18). Drop assays showed that *nse5*-ts1 (but not *nse5*-ts2) cells are sensitive to HU (Fig. 2*A*). One measure of replication correctness during replication stress is to monitor replisome association with stalled forks by ChIP. The recovered DNA from the ChIP was quantified by qPCR with primer pairs to two early-firing origins, *ARS305* and *ARS607*, with late-firing *ARS501* serving as a negative control (32–34). We determined the association of DNA polymerase ϵ by monitoring Myc-Pol2 recovery with stalled forks when cells were released into S phase in the presence of HU at the indicated time points. Compared with the wild type, we observed a reduction in polymerase association at both early-firing origins in *nse5*-ts1 cells (Fig. 2, *B* and *C*); however, recovery of Myc-Pol2 in *nse5*-ts2 cells was similar to wild type (Fig. 2*D*). Furthermore, there was a correlation between DNA polymerase ϵ stability and HU sensitivity (Fig. 2). Taken together with the data in Fig. 1, these results suggest that SUMO modification of Smc5 is not required for Smc5/6 complex functionality in response to HU, nor is Smc5 sumoylation a major contributing factor to survival during replication stress.

Phenotypic Analysis of nse5-ts and mms21-11 Cells—The loss of viability of *nse5*-ts1 cells after HU treatment and the notable decrease in Smc5 sumoylation for both alleles prompted us to analyze the genetic interactions between *NSE5* and the E3 SUMO ligase *MMS21*. The *nse5*-ts2/*mms21-11* double mutants were not more sensitive to HU than the single mutants alone (supplemental Fig. S2*A*). However, the *nse5*-ts1/*mms21-11* double mutants grew slowly on rich medium and showed synergistic sensitivity to HU (Fig. 3*A* and supplemental Fig. S2*A*). For this reason, we continued our analysis using the *nse5*-ts1 allele. First, we monitored Smc5 sumoylation, and in a side-by-side comparison, all cells carrying the *nse5*-ts1 allele were more deficient in Smc5 sumoylation than SUMO ligase-deficient *mms21-11* mutants (Fig. 3*B*).

Characterization of *nse5*-ts1/*mms21-11* cells involved monitoring the association of replisome components with forks by ChIP. DNA polymerases α and ϵ, as well as replication protein A, were measured when cells were released from α-factor into S phase in the presence of HU. For Myc-Rfa1, the 70-kDa subcomponent of replication protein A, we observed very little difference between the wild type and any of the mutants (supplemental Fig. S3, *A–D*). Fork-associated DNA polymerases α and ϵ were determined using HA-Pol1 and Myc-Pol2, respectively. We observed a reduction in polymerase association at *ARS305* and *ARS607* that was most pronounced in cells carrying the *nse5*-ts1 allele; however, *mms21-11* cells looked very similar to the wild type (Fig. 2, *C–F*, and supplemental Fig. S3, *E–G*). Compared with *mms21-11*, *nse5*-ts1 appears to be a more penetrant allele when forks initially stall, as there was little correlation between Mms21 ligase activity and replisome association.

To understand further the molecular basis of the HU sensitivity, we examined the kinetics and pattern of replication inter-

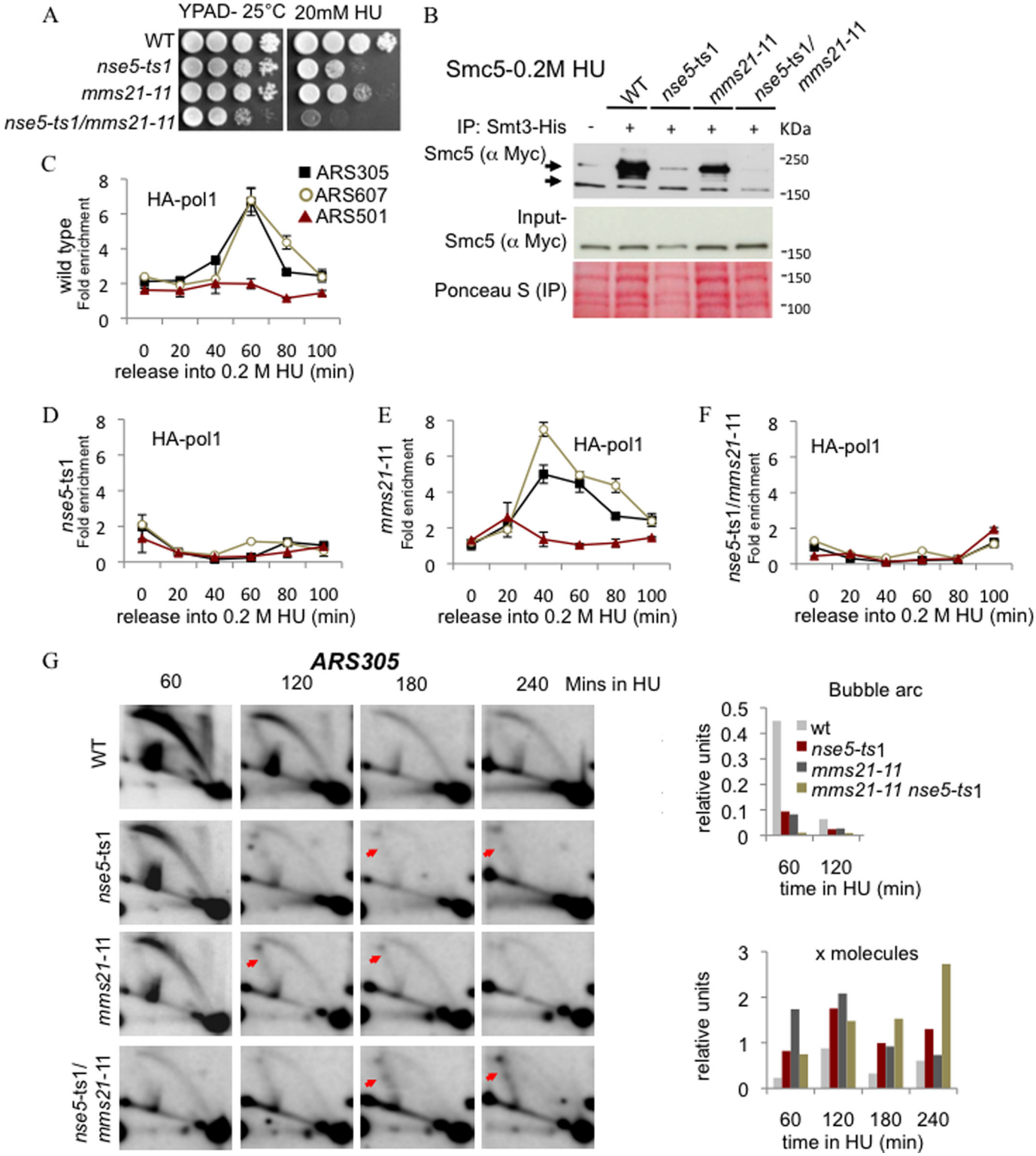

FIGURE 3. ***nse5*-ts1 and *mms21-11* cells accumulate X-shaped DNA structures during HU treatment.** *A*, drop assays (1:10 serial dilutions) with exponentially growing cultures were performed on YPAD ± medium containing the indicated concentrations of HU for WT (JC470), *nse5*-ts1 (JC1361), *mms21-11* (JC1908), and *nse5*-ts1/*mms21-11* (JC1320) cells at 25 °C. *B*, Smc5 sumoylation is further reduced in *nse5*-ts1 than in *mms21-11* mutant cells. Smc5 sumoylation was analyzed as described for Fig. 1*F* in WT (JC1157), *nse5*-ts1 (JC1156), *mms21-11* (JC1155), and *nse5*-ts1/*mms21-11* (JC1124) cells. *IP*, immunoprecipitation. *C–F*, ChIP with anti-HA antibody (F7) was performed at 25 °C on the following cells released from α-factor into YPAD + 0.2 M HU for HA-Pol1: WT (JC1805), *nse5*-ts1 (JC1471), *mms21-11* (JC1718), and *nse5*-ts1/*mms21-11* (JC1804) cells. *G*, two-dimensional gel analysis comparing WT (JC470), *nse5*-ts1 (JC1361), *mms21-11* (JC1908), and *nse5*-ts1/*mms21-11* (JC1320) cells that were arrested in G_1 with α-factor and released into YPAD + 0.2 M HU at 25 °C. The replication and recombination intermediates at the *ARS305* locus at 60, 120, 180, and 240 min after release into HU were visualized by two-dimensional gel electrophoresis, followed by Southern blot analysis. *Arrows* indicate the accumulated X-shaped DNA molecules.

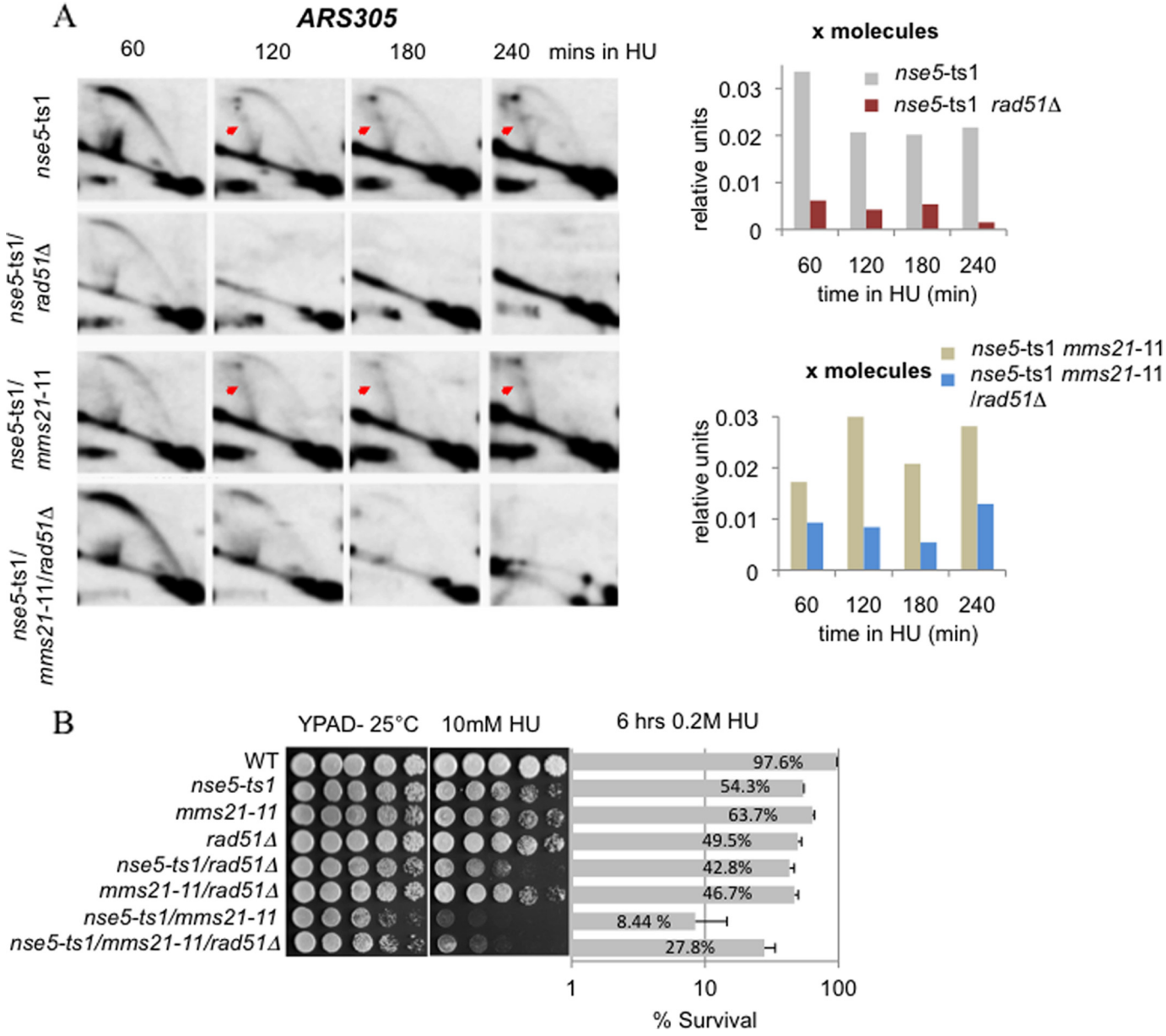

FIGURE 4. **Formation of X-shaped molecules in *nse5*-ts1 mutants is Rad51-dependent.** *A*, two-dimensional gel analysis comparing *nse5*-ts1 (JC1361), *nse5*-ts1/*rad51*Δ (JC2031), *nse5*-ts1/*mms21-11* (JC1320), and *nse5*-ts1/*mms21-11*/*rad51*Δ (JC2030) cells that were arrested in G_1 with α-factor and released into YPAD + 0.2 M HU at 25 °C. The replication and recombination intermediates at the *ARS305* locus at 60, 120, 180, and 240 min after release into HU were visualized by two-dimensional gel electrophoresis, followed by Southern blot analysis. *Arrows* indicate the accumulated X-shaped DNA molecules. *B*, drop assays (1:5 serial dilutions) with exponentially growing cultures were performed on YPAD ± medium containing 10 mM HU, and cell viability was monitored as colony outgrowth from asynchronous cultures after transient exposure to 0.2 M HU for 6 h at 25 °C, with values normalized to survival at time point 0 for WT (JC470), *nse5*-ts1 (JC1361), *mms21-11* (JC1908), *rad51*Δ (JC1362), *nse5*-ts1/*rad51*Δ (JC2031), *mms21-11*/*rad51*Δ (JC2032), *nse5*-ts1/*mms21-11* (JC1320), and *nse5*-ts1/*mms21-11*/*rad51*Δ (JC2030) cells.

mediates in *nse5*-ts1 and *mms21-11* cells by two-dimensional gel analysis. Psoralen cross-linking has allowed for enhanced detection of low-abundance X-shaped structures. Using a probe to *ARS305* (supplemental Fig. S4), we observed that bubble intermediates derived from origin firing and sister forks moving apart were significantly reduced in both *nse5*-ts1 and *mms21-11* mutants and were almost absent in *nse5*-ts1/*mms21-11* cells in the presence of HU (Fig. 3*G*). This could be due to problems in origin firing or an increased propensity for fork collapse. In line with the latter hypothesis, we observed that at late time points, X-shaped DNA molecules accumulated in all mutants. This phenotype was most pronounced in *nse5*-ts1/*mms21-11* double-mutant cells at 240 min following HU treatment and suggests that replication forks had potentially regressed or had been remodeled into recombination-like structures in an attempt to repair (Fig. 3*G*). We noted that in two-dimensional gel analysis, *nse5*-ts2 cells did not accumulate X-shaped DNA structures and exhibited wild-type levels of initiation (supplemental Fig. S2*B*).

Given the involvement of the Smc5/6 complex in HR, we determined if the accumulation of X-shaped intermediates in HU-treated *nse5*-ts1 mutants is dependent on Rad51 (8, 38). Similar to previous reports of MMS exposure (8), the accumulation of X-shaped molecules after HU treatment in *mms21-11*

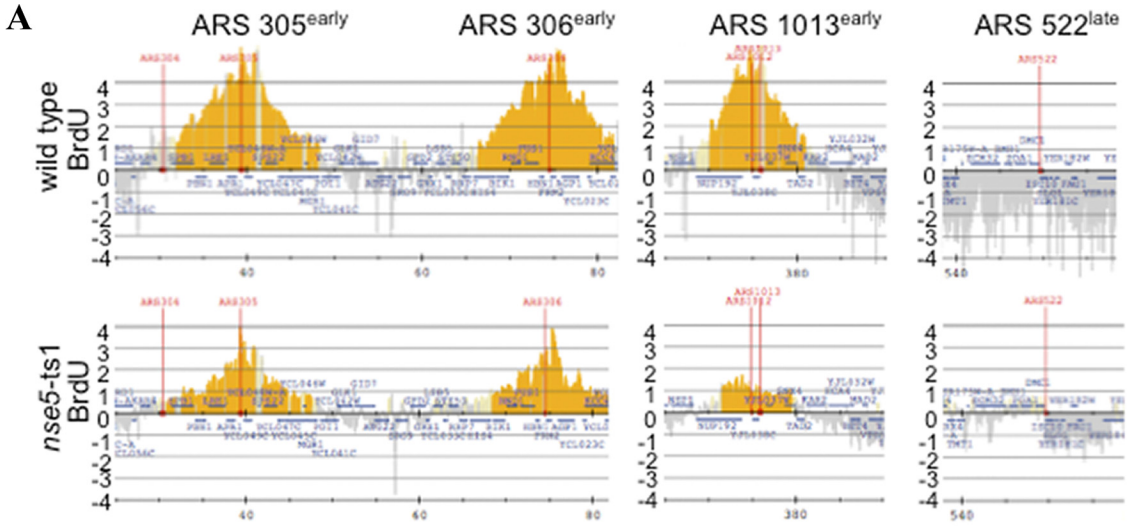

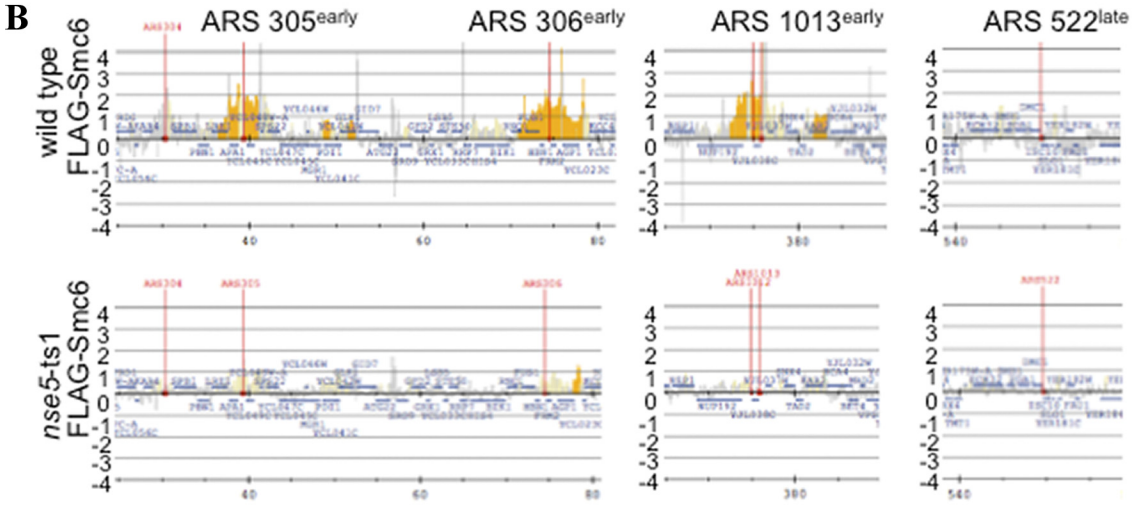

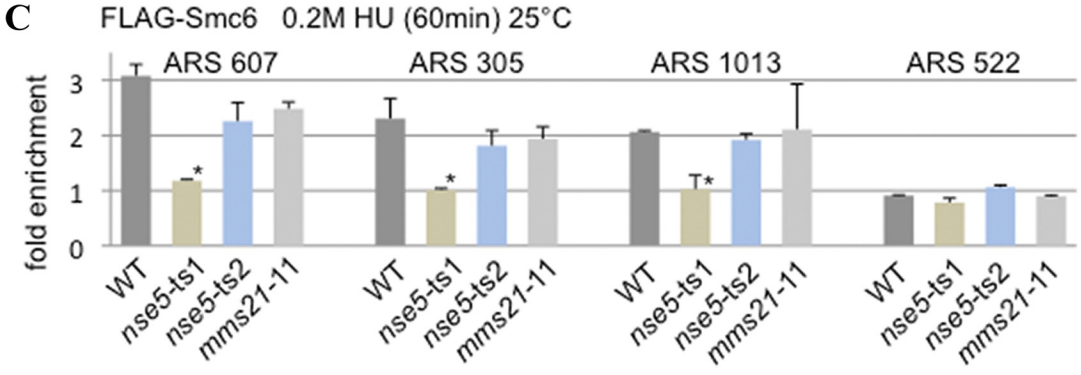

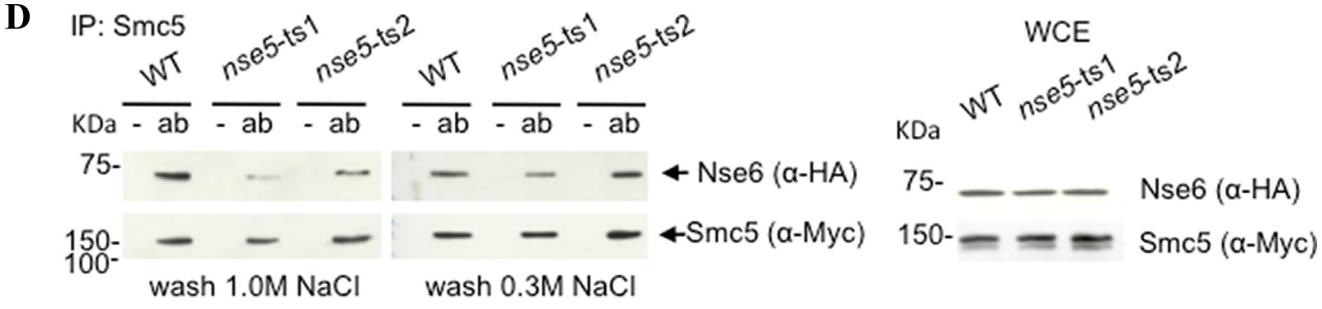

cells was Rad51-dependent (supplemental Fig. S5). Strikingly, in both *nse5*-ts1/*rad51*Δ and *mms21-11*/*nse5*-ts1/*rad51*Δ mutants, the X-shaped structures no longer persisted (Fig. 4*A*), indicating that their accumulation depends on Rad51-mediated recombination at HU-stalled forks rather than reversed forks that form upon replisome dissociation. Finally, we observed a partial suppression of HU sensitivity in *nse5*-ts1/*mms21-11* mutants when deleting *RAD51* (Fig. 4*B*), suggesting that aberrant HR structures, which persist at HU-stalled forks, contribute to the loss of cell viability.

The Smc5/6 Complex Shows Reduced Recruitment to Stalled Forks in nse5-ts1 Mutants—We wanted to understand the source of replication defects in *nse5*-ts1 cells. First, we monitored replication kinetics in wild-type and *nse5*-ts1 cells synchronized in G_1 and released into S phase in the presence of HU and BrdU. Newly synthesized DNA was labeled with BrdU for 60 min before immunoprecipitation and hybridization onto yeast genome tiling arrays (Fig. 5*A*). Consistent with both the two-dimensional gel analysis and ChIP for the replisome components (Fig. 3), cells harboring the *nse5*-ts1 allele exhibited a noticeable decrease in BrdU incorporation; however, sites of replication initiation remained identical to the wild type. Importantly, the lengths of the BrdU tracks were similar between wild-type and *nse5*-ts1 cells (Fig. 5*A*), suggesting similar fork rates. This is important because faster progression could have accounted for the reduction in replisome components detected at *ARS305* and *ARS607* in *nse5*-ts1 mutants and lower bubble and Y-arc signals by two-dimensional gel analysis (Fig. 3). Taken together, the data strongly support the interpretation that the loss of polymerase recovery in *nse5*-ts1 cells represents a decrease in replisome association with stalled replication forks. Finally, no enrichment was observed with BrdU at late-firing origins in *nse5*-ts1 cells (Fig. 5*A*), indicating that the S phase checkpoint remained intact.

The prominent replication phenotypes seen in *nse5*-ts1 cells prompted us to investigate whether the mutant allele influences Smc5/6 complex localization during replication stress. Although there was evidence for recruitment of the complex to HU-stalled forks in *S. pombe* by ChIP-qPCR (12), the presence of the complex at forks in *S. cerevisiae* has not been definitively established (4). We took a genome-wide approach and performed ChIP with FLAG-Smc6, as a marker for the Smc5/6 complex during stalls in replication, followed by hybridization onto tiling arrays. Cell lysis was carried out in liquid nitrogen, and an alternative antibody (anti-FLAG® monoclonal antibody M2) allowed for more sensitive detection of FLAG-Smc6 at HU-arrested forks. Using this methodology, Smc6 was consistently recovered at HU-stalled replication forks in wild-type cells (Fig. 5*B*), suggesting that its role in fork maintenance is direct in nature. There was a striking reduction in the recovery of Smc6 at sites of replication by both ChIP-chip and ChIP-qPCR in *nse5*-ts1 mutants (Fig. 5, *B* and *C*, and supplemental Fig. S6*A*). In contrast to *nse5*-ts1, localization of the Smc5/6 complex to stalled forks in *nse5*-ts2 and *mms21-11* mutants was not statistically different from the wild type (Fig. 5*C*). These data indicate that in *nse5*-ts1 cells, defects during replication stress arise because the Smc5/6 complex fails to be recruited to HU-stalled forks.

There are a least two conceivable explanations for why the Smc5/6 complex is not recruited to stalled forks in *nse5*-ts1 mutants. First, Nse5 could serve as the "recruiting factor" for complex localization, and important interactions are lost in *nse5*-ts1 cells. An alternative explanation is that the overall stability of the Smc5/6 complex is compromised in cells carrying the *nse5*-ts1 allele; therefore, it does not properly localize. To assess this, we monitored complex stability by measuring the association of Nse6 (the binding partner of Nse5) with Smc5 by co-immunoprecipitation. Nse6 was recovered with Smc5 in wild-type cells after washing in a high concentration of salt (1.0 M NaCl) (Fig. 5*D*). In *nse5*-ts1 mutants, there was a visible decrease in the recovery of Nse6 with Smc5; however, the complex did not completely dissociate because interactions were detected under low-salt conditions (0.3 M NaCl) (Fig. 5*D*). The loss of complex stability in *nse5*-ts1 mutants was not a result of lowered Nse5 protein levels, which were equivalent to the wild type (supplemental Fig. S6*B*). For *nse5*-ts2 cells, the recovery of Nse6 with Smc5 was slightly reduced, but not to the level of *nse5*-ts1 mutants (Fig. 5*D*), and Nse6-Smc5 association was indistinguishable from the wild type in 0.3 M NaCl (Fig. 5*D*). Taken together, our data suggest that Nse5 is essential for stable Smc5/6 complex association, and this is paramount for complex functionality at stalled forks.

DISCUSSION

One distinguishing feature of the Smc5/6 complex is the presence of additional components within the complex, namely Nse1–6. We have investigated the importance of Nse5 for Smc5/6 complex function by utilizing two mutant alleles, *nse5*-ts1 and *nse5*-ts2. We have demonstrated by three independent methods (two-dimensional gel analysis, ChIP-qPCR of replisome components, and BrdU/IP-chip) that cells carrying the *nse5*-ts1 allele have fork-associated defects under conditions of nucleotide depletion-associated stress. The data presented here are the first to show that Nse5 is essential for the complex integrity of Smc5/6, which in turn is necessary for its recruitment and functionality at stalled forks.

Nse5 interacts with SUMO, and our data suggest that this is through noncovalent interactions because Nse5 itself does not appear to be sumoylated. Although it is unclear what drives

FIGURE 5. **Smc6 recruitment to stalled forks is reduced in *nse5*-ts1 mutants.** BrdU/IP-chip (*A*) or ChIP-chip (*B*) with anti-FLAG antibody M2 was performed for FLAG-Smc6 in WT (CB207) and *nse5*-ts1 (CB1795) cells released from α-factor into 0.2 M HU for 60 min at 25 °C. The signal intensity ratio on a log 2 scale is shown on the *y axis*, and the chromosome coordinates are shown on the *x axis* for chromosomes III and X. All coordinates in the yeast genome are available in supplemental Data Sets S1–S4. *C*, ChIP-qPCR with anti-FLAG antibody M2 was performed for FLAG-Smc6 in WT (JC1594), *nse5*-ts1 (JC1665), *nse5*-ts2 (JC1913), and *mms21-11* (JC2075) cells that were arrested in G_1 with α-factor and released into YPAD + 0.2 M HU at 25 °C as described in the legend to Fig. 2 but with more stringent wash conditions, including 300 mM NaCl and 250 mM LiCl. A probability of $p = 0.001$ when comparing *t* values of *nse5*-ts1 and wild type (*) indicates that the differences are statistically significant. *D*, shown are the results from co-immunoprecipitation of Myc-tagged Smc5 and HA-tagged Nse6 (as described under "Experimental Procedures") with washes performed under conditions of 0.3 M NaCl or 1.0 M NaCl in WT (JC2229), *nse5*-ts1 (JC2230), and *nse5*-ts2 (JC2231) cells. *IP*, immunoprecipitation; *ab*, antibody; *WCE*, whole cell extract.

these interactions, both mutants show a dramatic decrease in interacting with SUMO when overexpressed in yeast two-hybrid analysis and a clear reduction of Smc5 sumoylation *in vivo*. The characterization of *nse5*-ts1 and *nse5*-ts2 mutants was instrumental in determining the significance of Smc5 sumoylation during replication stress. In many ways, the *nse5*-ts2 mutant we generated can be viewed as a separation of function allele. We observed wild-type patterns of replication intermediates and survival after HU treatment of *nse5*-ts2 mutants, which uncouples Smc5 sumoylation from Smc5/6 complex function at stalled forks. Smc5 sumoylation could be a "bystander effect" because of its proximity to the E3 ligase Mms21. The identification and mutation of the target lysine in Smc5 will be a necessary tool to address conclusively the functional outcome of Smc5 sumoylation.

The Smc5/6 complex is integrally involved in the resolution of DNA repair intermediates that form at collapsed replication forks. Indeed, several groups have demonstrated that recombination structures persist at collapsed forks in *smc5/6* mutants (8, 15, 39). What we have shown new here is that in *nse5*-ts1 and *mms21-11* cells, X-shaped structures arise when forks are stalled by HU. This suggests that the Smc5/6 complex also has a role during stalling to prevent fork collapse. Moreover, we have shown that the formation and resolution of these intermediates do not depend on Smc5 sumoylation, as X-shaped structures do not accumulate in *nse5*-ts2 cells, which are clearly deficient in Smc5 sumoylation. These data suggest that Smc5 sumoylation is not a prerequisite for complex functionality in response to HU or a major contributing factor to survival during replication stress. Nonetheless, these findings do not detract from a clear role for the Smc5/6 complex when forks stall. We have demonstrated that the Smc5/6 complex helps prevent replisome dissociation when forks stall, an event that would precede HR resolution and that is disrupted in *nse5*-ts1 mutants.

The accumulation of Rad51-dependent X-shaped structures at stalled forks in *mms21-11* and *nse5*-ts1 cells is consistent with the model that the Smc5/6 complex 1) prevents fork collapse and subsequent recombination-mediated fork restart and 2) promotes the resolution of such intermediates if/when they form. Our data are in line with those of Irmisch *et al.* (39) and the concept that the Smc5/6 complex has an "early" and "late" function during HU-induced fork stalling. The data shown here suggest that the early function involves complex localization, which helps stabilize the replisome through a mechanism in which Mms21 ligase activity is not that critical. Indeed, in contrast to *nse5*-ts1 cells, in which the complex fails to properly localize, replisome stability at stalled forks in *mms21-11* mutants remains largely intact. X-shaped molecules form during prolonged HU stalling in *nse5*-ts1 and *mms21-11* mutants, suggesting that forks either eventually collapse or try to restart via HR. The activity of Mms21 is important for the late function of resolving HR intermediates. Our data also suggest that in *mms21-11* mutants, the defects in HR resolution will ultimately be attributed to a misregulation in the sumoylation of yet-to-be determined targets, as Smc5 sumoylation appears dispensable. The identification of these targets will be critical for understanding the role of the Smc5/6 complex at stalled forks in its entirety.

Acknowledgments—We are grateful to E. Johnson for strains and very helpful discussions. We thank Damien D'Amours for instructive co-immunoprecipitation suggestions; X. Zhao for sharing anti-SUMO antibody; and S. Gasser, P. Hieter, and S. Ben-Aroya for strains. We thank all members of the Cobb laboratory for helpful discussions. The ABI 7900 sequence detector system at the Southern Alberta Cancer Research Institute was provided by the Alberta Cancer Foundation.

REFERENCES

1. Murray, J. M., and Carr, A. M. (2008) Smc5/6: a link between DNA repair and unidirectional replication? *Nat. Rev. Mol. Cell Biol.* **9,** 177–182
2. De Piccoli, G., Torres-Rosell, J., and Aragón, L. (2009) The unnamed complex: what do we know about Smc5/6? *Chromosome Res.* **17,** 251–263
3. Potts, P. R. (2009) The Yin and Yang of the MMS21-SMC5/6 SUMO ligase complex in homologous recombination. *DNA Repair* **8,** 499–506
4. Lindroos, H. B., Ström, L., Itoh, T., Katou, Y., Shirahige, K., and Sjögren, C. (2006) Chromosomal association of the Smc5/6 complex reveals that it functions in differently regulated pathways. *Mol. Cell* **22,** 755–767
5. Torres-Rosell, J., Machín, F., Farmer, S., Jarmuz, A., Eydmann, T., Dalgaard, J. Z., and Aragón, L. (2005) *SMC5* and *SMC6* genes are required for the segregation of repetitive chromosome regions. *Nat. Cell Biol.* **7,** 412–419
6. Pebernard, S., Schaffer, L., Campbell, D., Head, S. R., and Boddy, M. N. (2008) Localization of Smc5/6 to centromeres and telomeres requires heterochromatin and SUMO, respectively. *EMBO J.* **27,** 3011–3023
7. Choi, K., Szakal, B., Chen, Y. H., Branzei, D., and Zhao, X. (2010) The Smc5/6 complex and Esc2 influence multiple replication-associated recombination processes in *Saccharomyces cerevisiae*. *Mol. Biol. Cell* **21,** 2306–2314
8. Branzei, D., Sollier, J., Liberi, G., Zhao, X., Maeda, D., Seki, M., Enomoto, T., Ohta, K., and Foiani, M. (2006) Ubc9- and mms21-mediated sumoylation counteracts recombinogenic events at damaged replication forks. *Cell* **127,** 509–522
9. Sollier, J., Driscoll, R., Castellucci, F., Foiani, M., Jackson, S. P., and Branzei, D. (2009) The *Saccharomyces cerevisiae* Esc2 and Smc5/6 proteins promote sister chromatid junction-mediated intra-S repair. *Mol. Biol. Cell* **20,** 1671–1682
10. Hwang, J. Y., Smith, S., Ceschia, A., Torres-Rosell, J., Aragón, L., and Myung, K. (2008) Smc5/6 complex suppresses gross chromosomal rearrangements mediated by break-induced replications. *DNA Repair* **7,** 1426–1436
11. Miyabe, I., Morishita, T., Hishida, T., Yonei, S., and Shinagawa, H. (2006) Rhp51-dependent recombination intermediates that do not generate checkpoint signal are accumulated in *Schizosaccharomyces pombe rad60* and *smc5/6* mutants after release from replication arrest. *Mol. Cell. Biol.* **26,** 343–353
12. Ampatzidou, E., Irmisch, A., O'Connell, M. J., and Murray, J. M. (2006) Smc5/6 is required for repair at collapsed replication forks. *Mol. Cell. Biol.* **26,** 9387–9401
13. Pebernard, S., McDonald, W. H., Pavlova, Y., Yates, J. R., 3rd, and Boddy, M. N. (2004) Nse1, Nse2, and a novel subunit of the Smc5/6 complex, Nse3, play a crucial role in meiosis. *Mol. Biol. Cell* **15,** 4866–4876
14. Pebernard, S., Wohlschlegel, J., McDonald, W. H., Yates, J. R., 3rd, and Boddy, M. N. (2006) The Nse5-Nse6 dimer mediates DNA repair roles of the Smc5/6 complex. *Mol. Cell. Biol.* **26,** 1617–1630
15. Chen, Y. H., Choi, K., Szakal, B., Arenz, J., Duan, X., Ye, H., Branzei, D., and Zhao, X. (2009) Interplay between the Smc5/6 complex and the Mph1 helicase in recombinational repair. *Proc. Natl. Acad. Sci. U.S.A.* **106,** 21252–21257
16. Chavez, A., Agrawal, V., and Johnson, F. B. (2011) Homologous recombination-dependent rescue of deficiency in the structural maintenance of chromosomes (Smc) 5/6 complex. *J. Biol. Chem.* **286,** 5119–5125
17. Cost, G. J., and Cozzarelli, N. R. (2006) Smc5p promotes faithful chromosome transmission and DNA repair in *Saccharomyces cerevisiae*. *Genetics* **172,** 2185–2200

18. Hu, B., Liao, C., Millson, S. H., Mollapour, M., Prodromou, C., Pearl, L. H., Piper, P. W., and Panaretou, B. (2005) Qri2/Nse4, a component of the essential Smc5/6 DNA repair complex. *Mol. Microbiol.* **55,** 1735–1750
19. Zhao, X., and Blobel, G. (2005) A SUMO ligase is part of a nuclear multiprotein complex that affects DNA repair and chromosomal organization. *Proc. Natl. Acad. Sci. U.S.A.* **102,** 4777–4782
20. Andrews, E. A., Palecek, J., Sergeant, J., Taylor, E., Lehmann, A. R., and Watts, F. Z. (2005) Nse2, a component of the Smc5/6 complex, is a SUMO ligase required for the response to DNA damage. *Mol. Cell. Biol.* **25,** 185–196
21. Potts, P. R., and Yu, H. (2005) Human MMS21/NSE2 is a SUMO ligase required for DNA repair. *Mol. Cell. Biol.* **25,** 7021–7032
22. Johnson, E. S., and Gupta, A. A. (2001) An E3-like factor that promotes SUMO conjugation to the yeast septins. *Cell* **106,** 735–744
23. Takahashi, Y., Toh-e, A., and Kikuchi, Y. (2001) A novel factor required for the SUMO1/Smt3 conjugation of yeast septins. *Gene* **275,** 223–231
24. Johnson, E. S., and Blobel, G. (1997) Ubc9p is the conjugating enzyme for the ubiquitin-like protein Smt3p. *J. Biol. Chem.* **272,** 26799–26802
25. Duan, X., Sarangi, P., Liu, X., Rangi, G. K., Zhao, X., and Ye, H. (2009) Structural and functional insights into the roles of the Mms21 subunit of the Smc5/6 complex. *Mol. Cell* **35,** 657–668
26. Duan, X., Yang, Y., Chen, Y. H., Arenz, J., Rangi, G. K., Zhao, X., and Ye, H. (2009) Architecture of the Smc5/6 complex of *Saccharomyces cerevisiae* reveals a unique interaction between the Nse5/6 Subcomplex and the Hinge Regions of Smc5 and Smc6. *J. Biol. Chem.* **284,** 8507–8515
27. Hazbun, T. R., Malmström, L., Anderson, S., Graczyk, B. J., Fox, B., Riffle, M., Sundin, B. A., Aranda, J. D., McDonald, W. H., Chiu, C. H., Snydsman, B. E., Bradley, P., Muller, E. G., Fields, S., Baker, D., Yates, J. R., 3rd, and Davis, T. N. (2003) Assigning function to yeast proteins by integration of technologies. *Mol. Cell* **12,** 1353–1365
28. Ben-Aroya, S., Coombes, C., Kwok, T., O'Donnell, K. A., Boeke, J. D., and Hieter, P. (2008) Toward a comprehensive temperature-sensitive mutant repository of the essential genes of *Saccharomyces cerevisiae*. *Mol. Cell* **30,** 248–258
29. Aushubel, F. M., Brent, R., Kinston, R., Moore, D., Seidman, J. J., Smith, J., and Struhl, K. (1994) *Current Protocols in Molecular Biology*, Unit 13.14.1–13.14.17, John Wiley & Sons, New York
30. Wohlschlegel, J. A., Johnson, E. S., Reed, S. I., and Yates, J. R., 3rd (2006) Improved identification of SUMO attachment sites using C-terminal SUMO mutants and tailored protease digestion strategies. *J. Proteome Res.* **5,** 761–770
31. Vanoli, F., Fumasoni, M., Szakal, B., Maloisel, L., and Branzei, D. (2010) Replication and recombination factors contributing to recombination-dependent bypass of DNA lesions by template switch. *PLoS Genet.* **6,** 1–18
32. Tittel-Elmer, M., Alabert, C., Pasero, P., and Cobb, J. A. (2009) The MRX complex stabilizes the replisome independently of the S phase checkpoint during replication stress. *EMBO J.* **28,** 1142–1156
33. Cobb, J. A., Schleker, T., Rojas, V., Bjergbaek, L., Tercero, J. A., and Gasser, S. M. (2005) Replisome instability, fork collapse, and gross chromosomal rearrangements arise synergistically from Mec1 kinase and RecQ helicase mutations. *Genes Dev.* **19,** 3055–3069
34. Cobb, J. A., Bjergbaek, L., Shimada, K., Frei, C., and Gasser, S. M. (2003) DNA polymerase stabilization at stalled replication forks requires Mec1 and the RecQ helicase Sgs1. *EMBO J.* **22,** 4325–4336
35. Katou, Y., Kaneshiro, K., Aburatani, H., and Shirahige, K. (2006) Genomic approach for the understanding of dynamic aspect of chromosome behavior. *Methods Enzymol.* **409,** 389–410
36. Kegel, A., Betts-Lindroos, H., Kanno, T., Jeppsson, K., Ström, L., Katou, Y., Itoh, T., Shirahige, K., and Sjögren, C. (2011) Chromosome length influences replication-induced topological stress. *Nature* **471,** 392–396
37. Bjergbaek, L., Cobb, J. A., Tsai-Pflugfelder, M., and Gasser, S. M. (2005) Mechanistically distinct roles for Sgs1p in checkpoint activation and replication fork maintenance. *EMBO J.* **24,** 405–417
38. Liberi, G., Maffioletti, G., Lucca, C., Chiolo, I., Baryshnikova, A., Cotta-Ramusino, C., Lopes, M., Pellicioli, A., Haber, J. E., and Foiani, M. (2005) Rad51-dependent DNA structures accumulate at damaged replication forks in *sgs1* mutants defective in the yeast ortholog of BLM RecQ helicase. *Genes Dev.* **19,** 339–350
39. Irmisch, A., Ampatzidou, E., Mizuno, K., O'Connell, M. J., and Murray, J. M. (2009) Smc5/6 maintains stalled replication forks in a recombination-competent conformation. *EMBO J.* **28,** 144–155

Published online: January 28, 2014

Article

TRANSPARENT PROCESS OPEN ACCESS

THE EMBO JOURNAL

DNA bending facilitates the error-free DNA damage tolerance pathway and upholds genome integrity

Victor Gonzalez-Huici[1,†,§], Barnabas Szakal[1,§], Madhusoodanan Urulangodi[1], Ivan Psakhye[2], Federica Castellucci[1], Demis Menolfi[1], Eerappa Rajakumara[1], Marco Fumasoni[1], Rodrigo Bermejo[1,‡], Stefan Jentsch[2] & Dana Branzei[1,*]

Abstract

DNA replication is sensitive to damage in the template. To bypass lesions and complete replication, cells activate recombination-mediated (error-free) and translesion synthesis-mediated (error-prone) DNA damage tolerance pathways. Crucial for error-free DNA damage tolerance is template switching, which depends on the formation and resolution of damage-bypass intermediates consisting of sister chromatid junctions. Here we show that a chromatin architectural pathway involving the high mobility group box protein Hmo1 channels replication-associated lesions into the error-free DNA damage tolerance pathway mediated by Rad5 and PCNA polyubiquitylation, while preventing mutagenic bypass and toxic recombination. In the process of template switching, Hmo1 also promotes sister chromatid junction formation predominantly during replication. Its C-terminal tail, implicated in chromatin bending, facilitates the formation of catenations/hemicatenations and mediates the roles of Hmo1 in DNA damage tolerance pathway choice and sister chromatid junction formation. Together, the results suggest that replication-associated topological changes involving the molecular DNA bender, Hmo1, set the stage for dedicated repair reactions that limit errors during replication and impact on genome stability.

Keywords chromatin architecture; DNA damage tolerance; mutagenesis; replication; template switching

Subject Categories DNA Replication, Repair & Recombination

DOI 10.1002/embj.201387425 | Received 15 November 2013 | Revised 1 December 2013 | Accepted 3 December 2013 | Published online 28 January 2014

EMBO Journal (2014) 33, 327–340

Introduction

Damaged DNA templates are major obstacles during replication, inducing fork stalling and discontinuities in the replicated chromosomes. DNA damage tolerance (DDT) mechanisms are crucial to promote replication completion by mediating fork restart and filling of DNA gaps (Lopes *et al*, 2006; Branzei *et al*, 2008; Daigaku *et al*, 2010; Karras & Jentsch, 2010; Minca & Kowalski, 2010). Genetic work has delineated two main modes of DDT in all organisms: an error-free mode involving recombination in which one newly synthesized strand is used as a template for replication of the blocked nascent strand, and an error-prone mode involving translesion synthesis (TLS) and which is largely accountable for mutagenesis (reviewed in Friedberg, 2005; Branzei, 2011). Because increased mutations ultimately lead to genome instability and cancer (Nik-Zainal *et al*, 2012; Alexandrov *et al*, 2013), the molecular mechanisms underlying DDT pathway choice have implications for understanding cancer etiology and for cancer therapy. At present, the mechanisms underlying the error-free/error-prone DDT pathway switch remain little understood: on one hand, high expression of TLS polymerases in mitosis may represent a passive mechanism that favors error-free damage-bypass early during replication (Waters & Walker, 2006), in line with the observed correlation between replication timing and mutation rates (Lang & Murray, 2011); on the other hand, regulatory mechanisms, such as the ones involving post-translational modification of the polymerase clamp, PCNA, with SUMO and ubiquitin, modulate the recruitment of repair factors and TLS polymerases, thus influencing DDT pathway choice (Bergink & Jentsch, 2009).

PCNA modifications with SUMO and ubiquitin are crucial for DDT: mono-ubiquitylation of PCNA promotes translesion polymerase-mediated error-prone DDT (Stelter & Ulrich, 2003), Rad5-Mms2-Ubc13-dependent polyubiquitylation of PCNA acts in conjunction with a subset of homologous recombination factors to mediate error-free DDT by formation of sister chromatid junctions (SCJs) (Branzei

1 Fondazione Istituto FIRC di Oncologia Molecolare (IFOM), Milan, Italy
2 Department of Molecular Cell Biology, Max Planck Institute of Biochemistry, Martinsried/Munich, Germany
*Corresponding author. Tel: +39-02574303259; Fax: +39-02574303231; E-mail: dana.branzei@ifom.eu
§These authors contributed equally to this work.
†College of Life Sciences, University of Dundee, Dundee, UK
‡Instituto de Biología Funcional y Genómica, CSIC, Universidad de Salamanca, Salamanca, Spain

et al, 2008; Minca & Kowalski, 2010; Vanoli *et al*, 2010; Karras *et al*, 2013), and SUMOylated PCNA recruits Srs2 to chromatin, where it presumably prevents the access of the recombination machinery and inhibits unwanted recombination (Papouli *et al*, 2005; Pfander *et al*, 2005; Branzei *et al*, 2008; Karras *et al*, 2013). The recombination pathway prevented by SUMOylated PCNA is also known as the salvage pathway of DDT, whereas the Rad5-mediated pathway is commonly referred to as template switching. Notably, both these error-free DDT pathways mediate damage-bypass via the formation of SCJs, but may occupy distinct time windows in relation to DNA replication (Branzei *et al*, 2008; Karras *et al*, 2013).

Following the formation of damage-bypass SCJs, the Sgs1 helicase, homolog of human BLM that is mutated in cancer-prone Bloom syndrome patients, is thought to process together with the Top3 topoisomerase these intermediates to hemicatenanes, topological structures conjoining two DNA duplexes through a single-strand interlock, (Wu & Hickson, 2003; Liberi *et al*, 2005; Branzei *et al*, 2008; Karras & Jentsch, 2010; Cejka *et al*, 2012). Type IA topoisomerases—Top1 and Top3 in budding yeast—that catalyze strand passage through a reversible, enzyme-bridged, single-strand break can then resolve the resulting hemicatenanes (Wang, 2002). When Sgs1 functionality is impaired, the SCJs arising during error-free DDT are resolved by crossover-prone nucleases (Ashton *et al*, 2011; Szakal & Branzei, 2013), leading to elevated sister chromatid exchanges and loss of heterozygosity events that may ultimately drive chromosomal instabilities underpinning tumorigenesis (Wechsler *et al*, 2011; Szakal & Branzei, 2013).

High mobility group box (HMGB) proteins are abundant, multifunctional proteins with genome architectural capacity conferred by their ability to bend DNA, in the process creating DNA topologies that can impinge on the assembly of nucleoprotein structures (reviewed in Thomas & Travers, 2001; Stros, 2010). Notably, HMGB1 binds with high affinity to hemicatenanes (Stros *et al*, 2004; Jaouen *et al*, 2005). The *Saccharomyces cerevisiae* HMGB protein, Hmo1 - the closest ortholog of HMGB1 in yeast-, shows synthetic lethal interactions with *top3*Δ (Gadal *et al*, 2002), and binds with preference to single stranded (ss) DNA and to DNA with altered conformations, showing reduced DNA sequence specificity (Kamau *et al*, 2004; Bauerle *et al*, 2006; Xiao *et al*, 2010). In addition, in *hmo1* mutant cells, spontaneous and damage-induced mutagenesis is increased (Alekseev *et al*, 2002; Kim & Livingston, 2006, 2009), suggesting a possible role for Hmo1 in DDT or its regulation. It is of note that while mutation rates vary along chromosomes and correlate with replication timing (Lang & Murray, 2011), the underlying mechanisms accounting for the preferred usage of error-free DDT early in S phase remain elusive.

Here we show that Hmo1 has an early regulatory role, coincident with DNA replication, in error-free DDT pathway choice by channeling lesions towards the Rad5-Mms2-Ubc13-mediated pathway of template switching, while preventing mutagenic bypass and toxic recombination. We uncover that error-free DDT pathway choice, previously shown to be controlled by SUMOylated PCNA and its interactors Srs2 and Elg1, is uncoupled from the SCJ formation process *per se*. While Srs2 and Elg1 do not play a discernible role in SCJ formation, Hmo1 affects also this latter process. The time window for Hmo1 action in SCJ formation overlaps with the one of the Rad5-Mms2-Ubc13, being predominant early during replication. Importantly, these Hmo1 functions in error-free DDT are largely mediated via its carboxy (C)-terminal domain, previously shown to promote DNA bending. We additionally find that Hmo1 promotes topological transitions related to catenane/hemicatenane formation/stabilization during unperturbed growth and that this function is also largely dependent on its C-terminal domain. Together, the results indicate that the Hmo1-mediated topological pathway involving DNA bending represents a new replication-associated regulatory mechanism that facilitates error-free DDT and influences the error-free/error-prone DDT switch.

Results

Hmo1 functionally interacts with the Rad5-Mms2-Ubc13 error-free DDT pathway

Hmo1 and its human ortholog, HMGB1, exhibit high affinity for DNA hemicatenanes and other types of DNA with altered conformations such as ssDNA and DNA cruciform structures (Bianchi *et al*, 1989; Lu *et al*, 1996; Kamau *et al*, 2004; Jaouen *et al*, 2005) forming during replication in unperturbed and genotoxic stress conditions (Lopes *et al*, 2003, 2006; Liberi *et al*, 2005; Branzei *et al*, 2008). Hmo1 is an abundant protein, associated with chromatin throughout the cell-cycle (Bermejo *et al*, 2009). Following replication in the presence of DNA damage (MMS), we found by ChIP-on-chip a statistically significant co-localization between Hmo1 clusters and the ones of Rfa1, the large subunit of RPA (*P*-value 1.80E-16), which presumably marks ssDNA regions (Supplementary Fig S1A). Indeed, after treatment with high doses of HU, which blocks replication by depleting dNTP pools, Rfa1 peaks were clustered around early origins of replication and were overlapping with the BrdU peaks marking ongoing DNA replication (Supplementary Fig S1B, *P*-value 3.10E-17), in line with findings showing that HU treatment induces replication fork stalling and accumulation of ssDNA regions in the proximity of origins of replication (Sogo *et al*, 2002; Feng *et al*, 2006). On the other hand, following treatment with sublethal doses of MMS, which does not slow down replication fork progression to the same degree as high HU concentrations, Rfa1 peaks were spread over much larger regions (Supplementary Fig S1A), supporting the notion that during replication in the presence of genotoxic stress, DNA gaps persist behind replication forks (Lopes *et al*, 2006). Coating of ssDNA gaps with RPA facilitates the recruitment of the Rad18 ubiquitin ligase (Davies *et al*, 2008), which together with the Rad6 ubiquitin conjugating enzyme and the Rad5-Mms2-Ubc13 ubiquitylation complex, induces PCNA mono- and polyubiquitylation (Hoege *et al*, 2002) and mediates postreplicative DDT (Daigaku *et al*, 2010; Karras & Jentsch, 2010). The overlap between Hmo1 and Rfa1 clusters in MMS-treated cells (Supplementary Fig S1A), together with previous reports indicating a role for Hmo1 in the control of mutagenesis (Alekseev *et al*, 2002; Kim & Livingston, 2006), prompted us to investigate a possible involvement of Hmo1 in DDT and the metabolism of DNA structures arising during recombination-mediated damage-bypass.

Two genetic pathways, the Rad51 and the Rad5-Mms2-Ubc13 pathways were identified to contribute to error-free DDT (Branzei *et al*, 2008; Karras *et al*, 2013). While *hmo1Δ* cells had wild-type (WT) levels of MMS resistance and the *hmo1Δ* mutation did not

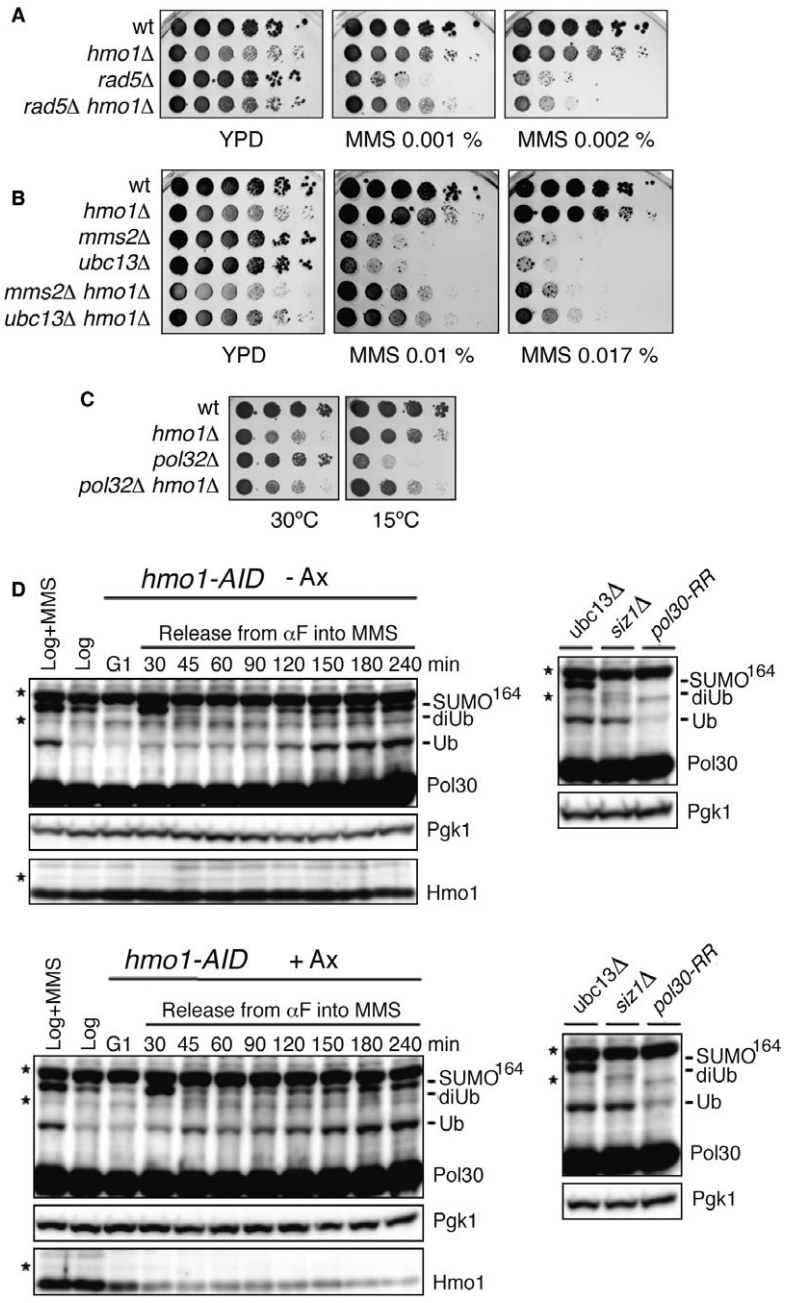

Figure 1. Hmo1 interacts functionally with the Rad5-Mms2-Ubc13 error-free DDT pathway.

A *HMO1* deletion rescues the MMS sensitivity of *rad5Δ*. wt (FY0113), *hmo1Δ* (HY3956), *rad5Δ* (HY0516), *rad5Δ hmo1Δ* (HY1518) cells were spotted.

B *HMO1* deletion rescues the MMS sensitivity of *mms2Δ* and *ubc13Δ*. wt (FY0113), *hmo1Δ* (HY1508), *mms2Δ* (HY0518), *ubc13Δ* (FY1490), *mms2Δ hmo1Δ* (HY1519), and *ubc13Δ hmo1Δ* (HY3959) were spotted.

C *HMO1* deletion rescues the cold sensitivity of *pol32Δ*. wt (FY0090), *hmo1Δ* (HY2714), *pol32Δ* (HY2719) and *hmo1Δ pol32Δ* (HY2706) were spotted.

D Hmo1 does not affect PCNA modifications with ubiquitin and SUMO. Western blot of Pol30 (PCNA) in an *hmo1-AID* conditional mutant (HY2174) following or not Hmo1 depletion by addition of auxin (Ax) before G1 arrest and release into MMS-containing media. Ubiquitylated and SUMOylated species are indicated. Hmo1 depletion control and Pgk1, used as loading control, are shown below. To the right, controls for lack of PCNA polyubiquitylation (*ubc13Δ*, Y2620), or SUMOylation (*siz1Δ*, Y1630), or both (*pol30-RR*, FY1487). Asterisks denote cross-reactive proteins.

increase or rescue the MMS sensitivity of *rad51*Δ cells (data not shown and see below), it partially but discernibly suppressed the damage sensitivity of *rad5Δ* cells in two different yeast backgrounds, DF5 (Fig 1A) and W303 (see below), suggesting a functional interaction between Hmo1 and Rad5. We further examined if this genetic relationship extended to other factors involved in PCNA polyubiquitylation. We found that the *hmo1Δ* mutation also partly suppressed the MMS sensitivity associated with

null mutations in *MMS2* and *UBC13* (Fig 1B), indicating that Hmo1 affects the usage of the Rad5-Mms2-Ubc13 error-free DDT pathway.

To further test Hmo1 implication in error-free DDT, we used a recently elucidated genetic readout (Karras & Jentsch, 2010). Deletion of *POL32*, encoding a nonessential subunit of the replicative DNA polymerase δ (Polδ) that is required for DNA synthesis during template switching (Vanoli *et al*, 2010), generates replication stress accompanied by cold sensitivity and induction of error-free DDT – and therefore of PCNA polyubiquitylation (Karras & Jentsch, 2010; Karras *et al*, 2013). Because mutations affecting PCNA polyubiquitylation (*mms2Δ*, *ubc13Δ*, *rad5Δ*, and *pol30-K164R*) suppress the cold sensitivity of *pol32Δ* cells (Karras *et al*, 2013), suppressors of the *pol32Δ* cold sensitivity phenotype are potentially new components or regulators of the error-free DDT pathway. We found that *hmo1Δ* also partly suppressed the slow growth phenotype at low temperatures of *pol32Δ* cells (Fig 1C), similarly to mutations in other components of the PCNA polyubiquitylation pathway, although to a smaller degree than those mutations (Supplementary Fig S1C). We note that *hmo1*Δ was reported to suppress the temperature sensitivity of other DNA Polδ mutants (Kim & Livingston, 2009), thus resembling also in this respect deletions of *RAD18, RAD5* and *MMS2-UBC13* (Giot *et al*, 1997; Branzei *et al*, 2002, 2004).

We then analyzed if Hmo1 affects PCNA post-translational modifications. Because *hmo1*Δ strains are slow growing, showing slower progression throughout the cell-cycle (Lu *et al*, 1996), and PCNA modifications with SUMO and ubiquitin are expected to be sensitive to cell-cycle changes and replication delays (Hoege *et al*, 2002), we established a conditional degron system (*hmo1-AID)*, in which Hmo1 depletion is induced by addition of auxin (Nishimura *et al*, 2009). Reduced levels of Hmo1 did not discernibly affect PCNA modifications with ubiquitin and SUMO (Fig 1D), suggesting that the effects manifested by Hmo1 on the Rad5-mediated error-free DDT pathway (Fig 1A and B) are not caused by alterations in PCNA modifications.

Hmo1 roles in DDT regulation and SCJ formation are manifested during DNA replication

While the ability of cells to deal with exogenous DNA damage is not affected by restricting the expression of key DDT genes to the G2/M phase of the cell-cycle (Daigaku *et al*, 2010; Karras & Jentsch, 2010), other results suggest an early role for the Rad5 pathway during replication and SCJ formation (Branzei *et al*, 2008; Minca & Kowalski, 2010; Karras *et al*, 2013). To address if the role(s) of Hmo1 in regulating the Rad5 pathway (see Fig 1) are normally manifested in S- or G2/M phases of the cell-cycle, or independently of the cell-cycle phase, we applied the S and G2 tags to *HMO1*. These tags restrict the expression of tagged proteins to specific phases of the cell-cycle, due to control elements of cyclin Clb6 or Clb2, respectively (Karras & Jentsch, 2010; Hombauer *et al*, 2011). When the S-tag- and G2-tag-containing DNA cassettes were integrated directly upstream of the *HMO1* open reading frame at its endogenous locus, the resulting fusion proteins were indeed largely restricted during the cell-cycle as assessed by comparing the expression of these proteins with the ones of Clb2 (Fig 2A). When we further combined these *hmo1* alleles with a *rad5*Δ mutation, we found that specifically the *G2-HMO1* allele resembled *hmo1*Δ in its ability to suppress *rad5*Δ MMS sensitivity. Thus, Hmo1 role in regulating the Rad5 pathway is manifested during replication.

The culmination of error-free DDT is the formation of SCJs, later resolved by Sgs1-Top3 (Branzei *et al*, 2008). To address if Hmo1 also affects the formation or the stability of SCJs generated during error-free DDT, we studied by 2D gel electrophoresis the profile of replication intermediates arising at an early, efficient origin of replication, *ARS305*, when yeast cells replicate in media containing MMS (Fig 2B). Because in *sgs1*Δ cells the processing of the resulting recombination intermediates is impaired and SCJs forming during error-free DDT accumulate (Liberi *et al*, 2005; Branzei *et al*, 2008), we used this genetic background as a tool to address a possible role for Hmo1 in this process. Furthermore, since *hmo1*Δ strains are slow-growing (Lu *et al*, 1996) and the profile of replication intermediates can be severely impacted by the cell-cycle/replication status, we used again the *hmo1-AID* degron system described above (see Fig 1D) to induce Hmo1 depletion. *sgs1*Δ *hmo1-AID* cells grow normally, but Hmo1 depletion at the beginning of replication correlated with a decrease in the amount of SCJs (Fig 2B, 60–120 min panels), which gradually increased following prolonged MMS treatment (Fig 2B, 180–240 min panels). Thus, Hmo1 facilitates SCJ formation/stability in the same time window with the one reported for Rad5-Mms2-Ubc13 (Karras *et al*, 2013), being predominant early during replication. Furthermore, these results indicate that Hmo1 depletion does not significantly impair the functionality of the salvage recombination pathway that normally promotes SCJ formation later in the cell-cycle (Branzei *et al*, 2008; Karras *et al*, 2013).

To examine if the above 2D gel results might reflect a role for Hmo1 in promoting SCJ stability rather than their formation, we used again an *sgs1Δ hmo1-AID* strain but induced Hmo1-AID depletion after the initiation of SCJ formation (1 h after the cells were released from G1 arrest into S phase, Supplementary Fig S2). Although under these conditions Hmo1 depletion also occurred efficiently, it did not anymore correlate with reduced SCJ levels (Supplementary Fig S2), in contrast to its effect at the beginning of replication (Fig 2B, 60–120 min panels). Thus, following genotoxic stress, Hmo1 facilitates the usage of the Rad5 pathway, promoting template switching accompanied by SCJ formation early in S phase.

Hmo1 is a novel regulator of the DDT pathway choice that acts in parallel with Elg1 and Srs2

To understand the molecular mechanism by which Hmo1 facilitates the execution of the Rad5 pathway, we attempted to identify Hmo1 interacting proteins, using a candidate approach as well as yeast two-hybrid screens. We found initially by two-hybrid that Elg1, a regulator of the Rad5 pathway and a binding partner of PCNA (Parnas *et al*, 2010; Kubota *et al*, 2013), interacts physically with Hmo1. We then examined this interaction by *in vivo* pull-down assays. To this end, we purified recombinant GST and GST-Hmo1, immobilized these proteins on glutathione-sepharose beads, and incubated the beads with total cell lysates prepared from Elg1-FLAG yeast strains. In this way, we found that Elg1 is efficiently pulled-down to Hmo1 beads, even when the extract was treated with ethidium bromide, thus suggesting that the interaction between Hmo1 and Elg1 is not bridged by DNA (Fig 3A).

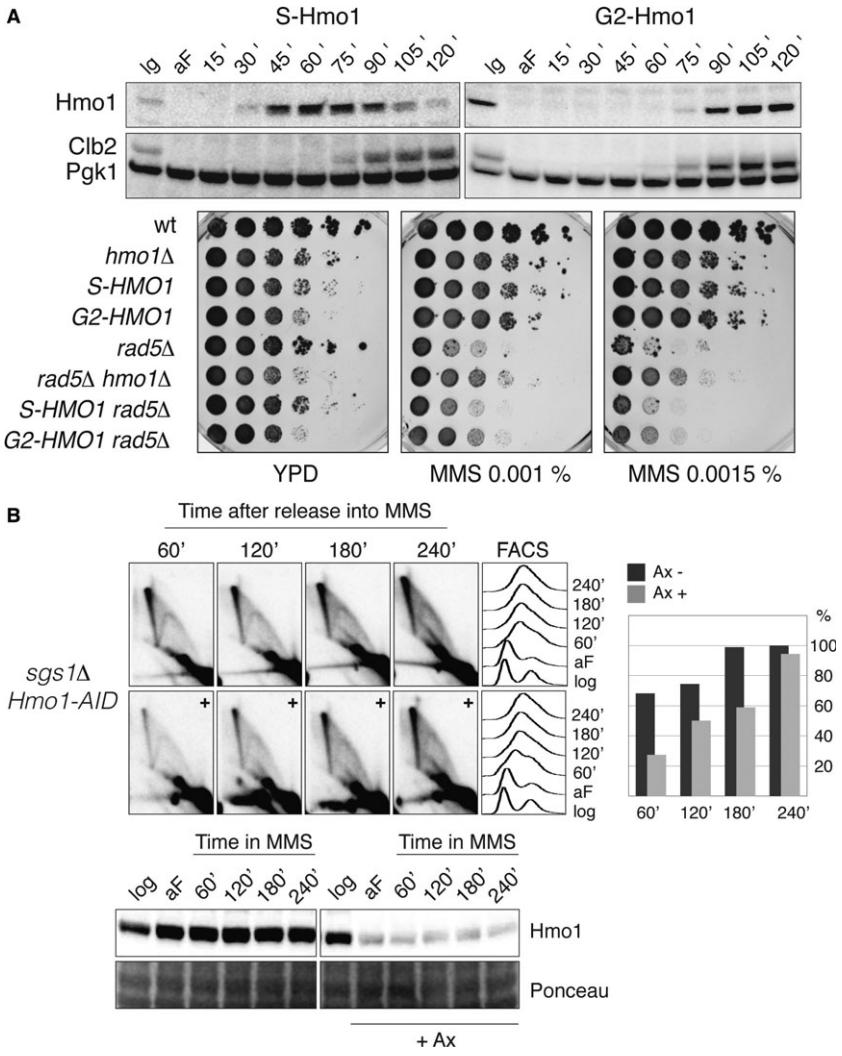

Figure 2. The roles of Hmo1 in Rad5 pathway regulation and SCJ formation are manifested during DNA replication.

A S-tag *HMO1* (*S-HMO1*, HY4324) and G2-tag *HMO1* (*G2-HMO1*, HY4325) cells were arrested in G1 phase and released into YPD at 28°C. Samples were collected at the indicated time points for Western blot analysis. The cell cycle progression was monitored using anti-Clb2 antibody; Pgk1 was used for loading control. Specifically the *G2-HMO1* allele partially rescues the MMS sensitivity of *rad5Δ* cells. wt (FY1296), *hmo1Δ* (HY1507), *S-HMO1* (HY4324), *G2-HMO1* (HY4325), *rad5Δ* (HY2682), *rad5Δ hmo1Δ* (HY3633), *S-HMO1 rad5Δ* (HY4355) and *G2-HMO1 rad5Δ* (HY4359) were spotted.

B Hmo1 promotes SCJ formation during template switching in S phase. *HMO1-AID sgs1Δ* (HY2176) cells were synchronized with alpha-factor (aF) and divided into two identical parts. One half of the culture was treated with auxin and released into YPD media containing 0.033% MMS in the presence of auxin (+), the other half was released into MMS-containing media without auxin treatment. At the indicated time points samples were taken for 2D gel, FACS and Western blot analysis. During quantification the highest value obtained for the X-molecules was considered as 100%. The efficiency of Hmo1 depletion was analyzed with anti-Hmo1 antibody via immunoblotting. Pgk1 was used for loading control.

The *elg1Δ* mutation suppresses the sensitivity of *rad5Δ*, *ubc13Δ*, and *mms2Δ* cells to MMS by a similar degree as the one conferred by *hmo1Δ* (Fig 3B, note the growth defect associated with *hmo1Δ*). However, the combination of *hmo1Δ* and *elg1Δ* mutations leads to a much better suppression of the *rad5Δ* sensitivity than the one conferred by single mutations (Fig 3B), attesting to the individual roles of Elg1 and Hmo1 in error-free DDT regulation and indicating that the distinct modulatory actions of Elg1 and Hmo1 on the Rad5 pathway are potentially coordinated via their physical interaction.

While the mechanism by which Elg1 regulates the Rad5 pathway remains elusive, it possibly involves a joint action of Elg1 with Srs2, the other known regulator of the Rad5-mediated DDT branch that acts by affecting the choice of the recombinational repair pathway (Rong *et al*, 1991; Papouli *et al*, 2005; Pfander *et al*, 2005). The interplay between Srs2 and Elg1 in error-free DDT regulation was suggested by their preferential binding to SUMOylated PCNA (Papouli *et al*, 2005; Pfander *et al*, 2005; Parnas *et al*, 2010) and the observation that simultaneous deletion of *SRS2* and *ELG1* leads to a growth impairment that is partly improved by a SUMOylation-defective allele of PCNA (Parnas *et al*, 2010). The proposed mechanism envisages that while Srs2 disrupts toxic recombination events and makes space for the action of the Rad5 pathway (Aboussekhra *et al*, 1992; Krejci *et al*, 2003; Veaute *et al*, 2003; Papouli *et al*,

Published online: January 28, 2014
The EMBO Journal

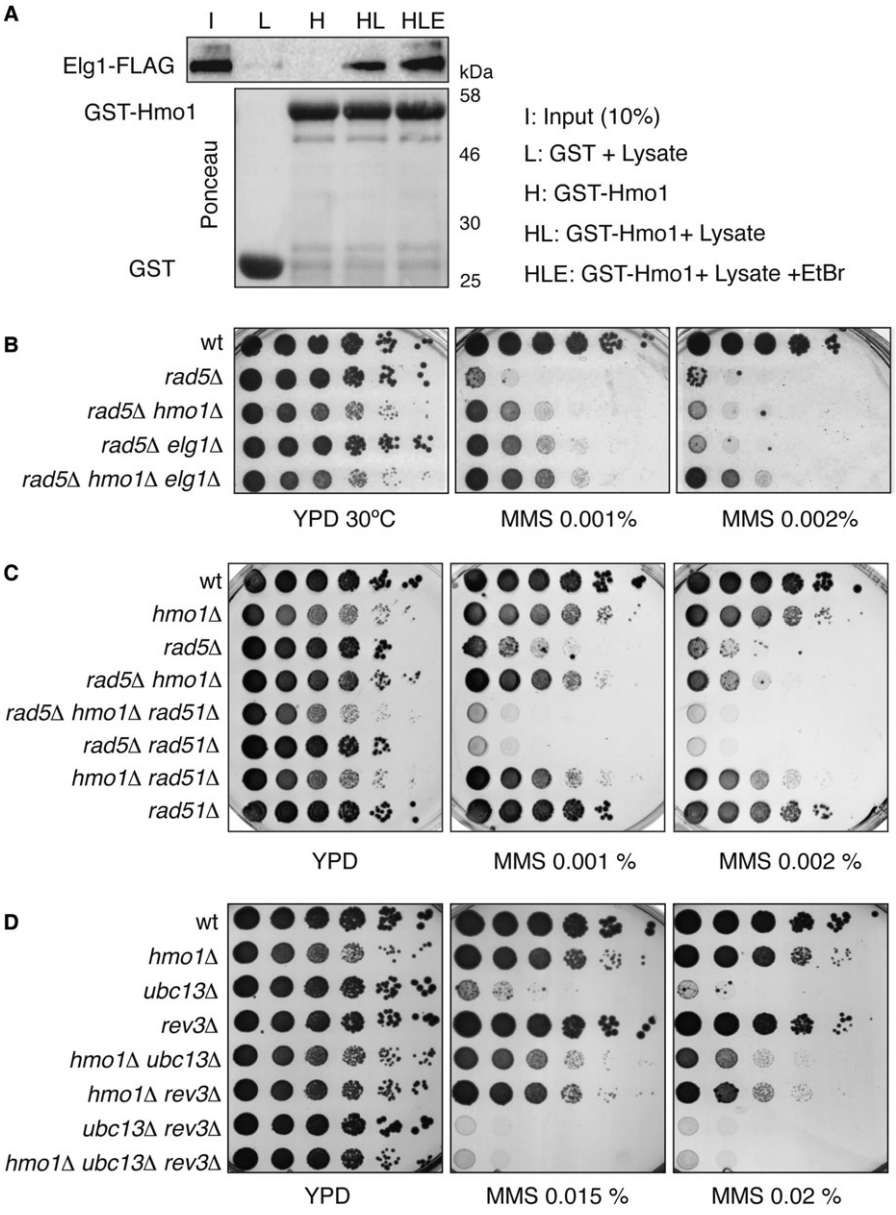

Figure 3. Hmo1 acts in parallel with Elg1 and Srs2 to promote Rad5-mediated error-free DDT.

A Hmo1 interacts physically with Elg1. *In vivo* pull-down assay. Recombinant GST-Hmo1 protein was tested for its ability to bind endogenous Elg1. The amount of GST and GST-Hmo1 protein used is shown by Ponceau staining. Total cell lysates prepared from yeast cells expressing Elg1-FLAG tagged strain (HY1976) were incubated with GST or GST-Hmo1 in the presence or absence of ethidium bromide. The protein complex formed on the beads was analyzed by immunoblotting using anti-FLAG antibody.

B *HMO1* and *ELG1* deletions additively rescue the MMS sensitivity of *rad5Δ*. wt (HY4104), *rad5Δ* (HY4098), *rad5Δ hmo1Δ* (HY4127), *rad5Δ elg1Δ* (HY4056) and *rad5Δ hmo1Δ elg1Δ* (HY4073) cells were spotted.

C *HMO1* deletion rescues the MMS sensitivity of *rad5Δ* cells by suppressing the recombination pathway. wt (FY0113), *hmo1Δ* (HY3957), *rad5Δ* (HY0516), *rad5Δ hmo1Δ* (HY1518), *rad5Δ hmo1Δ rad51Δ* (HY3943), *rad5Δ rad51Δ* (HY3948), *hmo1Δ rad51Δ* (HY3946) and *rad51Δ* (HY2651) strains were spotted.

D The survival of *hmo1Δ ubc13Δ* cells in MMS depends on the mutagenic pathway involving the translesion synthesis polymerase Rev3. wt (FY0090), *hmo1Δ* (HY1508), *ubc13Δ* (FY1490), *rev3Δ* (HY4416), *hmo1Δ ubc13Δ* (HY3960), *hmo1Δ rev3Δ* (HY4439), *ubc13Δ rev3Δ* (HY4417) and *ubc13Δ rev3Δ hmo1Δ* (HY4440) strains were spotted.

2005; Pfander *et al*, 2005), Elg1 may help unload (SUMOylated) PCNA from chromatin to facilitate DNA repair (Parnas *et al*, 2010; Kubota *et al*, 2013).

To further investigate the mechanism by which Hmo1 modulates Rad5-mediated DDT, we aimed at identifying the DDT pathways required for viability in *rad5Δ hmo1Δ* and *ubc13Δ hmo1Δ* cells. Similarly to the case previously elucidated for Srs2 (Rong *et al*, 1991; Aboussekhra *et al*, 1992; Papouli *et al*, 2005; Pfander *et al*, 2005), we found that the viability of *rad5Δ hmo1Δ* depended on the salvage recombination pathway involving Rad51

(Fig 3C) and the recently identified 9-1-1 activities (Karras *et al*, 2013) (Supplementary Fig S3A), but not on Ubc13 (Supplementary Fig S3B). In addition, Hmo1 was not required for the viability of *rad5Δ srs2Δ* cells exposed to MMS (Supplementary Fig S3C, note the growth defect associated with *hmo1Δ*). This latter result, together with the 2D gel analysis data showing that Hmo1 is dispensable for the formation of late SCJs (Fig 2B), likely arising via the action of the salvage pathway of recombination (Branzei *et al*, 2008; Karras *et al*, 2013), indicates that Hmo1 is not required for the execution of the salvage recombination pathway. Furthermore, we found that the viability conferred by *HMO1* deletion in mutants defective in the PCNA polyubiquitylation pathway of template switching depends on the TLS polymerase, Rev3 (Fig 3D). Thus, defects in the PCNA polyubiquitylation pathway in WT cells causes MMS hypersensitivity, whereas additional inhibition of *HMO1* cells allows other recombination- and TLS-mediated DDT pathways to operate efficiently. Together, these results allow us to conclude that Hmo1 is a new regulator of the error-free DDT pathway, acting in parallel with Srs2 and Elg1, to facilitate the Rad5-mediated error-free DDT pathway and influencing DDT pathway choice.

Uncoupling error-free DDT pathway choice from SCJ formation during template switching

The functionality of the Rad5 error-free DDT is reflected in the ability of cells to timely fill in DNA gaps (Torres-Ramos *et al*, 2002; Zhang & Lawrence, 2005) with the transient formation of SCJ intermediates (Branzei *et al*, 2008; Minca & Kowalski, 2010; Karras *et al*, 2013). However, whether the Rad5 pathway regulators, which direct lesions into the Rad5 pathway and/or facilitate its usage, also impact on SCJ formation is not known. The individual mutation of *srs2Δ* in a WT background does not affect SCJ levels (Liberi *et al*, 2005), and we found a similar profile of replication intermediates in WT and *elg1Δ* cells (Supplementary Fig S4). However, the low levels of SCJ intermediates and their transient nature in WT cells do not allow for conclusive answers in what regards a possible role for Srs2 and Elg1 in SCJ formation. In an *sgs1Δ* background, in which SCJ persistence facilitates the identification of genetic requirements (Liberi *et al*, 2005; Branzei *et al*, 2008; Vanoli *et al*, 2010), deletion of *SRS2* or *ELG1* leads to synthetic lethality or a slow growth phenotype (Mullen *et al*, 2001; Parnas *et al*, 2010), incompatible with the correct assessment of replication intermediate status by 2D gel analysis. To address a possible role for Srs2 and Elg1 in SCJ generation, we established a conditional mutant for *SGS1* (*Tc-SGS1*) in which Sgs1 translation is prevented upon addition of tetracycline (Kotter *et al*, 2009). Using this conditional allele, we could deplete Sgs1 and allow SCJ accumulation during replication (Fig 4 and data not shown). Deletion of *SRS2* and *ELG1* in *Tc-SGS1* strains did not affect cell fitness, thus making them suitable for 2D gel analysis of replication intermediates arising in one cell cycle. When Tc-Sgs1 depletion was induced during replication, *srs2Δ* and *elg1Δ* mutations did not discernibly reduce SCJ accumulation (Fig 4). These results reveal that the previously identified regulators of the Rad5 pathway usage, Elg1 and Srs2, which suppress *rad5Δ* sensitivity to MMS, do not affect SCJ formation during template switching. Thus, the function of guiding DDT pathway choice is uncoupled from the one(s) required for SCJ formation, and Hmo1 participates in both of these processes.

Hmo1-mediated DNA bending facilitates error-free DDT by template switching

We next aimed at addressing if changes in DNA topology induced by Hmo1-mediated DNA bending underlie its roles in DDT pathway choice or SCJ formation. Similar to mammalian HMGB proteins, Hmo1 contains two DNA-binding domains termed box A and box B, and a lysine rich C-terminal tail (Fig 5A). Of the DNA-binding domains of Hmo1, only box B corresponds to a consensus HMG box, while box A shows weak similarity. The HMG box is typically about 80 amino acids long and adopts an L-shaped fold composed of three α-helices. DNA binding, which occurs from the minor groove through intercalation of one or two hydrophobic residues, results in a sharp DNA bend and helical underwinding (Weir *et al*, 1993; Hardman *et al*, 1995). Biochemical studies indicated that box B is crucial for DNA binding, while box A plays only minor roles, affecting DNA bending by its interaction with the C-terminal tail of Hmo1 (Kamau *et al*, 2004; Bauerle *et al*, 2006; Xiao *et al*, 2010). The role of box A in bending is not fully understood as for certain assays measuring DNA bending, box A is dispensable (Xiao *et al*, 2010). In contrast, it has been clearly noted that the C-terminal tail of Hmo1 is crucial for DNA bending: Hmo1 C-terminal truncation variants are defective in DNA bending, while their DNA-binding affinity *per se* is not diminished (Bauerle *et al*, 2006; Xiao *et al*, 2010).

To study the effect of Hmo1-mediated DNA bending in DDT regulation, we deleted the C-terminal tail of Hmo1 to construct *hmo1-CΔ22* and *hmo1-CΔ64* mutants (Fig 5A and Supplementary Fig S5A). These Hmo1 variants are stable and *hmo1-CΔ22/64* strains do not show the growth defects characteristic of *hmo1Δ* (Fig 5A), suggesting that they are proficient in certain Hmo1 functions as also suggested by their previous biochemical characterization (Bauerle *et al*, 2006; Xiao *et al*, 2010). In what regards DDT pathway choice, we found that both *hmo1-CΔ*22 and *hmo1-CΔ64* alleles resembled *hmo1Δ* in their ability to suppress the *rad5Δ* sensitivity to MMS, although their effect was smaller than that of *hmo1Δ* (Fig 5A, DF5 background). We note that in a different yeast background, W303, in which the suppression conferred by *hmo1Δ* to *rad5Δ* is weaker than the one observed in DF5, the *hmo1-CΔ64* mutation suppresses *rad5*Δ sensitivity to MMS to the same degree as *hmo1*Δ (Supplementary Fig S5B). The reason underlying these background differences is unclear to us. Nevertheless, considering that *hmo1-CΔ* mutations partly suppress *rad5Δ* sensitivity to MMS in two different yeast backgrounds, we conclude that the C-terminus of Hmo1 is at least partly involved in DDT pathway choice. In addition, the *hmo1-CΔ* alleles showed increased spontaneous mutation rates (Fig 5B) and impaired damage-bypass via SCJ formation (Fig 5C), similarly to *hmo1*Δ or Hmo1 depletion (Figs 5B and 2B), respectively, thus substantiating the important role of the C-terminal tail of Hmo1 in error-free DDT. In all, these results suggest that Hmo1-mediated DNA bending facilitates channeling of DNA lesions into the Rad5 error-free DDT pathway and the execution of template switching via SCJ formation.

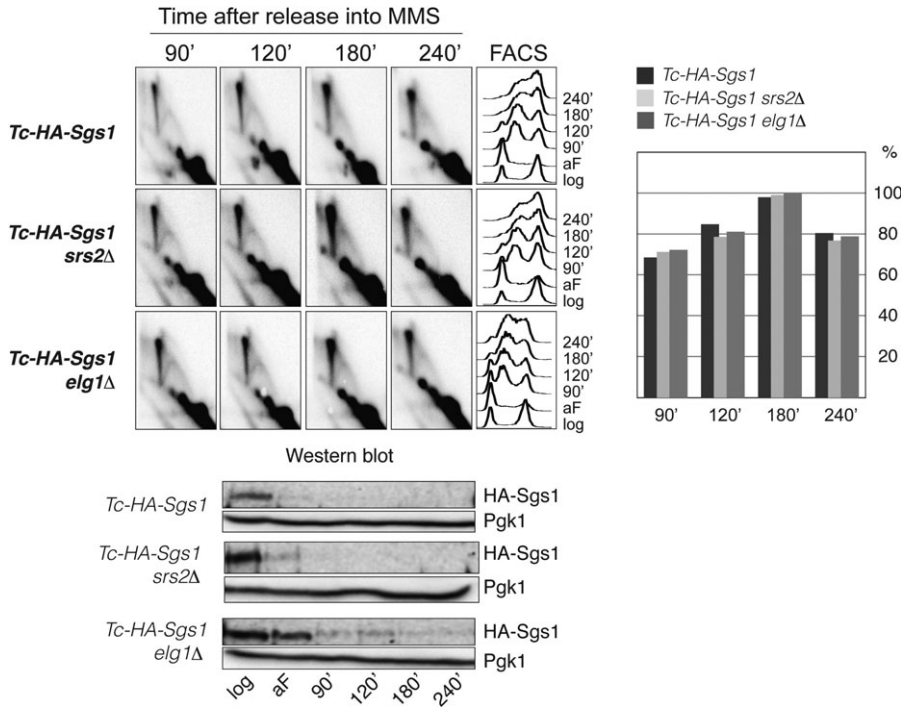

Figure 4. Srs2 and Elg1 involved in DDT pathway choice regulation are not required for SCJ formation during template switching.
Tc-Sgs1 (HY4017), *Tc-Sgs1 elg1Δ* (HY4320) and *Tc-Sgs1 srs2Δ* (HY4352) cells were synchronized with alpha-factor (aF) in the presence of tetracycline and released into YPD media containing 0.033% MMS in the presence of tetracycline. At the indicated time points samples were taken for 2D gel, FACS and Western blot analysis. During quantification, the highest value obtained for the X-molecules accumulating was considered as 100%. Depletion of Sgs1 (tagged with 3HA) was followed by Western blot using anti-HA antibody. Pgk1 was used for loading control.

Hmo1-mediated DNA bending facilitates formation of sister chromatid intertwinings

To further examine if Hmo1 role in template switching and SCJ formation (Figs 2B and 5C) is related to its role in altering DNA topologies in a manner that might facilitate sister chromatid interactions, we purified recombinant Hmo1 full-length, as well as an Hmo1 variant with a truncated C-terminus, and incubated increasing amounts of these Hmo1 proteins with Top1-relaxed plasmids. Addition of Hmo1, but not of the C-terminal truncated Hmo1 variant, promoted a gel retardation of the relaxed topoisomers (Supplementary Fig S5C). Since the migration pattern of topoisomers following Hmo1 addition is the one expected for supercoiled and nicked catenated plasmid dimers (Kegel *et al*, 2011), these findings indicate that Hmo1 mediates the formation or stabilization of catenanes/hemicatenanes via its C-terminal tail.

Hmo1 was previously reported to be deleterious in *top2* mutants for reasons that remained elusive. We asked if Hmo1 deleterious effect is related to its role in stabilizing catenanes/hemicatenanes via its C-terminal domain (Supplementary Fig S5C). Indeed, similarly to *hmo1Δ*, the *hmo1-CΔ22* and *hmo1-CΔ64* alleles also partially suppressed the temperature sensitivity phenotype of *top2-1* cells (Fig 5D). Together, these results indicate that the DNA-bending activity of Hmo1 mediates the formation of sister chromatid intertwinings that, under conditions of replication stress, facilitate replication by template switching.

Discussion

Replication is associated with DNA structural and topological changes as well as with specific post-translational modifications of DNA damage response factors that assist DDT and replication completion (Branzei & Foiani, 2010). RPA-coated ssDNA, accumulating following replication under conditions of genotoxic stress, activates the replication checkpoint (Mec1/Ddc2 in yeast and ATR/ATRIP in mammals), as well as DDT pathways (Zou & Elledge, 2003; Branzei & Foiani, 2010). The latter event appears to be mediated through RPA-dependent recruitment of Rad18 (Davies *et al*, 2008), which together with Rad6 and the Rad5-Mms2-Ubc13 complex promotes PCNA modification with mono- and polyubiquitin chains (Hoege *et al*, 2002), and induces translesion synthesis- and error-free-mediated DDT, respectively (Stelter & Ulrich, 2003; Papouli *et al*, 2005; Pfander *et al*, 2005; Branzei *et al*, 2008). The choice of the DDT pathway is crucial for genome integrity, as mutagenesis and hyper-recombination can lead to accumulation of deleterious mutations and chromosomal rearrangements that threaten genome integrity and promote cancer formation (Nik-Zainal *et al*, 2012; Alexandrov *et al*, 2013). In addition, while a correlation between replication timing and mutation rates was established (Lang & Murray, 2011), the genome surveillance mechanisms that promote genome integrity by facilitating error-free DDT early during replication remain largely unknown.

Published online: January 28, 2014

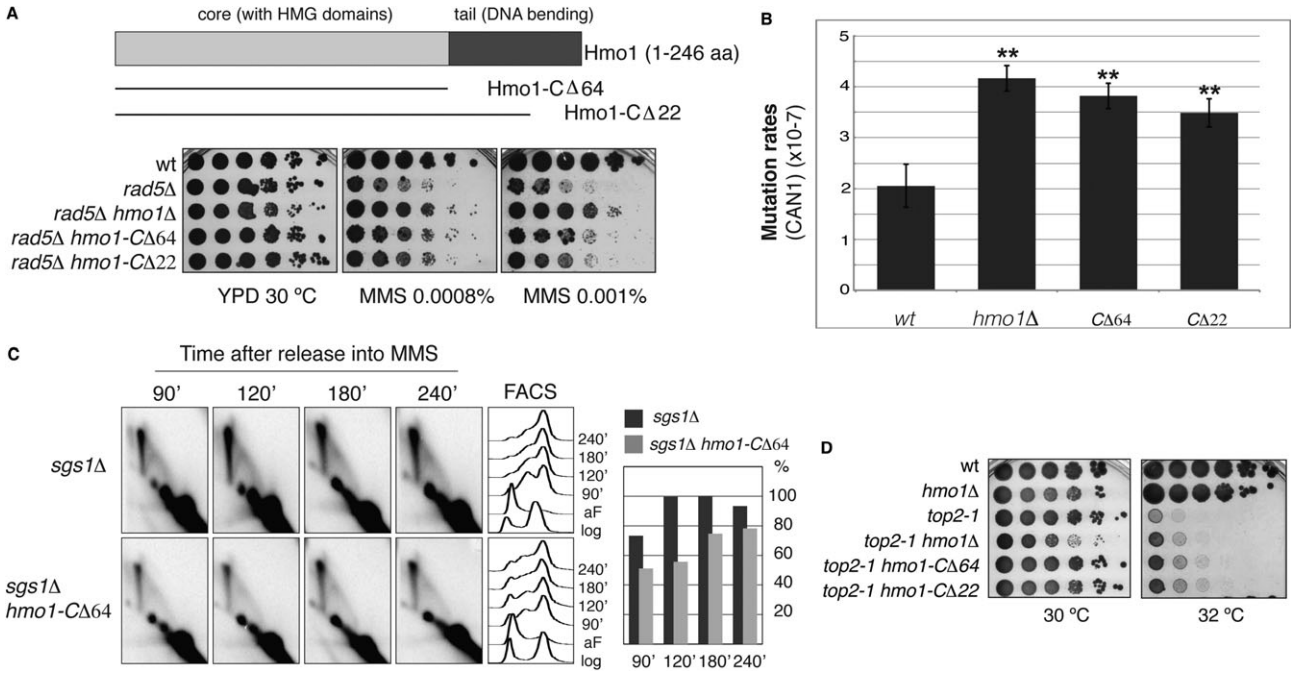

Figure 5. The C-terminal tail of Hmo1 required for DNA bending promotes Rad5-mediated error-free DDT and the formation of sister chromatid intertwinings *in vivo*.

A Scheme of Hmo1 and C-terminal truncation (Hmo1-CΔ) alleles. The Hmo1 C-terminal tail deletion partly suppresses the hypersensitivity of *rad5Δ* to MMS. wt (HY4104), *rad5Δ* (HY4098), *rad5Δ hmo1Δ* (HY4127), *rad5Δ hmo1-CΔ64* (HY4091) and *rad5Δ hmo1-CΔ22* (HY4108) strains were spotted.

B Hmo1 prevents spontaneous mutagenesis and its C-terminal tail is required for this function. Spontaneous mutagenesis at the *CAN1* locus is shown for the indicated mutants. wt (FY0108), *hmo1Δ* (HY1508), *hmo1-CΔ64* (HY3893) and *hmo1-CΔ22* (HY3895) cells were used. Values and associated error-bars represent averages and their standard deviations from 3 independent experiments. ** denotes a highly significant *P*-value ($P < 0.01$).

C Hmo1 promotes SCJ formation during template switching via its C-terminal tail. *sgs1Δ* (FY1060) and *sgs1Δ hmo1-CΔ64* (HY4303) cells were synchronized with alpha-factor (aF) and released into YPD media containing 0.033% MMS. At the indicated time points samples were taken for 2D gel and FACS analysis. In the quantification, the highest value obtained for the X-molecules accumulating was considered as 100%.

D The C-terminal tail of Hmo1 is deleterious in *top2-1* mutants. wt (FY1296), *hmo1Δ* (HY1507), *top2-1* (HY3362), *top2-1 hmo1Δ* (HY3363), *top2-1 hmo1-CΔ64* (HY3890) and *top2-1 hmo1-CΔ22* (HY3892) were spotted at permissive (30 °C) and semi-permissive (32 °C) temperatures for *top2-1*.

So far two well conserved mechanisms related to PCNA modifications have been shown to influence DDT pathway choice: one is related to the PCNA mono/poly-ubiquitylation status and affects the labor distribution between translesion synthesis-mediated error-prone damage bypass and Rad5-mediated error-free DDT, whereas the other regulatory mechanism is mediated by PCNA SUMOylation (Bergink & Jentsch, 2009; Branzei & Foiani, 2010). According to the current view, transient PCNA SUMOylation during S phase prevents unwanted recombination from occurring during replication. Factors such as Srs2 in yeast and PARI in human cells that directly bind to SUMOylated PCNA (Papouli *et al*, 2005; Pfander *et al*, 2005; Parnas *et al*, 2010; Moldovan *et al*, 2011), or Elg1/ATAD5 that interacts with SUMOylated PCNA in yeast (Parnas *et al*, 2010) and regulates the levels of PCNA (ubiquitylation) in human cells (Lee *et al*, 2010), affect genome stability likely by regulating the mechanism through which cells tolerate DNA lesions.

In addition to these protein interactions and post-translational modifications that affect DDT signaling and DDT pathway choice, replication is associated with various DNA topological changes. These topological transitions include accumulation of positive supercoil ahead of the replication forks, partly compensated by the rotation of the replisome along the DNA helix and accompanied by the formation of precatenanes behind replication forks (Postow *et al*, 2001; Wang, 2002), hemicatenations of the sister chromatids behind replication forks (Lucas & Hyrien, 2000; Lopes *et al*, 2003) and formation of sister chromatid bridges when replication forks pass through chromatin loops containing transcribed regions (Bermejo *et al*, 2009). HMGB proteins bind to hemicatenated/catenated structures *in vitro* (Bianchi *et al*, 1989) and Hmo1 may stabilize sister chromatid bridges proposed to arise at intergenic loci during replication (Bermejo *et al*, 2009). Moreover, HMGB proteins bind DNA with low sequence specificity, and their binding to DNA affects chromatin architecture by inducing sharp DNA bends and helical underwinding (Thomas & Travers, 2001; Stros, 2010). However, if and how chromatin architecture affects replication and the choice of the DNA repair pathway remained to date largely unknown.

Our present work revealed that the chromatin architectural HMGB protein, Hmo1, promotes the error-free DDT pathway during replication via at least two specific functions. First, Hmo1 facilitates channeling of replication-associated lesions towards the Rad5 pathway of error-free DDT, while preventing the salvage pathway of recombination (Fig 3C) and mutagenic bypass (Figs 3D and 5B), thus

contributing to the temporal separation and usage of template switching early during replication (Lang & Murray, 2011). We envisage that Hmo1-mediated bending may synergize with Elg1-mediated transactions (see Fig 3A and B) to fine-tune the levels of chromatin associated PCNA, setting the stage for error-free DNA repair (Fig 2A) and limiting the replication errors forming during damage-bypass (Fig 5B). Secondly, we found that Hmo1 facilitates template switching by promoting SCJ formation (Fig 2B). These functions of Hmo1 are both coincident with early DNA replication and are mediated by its C-terminal domain (Figs 2 and 5), which is crucial for Hmo1-mediated DNA bending and architectural/topological changes (Supplementary Fig S5C and Fig S5D). In all, these results suggest that topological changes associated with DNA replication facilitate error-free DDT by template switching, and thus impact on genome integrity.

In addition to sister chromatid bridges proposed to form upon encountering of replication forks with transcription units (Bermejo *et al*, 2009), replication-dependent SCJs, hypothesized to represent hemicatenanes, may form behind replication forks even in unperturbed conditions (Lucas & Hyrien, 2000; Benard *et al*, 2001; Lopes *et al*, 2003; Robinson *et al*, 2007). When replication-related X-molecules, encounter GGA/TTC repeats, homology-driven junctions substitute the original asymmetric hemicatenanes (Follonier *et al*, 2013). Thus, hemicatenanes or related topological structures may facilitate homology-mediated annealing to the same template strand in case of direct repeats. By analogy, in case of replication in the presence of genotoxic stress, we speculate that topological constrains arising during replication may facilitate annealing of the gap-containing region to the homologous sister duplex and promote template switching (Fig 6, I). As HMGB proteins show high affinity for cruciform structures (Bianchi *et al*, 1989; Stros *et al*, 2004; Jaouen *et al*, 2005), it is possible that Hmo1, via its ability to bind hemicatenanes and catenated sister chromatid bridges, prevents their dissolution upon encountering ssDNA gaps, thereby facilitating annealing of the ssDNA gap into the homologous duplex (Fig 6, II) and formation of subsequent SCJs generated during template switching (Fig 6, III–V).

In addition to the model proposed above, and not mutually exclusive, Hmo1 may promote template switching and SCJ formation via its reported ability to induce formation of chromatin loops via DNA-bending (Xiao *et al*, 2010). We envisage that under conditions of DNA damage, these chromatin loops will often contain ssDNA gap regions and would mediate homology search by engaging in inter-molecular interaction with the sister homologous duplex (Fig 6, II). We note that a closed circular nucleofilament of the Rad51 bacterial ortholog, RecA, efficiently invades a duplex (Bianchi *et al*, 1983). Furthermore, the Rad51 nucleofilament contained in the loop would promote extensive pairing with the homologous sequence from the donor duplex, thereby facilitating homologous recombination (De Vlaminck *et al*, 2012). This would lead to efficient re-annealing of the parental strands (Mozlin *et al*, 2008; Vanoli *et al*, 2010) and exposure of the newly synthesized strand for DNA synthesis (Fig 6, III), thus facilitating template switching (Fig 6, IV–V).

In conclusion, our results suggest that replication-associated chromatin architectural changes act as a novel layer of regulation, besides the molecular switch mediated by PCNA ubiquitylation/SUMOylation, to control DDT pathway choice and to promote error-free replication under conditions of genotoxic stress. Our findings thus establish a link between replication-associated topological changes and DDT pathway choice, highlighting the role of chromatin architecture as an important modulator of genome integrity, by setting the stage for error-free replication and DNA repair.

Materials and Methods

Yeast strains

The strains used in this study are derivatives of DF5 or W303. The relevant genotypes are shown in Supplementary Table 1.

Growing conditions, cell cycle arrests and drug treatments

Unless otherwise indicated, strains were grown at 30°C in YPD medium, synchronized with 2 μg/ml α-factor and released in 0.033% MMS.

Genomic DNA extraction, FACS analysis and 2D gel technique

Purification of DNA was performed by the CTAB procedure; FACS and 2D gel analysis of DNA intermediates were performed as previously described (Branzei *et al*, 2008). DNA samples were analyzed by 2D gel using probes against *ARS305* following NcoI or EcoRV-HindIII digestion. Quantification of X-shaped intermediates was done using IMAGEQUANT software, as previously described (Branzei *et al*, 2008) and as detailed in the Supplementary Data 1. Each experiment was independently performed at least twice and a representative experiment is shown.

ChIP-on-chip

These procedures are derived from the ChIP-on-chip protocol previously described (Bermejo *et al*, 2009) and detailed in the Supplementary Information Anti-PK SV5-Pk1 antibody (AbD Setotec) and anti-BrdU antibodies (MI-11-3 from MBL) were employed. ChIP-on-chip experiments were independently performed at least twice and a representative experiment is shown. Evaluation of the significance of protein cluster distributions was performed as described in (Bermejo *et al*, 2009).

Two-hybrid screens

Yeast two-hybrid screening was performed by Hybrigenics Services, S.A.S., Paris, France (http://www.hybrigenics-services.com). Further information is given in the Supplementary Data 1.

Mutagenesis assays

Spontaneous mutation rates were estimated using the maximum-likelihood approach and as described in the Supplementary Data 1.

Hmo1 protein expression and purification

The procedure used to express Hmo1 and Hmo1-CΔ64 proteins is detailed in the Supplementary Data 1.

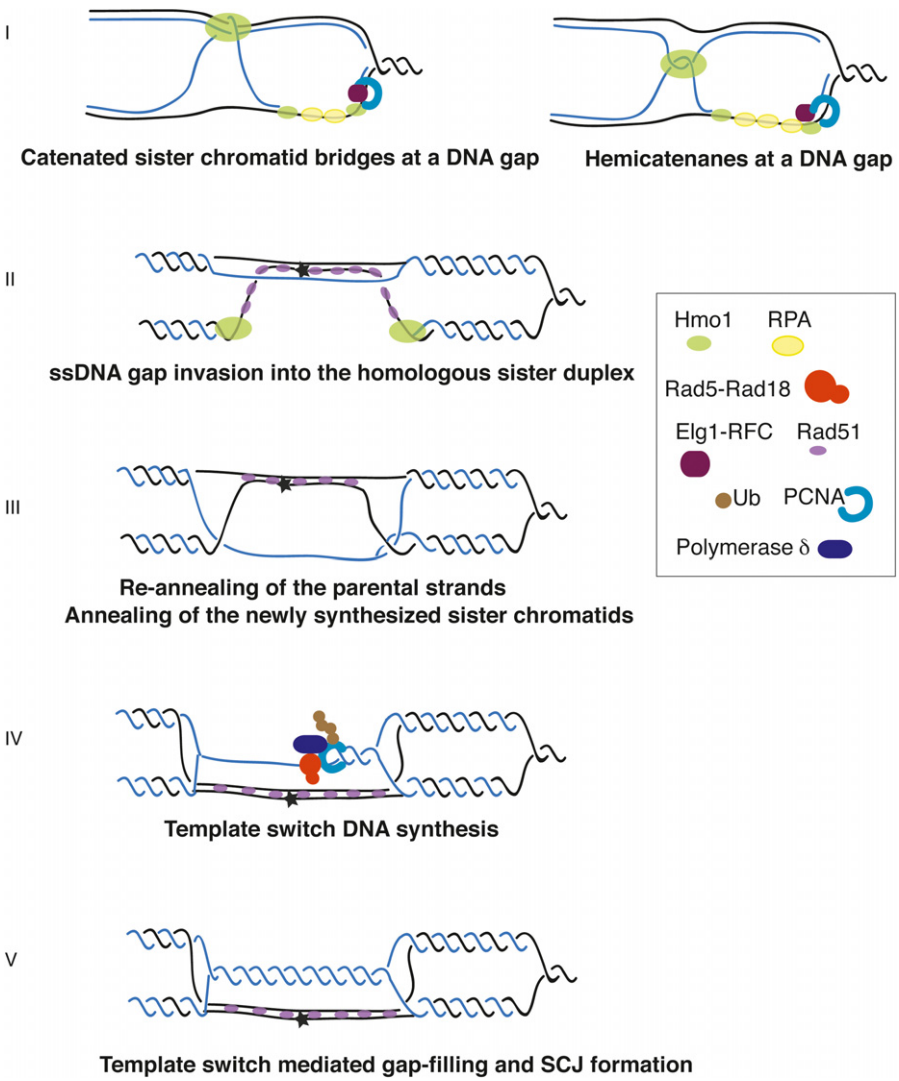

Figure 6. Hmo1 influences the S-phase chromosomal architecture creating a context favourable for error-free DDT by template switching.
A hypothetical model for Hmo1-mediated topological transitions promoting template switching. Parental DNA is shown in black, the newly synthesized DNA in blue. The asterisk indicates a DNA lesion. Sister chromatid bridges (Bermejo *et al*, 2009) and hemicatenane structures (Lopes *et al*, 2003) arising during replication could be stabilized by Hmo1 (Bianchi *et al*, 1989; Jaouen *et al*, 2005) (I). These topological constrains can facilitate gap-filling via template switching by bringing in proximity the homologous sister duplex (I). In addition to this, or alternatively, via its ability to bend DNA, Hmo1 may promote looping of a DNA region containing the DNA gap, facilitating strand invasion by inducing extensive pairing/annealing of the invading Rad51 filament with the homologous duplex (II). This would lead to re-annealing of the parental strands (in black), and exposure of the newly synthesized strand (in blue) (III). Extension of the 3 end proximal to the gap by Polδ and Rad5-mediated PCNA polyubiquitylation (Branzei *et al*, 2008; Vanoli *et al*, 2010) using the newly synthesized chromatid as template (IV) would lead to formation of template switch intermediates containing SCJs (V).

DNA supercoiling assay

The assay was performed by relaxing 1 μg of plasmid YIplac211 with 1 U of wheat-germ Topoisomerase I (Promega) for 1 h at 37°C. The indicated amounts (in μg) of full-length or C-terminal truncated Hmo1 were added and the reaction was left for the time indicated (15 or 60 min). The reactions were stopped by addition of 3% SDS and DNA ethanol-precipitated prior to resuspending and loading onto a 0.6% agarose gel in 1× TBE buffer. Electrophoresis was performed at 45 V for 15 h. We also performed phenolization prior to ethanol-precipitation, obtaining analogous results.

In vivo pull-down assay

Approximately 5 μg of bacterially expressed GST and GST-Hmo1 proteins were immobilized on 30 μl of glutathione-Sepharose 4B beads. For *in vivo* pull-down assay, extracts were prepared from Elg1-FLAG cells arrested with α factor (G1) and released in YPD with and without 0.033% MMS for 20 min. Approximately 2.5 mg of total cell lysates were incubated with GST and GST-Hmo1 proteins at 4°C in Tris-HCl buffer (Tris pH 7.5, 150 mM NaCl, 1 mM DTT, 1 mM EDTA, 10% glycerol, 0.1% Triton X-100 and Protease inhibitor cocktail) for 2 h, in the presence or absence of 0.5 mg/ml of ethidium bromide. The beads were washed twice with Tris-HCl

buffer and twice with Tris-HCl buffer containing 500 mM NaCl. The protein complexes formed on the beads were subjected to 10% SDS-PAGE and analysed by immunoblotting using anti-FLAG-M2 antibody (Sigma). The proteins were visualized by enhanced chemiluminescence (ECL), according to the manufacturer's instructions (Amersham ECL Plus).

Supplementary information for this article is available online: http://emboj.embopress.org

Acknowledgements
We thank S Brill for sharing Hmo1 antibodies, T Abe, M Bianchi, M Foiani for critical reading of the manuscript, GI Karras for technical suggestions on PCNA blots, W Carotenuto and A Cocito for help with statistical analysis of the microarray results, and the anonymous referee/arbitrator for useful suggestions on highlighting the general implications of our findings. SJ is supported by Max Planck Society, Deutsche Forschungsgemeinschaft, Fonds der chemischen Industrie, Center for Integrated Protein Science Munich, and Louis-Jeantet Foundation; DB, by the ERC grant REPSUBREP 242928, the AIRC grant IG10637, the Telethon grant GGP12160 and by FIRC.

Author contributions
The experiments were designed and conceived by DB, executed by BS, VGH, MU, IP, FC, DM, ER, MF, and DB. RB contributed advice on ChIP experiments. All authors contributed reagents, strains and participated in data analysis. DB wrote the paper, with IP and SJ contributing to the edition of the text.

Conflicts of interests
The authors declare that they have no conflict of interest.

References

Aboussekhra A, Chanet R, Adjiri A, Fabre F (1992) Semidominant suppressors of Srs2 helicase mutations of *Saccharomyces cerevisiae* map in the RAD51 gene, whose sequence predicts a protein with similarities to procaryotic RecA proteins. *Mol Cell Biol* 12: 3224 – 3234

Alekseev SY, Kovaltsova SV, Fedorova IV, Gracheva LM, Evstukhina TA, Peshekhonov VT, Korolev VG (2002) HSM2 (HMO1) gene participates in mutagenesis control in yeast *Saccharomyces cerevisiae*. *DNA Repair* 1: 287 – 297

Alexandrov LB, Nik-Zainal S, Wedge DC, Aparicio SA, Behjati S, Biankin AV, Bignell GR, Bolli N, Borg A, Borresen-Dale AL, Boyault S, Burkhardt B, Butler AP, Caldas C, Davies HR, Desmedt C, Eils R, Eyfjord JE, Foekens JA, Greaves M *et al* (2013) Signatures of mutational processes in human cancer. *Nature* 500: 415 – 421

Ashton TM, Mankouri HW, Heidenblut A, McHugh PJ, Hickson ID (2011) Pathways for holliday junction processing during homologous recombination in *Saccharomyces cerevisiae*. *Mol Cell Biol* 31: 1921 – 1933

Bauerle KT, Kamau E, Grove A (2006) Interactions between N- and C-terminal domains of the *Saccharomyces cerevisiae* high-mobility group protein HMO1 are required for DNA bending. *Biochemistry* 45: 3635 – 3645

Benard M, Maric C, Pierron G (2001) DNA replication-dependent formation of joint DNA molecules in *Physarum polycephalum*. *Mol Cell* 7: 971 – 980

Bergink S, Jentsch S (2009) Principles of ubiquitin and SUMO modifications in DNA repair. *Nature* 458: 461 – 467

Bermejo R, Capra T, Gonzalez-Huici V, Fachinetti D, Cocito A, Natoli G, Katou Y, Mori H, Kurokawa K, Shirahige K, Foiani M (2009) Genome-organizing factors Top2 and Hmo1 prevent chromosome fragility at sites of S phase transcription. *Cell* 138: 870 – 884

Bianchi M, DasGupta C, Radding CM (1983) Synapsis and the formation of paranemic joints by *E. coli* RecA protein. *Cell* 34: 931 – 939

Bianchi ME, Beltrame M, Paonessa G (1989) Specific recognition of cruciform DNA by nuclear protein HMG1. *Science* 243: 1056 – 1059

Branzei D (2011) Ubiquitin family modifications and template switching. *FEBS Lett* 585: 2810 – 2817

Branzei D, Foiani M (2010) Maintaining genome stability at the replication fork. *Nat Rev Mol Cell Biol* 11: 208 – 219

Branzei D, Seki M, Enomoto T (2004) Rad18/Rad5/Mms2-mediated polyubiquitination of PCNA is implicated in replication completion during replication stress. *Genes Cells* 9: 1031 – 1042

Branzei D, Seki M, Onoda F, Enomoto T (2002) The product of *Saccharomyces cerevisiae* WHIP/MGS1, a gene related to replication factor C genes, interacts functionally with DNA polymerase delta. *Mol Genet Genomics* 268: 371 – 386

Branzei D, Vanoli F, Foiani M (2008) SUMOylation regulates Rad18-mediated template switch. *Nature* 456: 915 – 920

Cejka P, Plank JL, Dombrowski CC, Kowalczykowski SC (2012) Decatenation of DNA by the *S. cerevisiae* Sgs1-Top3-Rmi1 and RPA complex: a mechanism for disentangling chromosomes. *Mol Cell* 47: 886 – 896

Daigaku Y, Davies AA, Ulrich HD (2010) Ubiquitin-dependent DNA damage bypass is separable from genome replication. *Nature* 465: 951 – 955

Davies AA, Huttner D, Daigaku Y, Chen S, Ulrich HD (2008) Activation of ubiquitin-dependent DNA damage bypass is mediated by replication protein a. *Mol Cell* 29: 625 – 636

De Vlaminck I, van Loenhout MT, Zweifel L, den Blanken J, Hooning K, Hage S, Kerssemakers J, Dekker C (2012) Mechanism of homology recognition in DNA recombination from dual-molecule experiments. *Mol Cell* 46: 616 – 624

Feng W, Collingwood D, Boeck ME, Fox LA, Alvino GM, Fangman WL, Raghuraman MK, Brewer BJ (2006) Genomic mapping of single-stranded DNA in hydroxyurea-challenged yeasts identifies origins of replication. *Nat Cell Biol* 8: 148 – 155

Follonier C, Oehler J, Herrador R, Lopes M (2013) Friedreichs ataxia-associated GAA repeats induce replication-fork reversal and unusual molecular junctions. *Nat Struct Mol Biol* 20: 486 – 494

Friedberg EC (2005) Suffering in silence: the tolerance of DNA damage. *Nat Rev Mol Cell Biol* 6: 943 – 953

Gadal O, Labarre S, Boschiero C, Thuriaux P (2002) Hmo1, an HMG-box protein, belongs to the yeast ribosomal DNA transcription system. *EMBO J* 21: 5498 – 5507

Giot L, Chanet R, Simon M, Facca C, Faye G (1997) Involvement of the yeast DNA polymerase delta in DNA repair in vivo. *Genetics* 146: 1239 – 1251

Hardman CH, Broadhurst RW, Raine AR, Grasser KD, Thomas JO, Laue ED (1995) Structure of the A-domain of HMG1 and its interaction with DNA as studied by heteronuclear three- and four-dimensional NMR spectroscopy. *Biochemistry* 34: 16596 – 16607

Hoege C, Pfander B, Moldovan GL, Pyrowolakis G, Jentsch S (2002) RAD6-dependent DNA repair is linked to modification of PCNA by ubiquitin and SUMO. *Nature* 419: 135 – 141

Hombauer H, Srivatsan A, Putnam CD, Kolodner RD (2011) Mismatch repair, but not heteroduplex rejection, is temporally coupled to DNA replication. *Science* 334: 1713 – 1716

Jaouen S, de Koning L, Gaillard C, Muselikova-Polanska E, Stros M, Strauss F (2005) Determinants of specific binding of HMGB1 protein to hemicatenated DNA loops. *J Mol Biol* 353: 822 – 837

Kamau E, Bauerle KT, Grove A (2004) The *Saccharomyces cerevisiae* high mobility group box protein HMO1 contains two functional DNA binding domains. *J Biol Chem* 279: 55234 – 55240

Karras GI, Fumasoni M, Sienski G, Vanoli F, Branzei D, Jentsch S (2013) Noncanonical role of the 9-1-1 clamp in the error-free DNA damage tolerance pathway. *Mol Cell* 49: 536 – 546

Karras GI, Jentsch S (2010) The RAD6 DNA damage tolerance pathway operates uncoupled from the replication fork and is functional beyond S phase. *Cell* 141: 255 – 267

Kegel A, Betts-Lindroos H, Kanno T, Jeppsson K, Strom L, Katou Y, Itoh T, Shirahige K, Sjogren C (2011) Chromosome length influences replication-induced topological stress. *Nature* 471: 392 – 396

Kim H, Livingston DM (2006) A high mobility group protein binds to long CAG repeat tracts and establishes their chromatin organization in *Saccharomyces cerevisiae*. *J Biol Chem* 281: 15735 – 15740

Kim H, Livingston DM (2009) Suppression of a DNA polymerase delta mutation by the absence of the high mobility group protein Hmo1 in *Saccharomyces cerevisiae*. *Curr Genet* 55: 127 – 138

Kotter P, Weigand JE, Meyer B, Entian KD, Suess B (2009) A fast and efficient translational control system for conditional expression of yeast genes. *Nucleic Acids Res* 37: e120

Krejci L, Van Komen S, Li Y, Villemain J, Reddy MS, Klein H, Ellenberger T, Sung P (2003) DNA helicase Srs2 disrupts the Rad51 presynaptic filament. *Nature* 423: 305 – 309

Kubota T, Nishimura K, Kanemaki MT, Donaldson AD (2013) The Elg1 replication factor C-like complex functions in PCNA unloading during DNA replication. *Mol Cell* 50: 273 – 280

Lang GI, Murray AW (2011) Mutation rates across budding yeast chromosome VI are correlated with replication timing. *Genome Biol Evol* 3: 799 – 811

Lee KY, Yang K, Cohn MA, Sikdar N, D'Andrea AD, Myung K (2010) Human ELG1 regulates the level of ubiquitinated proliferating cell nuclear antigen (PCNA) through its interactions with PCNA and USP1. *J Biol Chem* 285: 10362 – 10369

Liberi G, Maffioletti G, Lucca C, Chiolo I, Baryshnikova A, Cotta-Ramusino C, Lopes M, Pellicioli A, Haber JE, Foiani M (2005) Rad51-dependent DNA structures accumulate at damaged replication forks in sgs1 mutants defective in the yeast ortholog of BLM RecQ helicase. *Genes Dev* 19: 339 – 350

Lopes M, Cotta-Ramusino C, Liberi G, Foiani M (2003) Branch migrating sister chromatid junctions form at replication origins through Rad51/Rad52-independent mechanisms. *Mol Cell* 12: 1499 – 1510

Lopes M, Foiani M, Sogo JM (2006) Multiple mechanisms control chromosome integrity after replication fork uncoupling and restart at irreparable UV lesions. *Mol Cell* 21: 15 – 27

Lu J, Kobayashi R, Brill SJ (1996) Characterization of a high mobility group 1/2 homolog in yeast. *J Biol Chem* 271: 33678 – 33685

Lucas I, Hyrien O (2000) Hemicatenanes form upon inhibition of DNA replication. *Nucleic Acids Res* 28: 2187 – 2193

Minca EC, Kowalski D (2010) Multiple Rad5 activities mediate sister chromatid recombination to bypass DNA damage at stalled replication forks. *Mol Cell* 38: 649 – 661

Moldovan GL, Dejsuphong D, Petalcorin MI, Hofmann K, Takeda S, Boulton SJ, D'Andrea AD (2011) Inhibition of homologous recombination by the PCNA-interacting protein PARI. *Mol Cell* 45: 75 – 86

Mozlin AM, Fung CW, Symington LS (2008) Role of the *Saccharomyces cerevisiae* Rad51 paralogs in sister chromatid recombination. *Genetics* 178: 113 – 126

Mullen JR, Kaliraman V, Ibrahim SS, Brill SJ (2001) Requirement for three novel protein complexes in the absence of the Sgs1 DNA helicase in *Saccharomyces cerevisiae*. *Genetics* 157: 103 – 118

Nik-Zainal S, Alexandrov LB, Wedge DC, Van Loo P, Greenman CD, Raine K, Jones D, Hinton J, Marshall J, Stebbings LA, Menzies A, Martin S, Leung K, Chen L, Leroy C, Ramakrishna M, Rance R, Lau KW, Mudie LJ, Varela I *et al* (2012) Mutational processes molding the genomes of 21 breast cancers. *Cell* 149: 979 – 993

Nishimura K, Fukagawa T, Takisawa H, Kakimoto T, Kanemaki M (2009) An auxin-based degron system for the rapid depletion of proteins in nonplant cells. *Nat Methods* 6: 917 – 922

Papouli E, Chen S, Davies AA, Huttner D, Krejci L, Sung P, Ulrich HD (2005) Crosstalk between SUMO and ubiquitin on PCNA is mediated by recruitment of the helicase Srs2p. *Mol Cell* 19: 123 – 133

Parnas O, Zipin-Roitman A, Pfander B, Liefshitz B, Mazor Y, Ben-Aroya S, Jentsch S, Kupiec M (2010) Elg1, an alternative subunit of the RFC clamp loader, preferentially interacts with SUMOylated PCNA. *EMBO J* 29: 2611 – 2622

Pfander B, Moldovan GL, Sacher M, Hoege C, Jentsch S (2005) SUMO-modified PCNA recruits Srs2 to prevent recombination during S phase. *Nature* 436: 428 – 433

Postow L, Crisona NJ, Peter BJ, Hardy CD, Cozzarelli NR (2001) Topological challenges to DNA replication: conformations at the fork. *Proc Natl Acad Sci USA* 98: 8219 – 8226

Robinson NP, Blood KA, McCallum SA, Edwards PA, Bell SD (2007) Sister chromatid junctions in the hyperthermophilic archaeon *Sulfolobus solfataricus*. *EMBO J* 26: 816 – 824

Rong L, Palladino F, Aguilera A, Klein HL (1991) The hyper-gene conversion hpr5-1 mutation of *Saccharomyces cerevisiae* is an allele of the SRS2/RADH gene. *Genetics* 127: 75 – 85

Sogo JM, Lopes M, Foiani M (2002) Fork reversal and ssDNA accumulation at stalled replication forks owing to checkpoint defects. *Science* 297: 599 – 602

Stelter P, Ulrich HD (2003) Control of spontaneous and damage-induced mutagenesis by SUMO and ubiquitin conjugation. *Nature* 425: 188 – 191

Stros M (2010) HMGB proteins: interactions with DNA and chromatin. *Biochim Biophys Acta* 1799: 101 – 113

Stros M, Muselikova-Polanska E, Pospisilova S, Strauss F (2004) High-affinity binding of tumor-suppressor protein p53 and HMGB1 to hemicatenated DNA loops. *Biochemistry* 43: 7215 – 7225

Szakal B, Branzei D (2013) Premature Cdk1/Cdc5/Mus81 pathway activation induces aberrant replication and deleterious crossover. *EMBO J* 32: 1155 – 1167

Thomas JO, Travers AA (2001) HMG1 and 2, and related architectural DNA-binding proteins. *Trends Biochem Sci* 26: 167 – 174

Torres-Ramos CA, Prakash S, Prakash L (2002) Requirement of RAD5 and MMS2 for postreplication repair of UV-damaged DNA in *Saccharomyces cerevisiae*. *Mol Cell Biol* 22: 2419 – 2426

Vanoli F, Fumasoni M, Szakal B, Maloisel L, Branzei D (2010) Replication and recombination factors contributing to recombination-dependent bypass of DNA lesions by template switch. *PLoS Genet* 6: e1001205

Veaute X, Jeusset J, Soustelle C, Kowalczykowski SC, Le Cam E, Fabre F (2003) The Srs2 helicase prevents recombination by disrupting Rad51 nucleoprotein filaments. *Nature* 423: 309 – 312

Wang JC (2002) Cellular roles of DNA topoisomerases: a molecular perspective. *Nat Rev Mol Cell Biol* 3: 430 – 440

Waters LS, Walker GC (2006) The critical mutagenic translesion DNA polymerase Rev1 is highly expressed during G(2)/M phase rather than S phase. *Proc Natl Acad Sci USA* 103: 8971 – 8976

Wechsler T, Newman S, West SC (2011) Aberrant chromosome morphology in human cells defective for Holliday junction resolution. *Nature* 471: 642 – 646

Weir HM, Kraulis PJ, Hill CS, Raine AR, Laue ED, Thomas JO (1993) Structure of the HMG box motif in the B-domain of HMG1. *EMBO J* 12: 1311 – 1319

Wu L, Hickson ID (2003) The Blooms syndrome helicase suppresses crossing over during homologous recombination. *Nature* 426: 870 – 874

Xiao L, Williams AM, Grove A (2010) The C-terminal domain of yeast high mobility group protein HMO1 mediates lateral protein accretion and in-phase DNA bending. *Biochemistry* 49: 4051 – 4059

Zhang H, Lawrence CW (2005) The error-free component of the RAD6/RAD18 DNA damage tolerance pathway of budding yeast employs sister-strand recombination. *Proc Natl Acad Sci USA* 102: 15954 – 15959

Zou L, Elledge SJ (2003) Sensing DNA damage through ATRIP recognition of RPA-ssDNA complexes. *Science* 300: 1542 – 1548

Published online: January 28, 2014

Supplementary Figures and Figure Legends

Figure S1 relates to Figure 1

Supplementary Figure 1

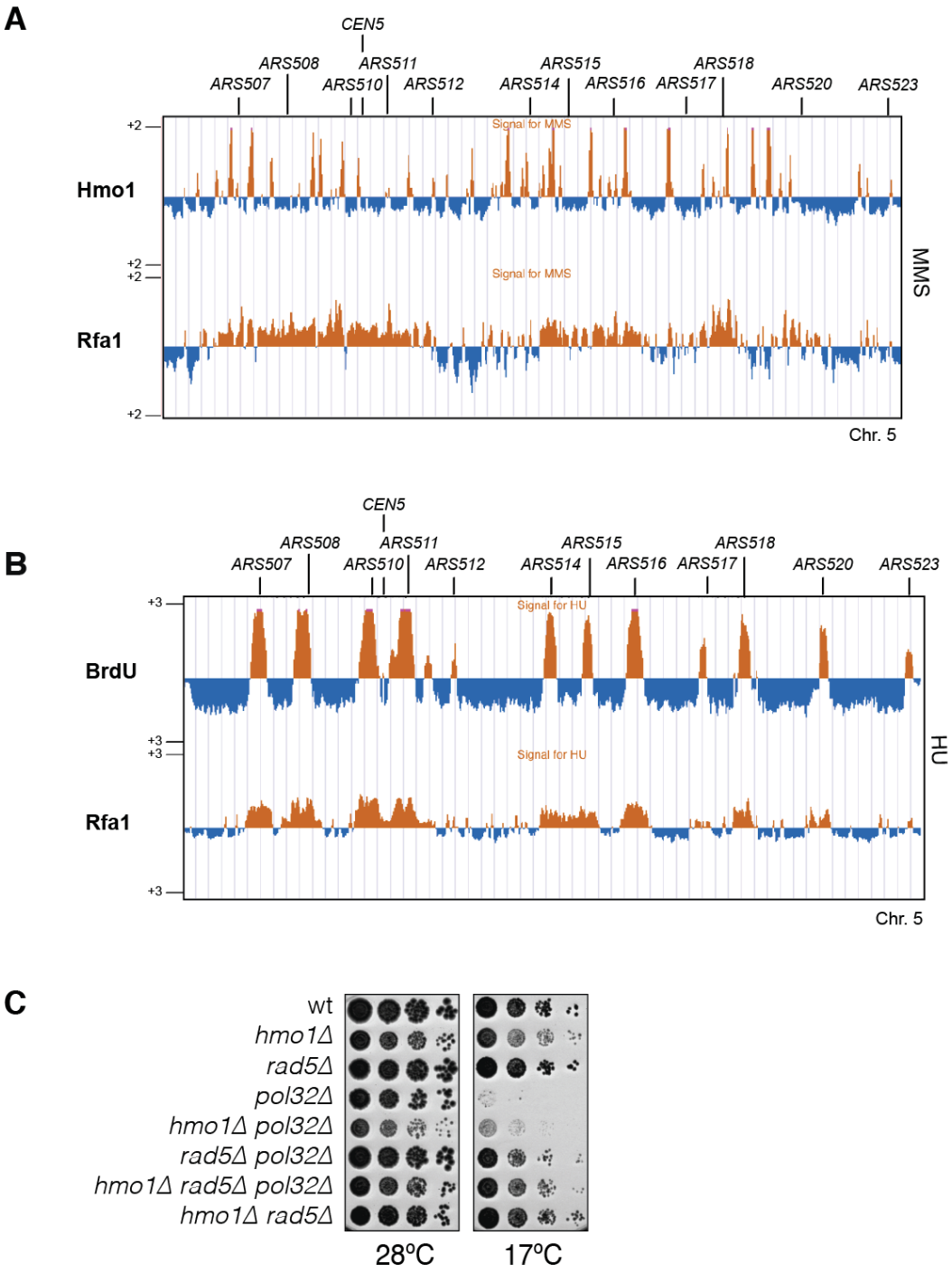

Figure S1. Genome-wide analysis of Hmo1 clusters following replication in the presence of genotoxic stress and characterization of *pol32* cold sensitivity suppression by *hmo1* . **(A)** Hmo1-6xPK (FY1687) and Rfa1-6xPK (HY3800) were released from G1 arrest in the presence of MMS 0.033% for 1 hour and processed for ChIP with antibodies specific to the PK epitope. Orange histogram bars in the y-axis show the average signal ratio of loci significantly enriched in the immunoprecipitated fraction along the indicated regions in log2 scale. Positions of *ARS* elements and *CENs* are indicated. **(B)** wt strains containing TK repeats to allow BrdU incorporation (FY1110) were released from G1 arrest in media containing 0.2M HU and BrdU for 90 min. Rfa1-6xPK (HY3800) strains were released in 0.2M HU media for 90 min. Samples were processed for ChIP with anti-BrdU antibodies or antibodies specific to the PK epitope. **(C)** wt (FY0090), *hmo1* (HY1508), *rad5* (Y1223), *pol32* (Y2593), *hmo1 pol32* (IP1136), *rad5 pol32* (Y2663), *hmo1 rad5 pol32* (IP1138), *hmo1 rad5* (IP1128) strains were spotted.

Acknowledgements

First, I would like to thank my supervisor, Dr. Dana Branzei, for her constant and amazing mentorship. She guided me through science and helped me to grow as a man and as a scientist in all these years spent together. I will be always grateful to her.
I would like to thank also my internal advisor, Prof. Marco Foiani, and my external advisor, Dr. Philippe Pasero, for their useful advices.
I thank all my collegues for friendship, scientific discussions and for everyday life in the lab. I thank also all the people of IFOM that help us with experiments and allow us to make great science in a so great institute.
A big thank goes to my family and friends for support and love.

Sometimes it's the people who no one imagines anything of, who do the things that no one can imagine.

Alan Turing